Surrogate-Assisted Evolutionary Algorithms

Ilya Loshchilov

Surrogate-Assisted Evolutionary Algorithms

Ph.D. Thesis

École Doctorale d'Informatique, ED 427

Université Paris-Sud 11

By **Ilya Gennadyevich LOSHCHILOV**

Presented and publicly defended :

On January 8 2013

In Orsay, France

With the following jury :

Frédéric Bonnans,	DR INRIA, INRIA Saclay, Ecole Polytechnique, France	(Examiner)
Michael Emmerich,	Assistant Professor, Leiden University, The Netherlands	(Examiner)
Christian Igel,	Professor, University of Copenhagen, Denmark	(Reviewer)
Una-May O'Reilly,	Principal Research Scientist, MIT CSAIL, USA	(Examiner)
Marc Schoenauer,	DR INRIA, INRIA Saclay, LRI/TAO, France	(Thesis Advisor)
Michèle Sebag,	DR CNRS, University of Paris-Sud 11, LRI/TAO, France	(Thesis Advisor)
François Yvon,	Professor, University of Paris-Sud 11, LIMSI/TLP, France	(Examiner)

Reviewers :

Christian Igel,	Professor, University of Copenhagen, Denmark
Yaochu Jin,	Professor, University of Surrey, UK

Inria Saclay - Île-de-France – TAO Project Team
1 rue Honoré d'Estienne d'Orves 91120 Palaiseau Cedex, France

Les algorithmes évolutionnaires à la base de méta-modèles scalaires

Thèse de doctorat

École Doctorale d'Informatique, ED 427

Université Paris-Sud 11

Par **Ilya Gennadyevich LOSHCHILOV**

Présentée et soutenue publiquement

Le 8 Janvier 2013

À Orsay, France

Devant le jury ci-dessous :

Frédéric Bonnans,	DR INRIA, INRIA Saclay, Ecole Polytechnique, France	(Examinateur)
Michael Emmerich,	Assistant Professor, Leiden University, The Netherlands	(Examinateur)
Christian Igel,	Professor, University of Copenhagen, Denmark	(Rapporteur)
Una-May O'Reilly,	Principal Research Scientist, MIT CSAIL, USA	(Examinatrice)
Marc Schoenauer,	DR INRIA, INRIA Saclay, LRI/TAO, France	(Directeur de Thèse)
Michèle Sebag,	DR CNRS, University of Paris-Sud 11, LRI/TAO, France	(Directrice de Thèse)
François Yvon,	Professor, University of Paris-Sud 11, LIMSI/TLP, France	(Examinateur)

Rapporteurs :

Christian Igel,	Professor, University of Copenhagen, Denmark
Yaochu Jin,	Professor, University of Surrey, UK

Inria Saclay - Île-de-France – TAO Project Team
1 rue Honoré d'Estienne d'Orves 91120 Palaiseau Cedex, France

Abstract

Evolutionary Algorithms (EAs) have received a lot of attention regarding their potential to solve complex optimization problems using problem-specific variation operators. A search directed by a population of candidate solutions is quite robust with respect to a moderate noise and multi-modality of the optimized function, in contrast to some classical optimization methods such as quasi-Newton methods. The main limitation of EAs, the large number of function evaluations required, prevents from using EAs on computationally expensive problems, where one evaluation takes much longer than 1 second.

The present thesis focuses on an evolutionary algorithm, Covariance Matrix Adaptation Evolution Strategy (CMA-ES), which has become a standard powerful tool for *continuous black-box optimization*. We present several state-of-the-art algorithms, derived from CMA-ES, for solving single- and multi-objective black-box optimization problems.

First, in order to deal with expensive optimization, we propose to use comparison-based surrogate (approximation) models of the optimized function, which do not exploit function values of candidate solutions, but only their quality-based ranking. The resulting self-adaptive surrogate-assisted CMA-ES represents a tight coupling of statistical machine learning and CMA-ES, where a surrogate model is build, taking advantage of the function topology given by the covariance matrix adapted by CMA-ES. This allows to preserve two key invariance properties of CMA-ES: invariance with respect to i). monotonous transformation of the function, and ii). orthogonal transformation of the search space. For multi-objective optimization we propose two mono-surrogate approaches: i). a mixed variant of One Class Support Vector Machine (SVM) for dominated points and Regression SVM for non-dominated points; ii). Ranking SVM for preference learning of candidate solutions in the multi-objective space. We further integrate these two approaches into multi-objective CMA-ES (MO-CMA-ES) and discuss aspects of surrogate-model exploitation.

Second, we introduce and discuss various algorithms, developed to understand, explore and expand frontiers of the Evolutionary Computation domain, and CMA-ES in particular. We introduce linear time Adaptive Coordinate Descent method for non-linear optimization, which inherits a CMA-like procedure of adaptation of an appropriate coordinate system without losing the initial simplicity of Coordinate Descent. For multi-modal optimization we propose to adaptively select the most suitable regime of restarts of CMA-ES and introduce corresponding alternative restart strategies. For multi-objective optimization we analyze case studies, where original parent selection procedures of MO-CMA-ES are inefficient, and introduce reward-based parent selection strategies, focused on a comparative success of generated solutions.

Résumé en Français

(abstract in French)

Les Algorithmes Évolutionnaires (AEs) ont été très étudiés en raison de leur capacité à résoudre des problèmes d'optimisation complexes en utilisant des opérateurs de variation adaptés à des problèmes spécifiques. Une recherche dirigée par une population de solutions offre une bonne robustesse par rapport à un bruit modéré et la multi-modalité de la fonction optimisée, contrairement à d'autres méthodes d'optimisation classiques telles que les méthodes de quasi-Newton. La principale limitation de AEs, le grand nombre d'évaluations de la fonction objectif, pénalise toutefois l'usage des AEs pour l'optimisation de fonctions chères en temps calcul.

La présente thèse se concentre sur un algorithme évolutionnaire, Covariance Matrix Adaptation Evolution Strategy (CMA-ES), connu comme un algorithme puissant pour *l'optimisation continue boîte noire*. Nous présentons l'état de l'art des algorithmes, dérivés de CMA-ES, pour résoudre les problèmes d'optimisation mono- et multi-objectifs dans le scénario boîte noire.

Une première contribution, visant l'optimisation de fonctions coûteuses, concerne l'approximation scalaire de la fonction objectif. Le meta-modèle appris respecte l'ordre des solutions (induit par la valeur de la fonction objectif pour ces solutions) ; il est ainsi invariant par transformation monotone de la fonction objectif. L'algorithme ainsi défini, saACM-ES, intègre étroitement l'optimisation réalisée par CMA-ES et l'apprentissage statistique de meta-modèles adaptatifs ; en particulier les meta-modèles reposent sur la matrice de covariance adaptée par CMA-ES. saACM-ES préserve ainsi les deux propriété clé d'invariance de CMA-ES : invariance i) par rapport aux transformations monotones de la fonction objectif; et ii) par rapport aux transformations orthogonales de l'espace de recherche.

L'approche est étendue au cadre de l'optimisation multi-objectifs, en proposant deux types de meta-modèles (scalaires). La première repose sur la caractérisation du front de Pareto courant (utilisant une variante mixte de One Class Support Vector Machone (SVM) pour les points dominés et de Regression SVM pour les points non-dominés). La seconde repose sur l'apprentissage d'ordre des solutions (rang de Pareto) des solutions. Ces deux approches sont intégrées à CMA-ES pour l'optimisation multi-objectif (MO-CMA-ES) et nous discutons quelques aspects de l'exploitation de meta-modèles dans le contexte de l'optimisation multi-objectif.

Une seconde contribution concerne la conception d'algorithmes nouveaux pour l'optimisation mono-objectif, multi-objectifs et multi-modale, développés pour comprendre, explorer et élargir les frontières du domaine des algorithmes évolutionnaires et CMA-ES en particulier. Spécifiquement, l'adaptation du système de coordonnées proposée par CMA-ES est couplée à une méthode adaptative de descente coordonnée par coordonnée. Une stratégie adaptative de redémarrage de CMA-ES est proposée pour l'optimisation multi-modale. Enfin, des stratégies de sélection adaptées aux cas de l'optimisation multi-objectifs et remédiant aux difficultés rencontrées par MO-CMA-ES sont proposées.

Acknowledgements

First and foremost I want to thank my advisors, Marc and Michèle, for a rich and friendly scientific environment they created. With a greatest pleasure I will remember all the adventures of thought we had together, some beautiful landscapes that we have noticed are still waiting for us. I will never forget the enormous forces you applied with great talent making me a better researcher.

I would like to use an opportunity to thank my previous advisors: my chess teacher, Vladimir Andreevich Zhukov who showed me that there is the pleasure of thinking, my history teacher, Yury Moiseevich Jarema who taught me to ask right questions, and my first scientific advisor, Leonid Ivanovich Babak who showed me the power of evolution.

I deeply thank Christian Igel and Yaochu Jin for closely reviewing my thesis and for many valuable comments and suggestions. I also would like to thank Frédéric Bonnans, Michael Emmerich, Una-May O'Reilly and François Yvon for kindly accepting to be members of the Jury, it is an honor for me.

I would like to thank all my friends from the TAO team and especially (in alphabetical order): Alvaro, Anne, Dawei, Gaetan, Jacques, Nikolaus, Mostepha, Mouadh, Ouassim, Riad, Weijia, Youhei and Zyed. I am especially grateful to Nikolaus and Anne for sharing their experience and for many fruitful discussions we had. This thesis would not have been possible without Marc, Michèle, Marie-Carol and Valérie who always were around to help me during the thesis.

I also thank all my new and old closest friends: Alexander, Arseniy, Gaetan, Ekaterina, Nikita, Petr, Timur, Valentin, Victor and Yury. The lovely time we spent together will forever stay in my memory.

Finally, I would like to warmly thank my Family: my parents Olga and Gennady, my brother Anton and my wife Anna. You are my happiness and my source of confidence that since we are together, tomorrow will be at least as good as today. When I get up in the morning and I feel myself falling in love, I still can not believe how lucky I am to be with you, my beauty and my treasure, my beloved Anna.

To Anna.

Contents

List of Figures

List of Tables

List of Algorithms

List of Acronyms

BBOB Black-Box Optimization Benchmarking

CMA-ES Covariance Matrix Adaptation Evolution Strategy

DOE Design of Experiments

EA Evolutionary Algorithm

EC Evolutionary Computation

ECDF Empirical Cumulative Distribution Function

ERT Expected Running Time

ES Evolution Strategy

GA Genetic Algorithm

GP Gaussian Process regression

MO-CMA-ES Multi-objective CMA-ES

MOEA Multi-objective Evolutionary Algorithm

NSGA-II Non-dominated Sorting Genetic Algorithm II

PR Polynomial Regression

RBF Radial Basis Function

SVM Support Vector Machine

Part I

General Introduction

Chapter 1

Introduction

1.1 Context/Motivation

The complexity of real-world problems is steadily growing, alongside with the computational power of supercomputers, clusters and graphics processing units. This growth maintains a permanent demand on powerful simulation and modelling frameworks, coupled with robust optimization algorithms; overall, the resolution of *advanced* real-world problems remains ever more expensive in terms of time and/or money. It is not uncommon to deal with real-world problems where one evaluation of a candidate solution requires a full laboratory experiment (e.g., protein's folding stability optimization [Chaput and Szostak, 2004], experimental quantum control [Roslund *et al.*, 2009], multi-objective optimization of Diesel combustion [Yagoubi, 2012]). A most common example of real-world problem consists of optimally tuning the hyper-parameters of a complex system (e.g., compiler optimization [Fursin *et al.*, 2005], job allocations in a computational grid [Tesauro *et al.*, 2007]), as opposed to using expert hand-crafted parameter settings.

Evolutionary Algorithms (EAs) have been thoroughly investigated in this context due to their ability to solve complex optimization problems by coupling problem-specific variation operators and selection operators:
Firstly, a search directed by a population of candidate solutions is quite robust with respect to a moderate noise and multi-modality of the objective function, in contrast to some classical optimization methods such as quasi-Newton methods.
Secondly, the role of variation operators is to explore the search space of potential solutions, taking into account already retrieved information about the problem. The − usually randomized − variation operators, together with the representation of the candidate solutions, encapsulate extensive prior knowledge about the problem domain.
Finally, selection is responsible for directing the search toward more promising regions on the basis of the current solutions, controlling the exploration versus exploitation trade-off.

These features make EAs very flexible and suitable for virtually any optimization problem provided that parametrized solutions can be comparatively assessed. Specifically, EAs are meant to address a wide range of optimization problems: involving a unimodal or multi-modal objective function; with or without noise; in a low- or high-dimensional search space; constrained or without constraints; involving a stationary or a dynamic objective ; involving a computationally expensive or cheap objective function; and last but not least, involving a single or multiple objective functions.

The Evolutionary Computation (EC) community has introduced a variety of approaches to address all abovementioned types of optimization problems. On the one

hand, these approaches have been empirically validated by practitioners, reporting a number of breakthrough applications (see, e.g., [Coello and Lamont, 2004, Yu *et al.*, 2008, Chiong *et al.*, 2011] among many others). On the other hand, the theoretical properties of some simple variants of the most successful approaches have been established and related to the first principles of optimization, specifically the natural gradient [Wierstra *et al.*, 2008, Arnold *et al.*, 2011, Akimoto and Ollivier, 2013].

In the meanwhile, rare position papers discuss the growing gap between the theory and the practice of EAs [Michalewicz, 2012]. The latter paper, reflecting the author's personal point of view based on 20 years of experience in the field of EC, invites to discuss the question of self-assessment in EC. It suggests that most generally and like many other scientific fields, EC is driven by two main forces: research and applications. In practice, some approaches are known to be the most efficient ones with respect to the current benchmark or real-world problems, whereas some other and perhaps less efficient approaches are considered to have more solid theoretical foundations, or to be more general, more flexible or more elegant. In this perspective, EC could itself be viewed as a black-box, non-stationary, multi-objective problem *per se*, with its deployment being shaped under simultaneous researcher and practitioner dynamic pressures. Along this line, the EC community collectively aims at building an *optimal Pareto set of optimization approaches*.

The lessons learned from multi-objective optimization are that, in order to build a dense Pareto front, one must mandatorily preserve the population diversity, and avoid discarding too easily the solutions which are dominated w.r.t. the current objectives. Despite their shortcomings, some solutions are found to pave the way toward truly non-dominated solutions in unfrequented regions of the Pareto front. In other words, the celebrated Exploitation versus Exploration trade-off should be considered at the level of algorithm design, too. Along this line, the contributions presented in this thesis and detailed below can be divided into two categories:

- In a first category (the exploitation category, Chapters 4 and 5), we present principled and efficient extensions of the prominent Covariance Matrix Adaptation Evolution Strategy (CMA-ES) [Hansen *et al.*, 2003], aimed at surrogate-based single-objective optimization [Jin, 2005] or surrogate-based multi-objective optimization [Knowles and Nakayama, 2008] and based on the tight coupling of stochastic optimization and statistical machine learning [Vapnik, 1995, Joachims, 2005].

- In a second category (the exploration category, Chapter 6), we present new stochastic optimization schemes, based on Adaptive Coordinate Descent (Section 6.1), with kernel-based change of representation (Section 6.4.1), or tackling the CMA-ES hyper-parameter tuning problem as a (very noisy) optimization problem (Section 6.3).

1.2 Main Contributions

As already said, the Covariance Matrix Adaptation Evolution Strategy (CMA-ES) and its variants are acknowledged to be the most efficient approaches in *continuous black-box optimization* [Hansen *et al.*, 2010b]. The first part of the presented contributions (the

"exploitation" part) proceeds by coupling statistical machine learning algorithms with CMA-ES, in order to address specific issues such as surrogate-based optimization and multi-objective optimization, while preserving all the invariance and robustness properties of CMA-ES.

The second part (the "exploration" part) investigates independent issues: hyper-parameter tuning; non-linear adaptive representations; reward-based multi-objective optimization.

1.2.1 Coupling CMA-ES with Statistical Machine Learning

One of the main limitations of EAs, the large number of function evaluations required for a reasonable accuracy of optimization, prevents EAs from being used on computationally expensive problems, where one evaluation takes more than one second and up to a few hours or a day[1].

A common way to reduce the overall number of function evaluations required to solve expensive optimization problems is to build surrogate (approximation) models and carefully treat the information available from the evaluated candidate solutions (see [Box and Wilson, 1951, Jin, 2005], Chapter 3).

ACM-ES In the spirit of the comparison-based CMA-ES approach, we used a comparison-based surrogate-learning approach, referred to as Ranking SVM [Herbrich *et al.*, 1999, Joachims, 2005]. The surrogate learning phase thus does not exploit the objective values of the available solutions, but only their ranks. In this way, the overall surrogate-based optimization approach is invariant under monotonous transformations of the objective function, a most desirable property.

A key contribution compared to the state of the art [Runarsson, 2006, Bouzarkouna *et al.*, 2010] is to reuse the covariance matrix built by CMA-ES itself within Ranking SVM; along this coupling, the overall approach called ACM-ES inherits CMA-ES invariance under orthogonal transformations of the search space.

A second contribution is to automatically and adaptively control the refreshment rate of the surrogate model (surrogate lifelength), depending on the empirical error of the previous surrogate model, under the assumption of a smooth variation of the optimal (unknown) surrogate along the search.

A third contribution is to interleave surrogate learning with the automatic online adjustment of the learning hyper-parameters, being reminded that the surrogate model quality critically depends on the learning hyper-parameters.

[1] This limitation is especially observable in the special, but quite common case of the unimodal noiseless continuous optimization, where gradient information is useful and quasi-Newton methods such as BFGS [Shanno, 1970], proposed 40 years ago, usually outperform most of advanced EAs [Hansen *et al.*, 2010b]. Unfortunately, this has become, directed by natural selection, a common practice in EC community to not view BFGS as an alternative approach, arguing that, anyway, the latter does not perform well on multi-modal and noisy functions. This may create a false impression about the performance of EAs in EC community, but does not create this impression among practitioners who *do* compare EAs with non-EC algorithms, such as BFGS and recently proposed NEWOUA [Powell, 2006]. We shall return to this point in Chapter 4.

The proposed algorithm, extensively benchmarked on the Black-Box Optimization Benchmarking (BBOB) [Hansen *et al.*, 2010a] framework against classical (BFGS [Shanno, 1970], NEWUOA [Powell, 2006], GLOBAL [Pal *et al.*, 2012]) and Evolutionary Algorithms, is shown to improve by a factor 2 to 4 on the state of the art.

ASM In the same spirit, Aggregated Surrogate Models (ASMs) inspired from the Support Vector Machine framework are used for multi-objective optimization.
A first approach aims at characterizing the current Pareto-front in the spirit of [Vapnik, 1995], as follows. On the one hand, One-Class SVM is used to characterize the (low-dimensional) region of the Pareto front like [Schölkopf *et al.*, 2001]; on the other hand, Regression SVM [Vapnik, 1995] is used to characterize the distance to the Pareto front. Both models together are used to estimate the progress toward the (true) Pareto front, by filtering the offspring estimated on the surrogate.
A second approach uses Ranking SVM to directly learn the Pareto dominance relation. A main originality of the approach compared to the state of the art in surrogate-based multi-objective optimization, is to characterize the Pareto front using *a single* surrogate (as opposed to, using a surrogate for each objective function), based on preference relations among solutions, e.g., based on Pareto dominance, Quality Indicators and Decision Maker preferences.
Likewise, an extensive benchmark of the two proposed approaches establishes that they improve on the state of the art by a factor 2.

1.2.2 Exploratory contributions

Three exploratory contributions inspired from CMA-ES are proposed:

- The first one called Adaptive Coordinate Descent (ACiD) hybridizes the simple Coordinate Descent approach with the CMA-ES adaptation of the problem representation.
  On the one hand, ACiD demonstrates a linear empirical complexity with respect to the problem dimensionality (as opposed to, at least quadratic in CMA-ES). On the other hand, ACiD can be extended to non-linear change of the problem representation by using the famed kernel trick [Vapnik, 1995].
  Comprehensive validation on BBOB shows that ACiD is competitive with CMA-ES.

- The second contribution is concerned with multi-objective optimization. In some cases, the failure of existing approaches is investigated and explained from the weakness of the parent selection procedures.
  A multi-objective reward function, measuring how much a parent contributes to the future populations, is designed and experimented. This approach measuring the "value" of an individual as opposed to its instant value, in the perspective of reinforcement learning [Sutton and Barto, 1998].

- Finally, the restart strategies of CMA-ES on multi-modal fitness landscape are analyzed. The optimal restart strategy is viewed as a sequential decision problem, setting in each restart the two CMA-ES hyper-parameters (the population size and

the initial mutation amplitude). The restart strategy is viewed as (yet another, but very noisy) optimization problem, and new restart strategies, with adaptive selection of the most suitable regime of restarts, are defined and validated.

1.3 Thesis Outline

Chapter 2 presents a historical overview of Evolutionary Computation and introduces Evolutionary Algorithms in the context of continuous black-box optimization, focusing on state-of-the-art algorithms for single-objective (respectively, multi-objective) optimization such as CMA-ES (respectively, MO-CMA-ES).

Chapter 3 presents a survey of popular techniques for surrogate model learning, exploitation and control, and reviews single- and multi-objective surrogate-assisted optimization algorithms.

Chapter 4 introduces surrogate-assisted versions of CMA-ES based on pre-selection of promising individuals and direct optimization of surrogate model, focusing on questions of surrogate hyper-parameters adaptation and surrogate exploitation control.

Chapter 5 extends surrogate-assisted CMA-ES with pre-selection to multi-objective optimization and discusses several ways to learn and incorporate preference information into surrogate models.

Chapter 6 provides a collection of CMA-like algorithms to explore prospective directions of the research in EC, including linear time Adaptive Coordinate Descent, new parent selection strategies for MO-CMA-ES and alternative restart strategies for CMA-ES.

Chapter 7 concludes the thesis and summarizes our contributions toward understanding of efficient continuous black-box optimization.

Part II

Background Review

Chapter 2

Evolutionary Algorithms for Continuous Black-Box Optimization

> *It may be said that natural selection is daily and hourly scrutinising, throughout the world, every variation, even the slightest; rejecting that which is bad, preserving and adding up all that is good; silently and insensibly working, whenever and wherever opportunity offers, at the improvement of each organic being in relation to its organic and inorganic conditions of life.*
> *Charles Darwin, 1859, On the Origin of Species, Chapter 4.*

The origins of the idea of natural selection can be traced as far as back to ancient Greeks philosophers Empedocles, Aristotle et al. A more contemporary and widely accepted version of this idea by Charles Darwin assumes the evolution of organic beings. In the present thesis, as well as in Evolutionary Computation, we assume that natural selection is a driving force of evolution not only for organic beings, but also for non-organic ones. In Section 2.1, we give a brief historical overview of the evolution of this concept in Evolutionary Computation domain. Section 2.2 introduces continuous black-box optimization and discusses main properties of black-box problems, which motivate the development of specific approaches to efficient optimization. We present the state-of-the-art Evolutionary Algorithms for single-objective (Section 2.3) and multi-objective (Section 2.4) continuous optimization. Finally, in Section 2.5, we conclude the Chapter and discuss some open questions of the field.

2.1 Historical Overview of Evolutionary Computation

Evolutionary Computation (EC) is the research field of nature- and evolution-inspired computational methods used to solve real-world problems, and their toy scientific models. We divide the history of the EC field into two parts: early approaches proposed before the first International Conference on Genetic Algorithms (ICGA) in 1985, and modern approaches proposed after this conference. According to an analysis by [Alander, 1994] of 2500 papers published on Genetic Algorithms, Evolution Strategies, Evolutionary Programming, etc., only 215 papers were published between 1957 and 1984, compared to 928 published between 1985 and 1990. Now the number of published papers per year is still growing, and while the exact number of papers is difficult to estimate, it might lie in order of tens of thousands, given that for one of the most cited researchers of the field of

evolutionary multi-objective optimization, Prof. Kalyanmoy Deb, the number of citation in the year of 2011 is about 6000 and about 45000 citations overall.

2.1.1 Early Approaches

"The Genetical Theory of Natural Selection" by Ronald Fisher [Fisher, 1930] is probably the second most influenced book on evolutionary biology after Darwin's book "On the Origin of Species" [Darwin, 1859].

Fisher claimed that natural selection is not Evolution, as it was identified in biological sciences, but an independent principle worthy of scientific study. He notices that the first decisive experiments, which opened in Biology this field of exact study, were due to a young mathematician, Gregor Mendel, whose statistical interests extended to physical and biological sciences (note that, experimental clarity of Mendel's work was later criticized by Fisher [Fisher, 1936]). According to Fisher, while the types of mind which result from training in mathematics and biology differ profoundly, this difference is not in the intellectual, but rather in imaginative faculty. The biologists are early introduced to the world with its immense variety of living things and amazing complexity, and they study this world as it is. The mathematicians instead deal with barest abstractions and often try to work in a wider domain than actual for a far better understanding of the actual. The difference of these two approaches lies not in intellectual methods and even less in the intellectual ability, but in an enormous and specialized extension of the imaginary faculty which each field has experienced.

It is interesting to note that Fisher studied the probability of improvement of mutation on a simple example of Sphere function $\sum_{i=1}^{n} x_i^2$. The initial solution is located on a distance $d/2$ from the center of the Sphere; the mutation operator performs a shift with radius r; the mutation is successful if new solution lies inside the Sphere, and unsuccessful otherwise. The limit of probability of improvement in this case is $0.5(1 - r/d)$, meaning that large mutations are usually unsuccessful and destructive, while small mutations are more successful, but lead to a slow progress of evolution. The latter observation was later confirmed and motivated the development of randomized optimization approaches with the adaptation of mutation step-size. Nowadays, both Evolutionary Computation and Population Genetic [Orr, 2000] show that the rate of adaptation is maximized for mutations of *intermediate size*.

Apart from Fisher's enormous contribution to statistics, he made the terms of natural selection and mutation mathematically more comprehensible for a wider scientific public. Another of his books, "The Design of Experiments" [Fisher, 1935] became the foundation for the field of Design of Experiments (DOE). This research on DOE for determining optimal conditions of chemical investigations was continued by a statistician George P. E. Box [Box and Wilson, 1951], the husband of one of Fisher's daughter Joan.

Probably inspired by Fisher's idea of small mutations and motivated by development of DOE methods which do not interrupt manufacturing processes during its optimization, George P. E. Box proposed Evolutionary Operation (EVOP) [Box, 1957]. One of the first real-world applications of Evolutionary Operation was described in [Box and Hunter, 1959] for 2-dimensional and 3-dimensional cases. In EVOP, a reason-

ably small hyper-rectangle centered in the current solution (current mean) is constructed such that the quality of the manufacturing process changes only slightly by using one of possible solutions from the hyper-rectangle. Then, the quality of solutions which lie on the corners of the hyper-rectangle is estimated and the solution with the best quality is chosen as the next mean of the hyper-rectangle. EVOP performs coordinate search with adaptive step-size and resembles the famous pattern/direct search algorithm of Hooke and Jeeves proposed later [Hooke and Jeeves, 1961]. At least 50 articles about EVOP were published during the first 10 years after its introduction. Box popularized the idea that artificial evolution can be useful for real-world optimization problems as well as Fisher showed that the natural selection can be mathematically studied.

The first computer-assisted experiments of Evolutionary Algorithms are often referred to Nils Aall Barricelli, who was visiting Princeton University in 1953, 1954. Barricelli emulated evolution of "organisms" to find the "decision function", that determines the next move for a player of several games such as Chess, Tax Tix et al. The work was published first in [Barricelli, 1954], then translated to [Barricelli, 1957]. David B. Fogel truly said [Fogel, 2006]: "Nils Barricelli remains a virtually unknown figure in the Evolutionary Computation community, but that is no reflection on his pioneering contributions and creative thoughts." Unfortunately, many other great researchers were also relatively unknown, such as Alex Fraser who simply proposed and implemented [Fraser, 1957] a pre-Genetic Algorithm with the population of individuals coded using binary strings, so-called (μ, λ) selection scheme and specific crossover and mutation operators (!).

[Bremmerman, 1958, Bremermann, 1962] discussed the idea of using evolution processes to solve optimization problems, making an analogy with DNA and using sequences of binary variables to code the solution. The author suggested to apply bit-flip mutation operation to each gene with a probability p, claiming that "In many cases optimal speed of improvement is reached for $p = 1/n$, where n = number of genes". This mutation probability has been proven by [Droste *et al.*, 1998] to be optimal on linear functions in order to reach expected running time $O(nlog(n))$ for (1+1)-Evolutionary Algorithm, where the generated by mutation offspring replaces the parent solution if it has better fitness function. The term of "fitness function" is also associated with the objective function $f : \mathbb{R}^n \mapsto \mathbb{R}$ in [Bremermann, 1962].

[Rastrigin, 1963b] (see also [Rastrigin, 1960, Rastrigin, 1963a]) discussed the advantages of randomized search methods on a real-world problem of lathe machine-tool parameter tuning. This machine-tool operates using many relatively simple single-point cutting tools, controlled by arms to produce objects of different geometry. The goal is to minimize a function $f(\boldsymbol{x})$ of the error of geometry of products by tuning $\boldsymbol{x}$, the positions of the arms. The author analyses possible scenarios of using Gauss-Seidel and Gradient-based methods and proposes to use a randomized search method. In this (1+1)-Evolutionary Algorithm, before each search step, all arms hold positions of the best solution (with the minimum error) found so far. Then, all arms should be simultaneously tuned by some random values to produce a new solution, which is accepted to be the new best solution only if it leads to a smaller $f(\boldsymbol{x})$. The mutation operation is not specified, and actually is not called "mutation", while this was probably meant, because the first part of the book discusses the importance of mutation for organic beings. The author also suggests to

adapt the mutation distribution ([Rastrigin, 1963b], p. 76) : "One can use a reward-based system, increasing the probability of those changes, which lead to improvements of quality of the system, i.e., to minimization of the criterion of similarity". The latter proposal was realized 30 years later in CMA-ES.

An idea of simultaneous mutation of problem parameters very similar to the Rastrigin's one was implemented by Hans-Paul Schwefel and Ingo Rechenberg in the 1960s. From Hans-Paul Schwefel's great book "Evolution and Optimum Seeking" [Schwefel, 1993] about "classical" and evolutionary optimization approaches of the 1960s and 1970s: "In 1963 two students at the Technical University of Berlin met and were soon to collaborate on experiments which used the wind tunnel of the Institute of Flow Engineering. During the search of the optimal shapes of bodies in a flow, which was then a matter of laborious intuitive experimentation, the idea was conceived of proceeding strategically. However, attempts with the coordinate and simple gradient strategies were unsuccessful. The one of the students, Ingo Rechenberg, now Professor of Bionics and Evolutionary Engineering, hit upon the idea of trying random changes in the parameters defining the shape, following the example of natural mutations. The evolution strategy was born." First simulations of different versions of two membered (one parent generates one offspring) (1+1)-Evolution Strategies (ESs) were performed on the first digital computer Zuse Z23 of Technical University of Berlin [Schwefel, 1965]. Theoretical analysis of these strategies and first proposals of μ multi-membered strategies $(\mu + 1)$ were published later in Ingo Rechenberg's doctorate thesis [Rechenberg, 1973]. Unfortunately, between 1976 and 1985 the research on ESs suffered from insufficient financial support [Schwefel, 1993].

Another key sub-field of Evolutionary Computation, Evolutionary Programming was invented by Lawrence J. Fogel also in the 1960s, leading to the book "Artificial Intelligence through Simulated Evolution" [Fogel *et al.*, 1966]. Fogel proposed to evolve the population of Finite State Machines (FSMs) to solve problems of prediction and control in an environment, defined as a set of sequences from a finite alphabet. All FSMs of the population are initially identical. Each FSM uses known part of the environment (previously observed symbols) to predict the next symbol from the unknown environment. The rate of this prediction is used as the fitness function. At each iteration of the algorithm, a mutation operator is applied to each FSM to generate an offspring solution. The best half of a mixed population of parents and offspring becomes the new population. This loop is repeated for several iterations, then the best machine is taken to predict the new symbol of the environment, the output symbol is attached to the environmental string. Fogel proposed several mutation operators to add and delete states and change links of FSMs. The process is named Evolutionary Programming probably in contrast to Linear Programming, Dynamic Programming and Quadratic Programming.

[Schumer and Steiglitz, 1968] proposed Adaptive Step-Size Random Search (ASSRS), an adaptive version of Fixed Step-Size Random Search (FSSRS) [Rastrigin, 1960, Rastrigin, 1963a, Mutseniyeks and Rastrigin, 1964]. They provided proofs for Optimal Step-Size Random Search (OSSRS) on unimodal functions and showed that: i). the optimal step-size is proportional to the distance to the optimum, similar results were obtained later for (1+1)-ES [Auger and Hansen, 2006]; ii). there is an optimal probability of improvements for ASSRS (see the 1/5th rule proposed later in [Rechenberg, 1973]); iii). the

average number of function evaluations to reach a desired accuracy (relative to starting point) is linear in the problem dimension. Since the distance to the optimum is usually unknown, only an approximation of the optimal step-size can be estimated. In ASSRS strategy two alternative solutions are generated by mutation of the current best solution by a random sampling in the hyper-sphere with two different radii/step-sizes. The step-size which generated the best solution (made the best improvement) is used for the next iteration. Experimental results demonstrated that Newton-Raphson method with Hessian approximation by finite differences outperforms ASSRS by a factor of about 2 on Sphere function $f(\boldsymbol{x}) = \sum_{i=1}^{n} x_i^2$ for $n > 20$, while on $\sum_{i=1}^{n} \boldsymbol{x}_i^4$ function ASSRS outperforms Newton-Raphson and simplex methods already for $n > 10$. It should be noted that ASSRS finds target fitness function $f_{target} = 10^{-8}$ after about $80n$ function evaluations, i.e., it shows the same performance as (1+1)-ES with the 1/5-th rule [Auger, 2009].

In 1975 John H. Holland wrote his book "Adaptation in Natural and Artificial Systems" [Holland, 1975], where he proposed Genetics Algorithms (see also Genetic/Adaptive Plans [Holland, 1969]). Indeed, Genetic Algorithms (GAs) were born from the "soup" of ideas of earlier researchers (some of these researchers were mentioned above). The key contribution of Holland was not only to identify what is relevant in this "soup", but to respect the following scientific trade-off: i). provide a simplified and at the same time rich theory of how the adaptation and evolution work; ii). provide a working algorithmic framework to simulate the evolution for solving real-world problems and their scientific toy models. In Holland's GA, the population were represented by chromosomes, candidate solutions of the problem, using binary coded "genes". The selection operator allows chromosomes with better fitness function (objective function) to produce offspring more often. The recombination procedure consists of crossover, mutation and inversion. Crossover exchanges sub-parts of parents chromosomes, mutation randomly changes randomly selected "genes", inversion reverses the ordering of "genes" in the chromosome. Holland also proposed the so-called Schema Theorem to provide theoretical evidence of GA convergence, however it was later criticized [Burjorjee, 2008, Antonisse, 1989] for making unacceptably strong assumptions on the distribution of fitness over the genome set.

After World War II the basic research attracted significant funding resources. In 1950s and 1960s major research agencies over the world, such as DARPA, had been promised to solve key military problems using Artificial Intelligence (AI): speech recognition and understanding, automatic machine translation, creation of general purpose robots, etc. However, most of these ambitious problems were not solved (and still are open problems in our 21-th century) or used approaches were criticized (e.g., in "Perceptrons" book by Marvin Minsky [Minsky and Seymour, 1969]), that led to funding cuts. So-called AI Winter took place from the early 1970s to the early 1980s, when major agencies switched to "goal-oriented" research and AI research continued in a limited way, because major funding for projects was difficult to find. A frustration about AI also influenced the research in a future of the "newborn" field of Evolutionary Computation: "The general interest in this type of optimum seeking algorithms was not broad enough for there to be financial support" [Schwefel, 1993]. Another important aspect was the experimental nature of Evolutionary Algorithms, that required significant CPU resources for algorithm design phase in contrast to exact methods. The latter problem was partially solved with

the emergence of personal computers in the 1980s and 1990s, that led to a "boom" of Evolutionary Computation.

2.1.2 Modern Approaches

The first International Conference on Genetic Algorithms took place in Pittsburgh, USA in 1985 and definitely boosted the research on Genetic Algorithms. After a seminal book "Genetic Algorithms in Search, Optimization, and Machine Learning" [Goldberg, 1989] (with more than 50.000 citations), David E. Goldberg, invited by Hans-Paul Schwefel, visited 14th Symposium uber Operations Research, Ulm, Germany in 1989. Together with Yuval Davidor he presented Genetic Algorithms. The first "official" meeting of German and US Evolutionary Computation interests was during the first Parallel Problem Solving from Nature (PPSN) conference in Dortmund, Germany in 1990. Genetic Algorithms and Evolution Strategies were presented together with Genetic Programming [Koza, 1990], Simulated Annealing, Classifier Systems and Immune Networks.

The number of papers published on so-called modern approaches is at least by a factor of 1000 larger than for so-called early approaches. Therefore, we do not pretend to cover this topic in a short Section. Instead, we list the most widely used approaches and give their brief comparison analysis.

Genetic Algorithms

Genetic Algorithms (GAs) is a core of Evolutionary Computation, and probably the most common approach used for initial pedagogical studies of evolution-inspired optimization and search. A good starting point of such studies is Simple Genetic Algorithm (SGA), a Holland's GA, where binary-coded parent solutions compete with offspring solutions, generated after multi-point crossover and bit-flip mutation of parents. Real-Coded Genetic Algorithms (RCGA) [Wright, 1991] popularized the real-value representation of decision variables and enriched the set of variation operators, an example of state-of-the-art RCGA algorithm is the generalized generation gap (G3) model with efficient parent-centric recombination operator (G3-PCX) [Deb, 2005]. The key aspect of design of GA is the "right" choice of representation of candidate solutions for a given problem, such that the variation operators favor successful exploration and exploitation of the search space. An illustrative example is the Travelling Salesman Problem (TSP), where a candidate solution can be represented as a sequence/tour of cities which should be visited. To make new prospective sequences from the existed ones, problem-specific variation operators can be used instead of classical crossover and mutation operators, which may create infeasible solutions (e.g., with more than one visit of the same city [Radcliffe and Surry, 1994]).

It would be unfair to think of Genetic Algorithms only in terms of their comparative performance on specific optimization problems. The GAs is, first of all, a quite general and flexible factory/template of new approaches. The flexibility of GAs allowed to explore a wide range of ideas, such as the study of diversity preservation in multi-modal optimization [Mahfoud, 1995, Sareni and Krahenbuhl, 1998]. Despite a huge progress made in 1990s, the research on GAs substantially stagnated in 2000s, at least in the domain of continuous single-objective optimization, where problem-specific approaches such as Evolution Strategies became the method of choice. In multi-objective optimization, GAs

made a long step forward (e.g., Non-dominated Sorting Genetic Algorithms-II (NSGA-II) [Deb *et al.*, 2002]), which other Evolutionary Computation approaches still try to follow.

Evolution Strategies

Evolution Strategies from the beginning have addressed continuous optimization (though discretized in the early approaches). Several attempts to extend ESs to mixed-integer optimization [Bäck and Schütz, 1995, Li *et al.*, 2006], unfortunately, have not attracted enough attention in the field. The latest results show that mixed-integer optimization is challenging and the premature convergence is possible even for relatively simple problems [Hansen, 2011, Li *et al.*, 2011].

In this thesis, we focus on ESs as a prospective approach specifically developed for continuous optimization, we give a detailed description of ESs in Section 2.3.1.

Estimation of Distribution Algorithms

In contrast to many EAs, where the distribution of candidate solutions is defined implicitly by variation operators, in Estimation of Distribution Algorithms (EDAs) [Larrañaga and Lozano, 2002] the sampling of new solutions is explicitly defined by a chosen probabilistic model, e.g., multi-variate normal distribution. The baseline EDA algorithms are: Univariate Marginal Distribution Algorithm (UMDA) [Mühlenbein and Mahnig, 2002], Estimation of Multivariate Normal Algorithm (EMNA) [Larrañaga and Lozano, 2002], Cross-Entropy Method (CEM) [Rubinstein and Kroese, 2004].

Ant Colony Optimization

Ant Colony Optimization (ACO) was proposed by Marco Dorigo in his PhD thesis [Dorigo, 1992]. ACO is an optimization technique (often viewed as an EDA) which imitates the behavior of ants to solve (usually) combinatorial optimization problems. As well as natural ants, simulated ants are seeking for a path between their colony and a source of the food. They lay down pheromone trails such that other ants will more likely to follow these trails and may reinforce attractiveness of the shortest path to the food. Trail evaporation reduces pheromone values of all trails over time, that allows to preserve some diversity in optimal path seeking.

Early ACO algorithms were aimed to solve TSP problem, but further were extended to a wide range of combinatorial problems [Dorigo and Stützle, 2003]: scheduling, vehicle routing, quadratic assignment, set covering problems, etc.

The main criticism of ACO algorithms can be demonstrated on the TSP problem (a similar criticism is also relevant for EAs in general) . Problem-specific approaches, such as modified Lin-Kernigan heuristic, implemented in LKH-2.0 library are able to solve this toy problem optimally for tens of thousands of cities (85.900 cities in [Applegate *et al.*, 2009]) and efficiently for millions of cities in linear time [Helsgaun, 2009]. The best known solution for the World TSP Tour of 1.904.711 cities was found by LKH-2.0 in October 25, 2011. It has length at most 0.0477% greater than the length of an optimal tour (estimated as the best lower bound established using Concorde TSP code). It seems that these results are better than the results of ACO algorithms, for which the instances of few thousands cities are already difficult to solve with and without 3-opt local search [Oliveira *et al.*, 2011].

A common and quite fair answer to this criticism is: i). ACO algorithms are aiming to find a general approach, which will be useful for a wide range of combinatorial problems

(this is also true for "classical" approaches); ii). ACO algorithms investigate optimization problems in a nature-inspired way, trying to fulfill the gap of understanding between optimization theory and evolutionary biology. These two things are both relevant for other EC approaches. Some progress in generalization was recently made when ACO algorithms for continuous optimization ($\text{ACO}_{\mathbb{R}}$) were proposed [Socha and Dorigo, 2008] and uncovered some similarity with the CMA-ES algorithm.

Genetic Programming

Genetic Programming (GP) was proposed by Nichael L. Cramer during the first ICGA conference in 1985 [Cramer, 1985] and later popularized by John R. Koza [Koza, 1990, Koza, 1992]. Genetic Programming is an evolution-inspired technique which imitates artificial evolution of computer programs that perform a used-predefined task. GP can be viewed as a GA with a specific representation of individuals, usually in tree structure, and variation operators defined for this tree. In contrast to other optimization techniques, the number of components (variables) representing a candidate solution is usually dynamically changing during the search. This often favors extensive search in the space of possible topologies, instead of intensive parametric search for a given topology. As a consequence, the final programs are often too complex for relatively simple problems. To control this *bloat*, the minimization of the program size/complexity can be set as the second objective after the program's fitness, leading to a multi-objective version of GP [Koza, 1992]. It is reported by John R. Koza, that analog electronic circuits, designed using GP often reinvent or/and outperform patented solutions, found by humans. However, the search in the space of possible topologies is usually heavily constrained by a designer and user of Electronic Design Automation tools. In Microwave frequency range, this becomes especially important, because lumped elements are not sufficiently precise anymore and should be replaced by approximated model for a given technological process, where each element typically has several variables. The fitness computation also becomes more expensive. Thus, parametric optimization becomes much more important than it is usually assumed in GP, and a reasonable trade-off between topological and parametric search should be found [Loshchilov, 2009].

Differential Evolution

Differential Evolution (DE) was proposed by Rainer Storn and Kenneth Price [Storn and Price, 1995] and became especially popular in recent few years thanks to relative simplicity and efficiency of this method. Basically, the original DE adds the weighted difference between two population vectors to a third vector. Each individual $\boldsymbol{x}_i$ of current population generates one offspring, which will replace the parent in the next generation if it has better fitness. The offspring $\boldsymbol{y}_i$ is a copy of the parent $\boldsymbol{x}_i$, except that some variables $x_{i,j}$ should be modified: i). randomly picked variable index j_{rand} among n variables; ii). all variables selected with the *crossover probability* CR. If a modification of offspring's variable $y_{i,j}$ is needed, the new value is computed in the following way:

$$y_{i,j} = x_{a,j} + F(x_{b,j} - x_{c,j}), \tag{2.1}$$

where $F \in [0, 1]$ is so-called *differential weight* and a, b, c are indexes of individuals from the current population. These three or more individuals are usually different from $\boldsymbol{y}_i$ and are chosen depending on the specific mutation strategy of DE.

DE typically has only few parameters (population size, CR, F) and several mutation strategies. This allowed DE community to develop a set of techniques for offline [Storn and Price, 1997] and online parameter tuning [Brest *et al.*, 2006], as well as efficient *adaptive operator selection* methods [Fialho *et al.*, 2010]. The latter methods add to DE the robustness it was missing, and would be useful also in other fields of EC.

Particle Swarm Optimization

The concept of Particle Swarm Optimization (PSO) was discovered by James Kennedy and Russell Eberhart [Kennedy and Eberhart, 1995] through simulation of a simplified social model of bird flocking, fish schooling, etc. In PSO the population is represented as a swarm of particles (individuals), which are seeking for the optimum of a function $f(\boldsymbol{x})$. Each particle i has its current position $\boldsymbol{x}_i$, best position $\boldsymbol{p}_i$ it visited so far and the velocity $\boldsymbol{v}_i$, which is simply the difference (shift) between its new and old position in the decision space. The shift for each particle i and decision variable j is computed in the following way:

$$v_{i,j} = \omega v_{i,j} + c_1 r_p (p_{i,j} - x_{i,j}) + c_2 r_g (g_j - x_{i,j}), \tag{2.2}$$

where $r_p, r_g \sim U[0,1]$ are drawn uniformly, $\mathbf{g}$ is the swarm's best know position and ω, c_1, c_2 are control parameters of the algorithm.

The use of current best solution in variation operators favors fast convergence on unimodal functions, and may lead to premature convergence on multi-modal functions. A number of techniques to avoid the premature convergence to local optima have been proposed such as update of velocity of a particle using best $\boldsymbol{p}$ locations of other particles [Liang *et al.*, 2006]. Another approach to preserve the diversity is, instead of using global swarm's best particle $\boldsymbol{g}$ for variation, to use the best one of some local "sub-swarm", supposing that the swarm has some topological structure. This structure can be fixed (original global star, local star, von Neumann neighborhood [Kennedy and Mendes, 2002]), but there are also approaches to adapt the topological structure during the search [Elshamy *et al.*, 2007].

Other Approaches

Particle Swarm and Ant Colony Optimization algorithms proposed in the early 1990s inspired a wide range of so-called Swarm Intelligence (SI) approaches, which have become especially popular since the early 2000s, one can say that they have been replacing GAs. Swarm Intelligence is usually associated with a population of relatively simple agents, whose collective interaction leads to the emergence of "intelligent" global behavior. Many SI algorithms have been proposed in recent years [Blum and Merkle, 2008]: artificial bee colony algorithm, bat algorithm, Cuckoo search, firefly algorithm, harmony search and many others. Some of these approaches imitate interesting processes, observed in nature, that probably will lead to their better understanding.

However, a common criticism, which is also relevant to the whole EC community, is that most of these approaches have very weak theoretical background and a lack of mathematical proofs of their efficiency. In some cases the lack of theoretical analysis of the algorithm can be compensated by empirical observations of its good performance. To assess the performance correctly, a precise experimental setup and procedure should be defined. Unfortunately, this is often not the case for many papers published in EC commu-

nity every year, that makes the evolution of optimization approaches even more noisy, than probably it is already because of No Free Lunch Theorem [Wolpert and Macready, 1997]. To reduce the risk of biased benchmarking, in this thesis, we extensively use BBOB framework. Another point of criticism is well illustrated in the paper "A Rigorous Analysis of the Harmony Search Algorithm: How the Research Community can be Misled by a "Novel" Methodology" [Weyland, 2010], there the author discusses obvious similarities between Harmony Search Algorithm and Evolution Strategies.

To answer the mentioned above criticism, we should again re-think the evolution of the EC field as multi-objective optimization, as described in Section 1.1. From this point of view, we indeed need some diversity of algorithms, because it might be too "greedy" to view the performance of the algorithm as the only (single) objective. However, we are more or less sure that we do not want to have "bad clones" of already existing approaches, without giving any credits, because this adds an artificial noise to the algorithm diversity measure. We also do not want to add any noise to the algorithm performance measure due to messy experimental validation procedures.

2.2 Continuous Black-Box Evolutionary Optimization

In the *black-box scenario*, we want to *minimize (without loss of generality) an objective (cost, fitness) function*

$$f : \mathbb{R}^n \mapsto \mathbb{R} \tag{2.3}$$

The function is called *black-box*, because no specific assumption on function is made, f is also called *continuous black-box function* as decision variables $\boldsymbol{x}$ are continuous variables.

The objective of *black-box optimization* is to find one or a set of solutions $\boldsymbol{x}$ with as small values $f(\boldsymbol{x})$ as possible, using as small number of function evaluations as possible. We suppose that all information (except dimension n) about the black-box function f comes from evaluations of candidate solutions $\boldsymbol{x}$ with f. The number of function evaluations used is a common *search costs* measure, which characterizes the amount of information acquired about the f during the optimization process.

There are several properties of f which can make its black-box optimization difficult. Below we list and comment some of these properties (see also [Hansen *et al.*, 2008]).

Multi-Modality

A *local minimum* (optimum of minimization) of an unconstrained function f is a vector $\boldsymbol{x}^l \in \mathbb{R}^n$ such that there is a *neighborhood* N of $\boldsymbol{x}^l$ with no better points than $\boldsymbol{x}^l$:

$$\forall \boldsymbol{x} \in N \cap \mathbb{R}^n, f(\boldsymbol{x}) \geq f(\boldsymbol{x}^l) \tag{2.4}$$

A *global optimum* is a vector $\boldsymbol{x}^g \in \mathbb{R}^n$, such that there is no $\boldsymbol{x}^l \in \mathbb{R}^n$ better than $\boldsymbol{x}^g$:

$$\forall \boldsymbol{x} \in \mathbb{R}^n, f(\boldsymbol{x}) \geq f(\boldsymbol{x}^g) \tag{2.5}$$

An objective function f is called *multi-modal* if it has more than one optimum. The optimization of multi-modal function is difficult, because usually there are no guarantees that the optimum that was found after the optimization by the algorithm is the global one. Therefore, to increase the chance to find the global optimum, several local optima should be explored in one optimization run or during several restarts. There is no consensus about the best global strategy for multi-modal optimization, two the most commonly used are: i). to preserve some diversity of solutions during the search, using niching approaches to explore local optima and hopefully find the global one(s) [Singh and Deb, 2006]; ii). to increase the probability to find the global optima performing multiple restarts with the same or different parameter settings of the algorithm (see Section 6.3.3). Multi-modal functions have typically much more complicated fitness landscapes than the unimodal ones, because of (sometimes large) basins of attraction located around the local optima.

High-Dimensionality

The volume of the search space increases exponentially with n, the number of decision variables. This can be illustrated on a simple example: first, place 100 points in a real interval $[0, 1]$; then to have a similar coverage in terms of distance between points in 10-dimensional space requires $100^{10} = 10^{20}$ points. Therefore, some optimization techniques, useful for small dimensions such as full coverage of the search space, become useless for large dimensions. This effect is called *the curse of dimensionality* [Richard Bellman, 1957]. Many important concepts such as proximity, distance, or neighborhood, become less meaningful with increasing dimensionality, due to a loss of contrast of distances [Houle *et al.*, 2010].

When comparing different optimization techniques it is important to mention the dimension range for which this comparison is considered. Many optimization algorithms do not scale in practice for extremely large dimensions ($n >> 100$), because their computational complexity and/or memory requirements grow too quickly with n, say cubically and quadratically, respectively.

Non-Separability

A function f is called *separable* if the optimum of this function can be achieved by performing n independent *one-dimensional* searches along each independent coordinate. Optimization of separable functions can break the curse of dimensionality, because the problem complexity grows linearly with n. A function f is called *non-separable* if the optimum of f cannot be achieved by one-dimensional searches and *partially-separable* if f is non-separable and has blocks of coordinates which can be optimized separately.

Many real-world problems are partially-separable, because humans tend to view the world as a structured system/object. Structured view of the world favors extensive use of decomposition, which allows to separately solve sub-problems of a large partially-separable problem. The decomposition is a common approach for complex design and optimization problems, such as design of a new car or airplane. We also often tend to simplify our daily life using decomposition: we first brush our teeth, then we drive a car to our workplace, then we work. However, some people find that it is better to do these things simultaneously.

The separability is probably the first property of the problem which should be checked when analyzing the performance of an optimizer on a benchmark or real-world problem. Some algorithms explicitly or implicitly exploit the separability, and, therefore, usually perform quite well on separable problems. The number of function evaluations to reach the optimum or some target objective value then may scale almost linearly with n. The separability of a problem or any other property of course should be exploited to improve the search *when automatically detected*. However, most of the well-known benchmark problems are separable and many optimizers have become *overfitted* [Hawkins, 2004] to this property - they perform well on benchmark problems, but fail on real-world problems which are often non-separable or partially-separable. A simple check against this kind of overfitting is to rotate the search space, such that f still has the same topology, but is not separable anymore. The overfitting to separability has misled many designers of algorithms and may be viewed as a drawback of such approaches as GAs, PSO, etc (a detailed analysis can be found in [Salomon, 1995, Hansen *et al.*, 2008]). A prospective direction of the research is to adaptively identify and learn the linkage between the variables [Tezuka *et al.*, 2004, Oliwa and Rasheed, 2012], that may allow to exploit the separability *when it is detected*.

Noisy

A function $\tilde{f}$ is called *noisy* if for a given $\boldsymbol{x}$ different $\tilde{f}(\boldsymbol{x})$ values can be observed , perturbed by some random component ξ. Optimization of noisy $\tilde{f}$ is called *noisy optimization*, which also often distinguishes two popular cases: i). the variance of the noise decreases to zero when approaching the optimum (*multiplicative noise*): $\tilde{f}(\boldsymbol{x}) = f(\boldsymbol{x})(1 + \xi)$; ii). the variance of the noise is lower bounded (*additive noise*): $\tilde{f}(\boldsymbol{x}) = f(\boldsymbol{x}) + \xi$. Both cases are widely presented in real-world problems, both make the optimization more difficult, because the information about the optimized function acquired from one function evaluation is less precise than in the *noise-less* case.

Theoretical analysis of optimization algorithms in noisy scenario usually becomes much more complicated and often requires to make some specific assumptions on the noise model ξ, hidden behind the evaluations of f. In a noisy environment, first derivatives are usually difficult or impossible to obtain, that limits the using of gradient-based methods. In a recently published paper by Jorge J. More and Stefan M. Wildy "Do You Trust Derivatives or Differences?" [More and Wild, 2012], the authors discuss why it is difficult to reliably compute derivatives or difference approximations for problems with high levels of noise. This fact among others motivated the development of *derivative-free* algorithms starting from Nelder-Mead algorithm [Nelder and Mead, 1965] and early Evolutionary Algorithms in the 1960s.

Ill-Conditioning

A convex-quadratic function $f(x) = \frac{1}{2}\boldsymbol{x}^T\boldsymbol{H}\boldsymbol{x}$, where $\boldsymbol{H}$ is symmetric positive definite,

is called *ill-conditioned* if the condition number of $\boldsymbol{H}$ is much larger than 1. The condition number of $\boldsymbol{H}$ is the ratio between its largest and smallest eigenvalue, and this is also equal to the squared rate between the longest and the shortest principal axes of the ellipsoid $\left\{\boldsymbol{x}|\boldsymbol{x}^T\boldsymbol{H}\boldsymbol{x}=1\right\}$. If the condition number is large, then this ellipsoid is very elongated. On an ill-conditioned function the length of search steps, performed in different directions of the decision space may differ by orders of magnitude to produce the same improvements of the objective function.

Ill-conditioned problems are difficult for optimization, because before we learn an appropriate metric we often make too short or too long search steps. Variable-metric methods, such as quasi-Newton methods (e.g., BFGS [Shanno, 1970]), learn the inverse of the Hessian of f and are able to "renormalize" the search steps. However, these algorithms often estimate the gradient using finite-difference methods, which suffer from numerical instability due to round-off errors when the condition number is large, say, larger than 10^4. Evolutionary variable-metric algorithms, such as CMA-ES [Hansen and Ostermeier, 2001], are usually more stable, because they do not need to estimate the gradient to learn an appropriate metric (e.g., CMA-ES learns the covariance matrix of successful steps, see Section 2.3.2).

Dynamic

A function $f(\boldsymbol{x},t)$ is called *dynamic*, because the objective value for a given $\boldsymbol{x}$ depends on the time-step t. It means that the function is changing in time: it may be a simple shift or rotation of the search space or any other change of f. In dynamic optimization the goal is to find the global optimum of f for a time-step t and, and in the best case, predict its location for time-steps $T > t$. However, this is often difficult to do, therefore, a less ambitious objective is considered - to track the progression of the optimum in through the space as closely as possible [Branke, 2001, Arnold and Beyer, 2002].

The dynamic version of any f usually becomes more difficult for optimization. This is especially true for the algorithms, which once make the decision about some part of the search space, exclude it forever from the later stages of the search (e.g., search space partition-based methods [Shi and Ólafsson, 2000]).

Deceptiveness

There is no clear definition of deceptive functions, a common example of deceptive function is a function, where a local optimum has much larger volume of the basin of attraction than the global optimum (a definition for binary settings can be found in [Goldberg *et al.*, 1992]). As a result, many optimizers can be misled by the local optimum and simply "do not see" the global one. This example, however, is not the best one and is rather related to the multi-modality.

It would be more fair to say that a function cannot be deceptive itself, but only with respect to a given (class of) optimization algorithm(s). A function f can be called *deceptive* for an algorithm $\mathcal{A}$, if the properties of f do not correspond to (hidden) assumptions of $\mathcal{A}$ on f *and* this leads to a bad performance of $\mathcal{A}$ on f with respect to a set of other optimizers and test problems (e.g., the rank of performance of $\mathcal{A}$ drops quickly on f). The deceptiveness is closely related to the questions of overfitting of algorithms to a given set of problem, and to No Free Lunch Theorem [Wolpert and Macready, 1997], which states that all algorithms have identically distributed performance when objective functions are

drawn uniformly at random.

Expensive

A function f is called *expensive* or *costly* if one evaluation of $f(\boldsymbol{x})$ for a given $\boldsymbol{x}$ is more costly in terms of chosen metric (time, money, etc.) than the cost of its optimization (excluding function evaluations) per function evaluation.

The optimization of expensive functions is difficult, because we are constrained by the relatively small number of function evaluations we can use. The fact that functions can be expensive in the sense described above motivates the existence of the whole field of optimization, because, otherwise, a pure random search would be probably a method of choice (the cheapest generator of $\boldsymbol{x}$ + almost free evaluations of $f(\boldsymbol{x})$).

Multi-objective

A problem is called *multi-objective* if there are m objectives $f_i(\boldsymbol{x})$ for $i = 1 \dots m$, which should be simultaneously optimized. If no specific preferences are given, the desirable output of *multi-objective optimization* is a Pareto set of optimal solutions, instead of a single solution, that is usually sufficient for single-objective optimization.

Multi-objective optimization is difficult because the multi-objective problem inherits properties of all single objectives and the optimization itself should take into account the criteria of multi-objective optimality, which are less obvious than for the *single-objective* case. We will discuss the multi-objective optimization in detail in Section 2.4.

2.3 Single-objective Continuous Evolutionary Algorithms

In this Section, we give a detailed description of Evolution Strategies and Covariance Matrix Adaptation Evolution Strategy for single-objective optimization. Despite the general name of this Section, we are biased to the discussion of ESs, mostly because their theoretical foundations are relatively well investigated [Hansen *et al.*, 2013], and they perform quite well on benchmark and real-world continuous optimization problems [Hansen *et al.*, 2010b, Hansen, 2012].

2.3.1 Evolution Strategies (ESs)

Evolution Strategies, introduced by Ingo Rechenberg and Hans-Paul Schwefel in the 1960s and 1970s [Schwefel, 1965, Rechenberg, 1973], are based on the idea of mutations of intermediate size, mainly represented by multivariate normal (Gaussian) mutations. In ESs a parent $\boldsymbol{m}^t$ of iteration/generation t generates its k-th offspring $\boldsymbol{x}_k \in \mathbb{R}^n$

$$\boldsymbol{x}_k = \mathcal{N}\big(\boldsymbol{m}, \sigma^2 \mathbf{C}\big) = \boldsymbol{m} + \sigma \cdot \mathcal{N}(\mathbf{0}, \mathbf{C}), \tag{2.6}$$

where $\mathbf{C} \in \mathbb{R}^{n \times n}$ is a (positive definite) covariance matrix and σ is a mutation step-size. The parent $\boldsymbol{m}$ also can be viewed as a mean of current mutation distribution. In each iteration of $(\mu^+_,\lambda)$-ES, λ offspring individuals are created from existing μ parent individuals. In a *plus* selection strategy, $(\mu+\lambda)$, μ best out of $\mu+\lambda$ individuals are chosen to become parents in the next generation. In a *comma* selection strategy, (μ, λ), parents never survive and $\mu < \lambda$ best offspring are chosen.

Algorithm 2.1: The (1+1)-ES with the 1/5th Rule

1: **given** $n \in \mathbb{N}_+$, $d_\sigma \approx 1 + n/3$
2: **initialize** $\boldsymbol{m}^{t=0} \in \mathbb{R}^n, \sigma^{t=0} > 0$
3: **repeat**
4: $\quad \boldsymbol{x}_1 = \boldsymbol{m}^t + \sigma^t \mathcal{N}(\mathbf{0}, \mathbf{I})$ // mutation
5: $\quad \sigma^{t+1} \leftarrow \sigma^t \exp(\frac{1}{d_\sigma}(\mathbb{E}\mathbb{1}_{f(\boldsymbol{x}_1)<f(\boldsymbol{m}^t)} - 1/5))$ // step-size update
6: $\quad$ **if** $f(\boldsymbol{x}_1) \leq f(\boldsymbol{m}^t)$ **then**
7: $\quad\quad \boldsymbol{m}^{t+1} = \boldsymbol{x}_1$ // selection of $\boldsymbol{x}_1$ as the new parent if it is better than $\boldsymbol{m}^t$
8: $\quad$ **end if**
9: $\quad t \leftarrow t + 1$
10: **until** *stopping criterion is met*

The research on ESs mainly focuses on questions of adaptation of $\mathbf{C}$ and (usually faster adaptation of) σ during the optimization, and the optimal parametrization of this adaptation. For a recent comprehensible overview of Evolution Strategies, the interested reader is referred to [Hansen *et al.*, 2013].

The 1/5th Success Rule

The 1/5th success rule is a basic step-size control strategy for randomized search, discovered in [Schumer and Steiglitz, 1968] and later, under its current name, in [Rechenberg, 1973]. Algorithm 2.1 implements (1+1)-ES with the 1/5th rule, where at iteration t a parent $\boldsymbol{m}^t$ generates an offspring $\boldsymbol{x}_1$ (line 4) with Gaussian mutation, defined by the step-size σ and an identity covariance matrix $\mathbf{C} = \mathbf{I}$. Setting the covariance matrix to the identity means that the variations of all variables are independent of each other, they are uncorrelated.

The generated offspring replaces its parent (lines 6-7) if it has at least as good fitness as its parent. The update of the mutation step-size (line 5) depends on the empirical probability that $f(\boldsymbol{x}_1) < f(\boldsymbol{m}^t)$, or in other words, $\mathbb{E}\mathbb{1}_{f(\boldsymbol{x}_1)<f(\boldsymbol{m}^t)}$. This information can be obtained from previous iterations. The target success rate 1/5 is chosen by Rechenberg [Rechenberg, 1973] after investigations of the optimal success rates of (1+1)-ES on Corridor (success rate ≈ 0.184) and Sphere (success rate ≈ 0.270) functions for $n \to \infty$.

The use of uncorrelated mutations limits the success of (1+1)-ES on non-linear functions. The preservation of the best solution (*elitism*) limits its application on multi-modal, noisy and dynamic functions.

Cumulative Step-Size Adaptation

The Cumulative Step-Size Adaptation Evolution Strategy (CSA or CSA-ES) proposed by [Hansen and Ostermeier, 1996] suggests to consider a path the population takes over a number of generations, an *evolution path*. The evolution path records the sum of consecutive successful steps to make a decision about possible corrections of the step-size. If successful steps are oriented into the same direction, they will sum up and the evolution path

Algorithm 2.2: The $(\mu/\mu_w, \lambda)$-ES with Cumulative Step-Size Adaptation

1: **given** $n \in \mathbb{N}_+$, $\lambda = 4 + 3\lfloor \ln n \rfloor$, $\mu = \lfloor \lambda/2 \rfloor$, $w_i = \frac{\ln(\mu+\frac{1}{2}) - \ln i}{\sum_{j=1}^{\mu}(\ln(\mu+\frac{1}{2}) - \ln j)}$ for $i = 1 \dots \mu$, $\mu_w = \frac{1}{\sum_{i=1}^{\mu} w_i^2}$, $c_\sigma = \frac{\mu_w + 2}{n + \mu_w + 3}$, $d_\sigma = 1 + c_\sigma + 2\max(0, \sqrt{\frac{\mu_w - 1}{n+1}} - 1)$
2: **initialize** $\boldsymbol{m}^{t=0} \in \mathbb{R}^n, \sigma^{t=0} > 0, \boldsymbol{p}_\sigma^{t=0} = \mathbf{0}$
3: **repeat**
4: **for** $k = 1, \dots, \lambda$ **do**
5: $\boldsymbol{x}_k = \boldsymbol{m}^t + \sigma^t \cdot \mathcal{N}(\mathbf{0}, \mathbf{I})$
6: $\boldsymbol{f}_k = f(\boldsymbol{x}_k)$
7: **end for**
8: $\boldsymbol{m}^{t+1} \leftarrow \sum_{i=1}^{\mu} \boldsymbol{w}_i \boldsymbol{x}_{i:\lambda}$ // the symbol $i : \lambda$ denotes i-th best individual on f
9: $\boldsymbol{p}_\sigma^{t+1} \leftarrow (1 - c_\sigma)\boldsymbol{p}_\sigma^t + \sqrt{c_\sigma(2 - c_\sigma)}\sqrt{\mu_w}\frac{\boldsymbol{m}^{t+1} - \boldsymbol{m}^t}{\sigma^t}$
10: $\sigma^{t+1} \leftarrow \sigma^t \exp(\frac{c_\sigma}{d_\sigma}(\frac{\|\boldsymbol{p}_\sigma^{t+1}\|}{\mathbb{E}\|\mathcal{N}(\mathbf{0},\mathbf{I})\|} - 1))$
11: $t \leftarrow t + 1$
12: **until** *stopping criterion is met*

will be relatively long in this direction. Since the same distance in this direction can be covered with larger steps, the step-size should be increased. If successful steps are opposite to each other, they sum up making the evolution path relatively short. In this case, the used step-size is too large and should be decreased. The *fundamental adaptation principle* of CSA is to decorrelate successfully selected mutation steps [Hansen and Ostermeier, 1996]: the adaptation should reduce the difference between the distributions of the actual evolution path and an evolution path under random selection.

Algorithm 2.2 outlines $(\mu/\mu_w, \lambda)$-ES with Cumulative Step-Size Adaptation. Initially chosen mean $\boldsymbol{m}^t$ of the mutation distribution (can be interpreted as an estimation of the optimum) is used to generate λ new solutions (lines 4-5) by adding a random uncorrelated Gaussian mutation. These λ solutions then should be evaluated on f (line 6). The old mean of the mutation distribution is stored in $\boldsymbol{m}^t$ and a new mean $\boldsymbol{m}^{t+1}$ is computed as a *weighted sum* of the best μ parent individuals selected among λ generated offspring individuals (line 8). The weights w are used to control the impact of selected individuals, weights are usually higher for better ranked individuals (line 1), but equal weights are also commonly used, leading to an $(\mu/\mu_I, \lambda)$-ES.

To update the evolution path $\boldsymbol{p}_\sigma$ using local information about a successful mutation step $\frac{\boldsymbol{m}^{t+1} - \boldsymbol{m}^t}{\sigma^t}$ (line 9), a decay/relaxation factor c_σ is used to decrease the importance of previously performed steps with time. A weight factor $c_u = \sqrt{c_\sigma(2 - c_\sigma)\mu_w}$ for the local successful step is set to normalize the variance of $\boldsymbol{p}_\sigma$ by solving the equation $1^2 = (1-c_\sigma)^2 + c_u^2$. The step-size update rule increases the step-size if the length of the evolution path $\boldsymbol{p}_\sigma$ is longer than the expected length of the evolution path under random selection $\mathbb{E}\,\|\mathcal{N}(\mathbf{0}, \mathbf{I})\|$, and decreases otherwise (line 10). Expectation of $\|\mathcal{N}(\mathbf{0}, \mathbf{I})\|$ is approximated by $\sqrt{n}(1 - \frac{1}{4n} + \frac{1}{21n^2})$. A damping parameter d_σ controls the change of the step-size.

The step-size adaptation of CSA is similar to the one of the 1/5th rule, but benefits

from using the global information stored in the evolution path. Non-elitist multi-parent selection strategy of $(\mu/\mu_w, \lambda)$-ES has many advantages over elitist (1+1)-ES (and $(1+\lambda)$-ES), it is suitable for (moderate) noisy [Arnold and Beyer, 2008] and dynamic optimization [Arnold and Beyer, 2002]. For a recent theoretical analysis of CSA on linear functions, the interested reader is referred to [Chotard *et al.*, 2012].

2.3.2 Covariance Matrix Adaptation Evolution Strategy

The Covariance Matrix Adaptation Evolution Strategy (CMA-ES) proposed by [Hansen and Ostermeier, 1996, Hansen and Ostermeier, 2001, Hansen *et al.*, 2003] has become a standard for continuous black-box evolutionary optimization. The main advantage over CSA comes from the use of correlated mutations instead of axis-parallel ones. The adaptation of the covariance matrix $\mathbf{C}$ allows to steadily learn appropriate mutation distribution and increase the probability of repeating the successful search steps.

The $(\mu/\mu_w, \lambda)$-CMA-ES is outlined in Algorithm 2.3: the original CMA-ES is recovered if set $c^- = 0$ in line 14, otherwise the pseudo-code presents a so-called weighted active CMA-ES [Hansen and Ros, 2010a].

Original CMA-ES

The procedure of the adaptation of the step-size σ in CMA-ES is inherited from CSA-ES and is controlled by $\boldsymbol{p}_\sigma$. However, it should be noted that successful steps are tracked in the space of sampling, i.e., in the isotropic coordinate system defined by principal components of $\mathbf{C}$. To find a pre-image $\boldsymbol{z}_k$ of a sampled point $\boldsymbol{x}_k$ in the space of sampling, a transform $\mathbf{C}^{t^{-\frac{1}{2}}} \frac{\boldsymbol{x}_k}{\sigma^t}$ is applied (as for $\boldsymbol{m}^{t+1} - \boldsymbol{m}^t$ in line 9), where $\mathbf{C}^{t^{-\frac{1}{2}}}$ is symmetric with positive eigenvalues such that $\mathbf{C}^{t^{-\frac{1}{2}}}\mathbf{C}^{t^{-\frac{1}{2}}}$ is the inverse of $\mathbf{C}^t$. If $\mathbf{B}\Lambda\mathbf{B}^T = \mathbf{C}$ is an eigendecomposition into an orthogonal matrix $\mathbf{B}$ and a diagonal matrix Λ, we have $\mathbf{C}^{-\frac{1}{2}} = \mathbf{B}\Lambda^{-\frac{1}{2}}\mathbf{B}^T$.

The covariance matrix update consists of two parts (line 14): rank-one update and rank-μ update. The rank-one update computes evolution path $\boldsymbol{p}_c$ of successful moves of the mean $\frac{\boldsymbol{m}^{t+1}-\boldsymbol{m}^t}{\sigma^t}$ of the mutation distribution in the given coordinate system (line 11), adapted in a similar way as for the evolution path $\boldsymbol{p}_\sigma$ of the step-size. To stall the update of $\boldsymbol{p}_c$ when σ increases rapidly, a h_σ trigger is used (line 10).

The rank-μ update computes a covariance matrix $\mathbf{C}^+$ as a weighted sum of covariances of successful steps of μ best individuals (line 12). In a similar way $\mathbf{C}^-$ is computed for μ worst individuals to be used for covariance matrix $\mathbf{C}$ update in weighted active CMA-ES. The update of $\mathbf{C}$ itself is a replace of previously accumulated information by a new one with corresponding weights of importance (line 14): c_1 for covariance matrix $\boldsymbol{p}_c^{t+1}\boldsymbol{p}_c^{t+1^T}$ of *rank-one update* [Hansen and Ostermeier, 2001], c_μ for $\mathbf{C}_\mu^+$ of *rank-μ update* [Hansen *et al.*, 2003], and c^- for $\mathbf{C}_\mu^-$ of *"active" rank-μ update* [Hansen and Ros, 2010a]. The coefficients c_1, c_μ, c^- and α_{old}^- are defined such that $c_1 + c_\mu - c^-\alpha_{old}^- \leq 1$.

The "right" parametrization of CMA-ES algorithm indeed is an open problem, most of the parameters of the algorithm were not proven mathematically to be optimal, but are chosen mostly based on algorithm designer's (including the author, Nikolaus Hansen)

Algorithm 2.3: The $(\mu/\mu_w, \lambda)$-CMA-ES

given $n \in \mathbb{N}_+$, $\lambda = 4 + \lfloor 3\ln n \rfloor$, $\mu = \lfloor \lambda/2 \rfloor$, $w_i = \frac{\ln(\mu+\frac{1}{2})-\ln i}{\sum_{j=1}^{\mu}(\ln(\mu+\frac{1}{2})-\ln j)}$ for $i = 1 \dots \mu$,
$\mu_w = \frac{1}{\sum_{i=1}^{\mu} w_i^2}$, $c_\sigma = \frac{\mu_w+2}{n+\mu_w+3}$, $d_\sigma = 1 + c_\sigma + 2\max(0, \sqrt{\frac{\mu_w-1}{n+1}} - 1)$, $c_c = \frac{4}{n+4}$,
$c_1 = \frac{2\min(1,\lambda/6)}{(n+1.3)^2+\mu_w}$, $c_\mu = \frac{2\,(\mu_w-2+1/\mu_w)}{(n+2)^2+\mu_w}$, $c^- = \frac{\mu_w}{4(n+2)^{1.5}+2\mu_w}$, $\alpha_{old}^- = 0.5$
initialize $\boldsymbol{m}^{t=0} \in \mathbb{R}^n, \sigma^{t=0} > 0, \boldsymbol{p}_\sigma^{t=0} = \mathbf{0}, \boldsymbol{p}_c^{t=0} = \mathbf{0}, \mathbf{C}^{t=0} = \mathbf{I}, t \leftarrow 0$
repeat
  for $k = 1, \dots, \lambda$ **do**
    $\boldsymbol{x}_k = \boldsymbol{m}^t + \sigma^t \times \mathcal{N}\big(\mathbf{0}, \mathbf{C}^t\big)$
    $\boldsymbol{f}_k = f(\boldsymbol{x}_k)$
  end for
  $\boldsymbol{m}^{t+1} \leftarrow \sum_{i=1}^{\mu} \boldsymbol{w}_i \boldsymbol{x}_{i:\lambda}$ // the symbol $i:\lambda$ denotes i-th best individual on f
  $\boldsymbol{p}_\sigma^{t+1} \leftarrow (1-c_\sigma)\boldsymbol{p}_\sigma^t + \sqrt{c_\sigma(2-c_\sigma)}\sqrt{\mu_w}\mathbf{C}^{t-\frac{1}{2}}\frac{\boldsymbol{m}^{t+1}-\boldsymbol{m}^t}{\sigma^t}$
  $h_\sigma = \mathbb{1}_{\|p_\sigma^{t+1}\| < \sqrt{1-(1-c_\sigma)^{2(t+1)}}(1.4+\frac{2}{n+1})\,\mathbb{E}\|\mathcal{N}(\mathbf{0},\mathbf{I})\|}$
  $\boldsymbol{p}_c^{t+1} \leftarrow (1-c_c)\boldsymbol{p}_c^t + h_\sigma\sqrt{c_c(2-c_c)}\sqrt{\mu_w}\frac{\boldsymbol{m}^{t+1}-\boldsymbol{m}^t}{\sigma^t}$
  $\mathbf{C}_\mu^+ = \sum_{i=1}^{\mu} w_i \frac{\boldsymbol{x}_{i:\lambda}-\boldsymbol{m}^t}{\sigma^t} \times \frac{(\boldsymbol{x}_{i:\lambda}-\boldsymbol{m}^t)^T}{\sigma^t}$
  $\mathbf{C}_\mu^- = \sum_{i=0}^{\mu-1} w_{i+1}\boldsymbol{y}_{\lambda-i:\lambda}\boldsymbol{y}_{\lambda-i:\lambda}^T$ with $\boldsymbol{y}_{\lambda-i:\lambda} = \frac{\left\| C^{t-1/2}(\boldsymbol{x}_{\lambda-\mu+1+i:\lambda}-\boldsymbol{m}^t)\right\|}{\left\| C^{t-1/2}(\boldsymbol{x}_{\lambda-i:\lambda}-\boldsymbol{m}^t)\right\|} \times \frac{\boldsymbol{x}_{\lambda-i:\lambda}-\boldsymbol{m}^t}{\sigma^t}$
  $\mathbf{C}^{t+1} = (1-c_1-c_\mu+c^-\alpha_{old}^-)\mathbf{C}^t + c_1 \underbrace{\boldsymbol{p}_c^{t+1}\boldsymbol{p}_c^{t+1^T}}_{\text{rank-one update}} + (c_\mu + c^-(1-\alpha_{old}^-))\underbrace{\mathbf{C}_\mu^+}_{\text{rank-}\mu\text{ update}} - \underbrace{c^-\mathbf{C}_\mu^-}_{\text{"}active\text{"}}$
  $\sigma^{t+1} \leftarrow \sigma^t \exp(\frac{c_\sigma}{d_\sigma}(\frac{\|\boldsymbol{p}_\sigma^{t+1}\|}{\mathbb{E}\|\mathcal{N}(\mathbf{0},\mathbf{I})\|} - 1))$
  $t \leftarrow t+1$
until *stopping criterion is met*

views on robustness of the CMA-ES. This relative robustness is also supported by empirical observations of CMA-ES performance on a few benchmark problems, such as Sphere function and rotated Ellipsoid function.

Weighted active CMA-ES

In the original CMA-ES only best μ out of λ individuals are used to estimate the local covariance matrix of successful steps to increase the probability of successful samples in the next iteration. The information about the remaining (worst $\lambda - \mu$) solutions is used only implicitly during the selection process.

In active $(\mu/\mu_I, \lambda)$-CMA-ES however, it has been shown that the worst solutions can be exploited to reduce the variance of the mutation distribution in unpromising directions [Jastrebski and Arnold, 2006], yielding a performance gain of up to a factor 2 for the active $(\mu/\mu_I, \lambda)$-CMA-ES with no loss of performance on any of tested functions. A recent extension of the $(\mu/\mu_w, \lambda)$-CMA-ES, *weighted* active CMA-ES [Hansen and Ros, 2010a]

(referred to as aCMA-ES for brevity) shows comparable improvements on a set of noiseless and noisy functions from the BBOB benchmark suite [Hansen *et al.*, 2010a]. In counterpart, aCMA-ES no longer guarantees the covariance matrix to be positive definite, possibly resulting in algorithmic instability. The instability issues can however be numerically controlled during the search; as a matter of fact they are never observed during the benchmarking on the BBOB test suite.

The main novelty of aCMA-ES is the exploitation of the worst solutions to compute $\mathbf{C}_\mu^- = \sum_{i=0}^{\mu-1} w_{i+1} \boldsymbol{y}_{\lambda-i:\lambda} \boldsymbol{y}_{\lambda-i:\lambda}^T$ (line 13), where $\boldsymbol{y}_{\lambda-i:\lambda} = \frac{\left\| \mathbf{C}^{t-1/2}(\boldsymbol{x}_{\lambda-\mu+1+i:\lambda} - \boldsymbol{m}^t) \right\|}{\left\| \mathbf{C}^{t-1/2}(\boldsymbol{x}_{\lambda-i:\lambda} - \boldsymbol{m}^t) \right\|} \times \frac{\boldsymbol{x}_{\lambda-i:\lambda} - \boldsymbol{m}^t}{\sigma^t}$. The covariance matrix estimation of these worst solutions is used to decrease the variance of the mutation distribution along these directions (line 14).

For a more detailed description of the original and active CMA-ES algorithms, the interested reader is referred to [Hansen *et al.*, 2003] and [Hansen and Ros, 2010a], respectively.

CMA-ES with restarts

There are several properties of black-box problems which may lead to a premature convergence of CMA-ES, among the most common are multi-modality and uncertainty. To increase the probability of finding the global optima, IPOP-CMA-ES [Auger and Hansen, 2005] and BIPOP-CMA-ES [Hansen, 2009] restart strategies for CMA-ES were proposed. In IPOP-CMA-ES, CMA-ES is restarted with double the population size each time the stopping criterion is met. BIPOP-CMA-ES has two regimes: one with large population, whose size doubles at each restart and one with small population, whose size is randomly chosen each restart. CMA-ES restarts under the first and the second regimes sequentially, such that two regimes have almost the same budget of function evaluations used so far. We will discuss these strategies in detail and propose two new alternative restart strategies in Section 6.3.3.

Natural Evolution Strategies

Natural Evolution Strategies (NES [Wierstra *et al.*, 2008]) is a "hot" topic in EC community. NES showed the attractiveness of the *natural gradient* as a general means to derive CMA-like optimization algorithms from the first principles. Natural gradient, first introduced by [Amari, 1998], has several advantages over plain gradient, it allows an algorithm to be invariant w.r.t. orthogonal transformations of the search space and an order-preserved transformations of the objective function. Let the vector θ represents all parameters used to define a sampling distribution for new offspring in the search space, then the natural gradient can be used to estimate an ascent in the θ-space toward higher expected fitness, i.e., the ascent in the original x-space and in the space of the algorithm parameters. If θ represents mean and covariance matrix of the multivariate normal distribution, a rank-μ CMA-like optimization algorithm can be recovered.

In this thesis, we do not use NES algorithms, while being elegant they are usually outperformed by CMA-ES algorithms and the most powerful versions of NES resembles CMA-ES. However, there are several very interesting features discovered for NES in the first

PhD thesis on the subject [Schaul, 2011]: hyper-parameters adaptation through *adaptive sampling* and reuse of already sampled individuals through *importance mixing*. Another interesting study of natural gradient-based optimization is the Information-Geometric Optimization (IGO) framework proposed in [Arnold *et al.*, 2011].

2.3.3 Why CMA-ES? Empirical Comparison with other Approaches

In this thesis, we intensively use CMA-ES as a baseline optimization algorithm for comparison and as a starting point to further improve optimization techniques in single- and multi-objective scenario (Section 2.4). It is used both in exploitation (Chapter 4 and Chapter 5) and exploration (Chapter 6) parts of this thesis, and in this Section, we present some arguments to convince the reader that the CMA-ES is a good candidate optimization algorithm.

Invariance properties of CMA-ES

The importance of invariances in science has long been acknowledged. In Computer Science in particular, the invariance of an algorithm with respect to a given transformation of the problem domain is a source of robustness, as any theoretical or empirical result that is demonstrated for a given problem instance can be extended to the whole class of problems obtained by applying the transformation. For instance, many bio-inspired optimization algorithms such as tournament-based EAs, PSO, or DE only rely on comparisons of the fitness function, making them invariant under any monotonous transformation of the fitness. From a theoretical perspective, this invariance property is a source of robustness [Gelly *et al.*, 2007]; from an algorithmic perspective, it removes the need to tune the algorithm hyper-parameters according to some (generally unknown) scale of the fitness function.

CMA-ES exhibits the following invariances:

- Invariance against rank-preserving transformation of f: if we apply a strictly increasing function $g : \mathbb{R} \mapsto \mathbb{R}$ to f, the optimization of f and $g \circ f$ is indifferent whether we minimize, e.g., f, f^3 or $f \times |f|^2$. As well as in all comparison-based optimization algorithms, the algorithm only depends on *the ranking* of function values (see Algorithm 2.3, line 8). Therefore it is as "easy" to optimize some non-convex or non-smooth functions as well as convex ones (it is also true for all comparison-based optimization algorithms).

- Invariance against angle preserving transformation of the search space (rotation, reflection, translation) if the initial search point(s) are transformed accordingly.

- Scale invariance if the initial scaling, e.g., σ^0, and the initial search point(s) are chosen accordingly.

The key invariance property which contributes the most into the good performance of the CMA-ES is invariance with respect to the rotation of the search space. Most of

Evolutionary Algorithms lack of this property and are therefore outperformed by CMA-ES on problems, where the algorithm may benefit from the learning of correlations between the variables, e.g., on non-separable problems [Hansen *et al.*, 2011]. Another important property of the CMA-ES is that it is almost parameter-less algorithm, and there is virtually only one parameter suggested to be tuned by the user - population size λ. Even for this parameter there is a default value, which depends on the problem dimension n and is "well-tuned" for unimodal functions (see also [Smit and Eiben, 2010] for offline parameter tuning of CMA-ES).

Performance on BBOB framework.

The number of function evaluations used to find a target function value f_{target} is a common metric, adopted from the very beginning of the field [Schumer and Steiglitz, 1968, Rechenberg, 1973] for "greedy" evaluation and comparison of EAs. The first International Contest on Evolutionary Optimization (1st ICEO) organized during the International Conference on Evolutionary Computation (ICEC) in 1996 was probably the first attempt to compare different continuous optimizers on a set of benchmark problem in a regime of competition. Differential Evolution managed to finish 3rd among 8 algorithms and after two non-evolutionary optimizers (one exploited function separability), this result definitely boosted the popularity of DE. [Bersini *et al.*, 1996] summarizes the results of the competition and presents a *brilliant argumentation* why organization of such competitions is important. We are agree with the vast majority of these arguments, which have become even more relevant in the last decade.

A more recent competition of optimizers, Congress on Evolutionary Computation 2005 - Session on Real-Parameter Optimization (CEC-2005), provided a more rigorous investigation of performance of 11 Evolutionary Algorithms on 25 unimodal and multi-modal 10- and 30-dimensional benchmark problems [Suganthan *et al.*, 2005]. A fitness-distance analysis of functions landscapes is given in [Müller and Sbalzarini, 2011]. Figure 2.1 from [Hansen, 2006] shows a comparative performance of 11 tested algorithms, including G-CMA-ES (a version of IPOP-CMA-ES [Auger and Hansen, 2005]). The higher the curve on the graph, the better the algorithm performs. For a given algorithm a value on axis-x (x-value) can be interpreted as a loss factor FEs/FEs$_{best}$ of number of function evaluations the algorithm has on (1 - (y-value))·100% of tested benchmark problems.

A relatively good performance of G-CMA-ES on CEC-2005 testbed attracted a lot of attention and in a long term has made CMA-ES "an algorithm to compare with". It has become a standard tool for real-world problem optimization, it also has more than one hundred real-world applications [Hansen, 2012] which can be considered as an empirical validation of its robustness. A detailed statistical analysis of the results of CEC-2005 contest is presented in [García *et al.*, 2009].

COmparing Continuous Optimizers (COCO [Finck *et al.*, 2010]) is a recent and quite successful platform to quantify and compare the performance of optimization algorithms in a scientifically decent and rigorous way. COCO provides means to run an optimization algorithm on a set of benchmark optimization problems, stores the information about evaluated points, post-processes the obtained information and, finally, prepares tables and

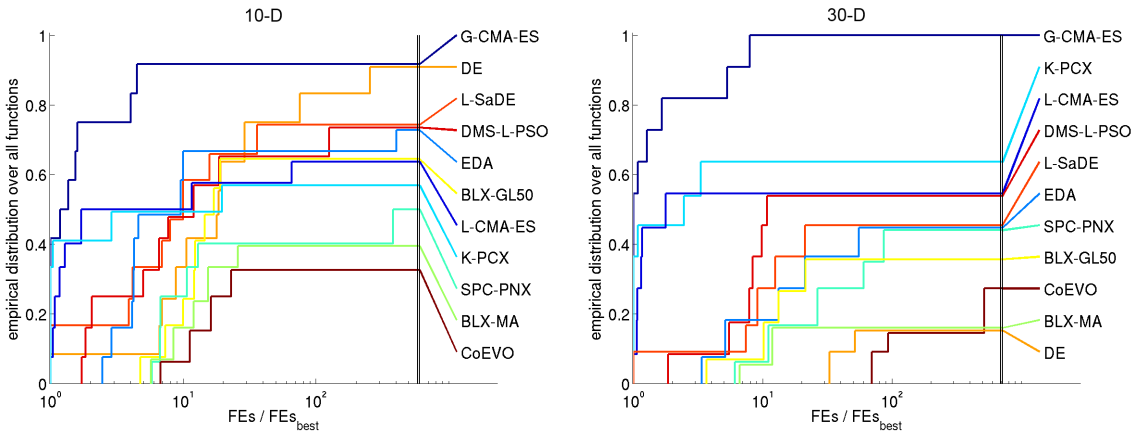

Figure 2.1: The graphs show the empirical cumulative distribution function of $\mathrm{FEs}/\mathrm{FEs}_{best}$ over different sets of function in dimension 10 (Left) and 30 (Right) for 11 tested Evolutionary Algorithms during the CEC-2005 optimization contest. FEs and FEs_{best} denote the expected number of function evaluations to reach the target function value by a given and the best performed algorithm, respectively. Large values of the graphs (the cumulative distribution function) are preferable, they correspond to smaller values of $\mathrm{FEs}/\mathrm{FEs}_{best}$.

figures to analyze the performance of the algorithm itself and in comparison with a set of already benchmarked algorithms. COCO has been used for the Black-Box-Optimization-Benchmarking (**BBOB** [Finck *et al.*, 2010]) workshops that took place during the Genetic and Evolutionary Computation Conference (GECCO) in 2009, 2010 and 2012.

BBOB provides 24 noise-less [Hansen *et al.*, 2009a] and 30 noisy [Hansen *et al.*, 2009b] benchmark problems with different properties: separable, non-separable, unimodal, multimodal, ill-conditioned, deceptive, functions with and without/weak global structure. All functions are defined and can be evaluated over $\mathbb{R}^n$, while the actual search domain is given as $[-5, 5]^n$. For the majority of functions the global optimum $\boldsymbol{x}^{opt}$ is *randomly drawn uniformly* in $[-4, 4]^n$. To derive non-separable functions from separable ones and to control the conditioning of the function, linear transformations are applied. Addition non-linear and symmetry breaking transformations are applied to a portion of $1/2^n$ of the search space to make some relatively simple functions less regular. All functions are defined for $n = 2, 3, 5, 10, 20$ (and $n = 40$ which is optional). The goal of optimization of function f is to reach $f_{target} = f_{opt} + \Delta f$ ($\Delta f = 10^{-8}$) function value using as few function evaluations as possible. The optimum function value f_{opt} is shifted in f-space and is different for each function. As an input for optimization of function f, only problem dimension n and the initial range for decision variables are provided. To collect "sufficient" amount of data and make statistical analyses of results more meaningful, 15 trials/runs of the benchmarked algorithm should be conducted on different instances of function f.

If an algorithm succeed to reach a target precision value $\Delta f_t = f_{target} - f_{opt}$ in a single run, then its *runtime* (RT) is the number of function evaluations used. If the algorithm fails, it can be restarted and run again. The Expected Running Time (ERT), the expected

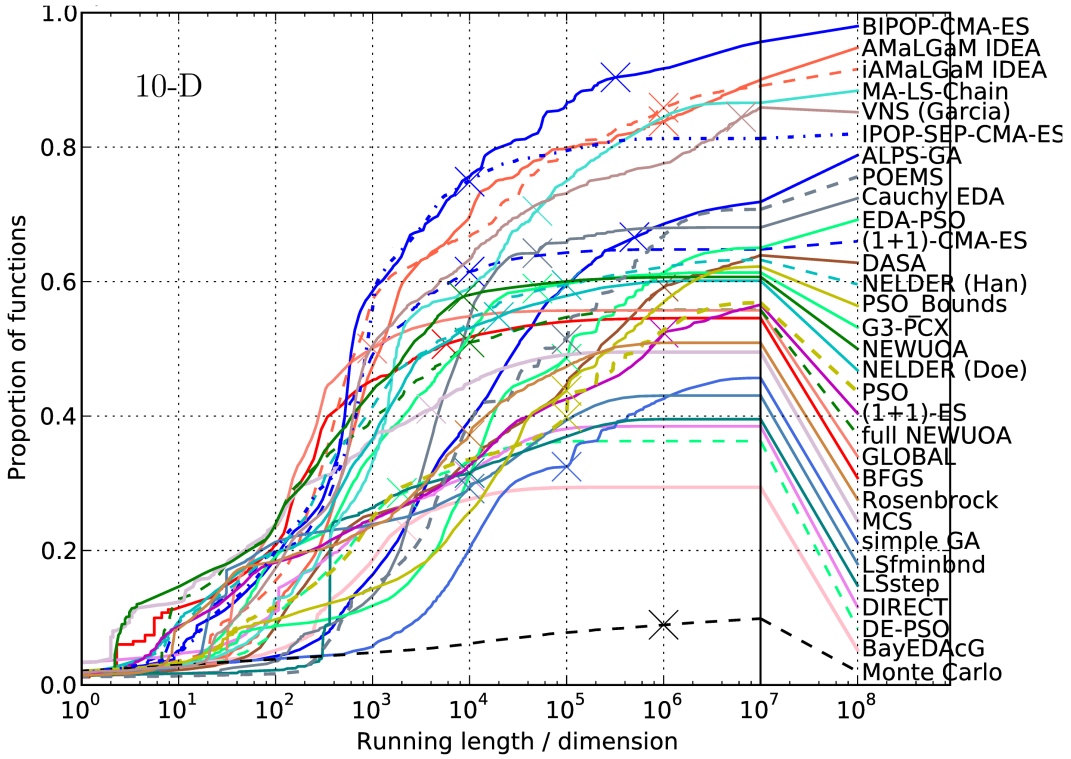

Figure 2.2: Empirical runtime distributions (runtime in number of function evaluations divided by dimension) on all noise-less functions of BBOB-2009 with $f_t \in [100, 10^8]$ in dimension **10**. See text for details.

number of function evaluations to reach a target function value for the first time is used for performance assessment. The ERT is computed as follows [Finck *et al.*, 2010]:

$$\mathrm{ERT}(f_{target}) = \frac{\#\mathrm{FEs}(f_{best} \geq f_{target})}{\#\mathrm{succ}}, \tag{2.7}$$

where the $\#\mathrm{FEs}(f_{best} \geq f_{target})$ is the number of function evaluations conducted in all trials, while the best function value was not smaller than f_{target} during the trial. The #succ is the number of successful trials.

To summarize the results from a set of benchmark problems Empirical Cumulative Distribution Functions (ECDFs) are used. The ECDF function $F : \mathbb{R} \mapsto [0, 1]$ is defined for a given set of real-valued data S, such that $F(x)$ equals the fraction of elements in S which are smaller than x. The function F is monotonous and a lossless representation of the (unordered) set S [Finck *et al.*, 2010].

Each graph in Figure 2.2 depicts the empirical cumulative distribution of RT of the annotated algorithm from BBOB-2009 on all noise-less functions $f_1 - f_{24}$ in dimension 10 [Hansen *et al.*, 2010b]. For each function-Δf_t-pair, 100 instances (problems) of RT are

generated, where each Δf_t is in $\left\{10^{1.8}, 10^{1.6}, 10^{1.4}, \ldots, 10^{-8}\right\}$, i.e., $\Delta f_t \in]10^2, 10^{-8}]$. Any given (x-value) in Figure 2.2 indicates a budget of function evaluations used, divided by dimension, to solve a given (y-value) proportion of problems (function-Δf_t-pairs). The graphs are monotonous by definition. Crosses indicate the maximum number of function evaluations observed for the respective algorithm. Results to the right of a cross are bootstrapped and are only comparable between algorithms with similar maximum number of function evaluations. The limit value to the right indicates the ratio of solved problems. The horizontal distance between graphs represents a difference in runtime for solving the same proportion of problems. The area between two graphs, up to a given y-value, is the average runtime difference (averaged on the log scale), arguably the most useful aggregated performance measure. The best algorithm covers the largest area under its graph [Hansen *et al.*, 2010b].

Figure 2.2 clearly shows that all benchmarked algorithms outperform Monte Carlo search method in a long run, for most of the algorithms the difference becomes significant already after $10^1 n$ function evaluations. BIPOP-CMA-ES outperforms all other algorithms after about $10^3 n$ function evaluations. It should be noted, that the most difficult function-Δf_t problems correspond to multi-modal functions and are located above the line of 0.6 (60% of problems solved) on y-axis. The performance of BIPOP-CMA-ES above this line, i.e., on multi-modal functions, can be explained by restart strategies used to increase the probability of finding the global optimum. The BIPOP restart scheme also outperforms IPOP scheme (see IPOP-SEP-CMA-ES) on the most difficult multi-modal functions. All BBOB-2009 algorithms with good performance on multi-modal functions strongly resemble CMA-ES (AMaLGaM IDEA, iAMaLGaM IDEA) or use CMA-ES as a local search (MA-LS-Chain, VNS).

The (1+1)-CMA-ES is a CMA version of (1+1)-ES presented by [Igel *et al.*, 2006]. The elitist (1+1) selection scheme tends to work well on unimodal functions, but suffers from premature convergence on multi-modal functions. State-of-the-art optimization algorithms from non-evolutionary community, derivative-free NEWUOA [Powell, 2006], quasi-Newton BFGS [Shanno, 1970] and GLOBAL method (clustering with local search using BFGS or Nelder-Mead [Pal *et al.*, 2012]), are very competitive with (1+1) CMA-ES algorithm on unimodal functions, but are outperformed by BIPOP-CMA-ES on multi-modal ones. However, these "classical" algorithms are not invariant to linear transformation of the objective function, that may be viewed as a potential drawback. Nevertheless as well as CMA-ES, they clearly **outperform** other Evolutionary Algorithms (PSO, GA, EDA-PSO, DE-PSO, G3-PCX) at least **by one order of magnitude** (this depends on n and functions discussed) in terms of ERT. *These observations motivated the exploitation ("greedy") part of this thesis, which consists of improving CMA-ES on unimodal functions, such that the "domination" of CMA-ES over "classical" approaches becomes obvious not only on difficult multi-modal and noisy functions, but also on "easy" unimodal functions.*

Limitations of CMA-ES.

While being a robust black-box optimizer, CMA-ES also has several limitations:

- **Space complexity**. CMA-ES adapts $\frac{n^2+n}{2}$ parameters in the covariance matrix

during the search. For large n, the storing of a single matrix with n^2 real-valued elements becomes intractable. On a typical PC this limitation is achieved for $n \approx 10^4$.

- **Time complexity**. CMA-ES performs eigendecomposition $\mathbf{B}\Lambda\mathbf{B}^T = \mathbf{C}$ of the covariance matrix, this procedure has a complexity of n^3, but can be postponed until after $n/10$ generations. Finally, the computational complexity scales between 10^{-8} and $10^{-7} \times n^2$ [Hansen, 2009], i.e., about 10-100ms per function evaluation for $n = 1000$, that can be considered to be too expensive for computationally *very cheap* functions.

- **Premature convergence**. With no surprise the algorithm may prematurely convergence to a local optimum on multi-modal functions. Surprisingly, a class of unimodal functions called HappyCat was found recently, where CMA-ES fails to find the minimizer [Beyer and Finck, 2012]. The behavior of CMA-ES on this class of problems is similar to the one observed when evolving at the edge of feasibility of constraint problems, where step-length control may fail because the mutation strength decreases exponentially fast such that the CMA-ES is not able to learn the covariance matrix [Beyer and Finck, 2012].

- **Large number of function evaluations required to find an optimum**. This can be viewed as general remark for all optimization algorithms, but becomes a less abstract limitation, when dealing with expensive optimization problems. Chapter 3 will address this limitation.

To address the above-described limitations of time and space complexities, several versions of CMA-ES with smaller than $\frac{n^2+n}{2}$ control parameters have been proposed. A recent baseline in this direction is IPOP-SEP-CMA-ES, also called separable IPOP-CMA-ES, with only n degrees of freedom [Ros and Hansen, 2008]. The algorithm has linear in n time and space complexity and, therefore, is suitable for large scale optimization, performing reasonably well on non-trivial optimization problems [Ros and Hansen, 2008].

The reasons of premature convergence of CMA-ES is an open question, which probably will become clearer by studying alternative variants of *online* parameter control in CMA-ES. For example, for the case of HappyCat problems, the effect of premature convergence can be reduced if a larger population size λ is used.

2.4 Multi-objective Evolutionary Algorithms

In this Section, we briefly describe the main concepts of multi-objective search and discuss reasons that make it difficult. Then we recall the history of Multi-objective Evolutionary Algorithms (MOEAs) and, finally, present Non-dominated Sorting Genetic Algorithm II (NSGA-II) and Multi-objective Evolutionary Algorithm (MO-CMA-ES), which will be used later in this study (see Chapter 5 and Section 6.2).

2.4.1 Main Concepts of Multi-objective Optimization

The optimization of the problem with 2 or more (often conflicting) objectives is called *multi-objective optimization*. The multi-objective problem is usually difficult to solve, because it inherits properties of individual objectives. Let us consider more formally, *without loss of generality*, a multi-objective *minimization* problem with n decision variables (parameters) and m objectives:

$$\begin{array}{ll} Minimize & \boldsymbol{y} = f(\boldsymbol{x}) = (f_1(\boldsymbol{x}), \ldots, f_m(\boldsymbol{x})) \\ where & \boldsymbol{x} = (x_1, \ldots, x_n) \in X \\ & \boldsymbol{y} = (y_1, \ldots, y_m) \in Y \end{array} \tag{2.8}$$

and where $\boldsymbol{x}$ is called the *decision vector*, X is the *decision (parameter) space*, $\boldsymbol{y}$ is the *objective vector*, and Y is the *objective space*. The multi-objective problem (MOP) may have constraints, in this case X should be defined as the *feasible decision space.*

Definition 1. (**Pareto dominance of vectors**). The objective vector $\boldsymbol{y}^1$ *dominates* the objective vector $\boldsymbol{y}^2$ $(\boldsymbol{y}^1 \prec \boldsymbol{y}^2) \overset{def}{\Longleftrightarrow} \Big(\boldsymbol{y}^1_j \leq \boldsymbol{y}^2_j$ for all $j \in \{1, \ldots, m\}$ and $\boldsymbol{y}^1_k < \boldsymbol{y}^2_k$ for at least one $k \in \{1, \ldots, m\}\Big)$.

Definition 2. (**Weak Pareto dominance of vectors**). The objective vector $\boldsymbol{y}^1$ *weakly dominates* the objective vector $\boldsymbol{y}^2$ $(\boldsymbol{y}^1 \preceq \boldsymbol{y}^2) \overset{def}{\Longleftrightarrow} \Big(\boldsymbol{y}^1_j \leq \boldsymbol{y}^2_j$ for all $j \in \{1, \ldots, m\}\Big)$.

Definition 3. (**Strict Pareto dominance of vectors**). The objective vector $\boldsymbol{y}^1$ *strictly dominates* the objective vector $\boldsymbol{y}^2$ $(\boldsymbol{y}^1 \prec\prec \boldsymbol{y}^2) \overset{def}{\Longleftrightarrow} \Big(\boldsymbol{y}^1_j < \boldsymbol{y}^2_j$ for all $j \in \{1, \ldots, m\}\Big)$.

Definition 4. (**Incomparability of vectors**). The objective vectors $\boldsymbol{y}^1$ and $\boldsymbol{y}^2$ are *incomparable* $(\boldsymbol{y}^1 \parallel \boldsymbol{y}^2) \overset{def}{\Longleftrightarrow} \big(\boldsymbol{y}^1 \not\preceq \boldsymbol{y}^2$ and $\boldsymbol{y}^2 \not\preceq \boldsymbol{y}^1\big)$.

Definition 5. (**Pareto Optimality of vectors**). The solution $\boldsymbol{x}^*$ and its corresponding objective vector $y^* = f(\boldsymbol{x}^*)$ are Pareto optimal $\overset{def}{\Longleftrightarrow}$ (there exists no $y \in Y$ such that $y \prec y^*$).

Definition 6. (**Approximation set/front**). Let $\mathcal{Y} \subseteq Y$ be a set of objective vectors. $\mathcal{Y}$ is called *approximation set* or *non-dominated set/front* or *Pareto front approximation* $\overset{def}{\Longleftrightarrow}$ (any vector of $\mathcal{Y}$ does not weakly dominate any other vector in $\mathcal{Y}$). Let denote Ω as a set of all approximation sets. Vectors of the non-dominated set/front are called *non-dominated vectors*.

Definition 7. (**Optimal Pareto set/front**). *Optimal Pareto set/front* is an approximation set of optimal Pareto solutions $\boldsymbol{x}^*$ and corresponding vectors $\boldsymbol{y}^*$.

Definition 8. (**Better set/front**). An approximation set A is better than an approximation set B $(A \rhd B) \overset{def}{\Longleftrightarrow} \big($ every $\boldsymbol{y} \in B$ is weakly dominated by at least one $\boldsymbol{y}^1 \in A$ and $A \neq B\big)$.

All dominance relations defined above for vectors are easily extendable for sets of vectors/solutions, by changing relations between variables to relations between vectors.

Performance Assessment

In order to compare the performance of two optimizers, one can run them to *minimize* some function f and depending on the output one can say which one performs better on this particular function. If f is a single-objective function, then this comparison is quite straightforward: the algorithm which usually (according to some statistical test on several runs) finds *better* solutions (smaller value of f) has a better performance on f. If f is a multi-objective function, the definition of the relation *better* is now more complicated, because the solution of (unimodal) multi-objective problem is not just one point, but a set of Pareto points. The relation *better* is defined by Definition 8 [Knowles *et al.*, 2006]. The problem arises when two sets are incomparable, but one needs to distinguish between them and find the more preferable one. It is usually difficult to define this preference criterion, because in multi-objective optimization two objectives are usually considered: i). minimize the distance to the optimal Pareto front; ii). maximize the diversity within the optimal Pareto set approximation. The problem of incomparability becomes even more serious as the number of objectives m increases [Deb *et al.*, 2001].

To compare output sets of multi-objective optimizers we will follow a widely accepted procedure suggested by [Zitzler *et al.*, 2002b, Knowles *et al.*, 2006] and use *Quality Indicators*.

Quality Indicators

The underlying idea of quality indicators is to quantify differences between approximation sets, by applying common mathematical metrics. Thus, even for incomparable approximation sets one can say which one is better w.r.t. a given quality indicator.

Definition 9. (**Unary quality indicator**). A *unary quality indicator* is a function $I : \Omega \to \mathbb{R}$, which assigns a real value to any approximation set $\mathcal{Y} \in \Omega$.

It is important to note that there exists no unary quality measure that is able to indicate whether a Pareto set approximation $\mathcal{Y}_1$ is better than a Pareto set approximation $\mathcal{Y}_2$ [Zitzler *et al.*, 2002b]. A better quality according to unary indicator in the best case can guarantee that $\mathcal{Y}_1$ is not worse than $\mathcal{Y}_2$, i.e., incomparable or better.

Definition 10. (**Binary quality indicator**). A *binary quality indicator* is a function $I : \Omega \times \Omega \to \mathbb{R}$, which assigns a real value to any pair of approximation sets $(\mathcal{Y}_1, \mathcal{Y}_2) \in \Omega \times \Omega$.

Properly designed binary quality indicators, in contrast to unary ones, are capable to indicate whether $\mathcal{Y}_1$ is better than $\mathcal{Y}_2$.

Definition 11. (**Pareto-compliant indicator**). The indicator $I : \Omega \to \mathbb{R}$ is *Pareto-compliant* $\overset{def}{\Longleftrightarrow}$ for every pair of approximation sets $\mathcal{Y}_1$ and $\mathcal{Y}_2$, for which $\mathcal{Y}_1 \preceq \mathcal{Y}_2$, $I(\mathcal{Y}_1)$ is not worse than $I(\mathcal{Y}_1)$.

The quality indicator is Pareto-compliant if it does not contradict the order induced by the Pareto-dominance relations. Many popular quality indicators are Pareto non-compliant (generational distance (GD), inverted generational distance (IGD), spread, coverage, etc. [Zitzler *et al.*, 2002b]), i.e., better quality of $\mathcal{Y}_1$ than of $\mathcal{Y}_2$ is possible even if $\mathcal{Y}_2 \prec \mathcal{Y}_1$. The use of such Pareto non-compliant quality indicators may mislead the performance assessment procedure. Detailed descriptions of other Pareto compliant indicators, In this thesis, we study multi-objective optimization algorithms using the Pareto-compliant *hypervolume indicator*. such as ϵ-indicator and $R2$ indicator are given in [Zitzler and Künzli, 2004] and [Brockhoff *et al.*, 2012], respectively.

Pareto Ranking

The Pareto ranks w.r.t. $A \subseteq Y$ of the points in A are iteratively determined. All non-dominated points in A (denoted $ndom_1(A)$ or simply $ndom(A)$), are given rank 1. The set $ndom(A)$ is then removed from A; from this reduced set, the non-dominated points (denoted $ndom_2(A)$) are given rank 2; the process continues until all points of A have received a Pareto rank. The Pareto rank of point $\boldsymbol{a} \in A$ is denoted $PR(\boldsymbol{a}, A)$. The sorting of points w.r.t. Pareto ranking criterion is called *non-dominated sorting* [Goldberg, 1989, Deb *et al.*, 2000].

Hypervolume Indicator

The *hypervolume* of a set of points A is sometimes also called "S-Metric" [Zitzler and Thiele, 1998]. Let $\boldsymbol{a}_{ref}$ denote a reference point, dominated by all points in A. The hypervolume of A is then the *volume* of the union of the hypercubes defined by one point of the set and $\boldsymbol{a}_{ref}$. Formally,

$$H(A) = Volume(\bigcup_{i=1}^{i=m} Rect(\boldsymbol{a}_i, \boldsymbol{a}_{ref})),$$

where $Rect(\boldsymbol{a}, \boldsymbol{b})$ is the hyper-rectangle whose diagonal is the segment $[\boldsymbol{ab}]$. It is clear that only the non-dominated points in A contribute to the hypervolume.

The *hypervolume contribution* of some non-dominated point $\boldsymbol{a}$ is defined as the difference between the hypervolume of the whole set A and that of the set from which $\boldsymbol{a}$ has been removed:

$$\Delta H(\boldsymbol{a}, A) = H(A) - H(A \backslash \{\boldsymbol{a}\})$$

Survival Selection

In multi-objective Evolutionary Algorithms μ parent individuals generate λ offspring. Since the population size is usually bounded, the question of *survival selection* of μ most promising / best individuals among $\lambda + \mu$ ones often arises. A common approach is to sort individuals / vectors of a set X with respect to a total preorder relation $\prec_X$. This relation is often based on two sorting criteria / quality indicators: i). a Pareto dominance-based indicator such as Pareto Ranking or Strength Pareto approach [Zitzler *et al.*, 2002a]; ii). a crowding-distance measure in NSGA-II [Deb *et al.*, 2000], distance to k-th nearest neigh-

bor in SPEA2 [Zitzler *et al.*, 2002a], hypervolume in SMS-EMOA [Emmerich *et al.*, 2005] and MO-CMA-ES [Igel *et al.*, 2007b]. Formally, $\prec_X$ is defined as follows:

$$\begin{aligned} x \prec_X \boldsymbol{y} \Leftrightarrow & I_1(\boldsymbol{x}, X) < I_1(\boldsymbol{y}, X) // \textit{ better dominance-based quality} \\ & \text{or} // \textit{ same dominance-based quality and better second sorting quality} \\ & I_1(\boldsymbol{x}, X) = I_1(\boldsymbol{y}, X) \text{ and } I_2(\boldsymbol{x}, X) > I_2(\boldsymbol{y}, X) \end{aligned} \tag{2.9}$$

The $\prec_X$ relation can be defined by a binary quality indicator, e.g., the one where the fitness of an individual $\boldsymbol{x}$ is associated with a "loss in quality" if $\boldsymbol{x}$ is removed from the population [Zitzler and Künzli, 2004].

2.4.2 Multiple Approaches to Multi-objective Optimization

The finding of solution(s) of multi-objective problems usually follows either the preference-based principle or the ideal principle [Deb and Kalyanmoy, 2001, Tusar, 2007], illustrated in Figure 2.3.

Following the *preference-based principle* (see Figure 2.3-Left), the multi-objective problem $f(\boldsymbol{x})$ is reformulated into a (series of) single-objective problem(s) $g(\boldsymbol{x})$ using some *preference* and/or *a priori* information about $f(\boldsymbol{x})$, e.g., the weights used for a weighted aggregation $g(\boldsymbol{x}) = \sum_{i=1}^{m} w_i f_i(\boldsymbol{x})$. The main advantage of the preference-based principle is that the solution of the multi-objective problem $f(\boldsymbol{x})$, reformulated as $g(\boldsymbol{x})$, can be found using one of many available single-objective optimizers. This fact made many preference-based "classical" optimization methods very popular in the 1960s-1990s: i). weighted sum methods with the aggregation as the one described above [Zadeh, 1963]; ii). ϵ-constraint method, where only one objective function is minimized, while other are ϵ upper-constrained [Marglin, 1967]; iii). goal programming techniques, where usually simplex method or linear programming is used to satisfy Decision Maker's goals and priorities [Charnes and Cooper, 1961, Tamiz *et al.*, 1998]. Some of these methods have several disadvantages: i). uniformly chosen weight vectors does not lead to a uniform set of Pareto-optimal solutions (e.g., in the weighted sum method); ii). non-convex parts of the Pareto front cannot be found (e.g., in the weighted sum method); iii). the results are very parameter-sensitive (e.g., in the ϵ-constraint method). The main disadvantage of the preference-based principle is that it usually provides only *one* solution of the multi-objective problem.

The *ideal principle* suggests to first find *all* Pareto-optimal solutions of the multi-objective problem (see Figure 2.3-Right), then choose one or several solutions taking into account the preference information. The method is ideal in the sense that it does not require any additional preference information to be given before the optimization. Thus, the preference-based choice of solutions is made with the complete information about the optimal Pareto front (or its approximation) found after the optimization. In practice we usually bound the maximum number of the Pareto-optimal solutions we are interested in.

Most multi-objective Evolutionary Algorithms (MOEAs) follow the ideal principle, while preference-based MOEAs also attract attention in the field. A promising

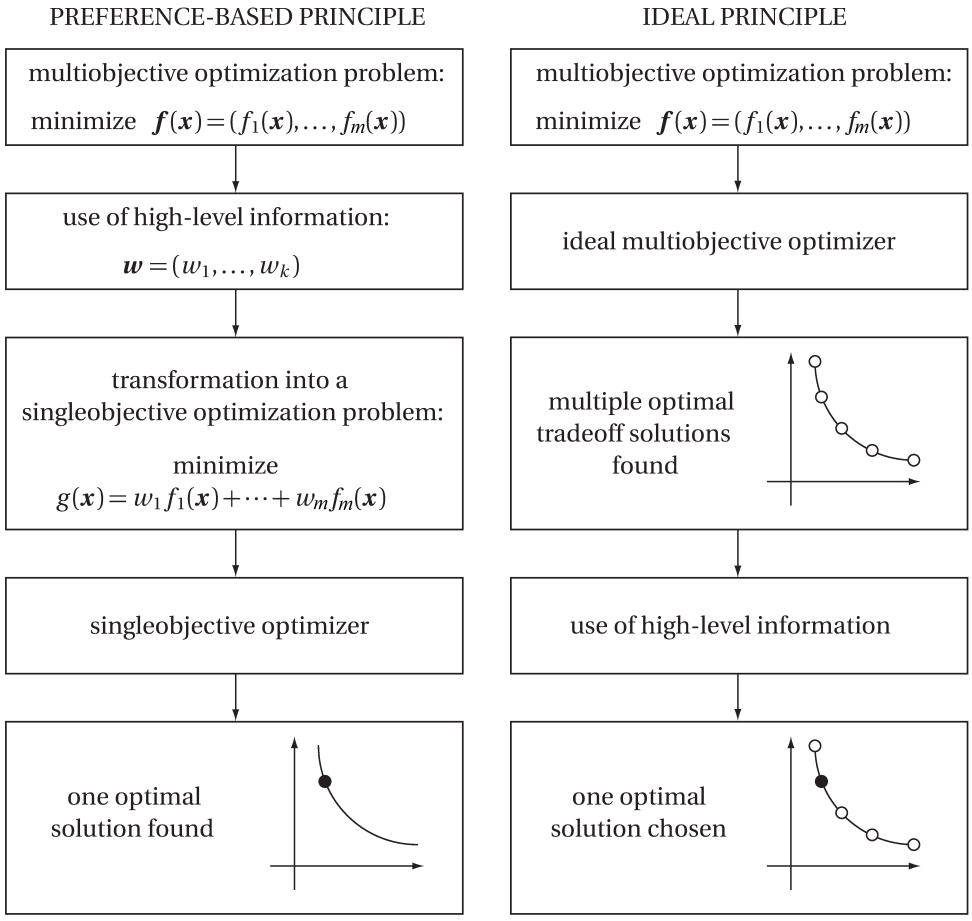

Figure 2.3: The preference-based principle (Left) and ideal principle (Right) of multiobjective optimization. The illustration is adapted from [Tusar, 2007].

algorithm in this direction would be a MOEA based on Decomposition (MOEA/D [Zhang and Li, 2007]), which simultaneously optimizes a number of single-objective aggregated optimization subproblems. It has been shown that the weights used for aggregation can be randomly uniformly assigned to each individual of the population in each generation or can be changed periodically during the optimization [Jin *et al.*, 2001a]. The second method combined with ES and CMA-ES usually outperforms the first method on high-dimensional ZDT problems [Jin *et al.*, 2001a].

Early MOEAs

The first MOEA algorithm, Vector Evaluated Genetic Algorithm (VEGA [Schaffer, 1985]), was a simple genetic algorithm with a modified selection step, where each sub-population has its own fitness-proportional based selection w.r.t. only one ob-

jective. Since the VEGA, the *environmental selection* has been recognized as the main difference between most MOEAs and their single-objective analogs. An important step of its understanding was made by Goldberg in his seminal book [Goldberg, 1989], where he discussed a concept of the non-dominated sorting, which was later implemented in the Non-dominated Sorting Genetic Algorithm (NSGA [Srinivas and Deb, 1994]).

The history of early approaches mainly represents the search for a suitable environmental selection mechanism for multi-objective optimization, the key contributors in this direction are the following algorithms:

- **First generation**. VEGA [Schaffer, 1985], Multi-Objective Genetic Algorithm (MOGA [Fonseca *et al.*, 1993]), NSGA [Srinivas and Deb, 1994], Niched-Pareto Genetic Algorithm (NPGA [Horn *et al.*, 1994]).
- **Second generation**. Strength Pareto Evolutionary Algorithm (SPEA [Zitzler and Thiele, 1998]), Pareto Archived Evolution Strategy (PAES [Knowles and Corne, 1999]), Non-dominated Sorting Genetic Algorithm II (NSGA-II [Deb *et al.*, 2000]), Strength Pareto Evolutionary Algorithm 2 (SPEA2 [Zitzler *et al.*, 2002a]).

One of the main achievements of the early approaches is the non-dominated sorting procedure and various secondary sorting criteria.

Modern MOEAs

After appropriate environmental selection schemes were found, many single-objective optimizers has been translated to their multi-objective versions:

- **Differential Evolution**. Pareto-frontier Differential Evolution (PDE [Abbass *et al.*, 2001]), Pareto Differential Evolution Approach (PDEA) [Madavan, 2002], Differential Evolution for Multi-objective Optimization (DEMO) [Robič and Filipič, 2005], Generalized Differential Evolution (GDE3 [Kukkonen and Lampinen, 2005]).
- **Particle Swarm Optimization**. Multi-objective Particle Swarm Optimization (MOPSO [Mostaghim and Teich, 2003]), MOPSO with Time Variant parameters (TV-MOPSO [Tripathi *et al.*, 2007]).
- **Evolution Strategy**. Multi-objective CMA-ES (MO-CMA-ES [Igel *et al.*, 2007b]).
- **Estimation of Distribution Algorithms**. Multi-objective EDA (MIDEA [Bosman and Thierens, 2005]), Regularity Model-Based Multi-objective EDA (RM-MEDA [Zhang *et al.*, 2008]).

However, not all above-described algorithms are "just" generalized versions of their single-objective variants. The RM-MEDA makes certain assumptions about the smoothness of $f(\boldsymbol{x})$ and induces from the Karush-Kuhn-Tucker condition (KKT) that the Pareto

set in the decision space represents a piecewise continuous $(m-1)$-dimensional manifold, where m is the number of objectives. As variation operations, RM-MEDA performs sampling of new individuals on $(m-1)$ largest principal components of distributions of local clusters, detected in the population. Thus, the variation operators are designed to increase the probability of successful sampling, taking into account the multi-objective context.

The Indicator Based Evolution Algorithm (IBEA) [Zitzler and Künzli, 2004] showed that the quality indicator itself can be used as a criterion for the environmental selection. Soon after that, the $\boldsymbol{S}$MS-EMOA [Emmerich *et al.*, 2005] algorithm demonstrated the advantages of using the hypervolume ($\boldsymbol{S}$-measure) as the second sorting criterion in the non-dominated sorting. This allowed to make a step toward Many-objective optimization ($m > 3$), where the widely used *crowding distance* measure fails to properly estimate the individual contribution of non-dominated points [Ishibuchi *et al.*, 2008]. However, the time complexity of the computation of the hypervolume indicator grows exponentially fast, and to make the hypervolume-based algorithm computationally suitable for large m, several Monte Carlo simulation schemes to approximate the exact hypervolume values have been proposed (e.g., HypE [Bader and Zitzler, 2011]). There is also certain progress in computation of the exact hypervolume: [Emmerich and Fonseca, 2011] proposes an algorithm for 3-dimensional objective space, which performs faster than the best known algorithm by a factor of $\sqrt{\ell}$, where ℓ is the number of points.

Despite the diversity of existed multi-objective algorithms worthy of scientific study, in this thesis, we focus on MO-CMA-ES because: i). the CMA-ES part of the algorithm was shown to be efficient in the single-objective case; ii). MO-CMA-ES already shows good results comparing to NSGA-II [Igel *et al.*, 2007b]; iii). self-adaptation mechanisms of CMA-ES make it more "sensitive/adaptive" to changes of the environment (see Section 6.2), while most MOEAs suffer from the lack of this crucial property.

2.4.3 Non-dominated Sorting Genetic Algorithm II (NSGA-II)

The Non-dominated Sorting Genetic Algorithm II (NSGA-II [Deb *et al.*, 2000]) is probably the most widely used multi-objective optimization algorithm. The NSGA-II (the second and drastically improved version of NSGA [Srinivas and Deb, 1994]) is an extension of GA for multi-objective optimization, where the $\prec_{\boldsymbol{X}}$ preference relation of the environmental selection is defined in the following way.

The dominance-based quality indicator I_1 is defined by Pareto ranking criterion: the sorting of individuals w.r.t. I_1, the *non-dominated sorting*, yields to several *approximation sets/non-dominated fronts*. Then, to order the individuals of the same non-dominated front $\mathcal{Y}$ the second quality indicator I_2, defined by *crowding distance* is applied. The crowding distance of an individual $\boldsymbol{x} \in \mathcal{Y}$ is computed as follows:

$$cd(\boldsymbol{x}, \mathcal{Y}) = \sum_{i=1}^{m} \frac{f_i(\boldsymbol{x}^+) - f_i(\boldsymbol{x}^-)}{max(f_i(y)|\forall y \in \mathcal{Y}) - min(f_i(y)|\forall y \in \mathcal{Y})}, \tag{2.10}$$

where $\boldsymbol{x}^+$ and $\boldsymbol{x}^-$ are right and left neighboring individuals of $\boldsymbol{x}$ on the objective i.

Algorithm 2.4: $(\mu+\lambda)$-NSGA-II

1: **given** $\mu \leftarrow 100, \lambda \leftarrow 100, p_c \leftarrow 0.9, p_m \leftarrow 1/n, \eta_c \leftarrow 15, \eta_m \leftarrow 20, t_{tour} \leftarrow 2$
2: **initialize** $t \leftarrow 0$, random parent population $\boldsymbol{Q}^{t=0}$;
3: **repeat**
4: **for** $k = 1, \ldots, \lambda$ **do**
5: **repeat**
6: $i_1 \leftarrow TournamentSelection(\boldsymbol{Q}^t, t_{tour})$;
7: $i_2 \leftarrow TournamentSelection(\boldsymbol{Q}^t, t_{tour})$;
8: **until** $i_1 = i_2$
9: **if** $\mathbb{U}(0,1) \leq p_c$ **then** $\{\boldsymbol{o}_1, \boldsymbol{o}_2\} \leftarrow SBXcrossover(\boldsymbol{x}_{i_1}, \boldsymbol{x}_{i_2}, \eta_c)$
10: **else** $\boldsymbol{o}_1 \leftarrow \boldsymbol{x}_{i_1}$; $\boldsymbol{o}_2 \leftarrow \boldsymbol{x}_{i_2}$
11: **if** $\mathbb{U}(0,1) \leq 0.5$ **then** $\boldsymbol{x}'_k \leftarrow \boldsymbol{o}_1$
12: **else** $\boldsymbol{x}'_k \leftarrow \boldsymbol{o}_2$
13: $\boldsymbol{x}'_k \leftarrow PolynomialMutation(\boldsymbol{x}'_k, p_m, \eta_m)$
14: $\boldsymbol{a}'^{t+1}_k \leftarrow \{\boldsymbol{x}'_k, \boldsymbol{y}'_k = f(\boldsymbol{x}'_k)\}$;
15: $\boldsymbol{Q}^t \leftarrow \boldsymbol{Q}^t \cup \{\boldsymbol{a}'^{t+1}_k\}$;
16: **end for**
17: $\boldsymbol{Q}^{t+1} \leftarrow \{\boldsymbol{Q}^t_{\prec:i} | 1 \leq i \leq \mu\}$ // Deterministic Selection according to $\prec_{\boldsymbol{Q}^t}$
18: $t \leftarrow t + 1$
19: **until** *stopping criterion is met*

The NSGA-II algorithm is outlined in Algorithm 2.4. In iteration $t = 0$, a population $\boldsymbol{Q}^{t=0}$ of μ individuals is randomly initialized. In each iteration t, the population $\boldsymbol{Q}^t$ generates λ offspring using variation operators of SBX crossover (with probability p_c and parameter η_c) and Polynomial mutation (with probability p_m and parameter η_m) [Deb and Goyal, 1996] (lines 4-15). Tournament-based parent selection is outlined in Algorithm 2.5. Each newly generated decision vector $\boldsymbol{x}'_k$ is evaluated and stored as an individual $\boldsymbol{a}'^{t+1}_k$ (lines 14-15). After the procedure of variation, $\mu + \lambda$ parent and offspring individuals are sorted (line 17) w.r.t. the partial preorder relation $\prec_{\boldsymbol{Q}^t}$ defined above. The time complexity analysis for NSGA-II as well as for many other multi-objective optimizers is given in [Jensen, 2003]. By setting $\lambda = 1$ and I_2 to the hypervolume indicator, the Algorithm 2.4 recovers $(\mu + 1)$-SMS-EMOA [Emmerich *et al.*, 2005]. In all experiments of this thesis we will *always* use NSGA-II *with* the hypervolume indicator as the second sorting criterion I_2, also referred to as S-NSGA-II.

2.4.4 Multi-objective CMA-ES (MO-CMA-ES)

Multi-objective
CMA-ES (MO-CMA-ES) proposed by [Igel *et al.*, 2007b, Igel *et al.*, 2007a] is based on CMA-ES adaptive paradigm to handle multiple objectives. MO-CMA-ES involves a set of μ $(1 + 1)$-CMA-ES algorithms [Igel *et al.*, 2006], each of which performs step-size and covariance matrix updates based on its own evolution path, and a Pareto-based survival

Algorithm 2.5: TournamentSelection

1: **given** t_{tour} // tournament size
2: $best \leftarrow \mathbb{U}(1, |A|)$
3: **for** $k = 2, \ldots, t_{tour}$ **do**
4: $\quad i_{cur} \leftarrow \mathbb{U}(1, |A|)$
5: $\quad$ **if** $i_{cur} < best$ **then**
6: $\quad\quad best \leftarrow i_{cur}$
7: $\quad$ **end if**
8: **end for**
9: **return** best

selection mechanism that selects μ individuals from the population of size $\mu + \lambda$ built in one iteration of the algorithm.

The $(\mu+\lambda)$-MO-CMA-ES (also referred to as $\mu_{MO} \times (1+1)$-MO-CMA-ES) is outlined in Algorithm 2.6. In iteration $t = 0$, a population $\boldsymbol{Q}^{t=0}$ of μ individual (1+1)-CMA-ES is randomly initialized. In each iteration t, the population $\boldsymbol{Q}^t$ generates λ offspring (1+1)-CMA-ES. To generate k-th offspring a parent $\boldsymbol{a}^t_{i_k}$ with index i_k is selected according to *ParentSelection* scheme (line 5). There are three baseline versions of MO-CMA-ES:

- **Generational $(\mu + \mu)$-MO-CMA-ES**. If $\lambda = \mu$ and *each* parent i_k generates *exactly one* offspring, i.e., $i_k = k$.
- **Steady-State $(\mu + 1)$-MO-CMA-ES or SS-MO-CMA-ES**. If $\lambda = 1$ and the parent i_k is *randomly uniformly drawn* from μ parents, i.e., $i_k = U(1, |\boldsymbol{Q}^t|)$.
- **Steady-State $(\mu_{\prec} + 1)$-MO-CMA-ES**. If $\lambda = 1$ and the parent i_k is selected among *non-dominated* points, i.e., $i_k = U(1, \mathrm{ndom}|\boldsymbol{Q}^t|)$

All parameters of the k-th (1+1)-CMA-ES including its mean of the mutation distribution $\boldsymbol{m}_k = \boldsymbol{x}_k$, its objective vector $\boldsymbol{y}_k = f(\boldsymbol{x}_k)$, its step-size σ_k, computed probability of success $\bar{p}_{\mathtt{succ},k}$ and evolution path of the step-size $\boldsymbol{p}_k$ are encapsulated in an element $\boldsymbol{a}_k$, which is called *individual*. When at iteration t an individual $\boldsymbol{a}^t_{i_k}$ is selected for mating it is just copied to an offspring individual $\boldsymbol{a}'^{t+1}_k$ (lines 5 - 6). The mating of $\boldsymbol{a}'^{t+1}_k$ consists of Gaussian mutation of its decision vector $\boldsymbol{x}^t_{i_k}$ (line 7). Then the fitness of newly generated offspring is computed (line 8) and it is added to the population $\boldsymbol{Q}^t$ (line 9). In the mating loop (4-9) λ new offspring individuals are added to the population, where each offspring is a simple copy of its parent with the mutated decision vector $\boldsymbol{x}'^{t+1}_{i_k}$ and the corresponding objective vector $\boldsymbol{y}'^{t+1}_k$.

The augmented population of parents and offspring is truncated to size μ after sorting w.r.t. $\prec_{\boldsymbol{Q}^t}$, defined in MO-CMA-ES as the non-dominated sorting + the hypervolume contribution indicator as the second sorting criterion (line 22). Before that, the CMA-ES parameters of both parent and offspring are updated depending on their *success* $\mathtt{succ}_{\boldsymbol{Q}^t}$ with respect to the parent and the population $\boldsymbol{Q}^t$. While the success measure $\mathtt{succ}_{\boldsymbol{Q}^t}$ can

Algorithm 2.6: $(\mu+\lambda)$-MO-CMA-ES — Generic MO-CMA-ES scheme

1: **given**
$d = 1 + \frac{n}{2\lambda}$, $p_{\texttt{succ}}^{\texttt{target}} = \frac{1}{5+\sqrt{\lambda}/2}$, $c_p = \frac{p_{\texttt{succ}}^{\texttt{target}}\lambda}{2+p_{\texttt{succ}}^{\texttt{target}}\lambda}$, $c_c = \frac{2}{n+2}$, $c_{cov} = \frac{2}{n^2+6}$, $p_{thresh} = 0.44$
2: **initialize** $t \leftarrow 0$, random parent population $\boldsymbol{Q}^{t=0}$
3: **repeat**
4: **for** $k = 1, \ldots, \lambda$ **do**
5: $i_k \leftarrow ParentSelection(\boldsymbol{Q}^t, k)$
6: $\boldsymbol{a}_k'^{t+1} \leftarrow \boldsymbol{a}_{i_k}^t$
7: $\boldsymbol{x}_k'^{t+1} \sim \boldsymbol{x}_{i_k}^t + \sigma_{i_k}^t \mathcal{N}\left(\boldsymbol{0}, \mathbf{C}_{i_k}^t\right)$
8: $\boldsymbol{a}_k'^{t+1} \leftarrow \left\{\boldsymbol{x}_k'^{t+1}, \boldsymbol{y}_k'^{t+1} = f(\boldsymbol{x}_k'^{t+1})\right\}$
9: $\boldsymbol{Q}^t \leftarrow \boldsymbol{Q}^t \cup \left\{\boldsymbol{a}_k'^{t+1}\right\}$
10: **end for**
11: **for** $k = 1, \ldots, \lambda$ **do**
12: $\bar{p}'^{t+1}_{\texttt{succ},k}, \bar{p}^t_{\texttt{succ},i_k} \leftarrow (1-c_p)\bar{p}'^{t+1}_{\texttt{succ},k} + c_p \texttt{succ}_{\boldsymbol{Q}^t}\left(\boldsymbol{a}_{i_k}^t, \boldsymbol{a}_k'^{t+1}\right)$
13: $\sigma_k'^{t+1}, \sigma_{i_k}^t \leftarrow \sigma_k'^{t+1} \exp\left(\frac{1}{d}\frac{\bar{p}'^{t+1}_{\texttt{succ},k} - p_{\texttt{succ}}^{\texttt{target}}}{1-p_{\texttt{succ}}^{\texttt{target}}}\right)$
14: **if** $\bar{p}'^{t+1}_{\texttt{succ},k} < \boldsymbol{p}_{\texttt{thresh}}$ **then**
15: $\boldsymbol{p}_{c,k}'^{t+1} \leftarrow (1-c_c)\boldsymbol{p}_{c,k}'^{t+1} + \sqrt{c_c(2-c_c)}\frac{\boldsymbol{x}_k'^{t+1} - \boldsymbol{x}_{i_k}^t}{\sigma_{i_k}^t}$
16: $\mathbf{C}_k'^{t+1} \leftarrow (1-c_{\texttt{cov}})\mathbf{C}_k'^{t+1} + c_{\texttt{cov}}\boldsymbol{p}_{c,k}'^{t+1}\boldsymbol{p}_{c,k}'^{g+1^T}$
17: **else**
18: $\boldsymbol{p}_{c,k}'^{t+1} \leftarrow (1-c_c)\boldsymbol{p}_{c,k}'^{t+1}$
19: $\mathbf{C}_k'^{t+1} \leftarrow (1-c_{\texttt{cov}})\mathbf{C}_k'^{t+1} + c_{\texttt{cov}}\left(\boldsymbol{p}_{c,k}'^{t+1}\boldsymbol{p}_{c,k}'^{t+1^T} + c_c(2-c_c)\mathbf{C}_k'^{t+1}\right)$
20: **end if**
21: **end for**
22: $\boldsymbol{Q}^{t+1} \leftarrow \left\{\boldsymbol{Q}^t_{\prec:i} | 1 \le i \le \mu\right\}$ // Deterministic Selection according to $\prec_{\boldsymbol{Q}^t}$
23: $t \leftarrow t+1$
24: **until** stopping criterion is met.

be defined in different ways, in original MO-CMA-ES it is defined as the $\prec_{\boldsymbol{Q}^t}$ preference. Parent's and offspring's success rates $\bar{p}'^{t+1}_{\texttt{succ},k}$ and $\bar{p}'^{t}_{\texttt{succ},k}$ are updated at each iteration using some decay factor c_p (line 12). In a similar way to that of the 1/5-th rule, the step-sizes of the parent and offspring are updated in line 13. Thus, if it survives, parent $a_k'^t$ will have an updated success rate and mutation step-size, while offspring $a_k'^{t+1}$ will also have an updated evolution path $\boldsymbol{p}_{c,k}'^{t+1}$ and an updated covariance matrix $\mathbf{C}_k'^{t+1}$ (lines 15-19), which account the information from the last mutation step.

The relatively good convergence of the MO-CMA-ES is due to its (1+1)-CMA-ES part, while the diversity/spread preservation is due to its hypervolume-based environmental selection procedure. There is a less strict variant of $\texttt{succ}_{\boldsymbol{Q}^t}$ success measure than $\prec_{\boldsymbol{Q}^t}$ [Voß *et al.*, 2010], where the offspring is successful if it is selected to the new population

$\boldsymbol{Q}^t$, more formally:

$$\texttt{succ}_{\boldsymbol{Q}^t}\left(a_{i_k}^t, a_k'^{t+1}\right) = \begin{cases} 1 & \text{if } a_k'^{t+1} \in \boldsymbol{Q}^{t+1} \\ 0 & \text{otherwise} \end{cases} \tag{2.11}$$

Another interesting extension of MO-CMA-ES is to use some recombination procedure for (1+1)-CMA-ES algorithms [Voß *et al.*, 2009]. The recombination consists of sharing the covariance matrix information between the neighborhood individuals, such than individuals with closer Mahalanobis distance in the decision space have larger weights of contribution in the recombination.

2.4.5 Benchmarking

Many ways of measuring the performance of multi-objective Evolutionary Algorithms have been proposed. In this study, we follow the guidelines of [Knowles *et al.*, 2006] and use only Pareto-compliant quality indicators, more particularly the widely used hypervolume indicator H. Let P be a μ-size approximation of Pareto front and let P^* be the approximate μ-optimal distribution of optimal Pareto points [Auger *et al.*, 2009]. The approximation error of the Pareto front is defined by $\Delta H(P^*, P) = H(P^*) - H(P)$. The optimization goal is to minimize $\Delta H(P^*, P)$ to have a better approximation of the optimal Pareto front of the initial multi-objective function $f(\boldsymbol{x})$.

The most popular sets of benchmark problems in the field are: the bi-objective ZDT problems [Zitzler *et al.*, 2000], the scalable DTLZ problems [Deb *et al.*, 2001] and the WFG problems with a wide variety of characteristics [Huband *et al.*, 2005]. ZDT problems are often considered to be too easy, e.g., the Pareto front is located on a boundary of the box-constrained decision space, this could bias the optimization process (see Section 6.2.2.2). They are also separable, and this is more advantageous for MOEAs with separable variation operators (NSGA-II, SPEA2, etc.). To make these problems more reliable, the IHR problems were proposed [Igel *et al.*, 2007b] as the shifted and rotated versions of the ZDT problems. Another interesting set of benchmark problems, inspired by the strategies for contructing test problems proposed in [Okabe *et al.*, 2004], is the LZ problems [Li and Zhang, 2009] with complicated Pareto fronts in decision space. In this thesis, we will benchmark MOEAs on ZDT, IHR and LZ problems.

2.5 Discussion

The historical overview of Evolutionary Computation presented in this Chapter is itself an evolution of approaches to optimization. This evolution is a constant fight against the complexity of the real-world that we try to conquer, solving more and more complex problems every day. Since the diversity of these problems is growing, a source of robustness as an ability to adequately solve them with a smallest number of changes in the used optimization technique has become an attractive property. The CMA-ES algorithm clearly demonstrates such robustness, originated in invariance properties of the CMA-ES with respect to rank-preserving transformations of the objective function and with respect to

the rotation of the search space. The empirical observations confirms that CMA-ES overall outperforms other techniques on a wide set of black-box single-objective optimization problems. While we do not observe in the literature such a clear "domination" (and vice versa) of MO-CMA-ES on multi-objective problems, we suppose that its better adaptation to the multi-objective context is worth of scientific study, while its (1+1)-CMA-ES part is already quite powerful. This research might lead to a more general CMA-like approach, derived from the first principles, which would work equally good on single- and multi-objective problems.

In this Chapter, we analyzed Evolutionary Algorithms separately for single- and multi-objective optimization. While many multi-objective optimizers may be recovered by changing the environmental selection of their single-objective analogs, the fundamental difference of these two cases may be more questionable. It would be interesting to know if a nature-driven "evolution of everything" (in a very global scale) exists, then whether this evolution is multi-objective or single-objective, but passed through the multi-objectivization? The multi-objectivization [Knowles *et al.*, 2001] consists in replacing the original objective by a set of objectives, or adding some new objectives to the original one. In certain cases multi-objectivization is shown to be favorable for the search of the global optimum [Knowles *et al.*, 2001]. We also might ask ourselves whether, e.g., the company which produces and sells cars is a multi-objective problem driven unit or just single-objective profit-oriented one, passed through the multi-objectivization? We suppose that the answers depend very much on the scale with which we look at these questions. While the multi-objective case is a more general one and should be viewed as our final goal, we believe that *most of colors to draw a picture of a feature general optimizer are already available* in the single-objective case.

Chapter 3

Surrogate-assisted Evolutionary Optimization

Much learning does not teach understanding.
Heraclitus, On the Univers.

In a black-box optimization scenario, the only available information about the objective function f comes from the evaluated candidate solutions. It is often assumed that the optimization algorithm estimates λ new candidate solutions at each iteration, then, updates its own hyper-parameters $\boldsymbol{\theta}$ (e.g., $\boldsymbol{m}, \sigma$ and $\mathbf{C}$ for CMA-ES) in such a way that the probability of sampling solutions with better fitness increases in a short and/or long term. One important thing here is that the algorithm often "forgets" previously evaluated solutions, assuming that all important information is already stored in the $\boldsymbol{\theta}$ hyper-parameters. However, the latter assumption is usually too strong, and most algorithms actually lose very important information, taking into account only the recently evaluated candidate solutions. This is a fundamental basis for learning an *approximation* or *surrogate model* $\hat{f}$ of f from a set of selected previously evaluated individuals, called *training points/individuals*. Thus, in principle all previously evaluated individuals can be checked and selected to build $\hat{f}$. The surrogate model $\hat{f}$ later can be used to give hints about where promising candidate solutions are located. An extreme case is when $\hat{f}$ replaces the original f and is used for direct optimization.

In this Chapter, we review the state-of-the-art techniques for surrogate-assisted evolutionary optimization. First we analyze recent trends in Machine Learning (Section 3.1) and describe the most popular techniques used for surrogate model learning. We focus on Support Vector Machines (SVMs) in Section 3.2, because we will use SVMs in this thesis to build surrogate models with nice invariance properties, such as invariance to rank-preserving transformation of the objective function. After the surrogate model has been built, it can be exploited in many different ways: in Section 3.3, we review the state-of-the-art techniques used for surrogate model control and exploitation in single- and multi-objective scenarios, focusing on Evolutionary Strategies and CMA-ES. Finally, in Section 3.4, we conclude the Chapter and discuss some prospective directions of the surrogate-assisted search.

3.1 Surrogate Models

Various surrogate modeling techniques have been proposed to replace the actual expensive simulations or experiments by cheap surrogate models. Figure 3.1 illustrates the history of

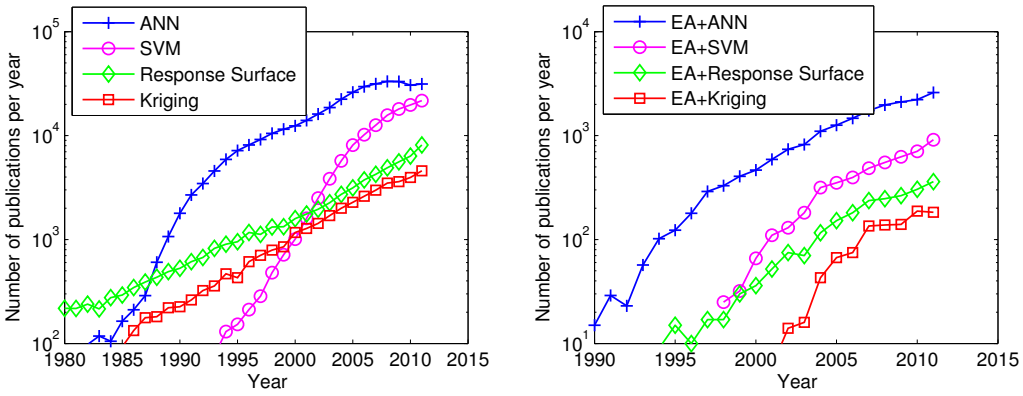

Figure 3.1: The history of publications reporting the use of the major surrogate techniques (**Left**) in all fields and (**Right**) with Evolutionary Algorithms, using Google Scholar data (see text for details).

publications reporting the use of the major surrogate techniques. Data was obtained using Google Scholar [Google, 2012] by a methodology proposed in [Viana and Haftka, 2008]. For each technique we searched articles with chosen keywords, e.g., for the response surface method (also referred to as Polynomial Regression (PR)) we used the following query: approximation OR metamodel OR regression OR prediction OR surrogate AND "response surface". Figure 3.1-**Left** illustrates the number of papers published in all fields. One can observe that the traditional polynomial response surface approach and Kriging approach grow every year in average by 10-15% in terms of number of publications per year. This can be viewed as a factor of growing of the field of theoretical and applied machine learning and optimization. One can also clearly observe the "boom" of artificial neural networks (ANN) in the late 1980s and the early 1990s, and a very similar "boom" of support vector machines (SVMs) 10 years later. The growth of popularity of ANN clearly stagnates for the last 5 years, while SVM might become the most popular approach in machine learning in the next few years.

To measure the popularity of surrogate techniques used with Evolutionary Algorithms (see Figure 3.1-**Right**) we searched using queries such as: "evolutionary algorithms" and "neural network". While the ranking of popularity of surrogate techniques is the same, the publications often correspond to the tuning of surrogate models (e.g., structures and weights of ANN, hyper-parameters of SVM) and not the surrogate-assisted optimization. Many publications only mention surrogate techniques but do not use them, other use them not for optimization but for, e.g., classification. Therefore, in order to estimate the popularity of techniques for surrogate-assisted optimization the absolute numbers should be divided by a factor from 10 to 50 for ANN and SVM and by some smaller factor for response surface and Kriging.

In this Section, we will describe only major techniques for surrogate model learning: Polynomial Regression in Section 3.1.1, Gaussian Processes in Section 3.1.2, Artificial Neural Networks in Section 3.1.3, Radial Basis Functions in Section 3.1.4 and Support Vector

Machines, which we will discuss *in detail* in Section 3.2. Many interesting approaches, such as Generalized Additive Models (GAMs [Hastie and Tibshirani, 1990]), Multivariate Adaptive Regression Splines (MARS [Friedman, 1991]) and Kernel Partial Least Squares (KPLS [Rosipal and Trejo, 2002]), are omitted for the sake of space.

3.1.1 Polynomial Regression (PR)

Polynomial regression is a form of *linear* regression which fits a *non-linear* model to a training set $\mathcal{D} = \{(\boldsymbol{x}_i, y_i), i = 1, \ldots, \ell\}$, where $\boldsymbol{x}_i \in \mathbb{R}^n, y_i \in \mathbb{R}$. A PR model that is linear in $\boldsymbol{\beta}$ can be expressed as follows [Myers, 1990, Atkeson *et al.*, 1997]:

$$\hat{f} = \tilde{\boldsymbol{x}}^T \boldsymbol{\beta}, \tag{3.1}$$

where $\boldsymbol{\beta}$ defines the complexity of the model. Linear (respectively, quadratic) polynomial regression models can be recovered by setting $\tilde{\boldsymbol{x}} = (x_1, \ldots, x_n, 1)$ (respectively, $\tilde{\boldsymbol{x}} = (x_1^2, \ldots, x_n^2, x_1x_2, \ldots, x_{n-1}x_n, x_1, \ldots, x_n, 1)$). The training points can be collected in a matrix equation

$$\left((\boldsymbol{W}\tilde{\boldsymbol{X}})^T \boldsymbol{W}\tilde{\boldsymbol{X}} \right) \boldsymbol{\beta} = (\boldsymbol{W}\tilde{\boldsymbol{X}})^T \boldsymbol{W}\boldsymbol{y}, \tag{3.2}$$

where $\tilde{\boldsymbol{X}} = (\tilde{\boldsymbol{x}}_1, \ldots, \tilde{\boldsymbol{x}}_\ell)^T$ is a matrix of $\tilde{\boldsymbol{x}}$ parameters of ℓ training points, $\boldsymbol{y} = (y_1, \ldots, \boldsymbol{y}_\ell)^T$, and $\boldsymbol{W} = \mathrm{diag}(1) \in \mathbb{R}^{\ell \times \ell}$ defines weights of training points. In global polynomial regression the weights of all training points are equal, the locally weighted regression with different weights is described in Section 3.3.2.2.

Estimating the parameters $\boldsymbol{\beta}$ using regression amounts to minimizing the *least square* loss criterion

$$A(\boldsymbol{q}) = \sum_{i=1}^{\ell} \left[(\hat{f}(\boldsymbol{x}_i, \boldsymbol{\beta}) - y_i)^2 \right] \tag{3.3}$$

by solving (3.2) using least square or gradient-based methods.

The Response Surface Methodology (RSM) proposed by [Box and Wilson, 1951] suggested to use quadratic PR models to perform a sequence of designed experiments (DOE) to obtain an optimal response from an analyzed function f. The terms PR and RSM are often used interchangeably.

If the target function f is smooth and its complexity is a priori known, then PR models may be a good choice. In practice, they are usually good for, e.g., quadratic or cubic landscapes, but often are not suitable for more complex multi-modal ones. An important drawback of PR models is that the computational complexity to find *exact* solution of the least square problems scales with $O(n_{param}^3)$, where n_{param} is the number of parameters of the model that scales itself with $O(n^2)$ for *quadratic* PR model. Therefore, the learning of quadratic PR model scales with $O(n^6)$, limiting the range of application to problems with $n \lesssim 15$ [Kern *et al.*, 2007].

3.1.2 Gaussian Processes (GP)

Kriging, also also referred to as Gaussian Process (GP) regression, was originally developed in geostatistics by a South African mining engineer called Danie Krige in the early 1950s and was further developed by [Matheron, 1963]. Kriging models are rather *global* than local surrogate models, hence more suited for larger experimental areas than the areas typically used in low-order polynomial regression models [Kleijnen, 2009].

A Gaussian process is a collection of random variables, any finite number of which have (consistent) Gaussian distributions [Rasmussen, 2004]. Therefore, the vector of function values $\boldsymbol{y}_\ell$ of training points can be viewed as only one sample of a multivariate Gaussian distribution with joint probability density $p(\boldsymbol{y}_\ell|\boldsymbol{X}_\ell)$, where $\boldsymbol{X}_\ell$ is the set of training points. Thus, the predictive distribution for a new test point $\boldsymbol{x}_{\ell+1}$ is obtained from $\ell+1$-dimensional joint Gaussian distribution for the outputs of the ℓ training points and the test point, by conditioning on the observed targets in the training set:

$$p(y_{\ell+1}|\boldsymbol{X}_{\ell+1}, \boldsymbol{y}_\ell) = \frac{p(\boldsymbol{y}_{\ell+1}|\boldsymbol{X}_{\ell+1})}{p(\boldsymbol{y}_\ell|\boldsymbol{X}_\ell)}, \tag{3.4}$$

It should be noted that the dimensionality of each probability density here equals the number of data points. The (3.4) can be simplified to [Büche *et al.*, 2004]

$$p(y_{\ell+1}|\boldsymbol{X}_{\ell+1}, \boldsymbol{y}_\ell) \propto \exp\left(-\frac{1}{2}\frac{(y_{\ell+1}-\hat{y}_{\ell+1})^2}{\sigma^2_{t_{\ell+1}}}\right), \tag{3.5}$$

a univariate Gaussian with mean and variance given by

$$\hat{y}_{\ell+1} = \boldsymbol{k}^T\mathbf{C}_\ell^{-1}\boldsymbol{y}_\ell, \tag{3.6}$$

$$\sigma^2_{t_{\ell+1}} = \kappa - \boldsymbol{k}^T\mathbf{C}_\ell^{-1}\boldsymbol{k}, \tag{3.7}$$

where the smooth covariance function between two point $\boldsymbol{x}_i$ and $\boldsymbol{x}_j$ is defined as

$$\mathbf{C}(\boldsymbol{x}_i, \boldsymbol{x}_j) = \theta_1\left(-\frac{1}{2}\sum_{i=k}^{n}\frac{(x_{i,k}-x_{j,k})^2}{r_k^2}\right) + \theta_2 + \delta_{ij}\theta_3. \tag{3.8}$$

The covariance vector $\boldsymbol{k}$ and variance κ can be expressed in terms of the covariance function as

$$k_i = \mathbf{C}(\boldsymbol{x}_i, \boldsymbol{x}_{\ell+1}), \quad i = 1, \ldots, \ell, \tag{3.9}$$

$$\kappa = \mathbf{C}(\boldsymbol{x}_{\ell+1}, \boldsymbol{x}_{\ell+1}) = \theta_1 + \theta_2 + \theta_3. \tag{3.10}$$

The optimization of hyper-parameters $\boldsymbol{\theta}= \{\theta_1, \theta_2, \theta_3, r_1, r_2, \ldots, r_\ell\}$ is a multi-modal function, therefore some combination of gradient-based (e.g., BFGS) and Evolutionary Algorithms (e.g., CMA-ES) can be used [Büche *et al.*, 2004].

The computational complexity of model training scales with $O(N\ell^3 + n\ell^2)$, where $N \geq 1$ denotes the number of iterations spent on hyper-parameters optimization by a gradient-based algorithm [Emmerich *et al.*, 2006b]. Each prediction of $\hat{f}$ scales with $O(\ell^2)$ in time and computation of σ scales with $O(\ell)$. Therefore, if ℓ is chosen very conservatively to be linear in n, then the computational complexity scales at least with $O(n^3)$.

3.1.3 Artificial Neural Network (ANN)

The perceptron [Rosenblatt, 1958] is a linear classifier whose output is a function applied on the weighted sum of its M inputs:

$$\hat{f}(\boldsymbol{x}, \boldsymbol{w}) = f_a \left(w_0 + \sum_{j=1}^{M} \boldsymbol{w}_j \boldsymbol{x}_j \right), \tag{3.11}$$

where $\boldsymbol{x}$ is the input with a corresponding weight vector $\boldsymbol{w}$, w_0 is a constant bias and $f_a : \mathbb{R} \mapsto \mathbb{R}$ the non-linear activation function.

A basic artificial neural network in the form of a Multilayer Perceptron (MLP) can be described as a perceptron whose input is the output of other perceptrons. The overall model of an ANN with one hidden layer of M perceptrons and an output layer with K outputs for $k = 1, \ldots, K$ takes the form [Bishop, 2006]:

$$\hat{f}_k(\boldsymbol{x}, \boldsymbol{w}) = f_a \left(\sum_{j=1}^{M} w_{kj}^{(2)} f_a \left(\sum_{i=1}^{n} w_{ji}^{(1)} x_i + w_{j0}^{(1)} \right) + w_{k0}^{(2)} \right), \tag{3.12}$$

where $\boldsymbol{w}$ is the vector of weights and the superscripts (1) and (2) indicate that the corresponding parameters are in the first and the second layers of the network, respectively. The activation function is often defined by a logistic sigmoid function $f_a(a) = 1/(1 + \exp(-a))$.

Since it is supposed that each training point $\boldsymbol{x}_i$ may have K values $f_1(\boldsymbol{x}_i), \ldots, f_K(\boldsymbol{x}_i)$, after optimizing the neural network we want to find the weight vector $\boldsymbol{w}$ that minimizes the mean square error on training points:

$$E = \frac{1}{\ell} \sum_{i=1}^{\ell} \sum_{k=1}^{K} (\hat{f}_k(\boldsymbol{x}_i) - f_k(\boldsymbol{x}_i)) \tag{3.13}$$

The main drawback of ANN is that the minimization of (3.13) during the model learning is a multi-modal problem, therefore popular approaches such as back-propagation [Bryson and Ho, 1975] and Newton's method may prematurely converge to local optima. An open question is how to *optimally* choose the structure of ANN: the number of hidden layers and perceptrons in each layer, connections between perceptrons. A state-of-the-art Evolutionary Algorithm HyperNEAT for evolving large-scale neural networks (simultaneous optimization of weights and structure, see also NEAT [Stanley and Miikkulainen, 2002]) with millions of connections can be found in [Stanley *et al.*, 2009].

3.1.4 Radial Basis Functions (RBFs)

The method of Radial Basis Functions (RBFs) [Orr, 1996] approximates f by using a linear combination of N_{RBF} (usually $N_{RBF} = \ell$) radially symmetric functions $h_i(\boldsymbol{x})$

$$\hat{f}(\boldsymbol{x}) = \sum_{i=1}^{N_{RBF}} w_i h_i(\boldsymbol{x}), \tag{3.14}$$

where $\boldsymbol{w}$ is the weight vector. Similarly to the polynomial regression optimal weights can be found by solving

$$\hat{\boldsymbol{w}} = \boldsymbol{A}^{-1}\boldsymbol{H}^T\hat{\mathbf{y}} \tag{3.15}$$

where $\boldsymbol{A}^{-1}$, the *variance matrix* is $\boldsymbol{A}^{-1} = (\boldsymbol{H}^T\boldsymbol{H})^{-1}$, where

$$\boldsymbol{H} = \begin{bmatrix} h_1(\boldsymbol{x}_1) & \cdots & h_{N_{RBF}}(\boldsymbol{x}_1) \\ \vdots & \ddots & \vdots \\ h_1(\boldsymbol{x}_\ell) & \cdots & h_{N_{RBF}}(\boldsymbol{x}_\ell) \end{bmatrix} \tag{3.16}$$

The variance matrix can be used to estimate the variance σ^2 of an independent error ϵ_i w.r.t. $h_i(\boldsymbol{x})$. The kernel function $h_i(\boldsymbol{x})$ (see Section 3.2 for definition of kernels) can be defined by polynomial kernel of degree d and linear splines, but usually is defined by Gaussian RBF [Bishop, 2006]. It is traditionally assumed that RBF networks have only one hidden layer [Orr, 1996], sharing some similarities with ANNs with one hidden layer.

As well as in GP, the computational complexity of RBG method scales at least with $O(\ell^3)$ because of the inversion of $\boldsymbol{A}$.

Because Support Vector Machines have been the preferred surrogate models in this thesis, the following Section details several variants of SVM.

3.2 Support Vector Machine (SVM)

Support Vector Machines (SVMs) and kernel-based learning methods have become popular since the 2000s for solving problems in classification, regression, and novelty detection. In this Section, we demonstrate the mathematical beauty of the SVM approach first for the case of simple linear classification and then show its extension to more complex tasks such as regression and ranking, which can be used for surrogate model learning.

3.2.1 Classification SVM

SVMs were initially proposed for linear classification by Vladimir Vapnik in [Vapnik, 1995], but have been developed by him together with Alexey Chervonenkis since the 1960s [Vapnik and Chervonenkis, 1971]. An important property of SVMs that made them popular is that the prediction model learning is a convex optimization problem, and so any local optimum is also a global optimum.

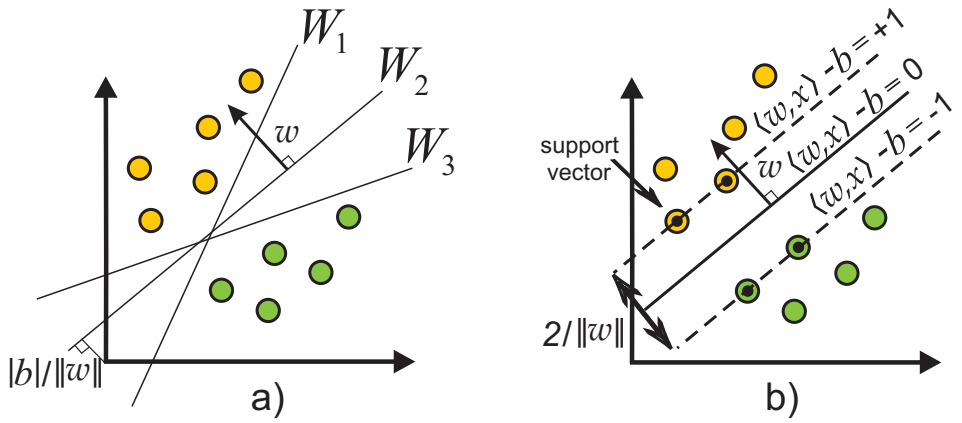

Figure 3.2: Linear separating hyperplanes for separable case of classification of yellow (class '+1') and green (class '-1') points.

3.2.1.1 Linear Separable Classification SVM

Considering a two-class training set $\mathcal{D} = \{(\boldsymbol{x}_i, y_i), i = 1, \ldots, \ell = N\}$, where $\boldsymbol{x}_i \in \mathbb{R}^n, y_i \in \{-1, +1\}$, classification problem consists of finding $\hat{f}_{classSVM}$ which can correctly classify all training points and predict classes of unseen test points.

The Optimal Hyperplane Suppose the training data $\mathcal{D}$ can be separated by a hyperplane

$$\langle \boldsymbol{w}, \boldsymbol{x} \rangle - b = 0, \tag{3.17}$$

where $\boldsymbol{w}$ is the norm to the hyperplane. Then, there are infinitely many such hyperplanes (see, e.g., $\boldsymbol{W}_1$, $\boldsymbol{W}_2$ and $\boldsymbol{W}_3$ in Figure 3.2-a), which separate the set of vectors $\mathcal{D}$ such that all points of one class (e.g., class '+1' of yellow points) lie on one side of the hyperplane (e.g., on the left side), while all points of another class (class '-1' of green points) lie on the opposite side of the hyperplane (on the right side).

A hyperplane is called the *optimal separating hyperplane* or *the maximum margin hyperplane* if the set of vectors $\mathcal{D}$ is separable without error and the distance between the closest vector to the hyperplane is maximal. More formally the separating hyperplane can be described as follows (after renormalization):

$$\begin{cases} \langle \boldsymbol{w}, \boldsymbol{x}_i \rangle - b \geq +1 & \text{if } \; y_i = +1 \\ \langle \boldsymbol{w}, \boldsymbol{x}_i \rangle - b \leq -1 & \text{if } \; y_i = -1, \end{cases} \tag{3.18}$$

or in a more compact notation as $y_i \left[\langle \boldsymbol{w}, \boldsymbol{x}_i \rangle - b \right] \geq 1$. It can be shown that the optimal hyperplane should satisfy the described above condition and minimize

$$\Phi(\boldsymbol{w}) = \frac{1}{2} \langle \boldsymbol{w}, \boldsymbol{w} \rangle = \frac{1}{2} ||\boldsymbol{w}||^2, \tag{3.19}$$

that corresponds to the maximization of the margin $2/||\boldsymbol{w}||$ between two classes of points.

Constructing The Optimal Hyperplane To find the optimal hyperplane one has to solve the following *primal* quadratic programming problem:

$$\begin{array}{l} \text{Minimize}_{\{\boldsymbol{w}\}} \ \frac{1}{2}||\boldsymbol{w}||^2 \\ \text{subject to the constraints } \ y_i \left[\langle \ \boldsymbol{w}, \boldsymbol{x}_i \ \rangle - b\right] \geq 1 \quad i = 1, \ldots, \ell \end{array} \tag{3.20}$$

Lagrange multipliers $\alpha_i, i = 1, \ldots, \ell$ can be introduced for each of the inequality constraints of (3.20) to i). replace the original constraints to constraints on the Lagrange multipliers themselves, which are much easier to handle; ii). formulate the problem only in terms of dot products between vectors, which will allow to generalize SVMs to non-linear classification and regression. The solution of (3.20) is given by the saddle point of the *primal* Lagrangian

$$L_P(\boldsymbol{w}, b, \alpha) = \frac{1}{2}\langle \ \boldsymbol{w}, \boldsymbol{w} \ \rangle - \sum_{i=1}^{\ell} \alpha_i \{y_i \left[\langle \ \boldsymbol{w}, \boldsymbol{x}_i \ \rangle - b\right] - 1\}, \tag{3.21}$$

The Lagrangian has to be minimized with respect to $\boldsymbol{w}$ and b and maximized with respect to $\alpha_i > 0$. At the saddle point, the solutions $\boldsymbol{w}_0$, b_0, and α^0 should satisfy the Karush-Kuhn-Tucker (KKT) conditions [Fletcher, 1987]

$$\frac{\partial L_P}{\partial \boldsymbol{w}}(\boldsymbol{w}_0, b_0, \alpha^0) = \boldsymbol{w}_0 - \sum_{i=1}^{\ell} \alpha_i^0 y_i \boldsymbol{x}_i = 0 \tag{3.22}$$

$$\frac{\partial L_P}{\partial b}(\boldsymbol{w}_0, b_0, \alpha^0) = \sum_{i=1}^{\ell} \alpha_i^0 y_i = 0 \tag{3.23}$$

From (3.22) and (3.23) we observe that the optimal hyperplane $\boldsymbol{w}_0$ is a linear combination of the training vectors:

$$\boldsymbol{w}_0 = \sum_{i=1}^{\ell} y_i \alpha_i^0 \boldsymbol{x}_i, \quad \alpha_i^0 \geq 0, \quad i = 1, \ldots, \ell \tag{3.24}$$

All points $\boldsymbol{x}_i$ with non-zero coefficients α_i^0 are called *support vectors*. In Figure 3.2-b support vectors have additional black dots inside the circle.

We can substitute equalities (3.22) and (3.23) into the *primal* form of Lagrangian (3.21) and obtain a particular *dual* form, called the Wolfe dual [Fletcher, 1987]:

$$\begin{array}{l} \text{Maximize } \ L_D(\alpha) = \sum_{i=1}^{\ell} \alpha_i - \frac{1}{2} \sum_{i=1}^{\ell} \alpha_i \alpha_j y_i y_j \langle \ \boldsymbol{x}_i, \boldsymbol{x}_j \ \rangle \\ \text{subject to } \ \alpha_i \geq 0, \quad i = 1, \ldots, \ell \end{array} \tag{3.25}$$

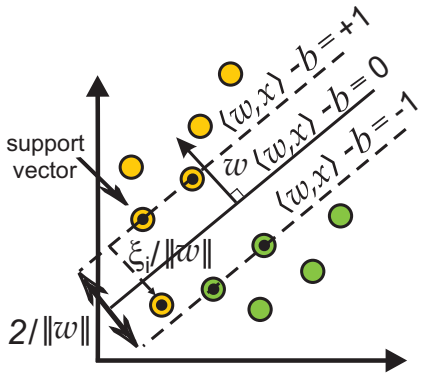

Figure 3.3: Linear separating hyperplanes for non-separable case of classification of yellow (class '+1') and green (class '-1') points.

The optimal solution α^0 of (3.25) can be used to predict the class of a point $\boldsymbol{x}$ computing the decision function

$$\hat{f}_{classSVM}(\boldsymbol{x}) = \text{sign}\left(\sum_{i=1}^{\ell} y_i \alpha_i^0 \langle\, \boldsymbol{x}_i, \boldsymbol{x}\,\rangle - b_0\right), \tag{3.26}$$

where b_0 is the threshold

$$b_0 = \frac{1}{2}\left[\langle\, \boldsymbol{w}_0, \boldsymbol{x}_{+1}\,\rangle + \langle\, \boldsymbol{w}_0, \boldsymbol{x}_{-1}\,\rangle\right], \tag{3.27}$$

where $\boldsymbol{x}_{+1}$ (respectively, $\boldsymbol{x}_{-1}$) is any support vector belonging to the class '+1' (respectively, to the class '-1').

3.2.1.2 Linear Soft Margin Classification SVM

The described above classification SVM is called *hard margin* SVM, because it assumes that the training data is separable by a linear classifier, and, therefore, the optimum solution leads to no error of classification in the training set. In the case where the training set is linearly non-separable, i.e., some of training points cannot be correctly classified (see, e.g., the yellow point in the left bottom corner in Figure 3.3), non-negative slack variables $\xi_i \geq 0$ are introduced to count and minimize the misclassification error. The *soft margin* SVM classification problem can be formulated as follows:

$$\begin{aligned} &\text{Minimize}_{\{\boldsymbol{w},\xi\}}\ \tfrac{1}{2}||\boldsymbol{w}||^2 + C\sum_{i=1}^{\ell}\xi_i \\ &\text{subject to}\ \begin{cases} y_i\left[\langle\, \boldsymbol{w}, \boldsymbol{x}_i\,\rangle - b\right] \geq 1 - \xi_i & i = 1, \ldots, \ell \\ \xi_i \geq 0, & i = 1, \ldots, \ell \end{cases} \end{aligned} \tag{3.28}$$

The constant C defines the trade-off and an aggregation weight of multi-objective problem of maximization of the margin and minimization of the error of misclassification. It also can be interpreted as an upper bound on the impact of the error of any given point.

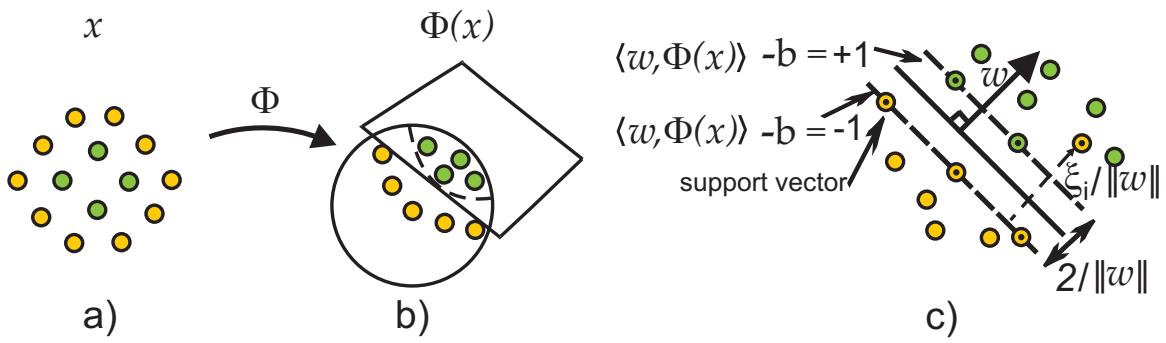

Figure 3.4: Linear separating hyperplanes for separable **(a)** and non-separable **(b)** cases of non-linear classification of yellow (class '+1') and green (class '-1') points.

The *dual* form of (3.28) is formulated as follows:

$$\begin{aligned} &\text{Maximize } L_D(\alpha) = \sum_{i=1}^{\ell} \alpha_i - \frac{1}{2} \sum_{i=1}^{\ell} \sum_{j=1}^{\ell} \alpha_i \alpha_j y_i y_j \langle \boldsymbol{x}_i, \boldsymbol{x}_j \rangle \\ &\text{subject to } \ 0 \leq \alpha_i \leq C, \quad i = 1, \ldots, \ell \end{aligned} \tag{3.29}$$

3.2.1.3 Non-linear Soft Margin Classification SVM

In case the training points cannot be successfully linearly classified in the original space $X \in \mathbb{R}^n$ (Figure 3.4-a), they can be mapped using a mapping Φ to some *feature* (possibly infinite dimensional) Euclidean space (to be an image $\Phi(X)$), where the classification error hopefully will be smaller (Figure 3.4-b), because the Vapnik-Chervonenkis (VC) dimension is higher [Vapnik and Chervonenkis, 1971].

Definition 12. (**The Vapnik-Chervonenkis dimension**). The Vapnik-Chervonenkis dimension, $VC(H)$, of hypothesis space H, defined over instance space X is the size of the *largest finite subset* of X shattered (isolated) by H. If arbitrary large finite sets of X can be shattered by H, then $VC(H) \equiv \infty$.

VC-dimension defines the *maximum* number of training points which can be *classified exactly for all possible labelings*. For a linear classifier defined in n-dimensional space $VC(H) = n + 1$.

VC dimension gives an estimate of the upper bound on "expected risk" $R(\alpha)$ (a measure of the error on unseen test data) of an α-parametrized learning machine with probability $1 - \eta$:

$$R(\alpha) \leq R_{emp}(\alpha) + \sqrt{\left(\frac{VC(H)(\log(2\ell/h) + 1) - \log(\eta/4)}{\ell} \right)}, \tag{3.30}$$

where $R_{emp}(\alpha)$ is the "empirical risk", i.e., the measured error on the training data, and ℓ is the size of the training set. The latter bound can be interpreted as follows: as the problem dimension increases, VC-dimension also increases that may decrease the

"empirical risk" since it becomes simpler to classify the training data, but also increase the upper bound of the "expected risk" on test data (in order to fix the bound, ℓ should be increased).

The mapping of the training set and the whole algorithm to a higher dimensional space may improve the generalization error, but computing this mapping may become computationally intractable for some Φ [Burges, 1998]. Fortunately, the formulation of SVM (3.29) does not require to explicitly know Φ, but only to know how to compute dot product of points. Hence if there exists a *kernel function* K defined on $\boldsymbol{X}$ such that $K(\boldsymbol{x}_i, \boldsymbol{x}_j) = \langle\, \Phi(\boldsymbol{x}_i), \Phi(\boldsymbol{x}_j) \,\rangle$ for all $(\boldsymbol{x}_i, \boldsymbol{x}_j)$ [Aizerman *et al.*, 1964], the problem (3.29) can be solved in $\boldsymbol{X}$. One example is the Radial Basis Function (RBF):

$$K_{RBF}(\boldsymbol{x}_i, \boldsymbol{x}_j) = \exp^{-||\boldsymbol{x}_i - \boldsymbol{x}_j||^2/2\sigma^2}, \tag{3.31}$$

where σ is a bandwidth parameter. RBF kernel maps any input point $\boldsymbol{x}_i$ onto a hyper-sphere of radius 1 since $K(\boldsymbol{x}_i, \boldsymbol{x}_i) = 1$.

According to Hilbert-Schmidt theory, $K(\boldsymbol{x}_i, \boldsymbol{x}_j)$ can be any symmetric function satisfying the following general *Mercel's* conditions [Vapnik, 1995]:

Theorem 1. *(Mercer) To guarantee that the symmetric function $K(u, v)$ form L_2 has an expansion*

$$K(\boldsymbol{u}, \boldsymbol{v}) = \sum_{k=1}^{\infty} a_k \langle\, \psi_k(\boldsymbol{u}), \psi_k(\boldsymbol{v}) \,\rangle \tag{3.32}$$

with positive coefficients $\alpha_k > 0$ (i.e., $K(\boldsymbol{u}, \boldsymbol{v})$ describes a dot product in some feature space), it is necessary and sufficient that the condition

$$\int\int K(\boldsymbol{u}, \boldsymbol{v}) g(\boldsymbol{u}) g(\boldsymbol{v}) d\boldsymbol{u} d\boldsymbol{v} > 0 \tag{3.33}$$

be valid for all $g \neq 0$ for which

$$\int g^2(\boldsymbol{u}) d\boldsymbol{u} < \infty \tag{3.34}$$

To extend the linear classification SVM to the non-linear case (see Figure 3.4-a,b) the "only" thing to do is to replace the dot product of points defined in the original decision space X (3.29) by $K(\boldsymbol{x}_i, \boldsymbol{x}_j)$ defined in the feature space $\Phi(X)$ as follows:

$$\begin{array}{l} \text{Maximize } \; L_D(\alpha) = \sum_{i=1}^{\ell} \alpha_i - \frac{1}{2} \sum_{i=1}^{\ell} \alpha_i \alpha_j y_i y_j K(\boldsymbol{x}_i, \boldsymbol{x}_j) \\ \text{subject to } \; 0 \leq \alpha_i \leq C, \quad i = 1, \ldots, \ell \end{array} \tag{3.35}$$

Thus, the decision function now is non-linear in the decision space:

$$\hat{f}_{classSVM}(\boldsymbol{x}) = \text{sign}\left(\sum_{i=1}^{\ell} y_i \alpha_i K(\boldsymbol{x}_i, \boldsymbol{x}) - b \right) \tag{3.36}$$

An efficient algorithm to find optimal α parameters of classification SVM can be found in [Platt, 1998].

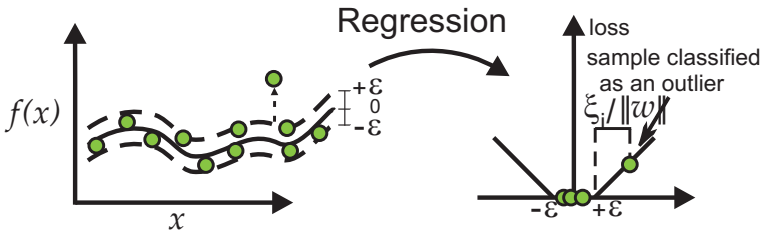

Figure 3.5: The soft margin $|\xi|_\epsilon$-loss setting for Support Vector Regression.

3.2.2 ϵ-Support Vector Regression (ϵ-SVR)

Considering a training set $\mathcal{D} = \{(\boldsymbol{x}_i, y_i), i = 1, \ldots, \ell\}$, where $\boldsymbol{x}_i \in \mathbb{R}^n, y_i \in \mathbb{R}$, ϵ-SVR proposed by [Vapnik, 1995] consists in finding a function $\hat{f}_{\epsilon SVR}$ that has at most ϵ deviation from the actual targets y_i for all training points, and at the same time is as flat/regular as possible (see Figure 3.5-a). ϵ-SVR does not take into account any approximation errors which are less than ϵ: this is defined by a so called ϵ-insensitive loss function $|\xi|_\epsilon$ [Smola and Schölkopf, 2004], illustrated in Figure 3.5-b and described as

$$|\xi|_\epsilon = \begin{cases} 0 \text{ if } |\xi| \leq \epsilon \\ |\xi| - \epsilon \quad \text{otherwise,} \end{cases} \tag{3.37}$$

The ϵ-SVR problem in primal form is defined as follows:

$$\begin{array}{l} \text{Minimize}_{\{\boldsymbol{w},\xi,\rho\}} \ \frac{1}{2}||\boldsymbol{w}||^2 + C\sum_{i=1}^{\ell}(\xi_i^{up} + \xi_i^{low}) \\ \text{subject to} \ \begin{cases} \langle \ \boldsymbol{w}, \boldsymbol{x}_i \ \rangle + b - y_i \leq \epsilon + \xi_i^{up}, \quad i = 1, \ldots, \ell \\ y_i - \langle \ \boldsymbol{w}, \boldsymbol{x}_i \ \rangle - b \leq \epsilon + \xi_i^{low}, \quad i = 1, \ldots, \ell \\ \xi_i^{up}, \xi_i^{low} \geq 0, \quad i = 1, \ldots, \ell, \end{cases} \end{array} \tag{3.38}$$

The dual problem in feature space is

$$\begin{array}{l} \text{Maximize} \ \ L_D(\alpha) = \sum_{i=1}^{\ell} y_i(\alpha_i^{up} - \alpha_i^{low}) - \epsilon\sum_{i=1}^{\ell}(\alpha_i^{up} + \alpha_i^{low}) \\ \qquad\qquad -\frac{1}{2}\sum_{i=1}^{\ell}\sum_{j=1}^{\ell}(\alpha_i^{up} - \alpha_i^{low})(\alpha_j^{up} - \alpha_j^{low})K(\boldsymbol{x}_i, \boldsymbol{x}_j) \\ \text{subject to} \ \begin{cases} 0 \leq \alpha_i^{up}, \alpha_i^{low} \leq C, \quad i = 1, \ldots, \ell \\ \sum_{i=1}^{\ell}(\alpha_i^{up} - \alpha_i^{low}) = 0 \end{cases} \end{array} \tag{3.39}$$

The prediction function of $f(x)$ is

$$\hat{f}_{\epsilon SVR}(\boldsymbol{x}) = \sum_{i=1}^{\ell}(\alpha_i^{up} - \alpha_i^{low})K(\boldsymbol{x}_i, \boldsymbol{x}) + b \tag{3.40}$$

The optimal α parameters and corresponding b can be found as described in [Smola and Schölkopf, 2004]. [Chang and Lin, 2001] proved that ϵ-SVR with pa-

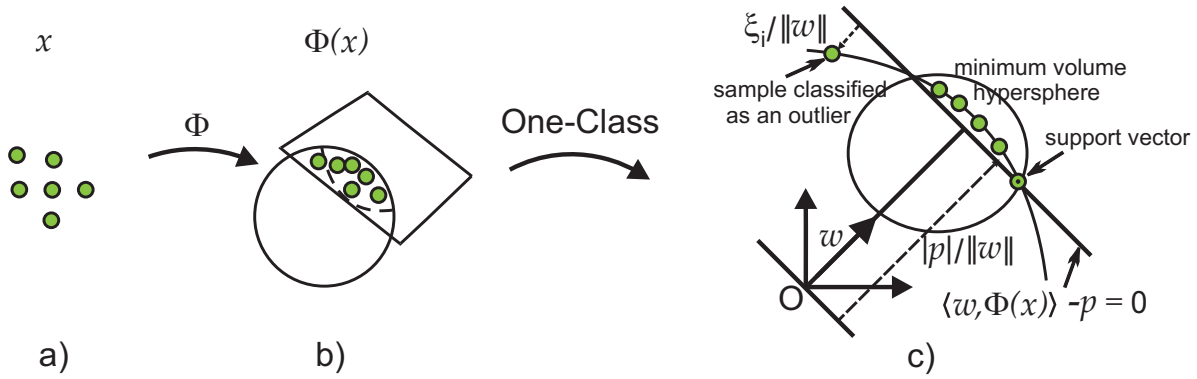

Figure 3.6: One-Class SVM maps training points of a single class **(a)** into the feature space **(b)** and separates them from the origin by the hyperplane **(c)** with maximum margin $\rho/||\boldsymbol{w}||$ to find the minimum volume hyperspace which encloses most of the training points.

rameters (C, ϵ) has the same solution as ν-Support Vector Regression (ν-SVR [Schölkopf *et al.*, 2000]) with parameters $(\ell C, \nu)$.

3.2.3 One-Class SVM

One-Class SVM was proposed by [Schölkopf *et al.*, 2001] for novelty and outliers detection. One-Class SVM learns a function $\hat{f}_{OneClassSVM}$ that takes the value +1 in "small" region capturing most of the training data and -1 elsewhere. The strategy is to separate the training data from the origin in the feature space by the hyperplane with maximum margin $\rho/||\boldsymbol{w}||$ (see Figure 3.6), and this is equivalent to finding the hyper-sphere with minimum volume that includes most of the training points [Tax and Duin, 2004]. Given training vector $\boldsymbol{x}_i \in \mathbb{R}^n, i = 1, \ldots, \ell$ without any class information, the primal problem of One-Class SVM is

$$\begin{aligned} &\text{Minimize}_{\{\boldsymbol{w},\xi,\rho\}}\ \tfrac{1}{2}||\boldsymbol{w}||^2 - \rho + \tfrac{1}{\nu\ell}\textstyle\sum_{i=1}^{\ell}\xi_i \\ &\text{subject to}\ \begin{cases} \langle\ \boldsymbol{w}, \boldsymbol{x}_i\ \rangle \geq \rho - \xi_i \quad i = 1, \ldots, \ell \\ \xi_i \geq 0, \quad i = 1, \ldots, \ell, \end{cases} \end{aligned} \tag{3.41}$$

where the parameter $\nu \in [0, 1]$ controls the trade-off between the radius of the hyper-sphere and the number of training points that it can hold, $\nu \in [0, 1]$ is also an upper bound on the fraction of outliers in the data set.

The dual problem in feature space is:

$$\begin{aligned} &\text{Minimize}\ \ L_D(\alpha) = \tfrac{1}{2}\textstyle\sum_{i=1}^{\ell}\sum_{j=1}^{\ell}\alpha_i\alpha_j y_i y_j K(\boldsymbol{x}_i, \boldsymbol{x}_j) \\ &\text{subject to}\ \begin{cases} 0 \leq \alpha_i \leq \frac{1}{\nu\ell}, \quad i = 1, \ldots, \ell \\ \sum_{i=1}^{\ell}\alpha_i = 1 \end{cases} \end{aligned} \tag{3.42}$$

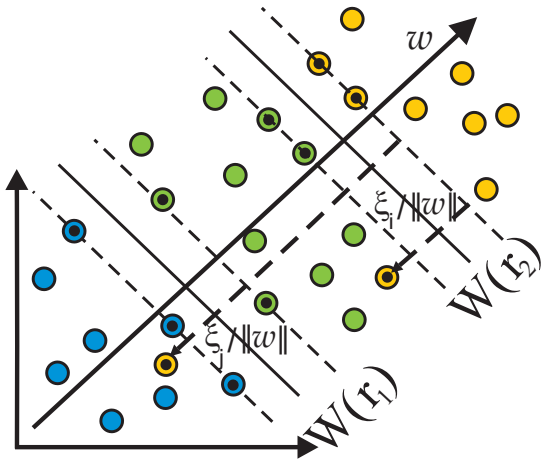

Figure 3.7: Three classes of points are illustrated: blue (rank 1), green (rank 2) and yellow (rank 3) points. The goal of ranking SVM is to find separated maximum-margin hyper-planes $\boldsymbol{W}(r_1)$ and $\boldsymbol{W}(r_2)$ with the norm $\boldsymbol{w}$ such that all points are correctly ranked w.r.t their score on $\boldsymbol{w}$.

The decision function is:

$$\hat{f}_{OneClassSVM}(\boldsymbol{x}) = \text{sign}\left(\sum_{i=1}^{\ell} y_i \alpha_i K(\boldsymbol{x}_i, \boldsymbol{x}) - \rho\right) \tag{3.43}$$

The optimal α parameters and corresponding ρ can be found as described in [Schölkopf *et al.*, 2001].

3.2.4 Ranking SVM

A new learning setting aimed at preference learning, a.k.a. *ordinal regression*, has been addressed within the SVM framework [Herbrich *et al.*, 1999, Joachims, 2005]. While preference learning can be cast as a classification problem on $X \times X$ (the class of $(\boldsymbol{x}, \boldsymbol{x}')$ is positive iff $\boldsymbol{x}$ is to be preferred to $\boldsymbol{x}'$), it may offer better generalization to formalize preference learning as an under-constrained regression problem, where the hypothesis h mapping X onto the real-valued space $\mathbb{R}$ is only required to satisfy $h(\boldsymbol{x}) > h(\boldsymbol{x}')$ whenever $\boldsymbol{x}$ is preferred to $\boldsymbol{x}'$. ϵ-SVR also can be used for ordinal regression (see Section 4.1.4).

Let $\mathcal{D} = \{\boldsymbol{x}_1, \ldots, \boldsymbol{x}_\ell\}$ and let $\mathcal{P}$ denote the set of m pairs (i, j) such that $\boldsymbol{x}_i$ is preferred to $\boldsymbol{x}_j$; the original formulation of rank-based SVM, involving all preference constraints, is as follows:

$$\text{Minimize}_{\{w,\xi\}} \frac{1}{2}||w||^2 + C \sum_{(i,j)\in\mathcal{P}} \xi_{i,j} \tag{3.44}$$

$$\text{subject to} \begin{cases} \langle w, x_i \rangle - \langle w, x_j \rangle \geq 1 - \xi_{i,j}, & \forall (i,j) \in \mathcal{P} \\ \xi_{i,j} \geq 0, & \forall (i,j) \in \mathcal{P} \end{cases} \tag{3.45}$$

where $\xi_{i,j}$ stands for the slack variable associated to the violation of the preference constraint associated to $(\boldsymbol{x}_i, \boldsymbol{x}_j)$.

The dual form in feature space is

$$\begin{array}{l}\text{Maximize}_{\{\alpha\}} L_D = \sum_{\forall(i,j)\in\mathcal{P}} \alpha_{ij} - \frac{1}{2}\sum_{\forall(i,j)\in\mathcal{P}}\sum_{\forall(u,v)\in\mathcal{P}} \alpha_{ij}\alpha_{uv}\left(K_{iu} - K_{iv} - K_{ju} + K_{jv}\right) \\ \text{subject to } 0 \leq \alpha_{ij} \leq C, \;\; \forall(i,j) \in \mathcal{P},\end{array} \tag{3.46}$$

where $K_{ij} = K(\boldsymbol{x}_i, \boldsymbol{x}_j)$.

The choice of constraints may significantly affect the model quality as well as the model learning computational complexity. Usually two cases are considered:

Linear in ℓ number of constraints , e.g., with $\ell - 1$ defined preference relations and corresponding constraints, when $\boldsymbol{x}_i$ is said to be preferred to $\boldsymbol{x}_{i+1}$ for $i = 1, \ldots, \ell - 1$. This may be sufficient for model learning, since the final chain will correctly rank all training individuals.

Super-linear/Quadratic in ℓ number of constraints , e.g., with 1.2ℓ (respectively, $\frac{(\ell-1)^2}{2}$ constraints), when $\boldsymbol{x}_i$ is preferred to some fraction of $\boldsymbol{x}_j$ for $i + 1 \leq j \leq \ell$ (respectively, to all $\boldsymbol{x}_j$ for $i + 1 \leq j \leq \ell$). This variant may be more robust if there is some uncertainty in preference relations.

We will discuss in detail both cases and the corresponding optimization procedures just before their application in Section 4.1.1 and Section 5.2.

When optimal α if found, the decision function that predicts the score of a test point $\boldsymbol{x}$ is defined as follows:

$$\hat{f}_{RankSVM}(\boldsymbol{x}) = \sum_{\forall(i,j)\in\mathcal{P}} \alpha_{ij}\left(K(\boldsymbol{x}_i, \boldsymbol{x}) - K(\boldsymbol{x}_j, \boldsymbol{x})\right) \tag{3.47}$$

The evaluated score of $\boldsymbol{x}$ allows to compute its rank with respect to the other evaluated points.

3.3 Surrogate-assisted Optimization

The basic idea of the surrogate-assisted optimization is to use one or several surrogate models $\hat{f}$ of the objective function f to improve the quality of the search (e.g., in terms of number of functions evaluations required to reach the optimum). It is usually assumed that the evaluation of f is expensive in terms of time or money and the learning of $\hat{f}$ is relatively cheap. $\hat{f}$ is learned/built from a set of pairs $(\boldsymbol{x}, f(\boldsymbol{x}))$ where actual f has been computed. $\hat{f}$ should be learned *optimally* for an algorithm $\mathcal{A}$ in the sense that there exists no $\hat{f}'$ such that $\hat{f}'$-assisted $\mathcal{A}$ performs statistically better than $\hat{f}$-assisted $\mathcal{A}$ (i.e., the optimum of f can be found faster in terms of number of function evaluations). Of course one can suppose that the *optimal* $\hat{f}$ in the sense described above should be equal to f, surprisingly this is not always the case. An illustrative example would be $f(\boldsymbol{x}) = \sum_{i=1}^{n} x_i^{10}$

and $\mathcal{A}$ is an algorithm which assumes a *quadratic* shape of f. In this case, $\hat{f}'(\boldsymbol{x}) \approx \sum_{i=1}^{n} x_i^2$ might be a better approximation *for this particular* algorithm $\mathcal{A}$ than $\hat{f}(\boldsymbol{x}) \approx \sum_{i=1}^{n} x_i^{10}$, because this $\hat{f}'$ corresponds to the class of functions the $\mathcal{A}$ was designed for, while the optimum of $\hat{f}'$ and f is the same. A similar effect was also investigated in the context of multi-modal optimization [Yew-Soon *et al.*, 2006], where a smoother approximation $\hat{f}'$ sometimes is preferred to a more precise approximation $\hat{f}$ of the rugged f, and is able to prevent the search from getting stuck in local optima.

The optimal learning of $\hat{f}$ and optimal interaction between $\hat{f}$ and $\mathcal{A}$ conceals many pitfalls and special cases in single- and multi-objective optimization, which we will discuss in this Section. A comprehensive survey of surrogate-assisted Evolutionary Algorithms can be also found in [Jin, 2005, Jin, 2011].

3.3.1 General Framework

A simple iteration of the surrogate-assisted algorithm is the following:

1. Learn $\hat{f}$ from training set of previously evaluated points $(\boldsymbol{x}, f(\boldsymbol{x}))$.
2. Use $\hat{f}$ in $\mathcal{A}$ (either by replacing f with $\hat{f}$, or by some other mechanism).
3. Compute additional points $(\boldsymbol{x}, f(\boldsymbol{x}))$.
4. Update training set.

In the following we will analyze in detail some steps of the described above procedure.

3.3.1.1 Model Quality Assessment

Without any doubts, the Mean Square Error (MSE) is the most popular model quality indicator in the literature. It is defined as follows:

$$\mathrm{MSE} = \frac{1}{\ell} \sum_{i=1}^{\ell} w_i (f(\boldsymbol{x}_i) - \hat{f}(\boldsymbol{x}_i))^2, \tag{3.48}$$

where $w_i = 1, i = 1, \ldots, \ell$ are the weights of the impact of each predicted $\hat{f}(\boldsymbol{x}_i)$ to the final error estimation.

This indicator was investigated in [Jin, 2003], where one important aspect was observed: *the Mean Square Error of the model only weakly correlates with the ability to select correct individuals*. This means that what we usually do (minimization of the MSE of the model) only weakly correlates with what we really need in comparison-based optimizers (only the correct ranking of individuals). The problem can be partially solved if the measure uses some rank-depended weighted error w_i. However, appropriate weights are usually unknown a priori.

[Jin, 2003] suggested to use the rank correlation coefficient [Spearman, 1904], given by

$$\rho^{(rank)} = 1 - \frac{6 \sum_{i=1}^{\lambda} d_i^2}{\lambda(\lambda^2 - 1)}, \tag{3.49}$$

as a measure for the monotonic relation between the ranks of two variables, where d_i is the difference between the ranks of the i-th offspring (among λ) individual based on the original fitness function and on the surrogate model. $\rho^{(rank)} = 1$ (respectively, $\rho^{(rank)} = -1$) when the model predicts correct (respectively, inverse) ranking of individuals. Again, weight coefficients can be defined to amplify the importance of better ranked individuals.

Rank-based quality indicators are *invariant* to rank-preserving transformations of the objective function, therefore, look quite promising for comparison-based Evolutionary Algorithms. However, they are rather unknown in the EC community, with a few exceptions [Ulmer *et al.*, 2004, Runarsson, 2006, Kern *et al.*, 2006, Ingimundardottir and Runarsson, 2011]. There is one simple reason for this: in most surrogate-assisted Evolutionary Algorithms there is no control of the model quality and the algorithm $\mathcal{A}$ uses the surrogate model $\hat{f}$ without online checking whether the model is good or not. This checking is usually done offline, such that the surrogate-assisted algorithm $\mathcal{A}$ does not fail, and this is usually achieved by setting quite conservative surrogate model hyper-parameters. The surrogate model quality indicators will attract much more attention when the comparison of different candidate surrogate models will become a common part of the learning procedure (see Section 4.3.2).

3.3.1.2 Training and Test Set Selection

Training set selection procedure should answer the question of which *training points* best represent the original function f to be used to build the *optimal* model $\hat{f}$. *Test set selection* is responsible for identifying which set of *test points* is best suitable for the model quality assessment.

Training Set Selection

There are three popular ways to select representative points for model learning:

1. **Best Points** Select ℓ points with the best fitness among all evaluated points seems to be a reasonable approach for unimodal noise-less optimization problems. If f is a noisy function, then this selection may become biased to noise-affected "lucky" points. If f is a multi-modal or noisy function, then the algorithm also may search far away or at a different scale from the subspace where best points were observed, therefore, $\hat{f}$ will be learned for a subspace which is far away from the actual optimal search subspace of $\mathcal{A}$.

2. **k-Nearest Neighbor Points** One can suppose that the k-nearest neighbor points ($k = \ell$) to some chosen point $\boldsymbol{m}$ (e.g., mean of the mutation distribution in ESs) best represent the actual search space and are good candidates for model learning. The Euclidean or Mahalanobis distance can be chosen as well as any other suitable similarity measure metric (see also clustering method for local models learning in [Liu *et al.*, 2009]). However, if f is a multi-modal function, it may happen that $\boldsymbol{m}$ is located around a local optimum visited by $\mathcal{A}$ many generations ago, and many of ℓ closest points to $\boldsymbol{m}$ may correspond to a small cluster of this local optimum, whose very precise learning may be undesirable.

3. **Recently Evaluated Points** One of the simplest strategy is to choose ℓ the most recently evaluated points, which are very likely to be reasonably good on f and relatively close to the actual search subspace of $\mathcal{A}$. This approach works reasonably well on noisy problems, but may be insufficiently "greedy", because it "forgets" promising individuals generated more than ℓ evaluations ago.

Optimal training and test set selection strategies depend on the surrogate modelling technique used and the optimization algorithm $\mathcal{A}$ (see Section 4.3.3.2), and probably should combine the described above approaches in some adaptive way.

Resampling Methods

Some approaches to model selection and validation such as *resampling methods* [Kohavi, 1995, Queipo *et al.*, 2005, Bischl *et al.*, 2012] can be applied almost independently on $\mathcal{A}$.

Split sample validation / Holdout With split sample validation, the whole dataset $\mathcal{D}$ of selected for model learning points is *splitted* into training set $\mathcal{D}_{training}$ and test set $\mathcal{D}_{test}$. The size of the test set $\ell_{test} = |\mathcal{D}_{test}|$ is usually smaller than the size of the training set $\ell = |\mathcal{D}_{training}|$, but still should be representative enough to estimate the generalization error and keep the confidence interval reasonably small. The test set is not used for model learning, because it would lead to overfitting. This limits the amount of information available for model learning and makes the estimate more biased. Another disadvantage is that the generalization error estimate is very sensitive to a particular split of training and test points.

Cross-validation In *k-fold cross-validation* [Stone, 1974] the dataset $\mathcal{D}$ is randomly splitted into k mutually exclusive subsets (*the folds*) $\mathcal{D}_1$,$\mathcal{D}_2$,...,$\mathcal{D}_k$. The cross-validation process is repeated k times, each time $i = 1, \ldots, k$, the model is trained and tested using training set $\mathcal{D}_i$ and test set $\mathcal{D}/\mathcal{D}_i$, respectively. The cross-validation estimate of accuracy is averaged over k estimates of each subset. In *leave-one-out cross-validation*, $k = \ell$ and the smallest possible test set $\mathcal{D}_i$ of only one test point ($|\mathcal{D}_i = 1|$) is considered. This procedure provides a good statistical estimate of accuracy, but may become computationally very expensive if $\mathcal{D}$ is large.

Bootstrap In contract to the cross-validation, where all subsets $\mathcal{D}_i$ are mutually exclusive, in *bootstrap* [Efron, 1979] the subsets are generated with replacement. Therefore, the probability of any point being chosen after ℓ trials is $(1/\ell)^\ell \approx e^{-1} \approx 63.2\%$ (for large ℓ), thus, only 63.2 % of $\mathcal{D}$ will be presented in the training set $\mathcal{D}_{training}$, while the remaining points form the test set $\mathcal{D}_{test}$. The final estimation of the error can be computed as the weighted sum of errors on the test and training sets. However, this still leads to a biased estimation of the generalization error, since some points are presented more than once in $\mathcal{D}_{training}$. An improvement version *.632 + bootstrap* was proposed in [Efron and Tibshirani, 1979], where the weights are corrected depending on a quantified relative overfitting rate.

A comprehensible analysis of successes and failures of the bootstrap and other resampling strategies is given in [Horowitz, 2001, Bickel *et al.*, 1997], and specifically for Evolu-

tionary Computation in [Tenne and Armfield, 2008, Bischl *et al.*, 2012]. Resampling approaches, while being powerful tools for accurate model quality estimation, still have only minor popularity in the EC community, mainly because of additional computations needed to re-learn the model several times. We envision that resampling approaches will become more relevant for complex multi-modal functions optimization and for surrogate-assisted algorithms, which tend to sample new candidate solution from mixed distributions, and, therefore, will need a careful estimation of the model error in different (disjoint) regions of the search space.

3.3.1.3 Selection of Surrogate Models and Hyper-parameters Adaptation

To build a surrogate model $\hat{f}$ of f for the surrogate-assisted optimization algorithm $\mathcal{A}$, a common approach is to choose a surrogate learning approach with suggested $\boldsymbol{\theta}$ hyper-parameters from the literature. This may become a difficult task in the context of surrogate-assisted optimization, because the ideal $\hat{f}$ depends on $\mathcal{A}$, the set of possible surrogate techniques to build this $\hat{f}$ is quite large (see Section 3.1 and Figure 3.1), and, finally, the suggested hyper-parameters are actually suggested for benchmark problems and not for the real-world problem at hand. An obvious solution to this problem is to consider multiple surrogates and get the best estimate of f. The two the most popular ways to aggregate the information from all surrogates in evolutionary and *non-evolutionary* optimization are the following [Viana and Haftka, 2008]:

1. **Best Surrogate** The idea to choose the best surrogate is obvious and probably was born on the same day when two surrogate models were built with different $\boldsymbol{\theta}$ hyper-parameters of the same surrogate technique. Since the earliest approaches [Zhang, 1993, Kohavi, 1995] the cross-validation has been intensively used for selecting surrogates. It is also a common practice in EC to build surrogate models using different techniques and then choose the best one for exploitation, for state-of-the-art approaches in this direction see [Viana, 2011].

2. **Weighted Average Surrogate (AWS)** [LeBlanc and Tibshirani, 1993] demonstrated that combining the estimators with some regularization can be useful for improving prediction performance. The *weighted average surrogate* $\hat{f}_{AWS}(\boldsymbol{x}) = \sum_{i=1}^{k} \hat{f}_k(\boldsymbol{x})$ is a weighted aggregation of k surrogate models $\hat{f}_i(\boldsymbol{x})$, where $\sum_{i=1}^{k} w_i = 1$. The option 'best surrogate' is also recovered if all weights but one are set to 0, and the option 'average surrogate' if all weights are equal. The averaging may guarantee some robustness, but an adaptation of the weights is definitely a more general and prospective strategy. A recent analysis of adaptive weights selection depending on error correlation, prediction variance and cross validation error for PRS, RBF, Kriging, GP, SVR surrogate models is given in [Acar and Rais-Rohani, 2009].

First papers on selection of surrogates were published many years before Evolutionary Computation even first time touched this subject, in the early 1990s. However, in the 2000s the EC community made a step further and many adaptive and self-adaptive approaches have been proposed. [Zhou *et al.*, 2007] shows that the combination of global and local

surrogate models performs better together than independently. [Shi and Rasheed, 2008] suggested to adaptively adjust the model complexity and the frequency of model usage according to time spent and model accuracy. An illustrative example of advances in surrogate model adaptation is the approach presented in [Gorissen *et al.*, 2009], where SVR, Kriging, ANN and Ensemble of surrogate models evolve *together* with their $\boldsymbol{\theta}$ hyper-parameters in a parallel Genetic Algorithm, and more successful surrogate models are better represented in the population.

3.3.1.4 Strategies of Surrogate Model Exploitation

The key aspect of surrogate-assisted optimization is to get and exploit maximum information from the surrogate model $\hat{f}$ of f, and this is usually realized in one of the following ways:

1. **Pre-selection of promising solutions** *Pre-selection* has become especially popular for Evolution Strategies [Emmerich *et al.*, 2002, Ulmer *et al.*, 2004], where λ individuals are generated at each iteration. In pre-selection strategy there are two popular options: i). generate $\lambda_{Pre} > \lambda$ individuals, then pre-select and evaluate only $\lambda' = \lambda$ (usually) best individuals according to $\hat{f}$; ii). generate $\lambda_{Pre} = \lambda$ individuals, pre-select and evaluate only $\lambda' < \lambda$ and use $\hat{f}$ estimate for ranking the other individuals. In both cases if $\hat{f}$ well approximates f, the overall number of function evaluations can be reduced thanks to a quicker (for the first case described above) or comparable (the second case with smaller than λ evaluations per generation) progress per generation toward the optimum of f.

2. **Surrogate-informed operators** All operators of Evolutionary Algorithms in principle may benefit from knowing more information about f or at least its good approximation $\hat{f}$. **Informed operators** [Rasheed and Hirsh, 2000] such as crossover [Anderson and Hsu, 1999] or mutation [Abboud and Schoenauer, 2002] provide the capability of quickly moving generated individuals toward regions with improved fitness.

3. **Direct optimization of the surrogate model** If $\hat{f}$ is a reasonably good approximation of f, then it can be used *in lieu* of f for optimization [Jin *et al.*, 2002]. A crucial point is to control the optimal time/number of generations that $\hat{f}$ should be used to obtain the maximum speedup and prevent the algorithm from divergence when $\hat{f}$ is imprecise.

The described above approaches are not that different from each other: the pre-selection when $\lambda_{Pre} > \lambda$ can be viewed as a Monte-Carlo search with the budget of λ_{Pre} function evaluations, and the pre-selection is actually an informed operator. They are also similar in the sense that in both cases a model quality based control should be used to maximize the speedup and prevent divergence. In this thesis, we will use both the pre-selection in Sections 4.2, 5.3 and direct optimization in Section 4.3.

It should be noted that some surrogate models, such as Kriging, provide not only an estimation of the fitness of a tested point, but also the level of uncertainty of this estimation. There is a sub-field of optimization (see, e.g., Efficient Global Optimization (EGO) algorithm in [Jones *et al.*, 1998]), which focuses on the *expected improvement* maximization $\mathbb{E}[max(f(\boldsymbol{x}) - Y, 0)]$, where Y is a random variable that models the uncertainty of the estimation of $f(\boldsymbol{x})$.

3.3.2 Single-objective Case

In this Section, we will focus on state-of-the-art surrogate-assisted Evolution Strategies.

3.3.2.1 Surrogate-assisted Evolution Strategies

Probably the first surrogate-assisted $(\mu + \lambda)$-ES and (μ, λ)-ES were proposed in [Papadrakakis *et al.*, 1998], where evaluations of an expensive structural optimization problem were replaced by a hidden-layer ANN trained by back-propagation. The authors suggested to re-learn the model at each iteration adding new training points randomly drawn from a Gaussian distribution with the mean located in the center of the decision space. They also reported that a speedup of a factor of 10 can nevertheless be obtained.

[Jin *et al.*, 2001b] proposed *individual-based* and *generation-based* evolution control strategies for surrogate-assisted search with CMA-ES. Individual-based strategy corresponds to the pre-selection strategy, where random (*random strategy*) or best (*best strategy*) *controlled* individuals may be evaluated on the expensive function. In generation-based strategy the whole population will be evaluated on the expensive function for η generations every κ generations, where $\eta \leq \kappa$. The authors found that in both cases about 50% of individuals should be evaluated in order to have a good final speedup, but employed only the generation-based strategy, because they found it more suitable for parallel implementation. It is suggested to set the fraction of generations $\frac{\eta}{\kappa}$ that $\hat{f}$ is optimized to be proportional to $\frac{E(k)}{E_{max}}$, where $E(k)$ and E_{max} are current and maximum model errors, respectively [1]. The cost function of the ANN-based surrogate is defined by

$$E = \frac{1}{\ell} \sum_{i=1}^{\ell} p(\boldsymbol{x}_i)(f(\boldsymbol{x}_i) - \hat{f}_{ANN}(\boldsymbol{x}_i))^2, \tag{3.50}$$

where $p(\boldsymbol{x}_i)$ is the weight for a sample $\boldsymbol{x}_i$, calculated using the covariance matrix $\mathbf{C}$ of CMA-ES:

$$p(\boldsymbol{x}_i) = exp(-\frac{1}{2}(\boldsymbol{x}_i - \boldsymbol{q})^T \mathbf{C}^{-1} (\boldsymbol{x}_i - \boldsymbol{q})), \tag{3.51}$$

where $\boldsymbol{q}$ is an individual in the current population to be refereed. To reduce the complexity of training set selection, all individuals with a weight smaller than a given threshold are discarded in learning.

[1] We found that we actually reinvented this simple idea in our surrogate-assisted CMA-ES, described in Section 4.3.1.3.

The experimental validation on 20-dimensional Ackley and Rosenbrock functions as well as on a real-world problem with computational fluid dynamics (CFD) simulations showed that the generation-based surrogate-assisted CMA-ES outperforms the original CMA-ES and that the weighted MSE estimation (3.50) is preferred to the original MSE estimation (3.48).

[Emmerich *et al.*, 2002] studied Kriging model based pre-selection strategy within (μ, κ, λ)-ES [Schwefel, 1993] with $\mu = 15$, $\lambda = 100$ and $\kappa = 5$, where the individuals that exceed the age of $\kappa = 5$ generations are eliminated from the selection procedure. The authors suggested to evaluate the best $\lambda' = 10$ individuals w.r.t. a criterion based on both the estimated value $\hat{f}(\boldsymbol{x})$ and the estimated local standard deviation $\hat{\sigma}(\boldsymbol{x})$ of the prediction RBF model:

$$S_c(\boldsymbol{x}) = \hat{f}(\boldsymbol{x}) - \alpha\hat{\sigma}(\boldsymbol{x}), \tag{3.52}$$

where α defines the selection trade-off between the most promising solutions with $\alpha = 0$ and promising solutions in still unexplored search areas with $\alpha > 0$. The experimental validation of the proposed surrogate-assisted algorithm showed that on unimodal functions the exploration ($\alpha = 1$) does not harm, but leads to a better convergence on multi-modal functions than $\hat{f}$-based selection ($\alpha = 0$).

[Ulmer *et al.*, 2003b] studied RBF networks based pre-selection strategy for (2,8)-ES with $\lambda_{Pre} = 30$ and (1+1)-ES with $\lambda_{Pre} = 10$ and concluded that the proposed meta-model assisted ES (MAES) performs better, especially on unimodal functions. Later [Ulmer *et al.*, 2003a] analyzed GP based pre-selection strategy similar to the one of [Emmerich *et al.*, 2002] for CMA-ES, where expected improvement was chosen as a selection criterion. The results confirmed the observations of [Emmerich *et al.*, 2002] that on multi-modal functions the expected improvement-based pre-selection should be preferred to "greedy" $\hat{f}$-based pre-selection. [Ulmer *et al.*, 2004] further studied SVR-based pre-selection strategy for (μ, λ) Main Vector Adaptation (MVA [Poland and Zell, 2001], a CMA-ES variant with linear time and space complexity). They proposed to adjust λ_{Pre}, depending on a model quality measure similar to the one proposed by [Jin, 2003] and defined as summed rank of all correctly selected individuals. At each generation t the actual model quality Q^t is compared to a quality Q^{rand} measured for the random model. The update procedure is the following:

$$\lambda_{Pre}^{t+1} = \begin{cases} \lambda_{Pre}^t + \frac{Q^{max} - Q^t}{Q^{max} - Q^{rand}}\delta_{\lambda_{Pre}} & \text{if } \; Q^t > Q^{rand} \\ \lambda_{Pre}^t - \frac{Q^{rand} - Q^t}{Q^{rand}}\delta_{\lambda_{Pre}} & \text{otherwise,} \end{cases} \tag{3.53}$$

where Q^{max} is the maximum possible quality. Experimental results of the proposed *C-MAES* on unimodal and multi-modal functions confirmed that the adaptation works well even in dynamically changing noisy environment, where the speedup up to a factor of 2 also can be achieved.

[Runarsson, 2004] found that it is always desirable to evaluate on f at least one best point among λ evaluated on $\hat{f}$, and proposed *approximate ranking procedure* which suggests to evaluate on f several additional points only if the model changes its ranking prediction of λ points (see the next Section for details).

[Poland, 2004] proposed an ES-like algorithm with quadratic meta-models, which showed the best results in the literature for an Evolutionary Algorithm on popular Rosenbrock benchmark problem, where it outperformed CMA-ES by a factor of 4. Unfortunately, the algorithm is not invariant to rank-preserving transformation and its performance probably will degrade significantly if f is scaled differently (also true for all regression to value based surrogate-assisted optimizers).

[Buche *et al.*, 2005] proposed Gaussian Process Optimization Procedure (GPOP) which suggests to repeat the following procedure. First, build a GP based model and directly optimize Eq. (3.52) by CMA-ES. When a local optimum for a given α is found, it can be evaluated on f and added to the training set. The training set consists of the union of the N_C closest points to the current best solution and the N_R most recently evaluated points. The search space for each local search is constrained by the hyper-rectangle around the current best solution. The GPOP outperforms CMA-ES on Sphere and Schwefel functions, but already for Rosenbrock the speedup is less than 2.0 for $n = 8, 16$ and less than 0.4 for $n = 32$. On multi-modal Rastrigin function GPOP is always outperformed by CMA-ES.

[Runarsson, 2006] first proposed to use *ordinal regression* and Ranking SVM as surrogate models in Evolutionary Computation. The author studied the performance of Ranking SVM based CMA-ES within the approximate ranking procedure and found that the surrogate-assisted version outperforms the original CMA-ES for $n \leq 5$, but shows no improvements for $n > 5$. The latter can be explained by the use of very small training set of only 60 training points. However, this paper has played an important role in the development of comparison-based surrogates that we will propose in Chapter 4.

[Hoffmann and Holemann, 2006] suggested to keep λ_{Pre} fixed, but adapt λ using the following formula, similar to (3.53):

$$\lambda^{t+1} = \begin{cases} max(\lambda^t - \frac{Q^{max}-Q^t}{Q^{rand}}\delta_\lambda, \mu) & \text{if } Q^t > Q^{rand} \\ min(\lambda^t + \frac{Q^{max}-Q^t}{Q^{max}-Q^{rand}}\delta_\lambda, \lambda_{Pre}) & \text{otherwise,} \end{cases} \tag{3.54}$$

Thus, the better the model - the smaller λ^{t+1}, and vice versa. The results of the proposed λ-controlled surrogate-assisted λ-*CMA-ES* are similar, but not directly comparable to [Ulmer *et al.*, 2004], where MVA was used as a baseline algorithm. A comparison in [Hebbel and Nisticò, 2008] confirmed that λ-CMA-ES and C-MAES have comparable performance on a robot's walking optimization problem. For a detailed analysis of different model quality indicators used to adapt λ the interested reader is refereed to [Gräning *et al.*, 2007].

3.3.2.2 The Local Meta-model CMA-ES (lmm-CMA-ES)

The local meta-model CMA-ES was first proposed by [Kern *et al.*, 2006] and later extended for large populations by [Bouzarkouna *et al.*, 2010] and for partially-separable functions by [Bouzarkouna *et al.*, 2011]. It is one of the most carefully designed surrogate-assisted CMA-ES algorithms.

Locally Weighted Regression In lmm-CMA-ES the locally weighted regression (LWR, [Atkeson *et al.*, 1997]) surrogate model $\hat{f}$ is build around each generated offspring

individual $\boldsymbol{q} \in \mathbb{R}^n$ using a set of training points $(\boldsymbol{x}_i, y_i), i = 1, \ldots, \ell$. The model error A is minimized w.r.t. the parameters $\boldsymbol{\beta}$ of the local model ($\hat{f} = \tilde{\boldsymbol{x}}^T \cdot \boldsymbol{\beta}$) at query point $\boldsymbol{q}$ and can be written as

$$A(\boldsymbol{q}) = \sum_{i=1}^{\ell} \left[(\hat{f}(\boldsymbol{x}_i, \boldsymbol{\beta}) - y_i)^2 K\left(\frac{d(\boldsymbol{x}_i, \boldsymbol{q})}{h}\right)\right], \tag{3.55}$$

where $K(.)$ is the kernel function and $d(\boldsymbol{x}_i, \boldsymbol{q})$ is the distance between data points $\boldsymbol{x}_i$ and $\boldsymbol{q}$, and h is the local bandwidth. [Kern *et al.*, 2006] investigated surrogates with different model complexity and reported that the best performance on test problems is achieved with the *full quadratic* surrogate models defined as

$$\hat{f}(\boldsymbol{x}, \boldsymbol{\beta}) = \boldsymbol{\beta}^T (x_1^2, \ldots, x_n^2, x_1 x_2, \ldots, x_{n-1} x_n, x_1, \ldots, x_n, 1)^T, \tag{3.56}$$

where $\boldsymbol{\beta} \in \mathbb{R}^{\frac{n(n+3)}{2}+1}$. The weights matrix $\boldsymbol{W}$ of Eq. (3.2) was set by [Kern *et al.*, 2006] to $\mathrm{diag}(\sqrt{K(d(\boldsymbol{x}_i, \boldsymbol{q})/h)}) \in \mathbb{R}^{\ell \times \ell}$. For the calculation of $d(x_j, \boldsymbol{q})$ [Kern *et al.*, 2006] proposed to use the covariance matrix $\mathbf{C}$ adapted by CMA-ES to take into account correlations between the variables and compute the Mahalanobis distance:

$$d(\boldsymbol{x}_j, \boldsymbol{q}) = \sqrt{(\boldsymbol{x}_j - \boldsymbol{q})^T \mathbf{C}^{-1} (\boldsymbol{x}_j - \boldsymbol{q})} \tag{3.57}$$

The kernel K is chosen to be bi-quadratic:

$$K(\zeta) = \begin{cases} (1-\zeta)^2 & \text{if } \zeta < 1, \\ 0 & \text{otherwise} \end{cases} \tag{3.58}$$

The bandwidth h is defined by the distance to the k-th nearest neighbor point to $\boldsymbol{q}$, where $k = n(n+3) + 2$ was chosen after some experimental analysis on Sphere, Ellipsoid and Rosenbrock functions.

Approximate Ranking Procedure In lmm-CMA-ES the surrogate model exploitation is controlled by the *approximate ranking procedure* [Runarsson, 2004], which suggests to evaluate with f only a fraction of λ new individuals if the ranking of some of λ individuals on surrogate models of the current and previous generations remains unchanged. In lmm-CMA-ES the original fitness evaluation procedure of CMA-ES is replaced by the following procedure, where initially all $n_b = \lambda$ individuals are evaluated on f, then the number of evaluated individuals per iteration is increased (starting with n_{init}) by $n_b = max\left(1, \lfloor \frac{\lambda}{10} \rfloor\right)$ as surrogate models show poor quality of prediction:

1. *build* λ models $\hat{f}_i(\boldsymbol{x})$ for all $i = 1, \ldots, \lambda$ individuals of the current population $(\boldsymbol{x}_i, f(\boldsymbol{x}_i))_{i \leq \lambda}$.

2. *rank* individuals according to their approximated value $\hat{f}(\boldsymbol{x})$: $\boldsymbol{x}_{i:\lambda_{n_{ic}=0}}$.

3. *evaluate* the best n_{init} individuals with the true objective function f and *add* their evaluations to the training set.

4. **for** $n_{ic} = 1, \ldots, \left\lfloor \frac{\lambda - n_{init}}{n_b} \right\rfloor$ **do**

   (a) *build* λ models $\hat{f}_i(\boldsymbol{x})$ for all $i = 1, \ldots, \lambda$ individuals of the current population $(\boldsymbol{x}_i, f(\boldsymbol{x}_i))_{i \leq \lambda}$.

   (b) *rank* individuals according to their approximated value $\hat{f}_i(\boldsymbol{x})$: $\boldsymbol{x}_{i:\lambda_{n_{ic}}}$.

   (c-1) **if** $(\boldsymbol{x}_{i:\lambda_{n_{ic}}} = \boldsymbol{x}_{i:\lambda_{n_{ic}-1}}$, for $i = 1, \ldots, \lambda)$ // *ranking of the* λ *best is the same* **then** the meta-model is accepted, GO TO STEP 5.

   (c-2) **if** $((n_{init} + n_{ic} n_b < \frac{\lambda}{4})$ **and** $(\boldsymbol{x}_{i:\lambda_{n_{ic}}} = \boldsymbol{x}_{i:\lambda_{n_{ic}-1}}$, for $i = 1, \ldots, \mu))$ // *less than one-fourth of the population is evaluated and ranking of the* μ *best is the same* **or** $((n_{init} + n_{ic} n_b \geq \frac{\lambda}{4})$ **and** $(\boldsymbol{x}_{1:\lambda_{n_{ic}}} = \boldsymbol{x}_{1:\lambda_{n_{ic}-1}}))$ // *at least one-fourth of the population is evaluated and the best individual is the same* **then** the meta-model is accepted, GO TO STEP 5.

   (d) *evaluate* the n_b best unevaluated individuals with the true objective function f and *add* their evaluations to the training set.

5. **if** $(n_{ic} > 2)$ **then** $n_{init} = min(n_{init} + n_b, \lambda - n_b)$.
   else if $(n_{ic} < 2)$ **then** $n_{init} = max(n_b, n_{init} - n_b)$.

In the original lmm-CMA-ES [Kern *et al.*, 2006], the model is accepted if the surrogate-based ranking of all λ individuals remains unchanged after adding new n_b points to the training set, this model acceptance criterion corresponds to line 4.(c-1) of the procedure described above. A less conservative model acceptance criterion described in line 4.(c-2) was proposed in [Bouzarkouna *et al.*, 2010], the corresponding algorithm is called nlmm-CMA-ES. When λ is large it becomes quite difficult to avoid small perturbations of ranking and keep it exactly the same after adding new batch of points. For this case if more than one-fourth of the population is already evaluated the new criterion suggests to accept the model if the ranking of the best individual does not change.

Performance of lmm-CMA-ES and nlmm-CMA-ES Performance of lmm-CMA-ES and different versions of nlmm-CMA-ES was tested on Sphere, Schwefel, Rosenbrock and Rastrigin functions in dimensions 2, 4, 8 and 16 [Kern *et al.*, 2006, Bouzarkouna *et al.*, 2011]. Both algorithms show a speedup between a factor of 1.1 and 6.7 (usually between 2 and 4) in comparison with the original CMA-ES. In contrast to the original lmm-CMA-ES, nlmm-CMA-ES is able to better keep this speedup for larger populations than the default $\lambda_{default} = 4 + 3 \lfloor log(n) \rfloor$. An important drawback of the algorithm was discussed already in [Kern *et al.*, 2006] and further studied in [Kern *et al.*, 2007]: the time complexity of the original algorithm scales with $O(n^6)$, limiting the range of application to problems with $n \lesssim 15$. Several alternative approaches were proposed in [Kern *et al.*, 2007] to reduce the time complexity to $O(n^4)$, however, the observed cost in terms of number of floating points operations per saved function evaluation still scales with $O(n^5)$ [Kern *et al.*, 2007].

Besides from the time complexity of the algorithm (relevant for both versions), lmm-CMA-ES has two other important drawbacks: i). the evaluation of individuals cannot be

efficiently parallelized; ii). the algorithm loses the invariance of the original CMA-ES w.r.t. rank-preserving transformation of f. Suppose that there are $\lambda_{default}$ CPUs and the evaluation of $\lambda_{default}$ individuals on the expensive f runs in parallel on each CPU independently, if the evaluations are not heterogeneous (see [Yagoubi and Schoenauer, 2012] for an analysis of heterogeneous case), then there are might be a speedup of the original CMA-ES by a factor of λ. In lmm-CMA-ES all individuals are evaluated in the batch of maximum size $n_b = \lfloor \lambda/10 \rfloor$, i.e., the evaluation of λ individuals will take $\frac{\lambda}{n_b} = 10$ times more time. Given that the speedup of lmm-CMA-ES is usually smaller than 10 in this scenario (in number of function evaluations), we will actually lose the time with comparison to the original CMA-ES. Therefore, the use of the nlmm-CMA-ES in the scenario of parallel evaluations does not make much sense for both default and large population sizes. The drawback of the lmm-CMA-ES is that it uses the metric regression (regression to value) in its quadratic meta-model, therefore scaling of f will change the meta-model and the quality of the approximation. This effect is observed for the Schwefel function $f_{Schwefel}(\boldsymbol{x}) = \sum_{i=1}^{n}(\sum_{j=1}^{i} x_j)^2$ and its scaled variant $f_{Schwefel^{1/4}} = (f_{Schwefel}(\boldsymbol{x}))^{1/4}$, where the speedups for nlmm-CMA-ES in dimension 4 is 5.4 and 2.9, respectively [Bouzarkouna *et al.*, 2010]. We suppose that the loss of invariance of CMA-ES w.r.t. rank-preserving transformation of f may lead to no speedup at all of lmm-CMA-ES on the same test problem under certain rank-preserving transformations of f. It also should be noted that all original problems in [Kern *et al.*, 2006, Bouzarkouna *et al.*, 2010] have local or global quadratic landscape, and this is desirable property for quadratic meta-models.

3.3.3 Multi-objective Case

Surrogate-assisted multi-objective evolutionary optimization is a relativity new field, which was born in the early 2000s and the majority of the papers were published during the last three-four years.

One of the first attempts to extend the surrogate-assisted evolutionary search to the multi-objective case was made by [Yang *et al.*, 2002], who proposed to build Kriging-based surrogates $\hat{f}_i$ for each objective f_i and enrich the training set using few points (usually only two or three) from a set of non-dominated points found after multi-objective optimization (and niching) of surrogates $\hat{f}_i$. [Farina, 2002] proposed a very similar approach with ANN-based surrogate models (see also ANN-NSGA-II [Nain and Deb, 2003]), where in order to increase the diversity of the training set, a point from the most unexplored area of the search space is evaluated (to find such point is an additional single-objective optimization problem). The concept of the direct optimization of surrogates $\hat{f}_i$ is quite trivial, but seems to be very reasonable if f_i can be approximated efficiently and problem dimension is relatively small.

Later [Voutchkov and Keane, 2006] studied the same approach and compared different types of Kriging, RBF and Polynomial models. The authors reported very interesting results: on 10-dimensional ZDT2 and ZDT3 functions the proposed surrogate-assisted algorithms using about 100 function evaluations find a Pareto front approximation comparable to the one found by NSGA-II after about 10000 evaluations (our indirect estimate). This is probably one of the most important results in the field one should keep in mind,

because it shows "the real" complexity of these ZDT functions.

Instead of learning m different $\hat{f}_i$ surrogate models, another approach is to learn and exploit only one global modal $\hat{f}_g$, which will aggregate the information about f. In ParEGO [Knowles, 2006], an extension of EGO algorithm for Pareto optimization, at each iteration the algorithm builds a randomly-weighted aggregated model $\hat{f}_g$. Then, the best solution found after optimization of $\hat{f}_g$ for a fixed number of generations is estimated and added to the training set. In contrast to the direct optimization of $\hat{f}_i$ surrogates that results to a set of non-dominated solutions, in ParEGO only one solution is obtained at each iteration, and, therefore, we should be able to properly formulate a priori our preferences (see the discussion of preference-based and ideal principles in Section 2.4.2).

[Emmerich and Naujoks, 2004] proposed CR-NSGA-II (NSGA-II with multiple Kriging-based surrogate models), where at each iteration only λ' the most promising points are evaluated on f_i (e.g., not dominated by μ parents) out of λ offspring evaluated on $\hat{f}_i$. [Emmerich *et al.*, 2006a] formalized the notion of expected improvement in multi-objective optimization in terms of hypervolume indicator, such that pre-selection is seeking to maximize contributing hypervolume minimizing Eq. (3.52), where α controls the trade-off between exploration and exploitation. [Ponweiser *et al.*, 2008] followed the idea of [Emmerich *et al.*, 2006a] to calculate expected hypervolume contribution of a potential solution and proposed the hypervolume selection-based EGO (SMS-EGO). SMS-EGO outperforms Par-EGO [Ponweiser *et al.*, 2008] and is comparable to MOEA/D-EGO [Zhang *et al.*, 2010], which extends MOEA/D to multi-objective optimization and is based on a simple pre-selection with some niching in the decision space.

To summarize, both approaches of building individual $\hat{f}_i$ and global $\hat{f}_g$ surrogates are popular, there is, however, a trend to build individual surrogates for each objective and optimize or pre-select solutions w.r.t. expected hypervolume contribution improvement. However, since this approach usually assumes sequential evaluation of solutions, it might be less promising in the scenario with parallel evaluations of solutions.

3.4 Discussion

Most of the surrogate modeling methods surveyed in this Chapter build a surrogate model $\hat{f}$ of the actual expensive function f which minimizes the mean square error of the prediction of *exact values* $f(\boldsymbol{x})$ of training points. However, there are some disadvantages of the use of MSE as a loss function for surrogate model learning and assessment:

1. MSE is only weakly correlated with the ability to correctly select best/prospective individuals [Jin, 2003], while the correct selection/ranking of individuals is the only thing that is needed from f in comparison-based evolutionary optimizers.

2. MSE is not invariant w.r.t. rank-preserving transformations of f, and hence so are not all MSE-based surrogate-assisted optimization algorithms.

3. MSE is not interpretable for a black-box f and can be used heavily as a quality indicator in surrogate model control procedures.

The disadvantages described above are also relevant for all quality indicators which use exact values of f and not only the information about comparison relations between the points, which is actually sufficient to build surrogate model. In this Chapter, we presented the Ranking SVM approach which learns the ranking of training points and predicts the score of test points. In contrast to PR, ANN, RBF, GP, Ranking SVM is invariant to rank-preserving transformations of f, that we believe (and will demonstrate) is the key source of robustness.

Another important aspect of surrogate modeling is the computational complexity of model learning and testing. GP, RBF and PR models scale at least with $O(\ell^3)$ and/or $O(n^3)$, and this limits their application to low-dimensional problems. ANNs are cheaper to compute, but the model quality heavily depends on the ANN's structure and the learning itself is a multi-modal problem. In contrast to ANNs, the learning of Ranking SVM model is a convex quadratic programming problem, whose optimum is unique and can be found by any quadratic programming solver. We will also show in Section 4.1 that the learning of Ranking SVM is much cheaper and typically scales with $O(\ell^2)$.

The choice of "appropriate" hyper-parameters (e.g., number of training points) for surrogate learning procedure is the key problem of efficient surrogate-assisted optimization. It would be desirable to have a way to automatically detect optimal hyper-parameters which are, indeed, algorithm- and problem-dependent. In Section 4.3, we will show how to automatically tune/optimize surrogate model hyper-parameters during the optimization of the expensive function, thus, significantly reducing the problem of optimal model learning and hyper-parameters selection.

Part III

Contributions

Chapter 4

Single-Objective Surrogate-Assisted CMA-ES

> *From the practical point of view, it is so urgently desirable to obtain the smallest probable error with a given number of subjects, that the method of rank must often have the preference even when we are dealing with two series of measurements properly comparable with one another.*
> *Charles Spearman, 1904, The Proof and Measurement of Association between Two Things.*

In this Chapter, we demonstrate the advantages of the use of ordinal regression over metric regression in surrogate-assisted optimization, and CMA-ES in particular. In Section 4.1, we analyze in detail the learning procedure of Ranking SVM, discuss the question of the choice of Kernel function and demonstrate comparative results of Ranking SVM and SVR. In Section 4.2, we present the surrogate-assisted rank-based CMA-ES (ACM-ES) algorithm, published in [Loshchilov *et al.*, 2010c], which is based on pre-selection of promising offspring on $\hat{f}$. In Section 4.3, we discuss the advantages and drawbacks of the original ACM-ES and propose the self-adaptive surrogate-assisted CMA-ES (s*ACM-ES), published in [Loshchilov *et al.*, 2012e, Loshchilov *et al.*, 2012b, Loshchilov *et al.*, 2012c]. The algorithm relies on iterative optimization of f for one generation and $\hat{f}$ for $\hat{n}$ generations, where $\hat{n}$ depends on the prediction quality of $\hat{f}$. We also show that hyper-parameters α used to build $\hat{f}$ can be adapted during the optimization, such that the user is only required to define the range of these parameters. The algorithm is experimentally validated on BBOB benchmark problems, where it shows best results for ill-conditioned problems, outperforming such algorithms as IPOP-aCMA-ES, BFGS and NEWUOA. In Section 4.4, we conclude the Chapter with a discussion and some perspectives for further research.

4.1 Ordinal Regression

The problem of predicting variables of ordinal scale is called *ordinal regression* or *learning to rank*, even though the latter is a broader term (see, e.g., [Li, 2011]). Ordinal regression can be viewed as a special case of *preference learning*, where the statement $\boldsymbol{x}$ is preferred to $\boldsymbol{y}$ can be simply expressed as an inequality relation $f(\boldsymbol{x}) > f(\boldsymbol{y})$ [Chu and Ghahramani, 2005b]. The goal of preference learning is to learn the underlying ordering $\hat{f}$ over the instances from these pairwise preference relations. Preference learning may deal with contradicting preferences, while in ordinal regression the transitivity is

usually assumed. We will analyze preference learning in a context of surrogate-assisted multi-objective optimization in Section 5.2. In this Section, we will investigate ordinal regression within Ranking SVM, proposed by [Herbrich *et al.*, 1999] and popularized by [Joachims, 2005, Chu and Keerthi, 2005].

4.1.1 Learning to Rank using Ranking SVM

One can rewrite the primal form of Ranking SVM Eq. (3.44) in a more general form with individual constraint violation weights C_i and desirable difference ϵ_i on $\hat{f}$ for each pair of preference constraints as follows:

$$\text{Minimize}_{\{w,\xi\}} \ \frac{1}{2}||w||^2 + \sum_{i=1}^{|\mathcal{P}|} C_i \xi_i \tag{4.1}$$

$$\text{subject to} \begin{cases} \langle w, x_a \rangle - \langle w, x_b \rangle \geq \epsilon_i - \xi_i, & i = 1, \ldots, |\mathcal{P}|; (a,b) \leftarrow \mathcal{P}_i \\ \xi_i \geq 0, & i = 1, \ldots, |\mathcal{P}|, \end{cases} \tag{4.2}$$

where $\mathcal{P}$ denote the set of pairs (a, b) such that $\boldsymbol{x}_a$ is preferred to $\boldsymbol{x}_b$.
Then, the dual form of Ranking SVM will have the following form:

$$\begin{aligned} &\text{Maximize}_{\{\alpha\}} L_D = \textstyle\sum_{i=1}^{|\mathcal{P}|} \alpha_i \epsilon_i - \frac{1}{2} \sum_{i=1}^{|\mathcal{P}|} \sum_{j=1}^{|\mathcal{P}|} \alpha_i \alpha_j \, dK_{ij} \\ &\text{subject to } 0 \leq \alpha_i \leq C_i \quad i = 1, \ldots, |\mathcal{P}|, \end{aligned} \tag{4.3}$$

where $dK_{ij} = K(x_a, x_b) - K(x_a, x_d) - K(x_c, x_b) + K(x_c, x_d)$ for two pairs of constraints $\mathcal{P}_i = (a, b)$ and $\mathcal{P}_j = (c, d)$.

One can solve Eq. (4.3) using Sequential Minimal Optimization (SMO) method proposed in [Platt, 1998] for classification and later extended for Regression SVM [Shevade *et al.*, 2000]. SMO suggests to sequentially optimize Eq. (4.3) by tunning minimum number of α parameters at a time (usually one or two). Then, Eq. (4.3) can be rewritten as a maximization w.r.t. some selected Lagrangian multiplier α_x as follows:

$$\begin{aligned} &\text{Maximize}_{\{\alpha_x\}} L_D = \alpha_x \epsilon_x - \alpha_x \textstyle\sum_{\forall i \neq x \in \mathcal{P}} \alpha_i dK_{xi} - \frac{1}{2} \alpha_x^2 dK_{xx} + L_{D_{constr}} \\ &\text{subject to } 0 \leq \alpha_x \leq C_x, \end{aligned} \tag{4.4}$$

where $L_{D_{const}}$ is the part of Lagrangian which is independent on α_x. If change α_x to $\alpha_x^* = \alpha_x + \Delta\alpha_x^*$, then Eq. (4.4) can be rewritten as follows:

$$\begin{aligned} &\text{Maximize}_{\{\Delta\alpha_x^*\}} \Delta L_D = \Delta\alpha_x^* \epsilon_x - \Delta\alpha_x^* \textstyle\sum_{i=1}^{|\mathcal{P}|} \alpha_i dK_{xi} - \frac{1}{2} \Delta\alpha^{*2}_x dK_{xx} \\ &\text{subject to } 0 \leq \alpha_x + \Delta\alpha_x^* \leq C_x, \end{aligned} \tag{4.5}$$

At the stationary point of the objective function (4.5) we have

$$\Delta\alpha_x^* = \frac{\epsilon_x - \sum_{i=1}^{|\mathcal{P}|} \alpha_i dK_{xi}}{dK_{xx}}, \tag{4.6}$$

where ϵ_x will be set to 1 for all experiments in this Chapter.

For the sake of completeness and to demonstrate the simplicity of the learning to rank approach, we present an efficient implementation of SMO for Ranking SVM in Algorithm 4.1. To reduce the computational complexity we pre-compute dK in lines 2-7, a temporary vector $\Delta\alpha_i^*, i = 1, \ldots, |\mathcal{P}|$ and matrix $DivdK_{ij}, i, j = 1, \ldots, |\mathcal{P}|$ in lines 12 and 14, respectively. The initial values of α parameters are set to constraint violation weights C in line 9, any other non-negative initial α would lead to the optimum, but probably with a smaller convergence rate. For n_{iter} iterations (lines 17-28) we select a Lagrangian multiplier α_{i_x} (line 18) and update it (line 28) using Eq. (4.6) to maximize the Lagrangian ΔL (line 23). New value α_{new} should be checked to satisfy $0 \leq \alpha_{new} \leq C_{i_x}$ (line 21), then for any non-zero $\Delta\alpha_{i_x}^*$ we always have $\Delta L > 0$[1]. The computational complexity of the algorithm scales with $O(n_{iter} n_{alpha})$, where n_{iter} should be chosen in order of $1000 n_{alpha}$ (see Section 4.1.2) and n_{alpha} will be set to $\ell - 1$ for all experiments in this Chapter. The computation of Kernel matrix $K \in \mathbb{R}^{\ell \times \ell}$ scales with $O(n\ell^2)$, i.e., $O(n^3)$ if $\ell = n$, but it usually has 10-100 times smaller constant factor than the one of the SMO optimization procedure. The memory complexity scales with $O(\ell^2)$, limiting the use of non-linear Kernels to $\ell \leq 10000$ on ordinary computers.

The simplest strategy to identify α_{i_x} with the largest potential increase of ΔL is to compute ΔL for all α_{i_x}. This allows to decrease the number of updates of $\Delta\alpha^*$ (lines 26), but the procedure itself is linear in ℓ, so there is a substantial gain in time only on first iterations of the algorithm before the distribution of improvements of Lagrangian become almost uniform for all α_{i_x}. We tried to apply gradient-based methods to optimize the dual form whose gradient information is available, but found no gains in terms of time. Finally, we use the simplest baseline procedure and iteratively choose all α_{i_x} (line 18). We also found that random permutation of indexes of α does not lead to a faster convergence.

In a machine learning context, Quadratic Programming (QP) problems such as (4.3) are usually optimized up to a given accuracy ϵ_{QP}. In this thesis, we adopt a different stopping criterion based on number of iterations n_{iter} because in the context of surrogate-assisted optimization we need to control the computational time spent on surrogate model learning, as surrogate-assisted optimization involves many steps of surrogate learning. As the number n_{iter} of iterations needed to reach precision ϵ_{QP} varies depending on the difficulty of the underlying QP, which itself varies along the search, we opted for specifying the number n_{iter} of iterations (directly visible in the computational cost) rather than ϵ_{QP} (since we cannot bound a priori n_{iter} needed to reach an accuracy ϵ_{QP}). Since our way of defining the stopping criterion is not common in Machine Learning, we present an analysis of n_{iter}-based stopping criterion and its comparison with ϵ_{QP}-based stopping criterion in Section 4.3.3.10.

[1] In an early version of the manuscript, the formula in line 23 was incorrectly given as $\Delta L \leftarrow \Delta\alpha dK_{i_x i_x}(\Delta\alpha_{i_x}^* - 0.50, 0.58, 0\Delta\alpha + 1)$. The term "+1" was introduced by a mistake both in the algorithm description and the source code, that led to a loss of perfomance of the learning algorithm in order of 1% in terms of time and number of iterations of SMO (while, the factor is problem-dependent), since the algorithm did not pass "$\Delta L > 0$" when necessary and several iterations among n_{iter} were lost. Thus, only about $0.99 n_{iter}$ were used instead of the declared $1.00 n_{iter}$. No significant difference of model quality is observed between the original and the corrected versions. However, the results presented in this Chapter are given for the original version except for Section 4.3.3.10

Algorithm 4.1: Rank SVM Dual problem optimization

given training points $\boldsymbol{x}_i, i = 1, \ldots, \ell$; Kernel matrix $K \in \mathbb{R}^{\ell \times \ell}$; pool of constraints $\mathcal{P}$; $n_{alpha} = |\mathcal{P}|$; $C \in \mathbb{R}^{n_{alpha}}$; n_{iter}
for $i = 1 \ldots n_{alpha}$ **do**
  for $j = 1 \ldots n_{alpha}$ **do**
    $(a, b) \leftarrow \mathcal{P}_i$; $(c, d) \leftarrow \mathcal{P}_j$
    $dK_{ij} = K(x_a, x_b) - K(x_a, x_d) - K(x_c, x_b) + K(x_c, x_d)$
  end for
end for
for $i = 1 \ldots n_{alpha}$ **do**
  $\alpha_i \leftarrow C_i$
end for
for $i = 1 \ldots n_{alpha}$ **do**
  $\Delta\alpha_i^* \leftarrow \frac{1 - \sum_{j=1}^{n_{alpha}} \alpha_j dK_{ij}}{dK_{ii}}$
  for $j = 1 \ldots n_{alpha}$ **do**
    $DivdK_{ij} \leftarrow \frac{dK_{ij}}{dK_{jj}}$
  end for
end for
for $i = 1 \ldots n_{iter}$ **do**
  $i_x \leftarrow i \; mod \; (n_{alpha} + 1)$
  $\alpha_{old} \leftarrow \alpha_{i_x}$
  $\alpha_{new} \leftarrow \alpha_{old} + \Delta\alpha_{i_x}^*$
  $\alpha_{new} \leftarrow max(min(\alpha_{new}, C_{i_x}), 0)$
  $\Delta\alpha \leftarrow \alpha_{new} - \alpha_{old}$
  $\Delta L \leftarrow \Delta\alpha dK_{i_x i_x}(\Delta\alpha_{i_x}^* - 0.5\Delta\alpha)$
  if $\Delta L > 0$ **then**
    for $j = 1 \ldots n_{alpha}$ **do**
      $\Delta\alpha_j^* \leftarrow \Delta\alpha_j^* - \Delta\alpha DivdK_{i_x j}$
    end for
    $\alpha_i \leftarrow \alpha_{new}$
  end if
end for
output: optimal α

4.1.2 Choice of Kernel Function

Performance of SVM algorithms may be significantly affected by a choice of kernel function. The most commonly used kernels are RBF kernel Eq. (3.31), Linear kernel defined as

$$K_{Linear}(\boldsymbol{x}_i, \boldsymbol{x}_j) = \boldsymbol{x}_i \boldsymbol{x}_j, \tag{4.7}$$

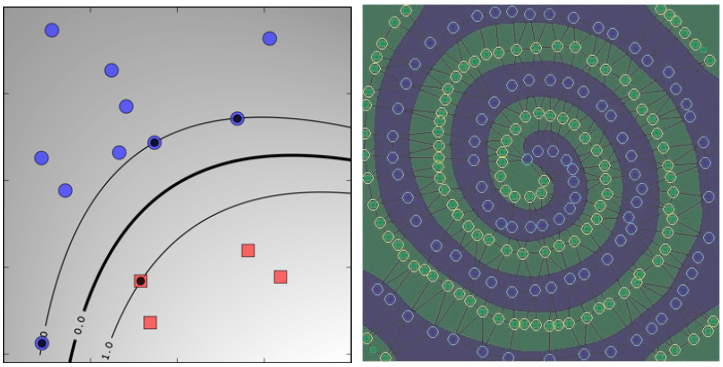

Figure 4.1: Examples of non-linear SVM classification using **(Left)** Polynomial kernel of degree 2 [Ben-Hur *et al.*,2008] and **(Right)** RBF kernel.

and *inhomogeneous* Polynomial kernel defined as

$$K_{inPoly}(\boldsymbol{x}_i, \boldsymbol{x}_j) = (\boldsymbol{x}_i \boldsymbol{x}_j + c)^d, \tag{4.8}$$

where $c > 0$ and d is polynomial degree (for difference of inhomogeneous and homogeneous ($c = 0$) kernels see [Scholkopf *et al.*, 1999]).

Polynomial kernels allow to solve non-linear classification (see Figure 4.1-**Left**) and regression problems with a decision boundary, whose flexibility is growing with d. The flexibility of RBF kernels allows to solve even so non-linear problems as the one shown in Figure 4.1-**Right**.

To choose an "appropriate" kernel for Ranking SVM we perform experiments on Sphere $f_{Sphere}(\boldsymbol{x}) = \sum_{i=1}^{n} x_i^2$ and Rosenbrock $f_{Rosen}(\boldsymbol{x}) = \sum_{i=1}^{n-1}(100.(x_i^2 - x_{i+1})^2 + (x_i - 1)^2)$ functions. To build a Ranking SVM based model $\hat{f}$ we first sort ℓ training points in ascending order w.r.t. chosen f and fill a pool of $\ell - 1$ constraints $\mathcal{P}$ such that each point $\boldsymbol{x}_i$ is preferred to points $\boldsymbol{x}_{i+1}$ for $i = 1, \ldots, \ell - 1$. For RBF kernel we set to $\sigma = c_{sigma}\sigma_x$, where σ_x is the average distance between training points. The trade-off constant C_i was set to $10^{C_{base}}$ for $i = 1, \ldots, \ell - 1$. When the model is build after SMO optimization as described in the previous Section, we measure model quality on $\ell_{test} = |\Lambda|$ points ordered after f as follows:

$$Err(\hat{f}) = \frac{2}{|\Lambda|(|\Lambda| - 1)} \sum_{i=1}^{|\Lambda|-1} \sum_{j=i+1}^{|\Lambda|} \mathbb{1}_{\hat{f},i,j} \tag{4.9}$$

where $\mathbb{1}_{\hat{f},i,j}$ holds true iff $\hat{f}$ violates the ordering constraint on pair (i, j).

In order to investigate the performance of Ranking SVM on different learning problems and for different kernel functions, we set c_{sigma} and C_{base} to the values which lead to the best results of $Err(\hat{f})$ observed on test points for different settings of c_{sigma} and C_{base}. For each pair of values c_{sigma} and C_{base}, the training set was filled using 100 (respectively, 250) training points randomly uniformly drawn from $[-2, 2]^n$ and evaluated on 10-dimensional

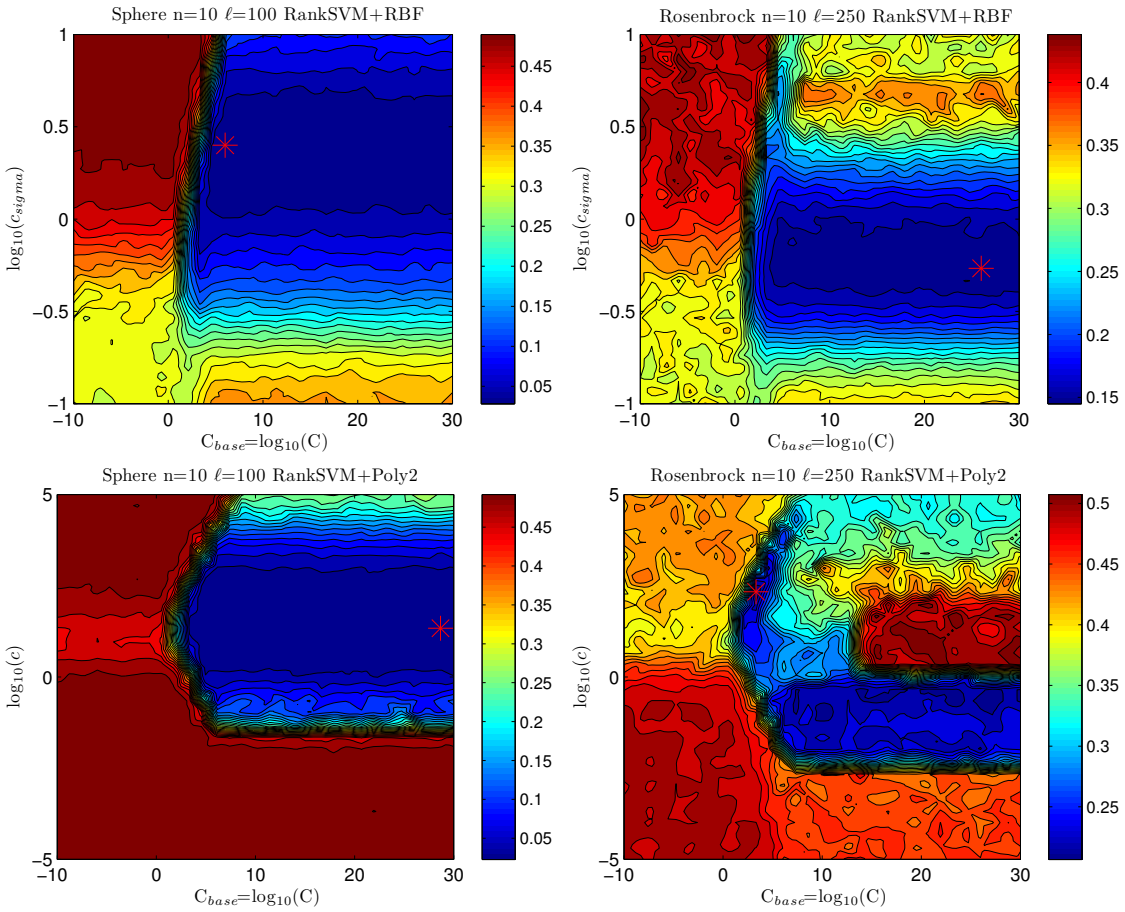

Figure 4.2: Average surrogate model error in (C_{base}, c_{sigma})-space (respectively, (C_{base}, c)-space) measured in 10 runs of Ranking SVM with RBF kernel (respectively, Polynomial kernel with degree 2) on **(Left)** Sphere and **(Right)** Rosenbrock functions in 10-D after 1000ℓ iterations of the SMO algorithm. The observed best pair of hyper-parameters is denoted as '*'.

Sphere (respectively, Rosenbrock) function. The test set was filled using $\ell_{test} = 1000$ test points from the same region. The 31 values of C_{base} (respectively, c_{sigma}) are uniformly taken from $[-10, 30]$ (respectively, $[-5, 5]$). The number of iterations of SMO n_{iter} was set to 1000ℓ (see Section 4.3.3.10 for a discussion).

Figure 4.2 shows the (C_{base}, c_{sigma})-space of Ranking SVM hyper-parameters for 10-dimensional Sphere and Rosenbrock functions. Indeed, the optimal hyper-parameters (with lowest $Err(\hat{f})$ values) are different for these problems. A basin (a region where $Err(\hat{f})$ is already small and tends to decrease slower) in (C_{base}, c_{sigma})-space of a relatively good performance is observed for both problems. As a simple estimator of optimal C^*_{base} and c^*_{sigma}, we originally tried to compute the mean/median of 1% (i.e., 9 out of

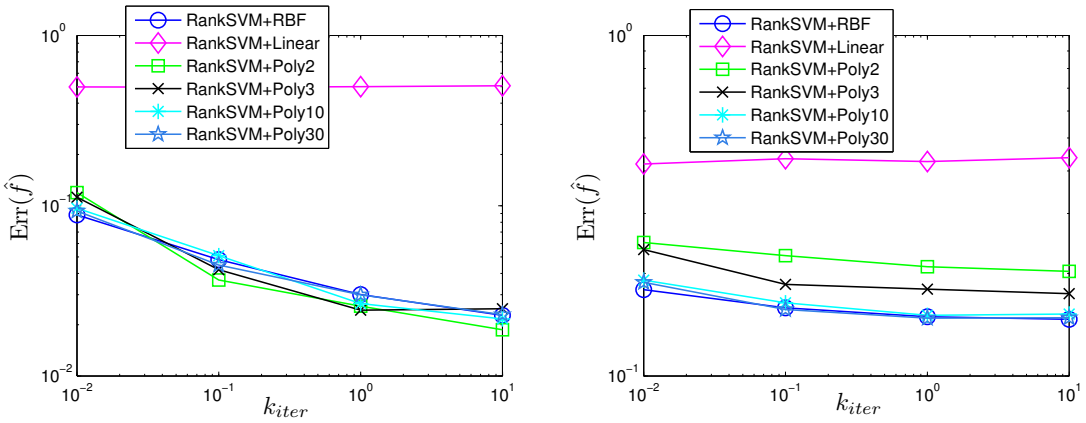

Figure 4.3: Average surrogate model error measured in 20 runs of Ranking SVM with different kernels on **(Left)** Sphere and **(Right)** Rosenbrock functions in 10-D after $k_{iter}1000\ell$ iterations of the SMO algorithm.

31×31=961) the best observed pairs of C_{base} and c_{sigma}. While this kind of averaging might be reasonable given that the estimations of $Err(\hat{f})$ are noisy, it also might be very harmful when $Err(\hat{f})$ in (C_{base}, c_{sigma})-space is multi-modal: the averaging of points from two good clusters may produce a point which is worse than the points of both clusters. The estimation of the global optimum of noisy multi-modal functions itself is an open scientific problem. Therefore, for the sake of simplicity, in this Section, the estimate of optimal hyper-parameters is set to the best pair of hyper-parameters C^*_{base}, c^*_{sigma}, observed in 31×31=961 experiments. The estimated $C^*_{base} = 6$ and $c^*_{sigma} = 0.4$ (respectively, $C^*_{base} = 26$ and $c^*_{sigma} = -0.2667$) for 10-dimensional Sphere function with 100 training points (respectively, Rosenbrock function with 250 training points).

For Polynomial kernel-based Ranking SVM a similar offline tuning procedure is applied, where instead of c_{sigma} the kernel parameter c (see Eq. 4.8) is varied in the range $[10^{-5}, 10^5]$. The estimated optimal values of C^*_{base} and c^* for Polynomial kernel-based Ranking SVM (see Figure 4.2) are used to plot the results shown in Figure 4.3 (see also Appendix A for several demonstrations of the (C_{base}, c)-space). The kernel matrix is additionally normalized [Graf and Borer, 2001] such that $\widetilde{K}_{ij} = K_{ij}/\sqrt{K_{ii}K_{jj}}$ (note that RBF-based kernel matrix is normalized by definition since $K_{ii} = 1$).

Figure 4.3 shows the average model error $Err(\hat{f})$ estimated on 10-dimensional Sphere and Rosenbrock functions for 20 runs of Ranking SVM with different kernels: RBF ('RankSVM+RBF'), Linear ('RankSVM+Linear'), Polynomial with $d = 2$ ('RankSVM+Poly2'), Polynomial with $d = 3$ ('RankSVM+Poly3'), etc. For RBF kernel-based (respectively, Polynomial kernel-based) Ranking SVM the estimated C^*_{base} and c^*_{sigma} (respectively, C^*_{base} and c^*) values are used. It should be noted that these values are estimated for a given SMO stopping criterion of $n_{iter} = k_{iter}1000\ell$ iterations individually for each $k_{iter} = 0.01, 0.1, 1, 10$, and Figure 4.3 investigates a dependency of $Err(\hat{f})$ on k_{iter} for different kernel functions.

Ranking SVM with Linear kernel has $Err(\hat{f})$ slightly below 0.5, where $Err(\hat{f})$ can be interpreted as the fraction of incorrectly predicted comparison relations. A random 50% prediction ($Err(\hat{f}) = 0.5$) is due to the fact that the functions are not linear. Quadratic Sphere function has probably the most suitable topography for Polynomial kernel with degree 2, so its good results are not surprising. Despite implicitly defined high degree of non-linearity, Polynomial kernels of higher degree also catch the topography of Sphere function, but likely due to a relatively successful offline parameter tuning (see Figure 1 in Appendix A). On Rosenbrock function, on the contrary, the degree 2 is insufficient and higher degree of non-linearity ($d > 2$) is needed to catch the "banana" topography of this function. Ranking SVM with RBF kernel and Polynomial kernel with degree 10 and 30 show good results on both functions. While the computational complexity of model learning is growing linearly with k_{iter}, the decrease of model error $Err(\hat{f})$ usually becomes slower for $k_{iter} > 1$ on *these* particular problems. In some cases, $Err(\hat{f})$ even increases with k_{iter} (see, e.g., 'RankSVM+Poly3' on 10-dimensional Sphere function). This might be due to one or a combination of the following effects:

- A larger number of iterations of SMO optimization leads to a *better* solution of the dual Ranking SVM problem, but the optimal solution of the dual problem not necessary leads to a smaller test error, while this is a goal of parametrization of the dual - to choose such parameters which will lead to a minimum test error.
- The estimated optimal hyper-parameters are located close to "bad" hyper-parameters in (C_{base}, c_{sigma})-space, and due to the stochasticity of the process, this might lead to a certain increase of $Err(\hat{f})$.

Indeed, the described above effects are very likely to be also relevant for online tuning of model hyper-parameters.

4.1.3 Ordinal Regression vs Metric Regression

Most surrogate approaches described in Section 3.1 are based on standard regression also referred to as *metric regression*. To analyze how sensitive metric regression to scaling of f we conducted several experiments with Support Vector Regression (see Section 3.2.2) and Ranking SVM.

The implementation of Support Vector Regression is derived from the Shark library [Igel *et al.*, 2008], where the gradient-based working set selection of QP sub-problem is used in contrast to the uniform selection used in this thesis (see Section 4.1.1). The gradient-based selection usually leads to a faster QP problem optimization per iteration of the learning algorithm, while each iteration is computationally more expensive. In order to calibrate n_{iter} iterations used to learn the model, we perfomed several experiments on 10-dimensional Sphere function for $\ell = 64, 100, 128, 256, 512, 1024, 2048$ and for 961 pairs of model hyper-parameters. We found that $n_{iter} = 1000\ell$ of Ranking SVM (including the cost of kernel matrix computation) corresponds to roughly $n_{iter} = 70\ell$ of SVR. Given that our Ranking SVM code was optimized to be computationally efficient, and in order to reduce a potential bias to Ranking SVM implementation, in the following we use $n_{iter} = 100\ell$

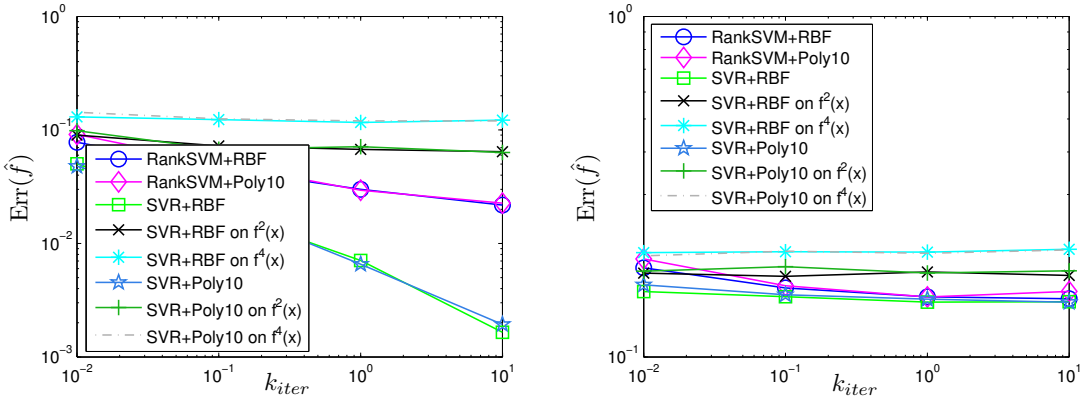

Figure 4.4: Average surrogate model error measured in 20 runs of Ranking SVM and Support Vector Regression (SVR) with different kernels on **(Left)** Sphere and **(Right)** Rosenbrock functions in 10-D after $k_{iter}1000\ell$ and $k_{iter}100\ell$ iterations of the SMO algorithm for Ranking SVM and SVR, respectively.

for SVR as an equivalent of $n_{iter} = 1000\ell$ of Ranking SVM. For all experiments in this Section we set ϵ of SVR to 0, but other values of ϵ lead to very similar results of these *noise-less* functions.

Figure 4.4 shows the results of Ranking SVM with RBF ('RankSVM+RBF') and Polynomial with $d = 10$ ('RankSVM+Poly10) kernels, Support Vector Regression with RBF and Polynomial kernels on the original function f ('SVR+RBF' and 'SVR+Poly10') and transformed functions $g = f^2$ ('SVR+RBF on $f^2(\boldsymbol{x})$' and 'SVR+Poly10 on $f^2(\boldsymbol{x})$') and $g = f^4$ ('SVR+RBF on $f^4(\boldsymbol{x})$' and 'SVR+Poly10 on $f^4(\boldsymbol{x})$'), where f is Sphere and Rosenbrock functions for Figure 4.4-**Left** and Figure 4.4-**Right**, respectively. Note that Sphere and Rosenbrock functions are positive everywhere.

The results for Ranking SVM are the same for the original and transformed versions, because the transformations of f do not change the ranking of training points. Our first observation is that 'SVR+Poly10' and 'SVR+RBF' demonstrate best performance on the original Sphere function f. However, the results of SVR on scaled functions f^2 and f^4 clearly show that the model accuracy quickly degrades as the transformed function less resembles the original *quadratic* function. For f^6 and f^8 SVR-based surrogate model tends to demonstrate even worse (comparable to random) prediction of test test points. This suggests that on one of the simplest optimization problems (e.g., a scaled version of Sphere function) metric regression may provide arbitrary bad results. On Rosenbrock function 'SVR+RBF' and 'SVR+Poly10' perform as well as 'RankSVM+RBF', but degrade quickly on f^2 and f^4.

The reasons of these results become clearer by looking at the space of model hyper-parameters for f, f^2 and f^4 (see Figure 2 in Appendix A). The bassin of hyper-parameters which corresponds to good performance on $Err(\hat{f})$ becomes much smaller on f^2 and f^4 (for *these particular* problems it becomes more difficult to find "good" mapping between the

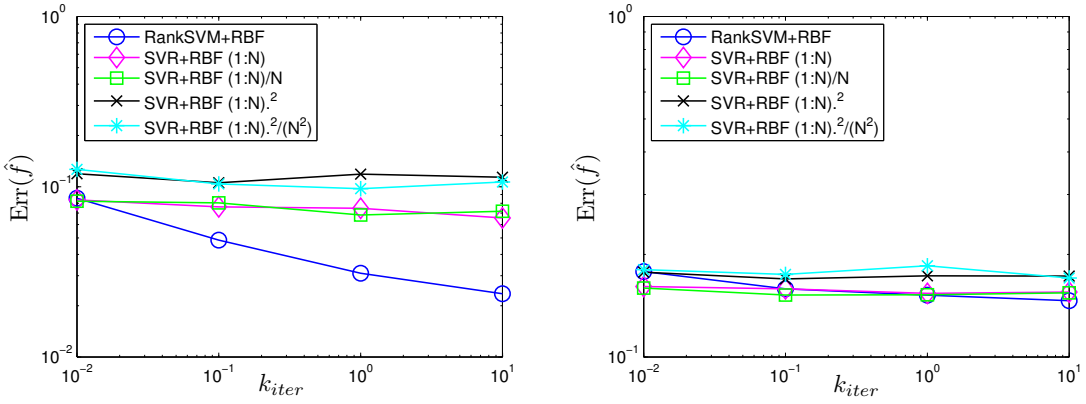

Figure 4.5: Average surrogate model error measured in 20 runs of Ranking SVM and Support Vector Regression (SVR) with different rank-based transformations of fitness values on **(Left)** Sphere and **(Right)** Rosenbrock functions in 10-D after $k_{iter}1000\ell$ and $k_{iter}100\ell$ iterations of the SMO algorithm for Ranking SVM and SVR, respectively.

decision and the objective space), and this is especially the case for the hyper-parameter C and $C_{base} = log(C)$. At a first look, it seems reasonably to scale C according to the scaling of f. However, in the black-box scenario we observe only f, so it is unclear how to scale C since the notion of "scaling" can be defined only with respect to another function. As can been seen in Figure 2 of Appendix A, the bassin of optimal model hyper-parameters is almost the same for f^2 and f^4 of Sphere function, but moves significantly for Rosenbrock function. Thus, even if the optimal bassin is known for f for a given range of C, it is still unclear how to scale the search range of C (to have a comparable chance to localize the optimal bassin during the offline tuning) for f^2 and f^4, since this scaling is problem-dependent.

In black-box optimization, the scaling of f is unknown *and* may vary locally during the search. A sophisticated procedure can be proposed to learn "optimal" scaling of f and adapt hyper-parameters of SVM accordingly. However, the results on Rosenbrock function suggest that presumably even using the original "preferred scenario" of scaling (which might be preferred to, e.g., f^{10}), the accuracy of SVR may be at best comparable to the one of Ranking SVM.

4.1.4 Ordinal Regression using Metric Regression Approaches

One can use metric regression to learn ranking of training points and predict the score of test points. The original "raw" objective function value of each training point should be modified such that it will depend only on the rank of this point.

The simplest rank-based fitness assignment scheme, referred to as '(1:N)', sets the fitness of each training point to be equal to its rank among $N = \ell$ training points. Since ℓ is usually growing with n, it might be reasonable to normalize new fitness values by ℓ to

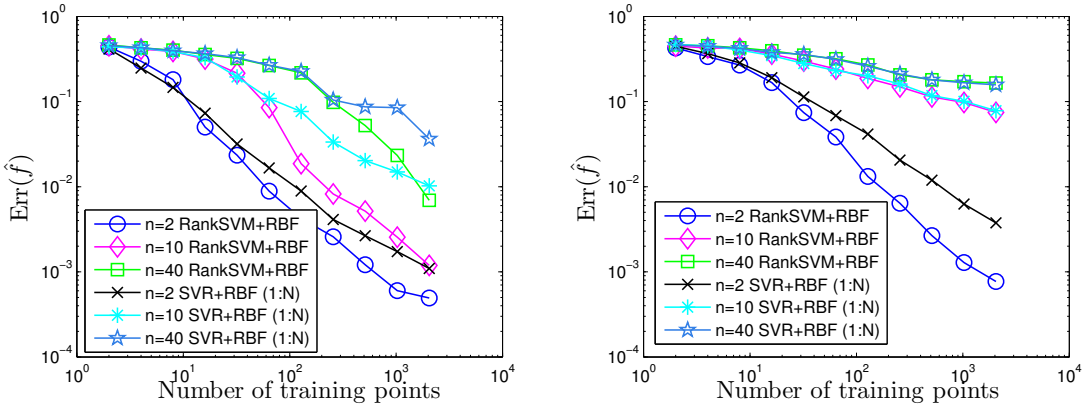

Figure 4.6: Average surrogate model error measured in 20 runs of Ranking SVM and Support Vector Regression (SVR) with different number of training points on **(Left)** Sphere and **(Right)** Rosenbrock functions in 10-D after 1000ℓ and 100ℓ iterations of the SMO algorithm for Ranking SVM and SVR, respectively.

the range $[1/N, 1]$: we call this scheme '$(1{:}N)/N$'. As was shown in the previous Section, quadratic shapes of fitness function may be beneficial for SVR. To check this hypothesis for rank-based SVR, we set the fitness of each training points to be equal to its squared and normalized squared rank value in '$(1{:}N).^2$' and '$(1{:}N).^2/(N^2)$' schemes, respectively.

It can be seen from Figure 4.5 and Figure 4.4 that rank-based SVR performs worse than metric-based SVR in its "preferred scenario" of scaling of f, but does not fail like metric-based SVR in its "worst scenario", e.g., on f^4, f^6, etc., because rank-based SVR is invariant to rank-preserving transformations of f. Rank-based SVR performs worse on 10-dimensional Sphere function, while on Rosenbrock function the difference is not significant. The normalization of rank-based fitness given to SVR sometimes even worsen the results, but usually has minor impact. The scaling of the rank-based fitness seems to be more important than the normalization, but quadratic scaling worsen the results on Sphere function and is not better on Rosenbrock function. We also tried to use other scaling schemes such as square root of rank '$(1{:}N).^{0.5}$', which slightly improves the results on Sphere, but worsen on Rosenbrock. Finally, the simplest '$(1{:}N)/N$' scheme probably should be taken as a baseline for a black-box function f, but its optimal parametrization in principle may be adapted during the optimization of f.

4.1.5 Ranking SVM vs Rank-based SVR

It was shown in the previous Sections that ordinal regression usually should be preferred to metric-regression, since the latter is sensitive to rank-preserving transformations of f. One should keep in mind that all conjectures and conclusions drawn from experimental results are supposed to be valid for a given parametrization of algorithms and on a given set of test functions. However, the results obtained on some functions, such as Sphere

function, can be generalized for a larger class of problems which resemble Sphere-like function at least around local and global optima, i.e., on later stages of the optimization of these problems we actually optimize Sphere-like function.

Figure 4.6 demonstrates the results of Ranking SVM and rank-based SVR for different number of training points $\ell = 2, 4, \ldots, 2048$ used to build $\hat{f}$ on **(Left)** Sphere and **(Right)** Rosenbrock functions in dimensions 2, 10 and 40 (see also Figure 3 and 4 of Appendix A). It can be seen that Ranking SVM outperforms SVR on Sphere function for $\ell > 10n$: this is very important result which among other reasons has determined our preferences to Ranking SVM. While on Rosenbrock function Ranking SVM outperforms SVR only for $n = 2$, for $n = 10, 40$ both algorithms have very similar performance.

The main difference between Ranking SVM and Rank-based SVR is that the latter is more constrained since target values of $\hat{f}$ are pre-defined for all training points, while in Ranking SVM only the minimum difference of target values is defined. Thus, Ranking SVM may find solutions of SVR constrained to have specific $\hat{f}$ values, but it is *also* open to a larger set of optimal solutions, which are unavailable for SVR. An important remark is that we analyzed the cheapest variant of Ranking SVM with only $\ell - 1$ constraints, a slightly larger number of constraints, say 1.2ℓ, may improve the robustness of the model learning on multi-modal and/or noisy functions.

The simple offline tuning procedure used in this Section allows to investigate the surrogate models hyper-parameters and to estimate their nearly-optimal values w.r.t. model error. However, the search range of these hyper-parameters still should be defined by the user, the estimation itself is computationally expensive and requires a quite large test set to be available, that is usually not the case (instead, a cross-validation procedure might be considered). Moreover, the adapted grid search procedure badly scales w.r.t. the number of hyper-parameters. In preliminary experiments of Section 4.2.2, for the sake of simplicity we use some fixed values of hyper-parameters found after some offline tuning. This is also the case for multi-objective surrogate-assisted search (see Chapter 5). However, an important contribution of this thesis is a procedure of surrogate model hyper-parameters adaptation by CMA-ES (see Section 4.3.2), which replaces the grid search and automates the resolution of the problem of model selection for the learning problem at hand.

4.2 ACM with Pre-selection

To the best of our knowledge, the only work investigating the use of Ranking SVM as surrogate model within a meta-model assisted EA published before [Loshchilov *et al.*, 2010c] was [Runarsson, 2006]; while the approach proposed in [Runarsson, 2006] was reported to bring small improvements over a CMA-ES baseline, a major issue regards the choice of the kernel, the Achilles heel of all SVM-based methods. Following the path opened by [Runarsson, 2006], in [Loshchilov *et al.*, 2010c] we investigated the use of Ranking SVM surrogate models within CMA-ES.

In this Section, we describe Ranking SVM-based CMA-ES, referred to as ACM-ES [Loshchilov *et al.*, 2010c] for (*alphabetically*) ranked CMA-ES. In Section 4.2.1, we discuss the advantages of the use of the Covariance Matrix adapted by CMA-ES, viewed as the

proper metric to look at the region of the fitness landscape currently explored, and which renders surrogate learning techniques invariant w.r.t. orthogonal transformations of f. In Section 4.2.2, we present pre-selection strategy used in ACM-ES and the algorithm itself. The experimental validation of the approach is reported in Section 4.2.3, and directions for further work are discussed in Section 4.2.4.

4.2.1 Toward Optimal Kernel Function: Invariance w.r.t. Orthogonal Transformations

In Section 3.3.2.2, we have described lmm-CMA-ES algorithm proposed by [Kern *et al.*, 2006], which predicts fitness of an offspring $\boldsymbol{q}$ by building a weighted quadratic meta-model $\hat{f}$ around $\boldsymbol{q}$. An important contribution made by [Kern *et al.*, 2006] was to use the covariance matrix adapted by CMA-ES to compute the weight of each training point $\boldsymbol{x}_j$, such that the weight decreases as the Mahalanobis distance $\sqrt{(\boldsymbol{x}_j - \boldsymbol{q})^T \mathbf{C}^{-1} (\boldsymbol{x}_j - \boldsymbol{q})}$ to the query point $\boldsymbol{q}$ increases. This covariance matrix-based Mahalanobis distance takes into account the correlations of the data (the Euclidean distance can be obtained by setting the covariance matrix to identity). Later, in order to decrease the computational complexity of lmm-CMA-ES [Kern *et al.*, 2007] studied different versions of lmm-CMA-ES. They pointed out more explicitly that

$$\sqrt{(\boldsymbol{x}_j - \boldsymbol{q})^T \mathbf{C}^{-1} (\boldsymbol{x}_j - \boldsymbol{q})} = \sqrt{\boldsymbol{x}'^T_j \boldsymbol{x}'_j}, \tag{4.10}$$

where $\boldsymbol{x}'_j$ is an image of $\boldsymbol{x}_j$ in some *transformed* space, defined as

$$\boldsymbol{x}'_j = \mathbf{C}^{-1/2} (\boldsymbol{x}_j - \boldsymbol{q}) \tag{4.11}$$

Later [Hansen, 2008] proposed Adaptive Encoding procedure which gradually learns an appropriate coordinate system and can be used in principle within any continuous optimizer. The author showed that CMA-ES can be viewed as Cumulative Step-size Adaptation algorithm performed in the transformed coordinate system, adapted by Adaptive Encoding procedure. The change of coordinates, defined from the current covariance matrix C and the current mean value m (this was also proposed before in [Kern *et al.*, 2007]), reads:

$$\boldsymbol{x}'_j = \mathbf{C}^{-1/2} (\boldsymbol{x}_j - \boldsymbol{m}) \tag{4.12}$$

We hence propose to define the kernel function (e.g., RBF kernel) directly to the covariance matrix (the idea was proposed in [Loshchilov *et al.*, 2010c] independently from a similar idea for Gaussian Processes proposed in [Kruisselbrink *et al.*, 2010]), with $\sigma > 0$:

$$K_C(\boldsymbol{x}_i, \boldsymbol{x}_j) = \mathrm{e}^{-\frac{(\boldsymbol{x}_i - \boldsymbol{x}_j)^T \mathbf{C}^{-1} (\boldsymbol{x}_i - \boldsymbol{x}_j)}{2\sigma^2}} \tag{4.13}$$

However, the computation of the kernel matrix with $\ell \times \ell$ elements may become computationally expensive if we need to compute Eq. (4.13) for each element. Instead, we can

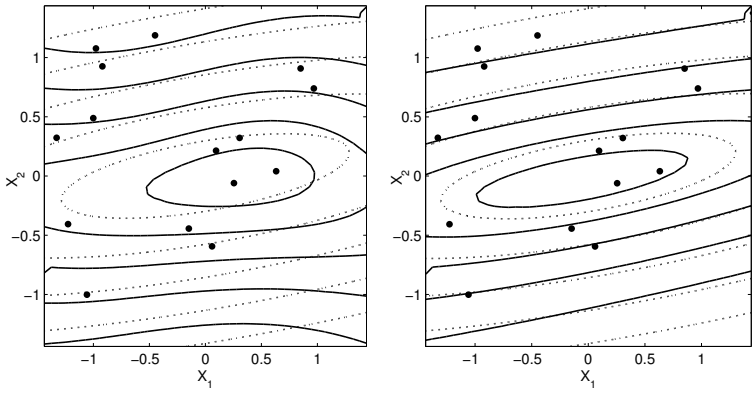

Figure 4.7: Contour plots of rotated Ellipsoid function (dotted lines) and Ranking SVM surrogates (solid lines) obtained with isotropic RBF kernel **(Left)** or covariance matrix-based transformed RBF kernel **(Right)**. The transformed RBF kernel is more appropriate than the isotropic one.

translate all training points to the feature space using Eq. (4.12), where all variables are as decorrelated as possible and the objective function more resembles the Sphere function, which is relatively easy to learn (see Figure 4.6). Then, in this feature space, we may use the Euclidean distance and compute σ, which we set to the average distance between training points.

Figure 4.7 displays surrogate models of 2-dimensional rotated Ellipsoid function f built on 15 the same training points using **(Left)** standard RBF kernel and **(Right)** transformed RBF kernel with Eq. (4.13), where $\mathbf{C}$ is set to the inverse of the Hessian of f. It can be seen that the use of the transformed RBF allows to obtain more satisfactory (bold) contour lines of the surrogate model to the (dotted) contour lines of the original Ellipsoid function, i.e., we may obtain a much better prediction of f if covariance matrix $\mathbf{C}$ is known. Fortunately, CMA-ES adapts $\mathbf{C}$ during the search, therefore, we may transform training and test points using Eq. (4.12) to make our surrogate modeling approach *invariant w.r.t. orthogonal transformation of the search space*. An important detail is that $\mathbf{C}^{-1/2}$ is already computed within CMA-ES, therefore the transformation comes at almost no additional cost.

We believe that the use of the transformation (4.12) may improve the performance of most of the surrogate techniques proposed for CMA-ES. For other EAs which do not adapt $\mathbf{C}$, the estimation of covariance matrix can be obtained performing Principal Component Analysis (PCA) of the training data. One should mention that the transformed kernel (4.13) shares certain similarities with the Fisher Kernel, relatively recently proposed by [Jaakkola *et al.*, 1999] and briefly reviewed in [Sewell, 2011].

4.2.2 Overview of ACM-ES

Having chosen the transformation of training and test points after Eq. (4.12), the integration of Ranking SVM as surrogate model within CMA-ES raises three main issues: i). how to train the surrogate model, i.e., how to select the current training points in the set of all points evaluated with the true objective function; ii). how to use the model within CMA-ES, without perturbing the delicate adaptive mechanism thereof, and iii). how to select the new points which will be evaluated with the true objective function.

Regarding the first issue, i.e., the selection of the training sample, several requirements have been identified. Firstly, the number ℓ of training samples must increase with the dimension n of the search space. Using statistical learning arguments, ℓ should be of the order of the VC dimension of the model space. Note that after transformation (4.12) the decision space is a variant of the Sphere function, in the best case, or a noisy multi-modal variant thereof in the worst case. A second requirement is that the training samples should not lie "too far" from the current mean $\boldsymbol{m}$ of the mutation distribution used by CMA-ES to generate its offspring, since the transformation defined by the current covariance matrix only aims at the local structure of the fitness landscape around $\boldsymbol{m}$. Finally, the analysis of preliminary experiments on the n-dimensional Sphere function shows that ℓ should increase proportionally to $\sqrt{n}$; the proportionality constant however remains problem-dependent as will be seen in Section 4.2.3. These ℓ selected points are the most recently evaluated points with the true fitness function (see Section 3.3.1.2 for a detailed discussion of different selection schemes). Figure 4.8 illustrates the whole optimization loop of ACM-ES, the training points selection corresponds to part **A**. The surrogate model learning using transformed after Eq. (4.12) training set corresponds to part **B**.

The second issue regards how to use the rank-based surrogate within CMA-ES. Using the surrogate model *in lieu* of the true fitness is a risky option due to the lack of guarantees about errors in regions outside the training sample (i.e., without model error-based control). A more conservative option thus is to use the surrogate model to pre-screen the offspring, generating many more *pre-children* than required, and keeping the best ones according the surrogate model. Such an approach however rapidly looses the offspring diversity, hindering the CMA-ES adaptive mechanism used to adapt the covariance matrix. Some trade-off between the optimization of the objective and the adaptation of the covariance matrix must thus be found.

The approach finally proposed is a two-step process. In order to prevent premature convergence, and interfere as little as possible with CMA-ES cumulative step-size adaptation, a large number λ_{Pre} of pre-children is drawn using the standard CMA Gaussian distribution; let them be noted $\boldsymbol{x}_1, \ldots \boldsymbol{x}_{\lambda_{Pre}}$, assuming with no loss of generality them to be ranked after the surrogate model (see Figure 4.8 part **C**). The λ offspring are obtained by iteratively drawing a real number $a < \lambda_{Pre}$ from distribution $\mathcal{N}(0, \sigma^2_{sel0})$ (where σ_{sel0} is a parameter of the algorithm), and retaining the pre-child with rank $\lfloor a \rfloor$ (see Figure 4.8 part **D**). The same procedure is followed to select the points to be evaluated according to the true objective function, with the same rationale: on the one hand, one should select the best points according to the current surrogate model; on the other hand, some diversity must be preserved. Finally, i). the point with top rank is selected and always

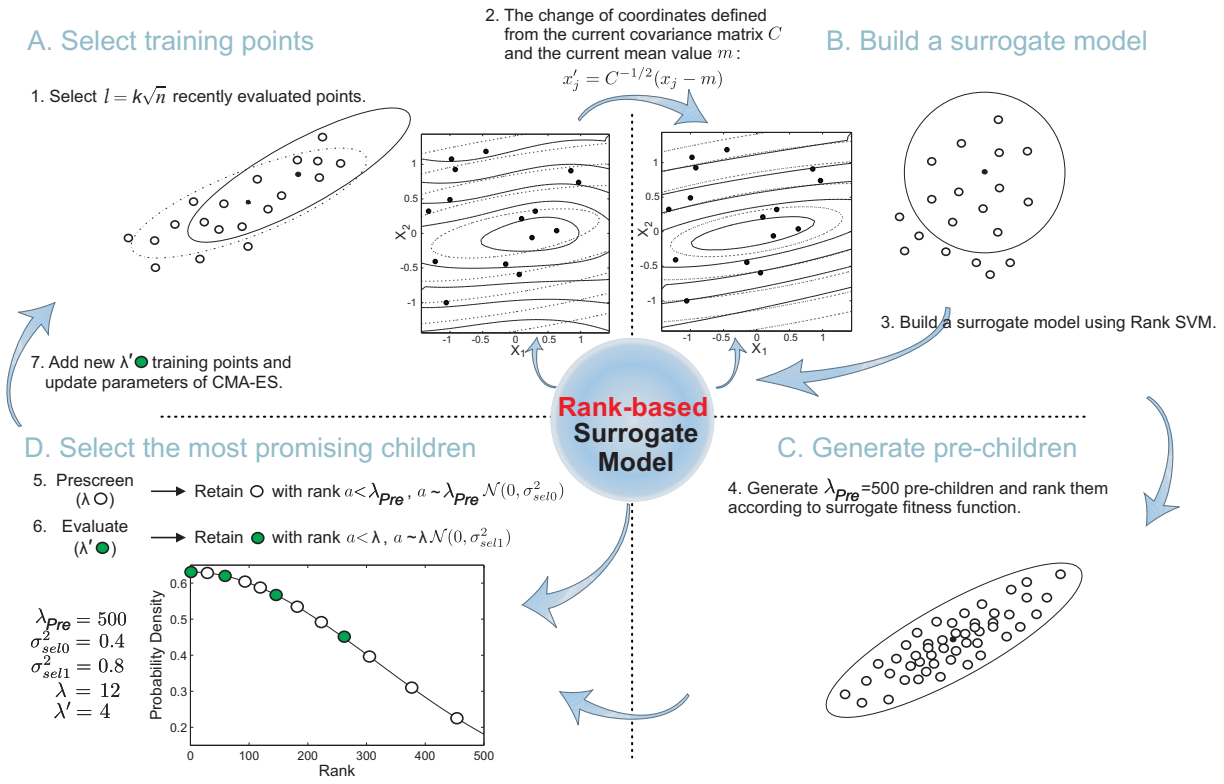

Figure 4.8: Optimization loop of the ACM-ES algorithm with pre-selection.

evaluated (as in the approximate ranking approach [Runarsson, 2004]); ii). other (λ'-1) points selected among the pre-children using a rank distribution $\mathcal{N}(0, \sigma^2_{sel1})$ are evaluated, using the same process as for the offspring selection albeit with a larger standard deviation ($\sigma_{sel1} > \sigma_{sel0}$). A typical distribution of the ranks of the λ offspring is depicted in Figure 4.8 Part **D**, where $\lambda = 12$ white circles are pre-selected among $\lambda_{Pre} = 500$ pre-children with $\sigma^2_{sel0} = 0.4$, while points that will be evaluated with the true fitness are represented by green circles ($\lambda' = 4$ and $\sigma^2_{sel1} = 0.8$).

In ACM-ES, a fixed number λ' of points is evaluated in each generation, thus bounding the complexity in terms of true fitness evaluation. The choice of the ratio λ/λ' thus controls the efficiency of the approach and the speedup w.r.t. the standard CMA-ES (where λ offspring are evaluated in each generation).

4.2.3 Experimental Validation

The experimental validation of ACM-ES investigates the performance of the approach comparatively to CMA-ES and nlmm-CMA, focussing on its scalability w.r.t. the problem dimension n, the robustness with respect to multi-modality, and with respect to the calibration of the surrogate training.

Seven uni- and multi-modal benchmark functions have been considered (see Table 4.1,

Table 4.1: Test functions, initialization intervals and initial std. dev. (from [Kern *et al.*, 2006; Bouzarkouna *et al.*, 2010]).

Name	Function	Init	σ^0
Noisy Sphere	$f_{NoisySphere}(\mathrm{x}) = (\sum_{i=1}^{n} x_i^2)\exp(\epsilon\mathcal{N}(0,1)$	$[-3,7]^n$	5
Ellipsoid	$f_{Elli}(\mathrm{x}) = \sum_{i=1}^{n} 10^{6\frac{i-1}{n-1}} x_i^2$	$[1,5]^n$	2
Schwefel	$f_{Schwefel}(\mathrm{x}) = \sum_{i=1}^{n} (\sum_{j=1}^{i} x_j)^2$	$[-10,10]^n$	10
Schwefel$^{1/4}$	$f_{Schwefel^{1/4}}(\mathrm{x}) = (f_{Schwefel}(x))^{1/4}$	$[-10,10]^n$	10
Rosenbrock	$f_{Rosenbrock}(\mathrm{x}) = \sum_{i=1}^{n-1} \left(100.(x_i^2 - x_{i+1})^2 + (x_i - 1)^2\right)$	$[-5,5]^n$	0.5
Ackley	$f_{Ackley}(\mathrm{x}) = -20\exp\left(-0.2\sqrt{\frac{1}{n}\sum_{i=1}^{n} x_i^2}\right) + \exp(\frac{1}{n}\sum_{i=1}^{n}\cos(2\pi x_i))$	$[1,30]^n$	14.5
Rastrigin	$f_{Rastrigin}(\mathrm{x}) = 10d + \sum_{i=1}^{n}(x_i^2 - 10.\cos(2\pi x_i))$	$[1,5]^n$	2

definitions in [Kern *et al.*, 2006] and [Bouzarkouna *et al.*, 2010]), with dimension n ranging in $[2, 40]$ except for the Rastrigin function. Within ACM-ES, CMA-ES is used with its default parameters [Hansen *et al.*, 2003]. Reported results are based on 20 independent runs. The stopping criterion is reaching target value 10^{-10}, with a maximum of $1000n^2$ function evaluations.

After preliminary experiments, the rank-based surrogate was trained using $\ell = \lfloor 30\sqrt{n} \rfloor$ samples for all functions, except for Ellipsoid and Rosenbrock where it was set to $\lfloor 70\sqrt{n} \rfloor$ (see Section 4.3.3.2). The maximum number of iterations of the SVM learning algorithm was arbitrarily set to $\lfloor 50000\sqrt{n} \rfloor$. The constraint weights C_i in Eq. (4.2) were set to $10^6(\ell - i)^{2.0}$, implying that the cost of rank-constraints violation quadratically increases for top-ranked samples. For all functions except Rastrigin, $\lambda' = \frac{\lambda}{3}$, $\sigma^2_{sel0} = 0.4$, $\sigma^2_{sel1} = 2\sigma^2_{sel0} = 0.8$, $\ell_{test} = 500$. For Rastrigin function $\sigma^2_{sel0} = \sigma^2_{sel1} = 0.6$.

4.2.3.1 Results and Discussion

Firstly, experiments are conducted to estimate the empirical complexity of the surrogate training and using, using $\lfloor 100\sqrt{n} \rfloor$ training points, stopping after $\lfloor 50000\sqrt{n} \rfloor$ iterations and assessing the surrogated model on 500 test points. The empirical complexity with respect to dimension n (Figure 4.9-**Left** in log scale) is 1.13, thus, slightly super-linear, contrasting with lmm-CMA complexity of $\mathcal{O}(n^6)$ (see Section 3.3.2.2 for a detailed discussion).

Secondly, the comparative validation of ACM-ES, nlmm-CMA and standard CMA-ES on all benchmark functions is reported in Table 4.2; lmm-CMA and nlmm-CMA results have been taken from original papers [Kern *et al.*, 2006] and [Bouzarkouna *et al.*, 2010] when available; those of CMA-ES have been recomputed[2]. Overall, ACM-ES outperforms lmm-CMA and nlmm-CMA algorithms on most problems, particularly so for problems with dimension $n > 4$. The invariance of ACM-ES w.r.t. monotonous transformations of the fitness is witnessed by its almost identical results on $f_{Schwefel}$ and $f_{Schwefel^{1/4}}$ functions, when the stopping criterion is adjusted accordingly (which is not the case for the results of Table 4.2). Likewise, the results on f_{Elli} confirm that ACM-ES also retains the good behavioral properties of CMA-ES with respect to the ill-conditioning of the fitness

[2] using the source code available at the website of Nikolaus Hansen: `http://www.lri.fr/~hansen/cmaes_inmatlab.html/`

Table 4.2: Computational effort SP1 (i.e., the average number of function evaluations of successful runs divided by proportion of successful runs), standard deviations and speedup performance (spu) of ACM-ES, (n)lmm-CMA-ES and CMA-ES. Results in the (n)lmm-CMA column are the best of those in [Kern *et al.*, 2006] and [Bouzarkouna *et al.*, 2010] (marked with leading "n:" for the latter). Successful runs are those who reached the target fitness value of 10^{-10}. The proportion of successful runs is given in parentheses if less than 100%. ϵ is the noise level (when relevant).

Function	n	λ	λ'	ϵ	ACM-ES		spu	(n)lmm-CMA		spu	CMA-ES	
$f_{Schwefel}$	2	6	3		186±5		2.0	**81±5**		4.5	370±32	
	4	8	3		289±9		3.0	**145±7**		6.0	879±60	
	5	8	3		344±9		3.2				1112±72	
	8	10	3		558±18		3.6	**282±11**		7.1	2010±82	
	10	10	3		801±36		3.3				2667±87	
	16	11	3		2204±74		2.3	**626±17**		8.2	5156±161	
	20	12	4		3531±179		2.0				7042±172	
	32	14	4		8933±337		1.7				15072±377	
	40	15	5		13440±281		1.7				22400±289	
$f_{Schwefel^{1/4}}$	2	6	3		551±12		2.8	**n:413±25**		3.7	1527±76	
	4	8	3		**783±8**		3.6	n:971±36		2.9	2847±109	
	5	8	3		**914±15**		3.8	n:1302±31		2.7	3505±114	
	8	10	3		**1366±25**		4.3				5882±146	
	10	10	3		**1774±37**		4.1				7220±206	
	16	11	3		**4193±88**		3.0				12411±198	
	20	12	4		**6138±82**		2.5				15600±294	
	32	14	4		**14796±310**		2.0				29378±330	
	40	15	5		**22658±390**		1.8				41534±466	
$f_{Rosenbrock}$	2	6	3		511±84		1.4	**n:252±52**		2.8	700±194	
	4	8	3		775±108		2.8	**n:719±54**	(0.85)	3.0	2187±376	(0.85)
	5	8	3		**854±89**		3.0	n:1014±94	(0.90)	2.5	2526±308	(0.95)
	8	10	3		**1388±139**		4.2	2494±511	(0.90)	2.3	5769±547	(0.85)
	10	10	3		**2059±143**	(0.95)	3.7				7669±691	(0.90)
	16	11	3		**5255±560**		3.1	7299±1154		2.2	16317±1281	(0.90)
	20	12	4		**11793±574**	(0.75)	1.8				21794±1529	
	32	14	4		**32261±2165**	(0.8)	1.6				52671±5587	
	40	15	5		**49750±2412**	(0.9)	1.6				82043±3991	
$f_{NoisySphere}$	2	6	3	0.35	413±114		1.0	**n:109±12**		3.7	407±61	(0.95)
	4	8	3	0.25	428±46		2.0	**n:236±19**		3.6	844±141	
	5	8	3	0.22	480±66		2.1				1014±68	
	8	10	3	0.18	**630±76**		2.6	n:636±33		2.6	1663±140	
	10	10	3	0.15	**766±90**	(0.95)	2.7				2058±148	
	16	11	3	0.13	**1119±115**		2.8	n:2156±216		1.4	3120±168	
	20	12	4	0.11	**1361±212**		2.8				3777±127	
	32	14	4	0.09	**1997±247**		2.9				5767±162	
	40	15	5	0.08	**2409±120**		2.9				7023±173	
f_{Ackley}	2	6	3		352±39		2.1	**n:227±23**		3.2	735±55	
	4	8	3		**540±29**	(0.95)	2.9				1577±83	
	5	8	3		**566±33**		3.4	n:704±24	(0.90)	2.2	1904±122	(0.95)
	8	10	3		**800±22**	(0.95)	3.8				3066±114	
	10	10	3		**892±28**		4.1	n:2066±119	(0.95)	1.8	3641±154	
	16	11	3		**1530±39**		3.7				5672±151	
	20	12	4		**1884±50**		3.5	8150±196		0.8	6641±108	
	32	14	4		**2747±62**		3.7				10063±203	
	40	15	5		**3690±80**		3.3				12084±247	
f_{Elli}	2	6	3		**393±19**		2.0				774±73	
	4	8	3		**582±24**		2.9				1688±11	
	5	8	3		**683±33**		3.4				2342±162	
	8	10	3		**1142±53**		4.0				4542±155	
	10	10	3		**1628±95**		3.8				6211±264	
	16	11	3		**4706±148**		2.8				13177±341	
	20	12	4		**8250±393**		2.3				19060±501	
	32	14	4		**27281±753**		1.6				44562±530	
	40	15	5		**33602±548**		2.1				69642±644	
$f_{Rastrigin}$	2	50	25		1640±242	(0.6)	1.2	**n:528±48**	(0.95)	3.6	1970±418	(0.85)
	5	140	70		23293±1374	(0.3)	0.5	**n:4037±209**	(0.60)	3.0	12310±1098	(0.75)

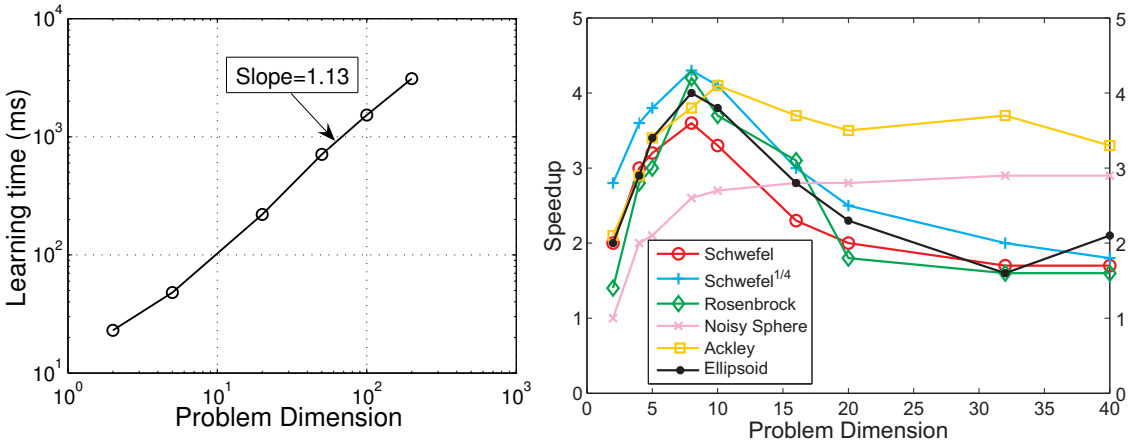

Figure 4.9: **Left**: the cost of model learning/testing increases quasi-linearly with n. **Right**: the average speedup and speedup for all problems except Rastrigin.

function. The speedup w.r.t. CMA-ES is depicted in Figure 4.9-**Right** versus the problem dimension n. Interestingly, the speedup reaches its peak for n ranging in 8..10, then it decreases – except on the Noisy Sphere function. A possible explanation is that the noise level is comparatively less when the dimension increases (as in [Bouzarkouna *et al.*, 2010]), enabling the regularization involved in the model optimization to counteract the noise effects.

On the negative side, ACM-ES performs poorly on $f_{Rastrigin}$ function, and only solves it marginally for dimensions $n > 8$. This failure is attributed to the fact that ACM-ES does not handle well multi-modal diversity; it tends to accelerate the premature convergence to a local optimum, thus amplifying the weakness of CMA-ES without restarts on this benchmark problem: the best-performing versions of CMA-ES require an increasing population size [Hansen, 2009]. Further work will consider the use of niching techniques as well as model quality control strategies to overcome this weakness.

4.2.4 Preliminary Conclusion

The main novelty of the proposed ACM-ES is that all steps of the algorithm preserve invariance with respect to *both* monotonous transformations of the fitness function and orthogonal transformations of the search space. Comparison-based invariance is enforced by using Ranking Support Vector Machines to learn the surrogate model; coordinate invariance is enforced through using the covariance matrix adapted by CMA-ES as SVM kernel. Experimental validation confirms both invariance claims, and demonstrates the merits of the approach in terms of fitness evaluations and scalability w.r.t. the space dimension.

The main weakness of the approach is due to the failure of the surrogate model to account for multi-modal landscapes, as shown on the Rastrigin function; some improvements,

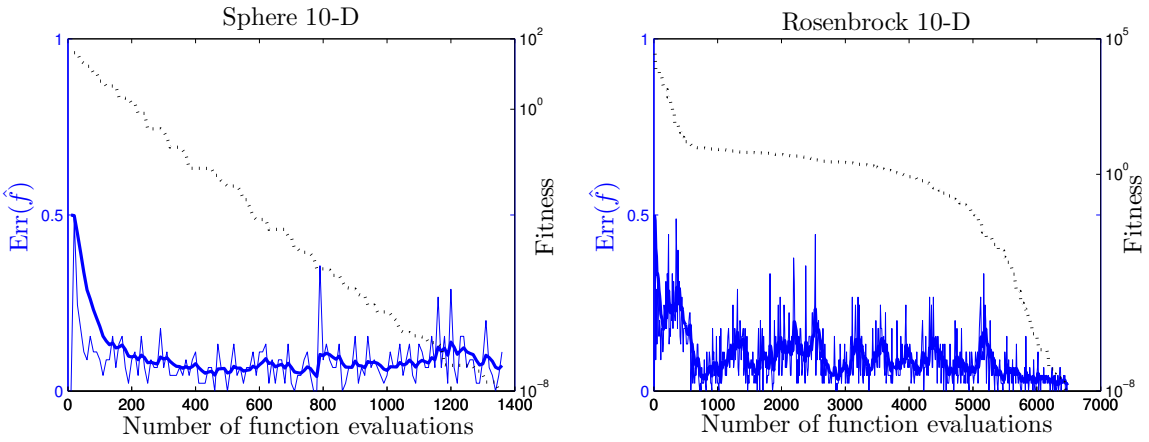

Figure 4.10: Rank-based surrogate error vs number of function evaluations, during a representative run of CMA-ES on 10-dimensional Sphere **(Left)** and Rosenbrock **(Right)** functions. See text for details.

e.g., related to model control, will be discussed in the next Section. Another issue regards the surrogate model hyper-parameters, which have been calibrated after preliminary experiments on the Sphere function conditionally to the carefully tuned hyper-parameters of CMA-ES [Hansen and Ostermeier, 2001]. A global approach, considering both sets of hyper-parameters in an integrated way, would be appropriate. Another perspective, pointed out in [Runarsson, 2004], is to extend the approach to constrained optimization.

4.3 Self-adaptive Surrogate-assisted CMA-ES

In this Section, we present a surrogate-adaptation mechanism (^{s*}) which can be used on top of any surrogate optimization approach. ^{s*} adapts online the number of generations after which the surrogate is re-trained, referred to as the surrogate *lifelength*; further, it adaptively optimizes during the search the surrogate hyper-parameters using an embedded CMA-ES module. A proof of principle of the approach is given by implementing ^{s*} on top of ACM-ES, a surrogate-assisted variant of CMA-ES, yielding the ^{s*}ACM-ES algorithm. To our best knowledge, the self-adaptation of the surrogate model within CMA-ES and by CMA-ES is a new contribution. The merits of the approach are shown as ^{s*}ACM-ES shows significant improvements compared to CMA-ES and ACM-ES on the BBOB-2012 noiseless and noisy testbeds.

The results of this Section have been published as [Loshchilov *et al.*, 2012e, Loshchilov *et al.*, 2012b, Loshchilov *et al.*, 2012c].

4.3.1 Preliminary Analysis

Following the characterization proposed in [Jin, 2005], ACM-ES, discussed in detail in the previous Section, is a surrogate-assisted optimizer with an individual-based evolution con-

trol. As in many other pre-selection methods (see Section 3.3.2.1 for a detailed overview), at each generation ACM-ES generates λ_{Pre} individuals, where λ_{Pre} is much larger than population size λ. Then λ_{Pre} pre-children are evaluated and ranked using surrogate model $\widehat{f}$. The most promising λ' (not always the best) pre-children are selected and evaluated using the true expensive function, yielding new points $(\boldsymbol{x}, f(\boldsymbol{x}))$. When the true objective function of λ' individuals is known, the ranking of other $\lambda - \lambda'$ points can be approximated.

While the experimental results demonstrate the improvements brought by ACM-ES on some functions (about 2-4 times faster than CMA-ES on Rosenbrock, Ellipsoid, Schwefel, Noisy Sphere and Ackley functions up to dimension 20, see Figure 4.9), they also show a loss of performance on the multi-modal Rastrigin function. Complementary experiments suggest that:

1. on highly multi-modal functions, the surrogate model happens to suffer from a loss of accuracy; in such cases some control is required to prevent the surrogate model from misleading the search;

2. surrogate-assisted algorithms may require a larger population size for multi-modal problems.

The lack of surrogate control appears to be an important drawback in ACM-ES. This control should naturally reflect the current surrogate accuracy. A standard measure of the rank-based surrogate error is given as the fraction of violated ranking constraints on the test set (see Section 3.3.1.1 and Eq. 4.9). Error value 0 (respectively, 0.5) corresponds to a perfect surrogate (respectively, random guessing).

4.3.1.1 Model Quality Estimation

Before doing surrogate-assisted optimization one should be sure that the model provides a reasonable prediction of the objective function. Figure 4.10 illustrates the surrogate model error during a representative run of CMA-ES (with re-training at each iteration, but without any exploitation of the model) on 10-dimensional Sphere **(Left)** and Rosenbrock **(Right)** functions using 100 and 250 training points, respectively. Thin blue curves correspond to the model error $Err(\hat{f})$ measured with Eq. (4.9) on λ offspring (test) solutions, which were not used to build $\hat{f}$. Dotted curves correspond to fitness of the mean m of the mutation distribution of CMA-ES. A fluctuation of $Err(\hat{f})$ is clearly observable because i). the model quality changes depending on used training points, hyper-parameters, etc.; ii). the estimation of $Err(\hat{f})$ is imprecise because λ is too small ($\lambda = 10$ for 10-dimensional problems). To make this estimation more robust one of the following approaches can be used:

1. Use larger λ. This may increase the overall runtime of CMA-ES.

2. Exclude some training points and use them as test points. These points should be located in the actual search region of CMA-ES. Exclusion of such points may worsen the model.

3. Use cross-validation, e.g., leave-one-out cross-validation (see Section 3.3.1.2). This may significantly increase the computational complexity of the algorithm.

4. Use some relaxation of $Err(\hat{f})$. The results may be sensitive to the parametrization of the relaxation (also true for all approaches described above).

For a better numerical stability without additional computational cost, we suggest to update the surrogate error using additive relaxation with relaxation constant β_{Err}:

$$Err(\hat{f}) = (1 - \beta_{Err})Err(\hat{f}) + \beta_{Err}Err(\hat{f})_{loc}, \tag{4.14}$$

where $Err(\hat{f})_{loc}$ is the *local* model error estimated on λ points of the current generation using Eq. (4.9). We experimentally found that $\beta_{Err} = 0.2$ represents a reasonable trade-off between the use of local and global information. This parameter indeed is problem- and model control approach-dependent. It can be adjusted if some relevant information about the problem at hand is available. As the initial setting of $Err(\hat{f})$ we choose a pessimistic value 0.5 (random prediction) to avoid a potential overestimation of $Err(\hat{f})$ in the first generations of CMA-ES. As can be seen in Figure 4.10, the relaxed model error (bold blue lines) is quite robust w.r.t. outliers, and at the same time is sensitive to local information.

4.3.1.2 Model Exploitation

As can be seen in Figure 4.10, after the first generations of CMA-ES, the surrogate error decreases to approximately 10%. This better than random prediction can be viewed as a source of information about the function which can be used to improve the search.

Let $\widehat{n}$ denote the number of generations a surrogate model is used, referred to as surrogate *lifelength*. In so-called generation-based evolution control methods [Jin, 2005], the surrogate $\widehat{f}$ is directly optimized for $\widehat{n}$ generations, without requiring any true (expensive) objective computations. Then, the following generation considers the objective function f, and yields instances to enrich the training set, relearn or refresh the surrogate and adjust some parameters of the algorithm. The surrogate lifelength $\widehat{n}$ can be fixed or adapted.

The above-described procedure, as well as several approaches which we will present in this Section, can be used in principle with any optimization algorithm. In this work, however, we consider CMA-ES and its active and restart versions by the reasons discussed in Section 2.3.3.

An experimental study of the impact of $\widehat{n}$ is displayed in Figure 4.11, showing the speedup reached by direct surrogate optimization on several 10-dimensional benchmark problems *vs* the number of generations $\widehat{n}$ the surrogate is used. A factor of speedup 1.7 is obtained for $\widehat{n}$= 1 on the Rotated Ellipsoid function, close to the optimal speedup 2.0. A speedup ranging from 2 to 4 is obtained for IPOP-aACM-ES with surrogates for $\widehat{n}$ *in* $[5, 15]$. As could have been expected again, the optimal value of $\widehat{n}$ is problem-dependent and widely varies. In the case of the Attractive Sector problem for instance, the surrogate model is imprecise and not useful, so $\widehat{n} = 0$ should be used (thus falling back to the original IPOP-aCMA-ES with no surrogate) to prevent the surrogate from misleading the search.

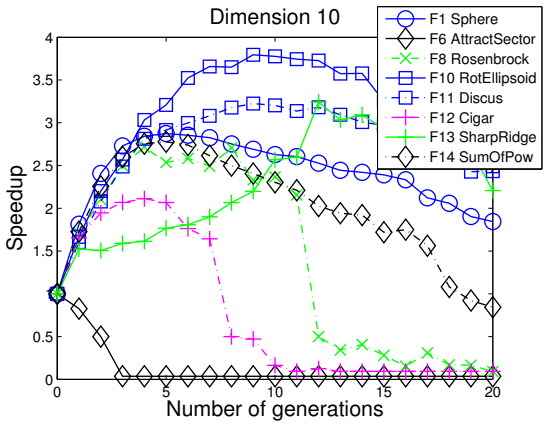

Figure 4.11: The speedup of IPOP-aACM-ES over IPOP-aCMA-ES, where speedup = 2.0 means that IPOP-aACM-ES with a given lifelength $\widehat{n}$ of the surrogate model, requires 2.0 times less computational effort SP1 (i.e., the average number of function evaluations of successful runs divided by proportion of successful runs) than IPOP-aCMA-ES to reach the target objective value of $f_{\mathrm{t}} = f_{\mathrm{opt}} + 10^{-8}$. The results of the IPOP-aCMA-ES are given when number of generations is zero.

4.3.1.3 Adjusting Surrogate Lifelength

A natural idea is then to adjust lifelength $\widehat{n}$ can be adjusted depending on the error made by the surrogate $\hat{f}$ on the new λ points evaluated on f. If this error is 0, then $\hat{f}$ is perfectly accurate and could have been used for some more generations before learning a new $\hat{f}$. In this case, lifelength $\widehat{n}$ is set to the maximum value $\widehat{n_{max}}$, which corresponds to the maximum theoretical speedup of the ^{s}*ACM-ES. If the error is circa 0.5, surrogate $\hat{f}$ provides no better indications than random guessing and thus misleads the optimization: $\widehat{n}$ is set to 0. More generally, considering an error threshold τ_{err}, we decided to adjust $\widehat{n}$ between $\widehat{n_{max}}$ and 0, proportionally[3] to the ratio between the actual error and the error threshold τ_{err} (bold curve in Figure 4.12):

$$\widehat{n} \leftarrow \left\lfloor \frac{\tau_{err} - \mathrm{Err}(\hat{f})}{\tau_{err}} \widehat{n_{max}} \right\rfloor . \tag{4.15}$$

4.3.1.4 Alternative Approaches to Surrogate Model Exploitation

To try to improve the results of ACM, we also tested a trust-region-based algorithm, where $\hat{f}$ is optimized to find a candidate solution $\boldsymbol{x}^*$ to be evaluated on f. The trust-region is bounded using the Mahalanobis distance defined by the covariance matrix of CMA-ES. We found that the results of ACM on Ellipsoid function can be improved, but

[3]Complementary experiments show that the best adjustment of $\widehat{n}$ depending on the surrogate error is again problem-dependent, but that the linear adjustment proposed here is a good compromise.

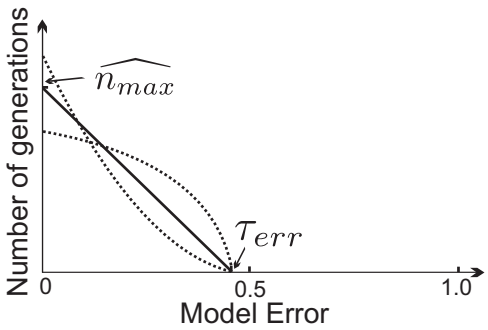

Figure 4.12: Number of generations $\widehat{n}$ versus surrogate error Err. Linear interpolation (bold curve) has been used in the experimental validation.

in larger dimensions ($n > 10$) this strategy becomes too "greedy", the training set is not sufficiently diverse to build an accurate $\hat{f}$. Thus, some diversity preservation procedure must be considered. The most important drawback of the trust-region-based search is the evaluation of (usually) only one solution on f per iteration. This makes the algorithm not suitable for parallel evaluations of solutions, which is the main source of speedup in real-world expensive optimization. Another important detail is that the algorithm actually not resembles anymore CMA-ES and its performance is not stable on noisy functions.

Instead of evaluating λ individuals after $\hat{n}$ generations on $\hat{f}$ we may use alternative strategies, e.g., evaluate on f one best or random individual per generation. We found that this may improve the results, however, there are at least two issues: i). again, the algorithm cannot be efficiently parallelized; ii). CMA-ES never observes the correct ranking of all individuals, thus, a potential misleading introduced by the surrogate model may be heavily corrected.

We also tested several strategies to control $\hat{n}$, including the following ones:

1. Optimal control of $\hat{n}$ can be viewed as an operator selection problem with a fixed number of arms/operators, e.g., 21 arms for $\hat{n} = 0, \ldots, 20$ (see Figure 4.11). To find an optimal $\hat{n}$, Multi-Armed Bandits paradigm can be applied (see, e.g., [Fialho *et al.*, 2010]). We also tested an Elo-based (chess rating system named after Arpad Elo, a master-level chess player) system, where in each game we check two arms i and j and the one whose $\lfloor \lambda/2 \rfloor$ offspring are statistically better wins the game. Using Elo-based approach we may find the rating for different $\hat{n}$, an important detail is that even if some arm is rarely used it may quickly reach high Elo rating if wins against another high-rated arm. The approach can be extended to the competition of teams of arms using generalized Elo-system proposed in [Dangauthier *et al.*, 2007, Coulom, 2007].

2. The search for an optimal $\hat{n}$ can be viewed as a one-dimensional noisy optimization problem. We may directly apply ESs to solve this problem. For each generated offspring defined by a decision variable $\hat{n}$ we run CMA-ES on $\hat{f}$ for $\hat{n}$ generations and evaluate one best, mean or random individual of the $\hat{n}$-th population on f.

Then, we may compare different alternatives (solutions) of $\hat{n}$, choose new mean of distribution, adapts parameters of ES and repeat the procedure again. It should be noted that the minimum variance must be fixed to prevent the algorithm from premature convergence on an integer value of $\hat{n}$, given that the problem is dynamic and noisy.

3. An alternative to the previously described strategy would be to consider only two candidate generations at a time, generations $\hat{n}$ and $\hat{n}+1$. We may run CMA-ES on $\hat{f}$ for $\hat{n}$ generation and evaluate $\lfloor \lambda/2 \rfloor$ individuals on f (without updating $\hat{f}$), then run for one more generation and evaluate the remaining $\lambda - \lfloor \lambda/2 \rfloor$ individuals. We may check whether $\hat{n}+1$-th individuals are statistically significantly better or not, if this is the case, we may increment $\hat{n}$ and vise versa. If there is no difference, then we may suppose that we are around the maximum of curves illustrated in Figure 4.11. However, it may happen that the one-dimensional curve is flat and we will (almost randomly) walk unreasonably far away. The latter becomes a problem if the model quality drops quickly, then we should quickly decrease $\hat{n}$, but doing so decrementally may take a long time so that the algorithm finally diverges. As an alternative we used Wilcoxon rank-sum test to estimate the significance of difference between $\hat{n}$-th and $\hat{n}+1$-th generations to set the scale of the increasing/decreasing factor of $\hat{n}$ correspondingly.

The described above approaches have at least three important drawbacks:

1. When λ points from different generations are evaluated, we have a dilemma to choose which state of CMA-ES will be used as the actual one for the next generation. We may compute this state as a weighted sum of all states, which were used to generate λ points. However, this may potentially introduce an instability to CMA-ES.

2. If the model quality drops relatively quickly, it may take some time to adjust $\hat{n}$ accordingly.

3. If the model is random guessing ($Err(\hat{f})$=0.5), then we will still need to check $\hat{n}=0$ (no surrogate mode used = no loss) and $\hat{n}=1$ (*one generation of divergence*). Thus, when the model badly predicts f, which is often the case on multi-modal and/or noisy functions, the algorithm will often diverge because of $\hat{n}=1$.

To summarize, we choose the approach described in Section 4.3.1.3 as a *baseline* for our experiments because it allows to prevent divergence if $\hat{f}$ is random guessing, the evaluation of all λ individuals can be easily parallelized, and the implementation of the approach is straightforward. However, we strongly believe that the other approaches described above are prospective and can be superior to the error model-based one under certain conditions.

4.3.2 Self-adaptive Surrogate-assisted CMA-ES

In this Section, we describe the novel surrogate adaptation mechanism resulting from previous discussions, which can be used in principle on top of any iterative population-based

optimizer without requiring any significant modifications thereof. The approach is illustrated on top of CMA-ES and ACM-ES. The resulting algorithm, ^{s*}ACM-ES, maintains a global hyper-parameter vector $\theta = (\theta_{opt}, \theta_{sur}, \widehat{n}, \mathcal{A}, \alpha)$, where:
• θ_{opt} stands for the optimization parameters of the outer CMA-ES used for expensive function optimization (see Figure 4.13);
• θ_{sur} stands for the optimization parameters of the internal CMA-ES used for surrogate model hyper-parameters optimization;
• $\widehat{n}$ is the number of internal generations during which the current surrogate model is used;
• $\mathcal{A}$ is the archive of all points $(\boldsymbol{x}_i, f(\boldsymbol{x}_i))$ for which the true objective function has been computed, exploited to train the surrogate function;
• α stands for the surrogate hyper-parameters.
All hyper-parameters are indexed by the current outer generation g; by abuse of notations, the subscript g is omitted when clear from the context.

4.3.2.1 Overview of ^{s*}ACM-ES

Let *GenCMA*(h,θ_h,$\mathcal{A}$) denote the elementary optimization module (here one generation of CMA-ES) where h is the function to be optimized (the true objective f or the surrogate $\widehat{f}$), θ_h denotes the current optimization parameters (e.g., CMA-ES step-size and covariance matrix, etc.) associated to h, and $\mathcal{A}$ is the archive of f. After each call of *GenCMA*, optimization parameters θ_h are updated; and if *GenCMA* was called with the true objective function f, archive $\mathcal{A}$ is updated and augmented with the new points $(\boldsymbol{x}, f(\boldsymbol{x}))$. Note that *GenCMA* can be replaced by any black-box optimization procedure, as long as it is able to update its own optimization parameters and the archive.

^{s*}ACM-ES starts by calling *GenCMA* for g_{start} number of generations with the true objective f, where θ_{opt} and $\mathcal{A}$ are respectively initialized to the default parameter of CMA-ES and the empty set (Algorithm 4.2, lines 4-7). In this starting phase, optimization parameter θ_{opt} and archive $\mathcal{A}$ are updated in each generation.

Then ^{s*}ACM-ES iterates a six-step process (Algorithm 4.2, lines 9 - 22, illustrated in Figure 4.13):

1 Learning surrogate $\widehat{f}$ using surrogate model hyper-parameters α (e.g., number of training points, parameters of kernel functions) and the current optimization parameters θ_{opt} such as covariance matrix C (procedure BuildSurrogateModel, line 9; Section 4.1.1).

2 Optimizing the surrogate $\widehat{f}$ for $\widehat{n}$ generations (lines 11-13). This step classically calls *GenCMA*($\widehat{f}$,θ_{opt},$\mathcal{A}$) for $\widehat{n}$ consecutive generations; θ_{opt} is updated accordingly while $\mathcal{A}$ is unchanged since this step does not involve any computation of the expensive f.

3 Optimizing the expensive function f for one generation (line 15). In this step, we sample and evaluate λ individuals on f and update θ_{opt} parameters of CMA-ES accordingly, updating and augmenting archive $\mathcal{A}$ with new $(\boldsymbol{x}, f(\boldsymbol{x}))$ points.

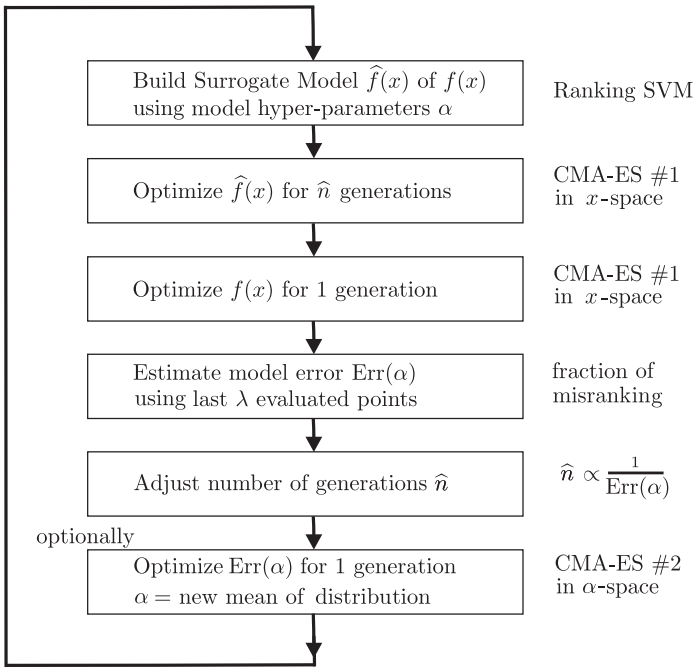

Figure 4.13: Optimization loop of the ^{s*}ACM-ES.

4 Estimating model error $Err(\hat{f})$ using Eq. (4.9) on λ recently evaluated points (line 17).

5 Adjusting the surrogate lifelength $\widehat{n}$ using Eq. (4.15) (line 19, Section 4.3.1.3).

6 Optimizing surrogate model hyper-parameters α (line 21).

The contribution regards the adjustment of the surrogate hyper-parameters α (e.g., the number of the training points in $\mathcal{A}$; the weights of the constraint violations in Ranking SVM, see Table 4.3), which are adjusted to optimize the quality of the surrogate Err (Eq. 4.9). Formally, to each surrogate hyper-parameter vector α is associated a surrogate error $\mathrm{Err}(\alpha)$ defined as follows (see Algorithm 4.3): hyper-parameter α is used to learn surrogate $\widehat{f}_\alpha$ using $\mathcal{A}_{g-1}$ as training set, and $\mathrm{Err}(\alpha)$ is set to the ranking error of $\widehat{f}_\alpha$(Eq. 4.9), using the most recent λ points from $\mathcal{A}_g - \mathcal{A}_{g-1}$ as test set.

The elementary optimization module *GenCMA*(Err,θ_{sur}) (in this study, we do not use the archive parameter here) is launched for one generation (line 21), and the mean of the CMA-ES mutation distribution is used (line 22) as surrogate hyper-parameter vector in the next surrogate building phase (line 9).

Hyper-parameters might be optimized for more than one generation, however, this would increase the overall computational complexity of the algorithm, because λ_{hyp} surrogates must be built at each generation. Since the hyper-parameters optimization problem is noisy, we suggest to perform one generation with a relatively large λ_{hyp} instead of few generations with a small λ_{hyp}.

Algorithm 4.2: ^{s*}ACM-ES

given $g \leftarrow 0$; Err $\leftarrow 0.5$; $\mathcal{A}_g \leftarrow \emptyset$;
$\theta_{opt} \leftarrow$ InitializationCMA(); // to optimize $f(x)$
$\theta_{sur} \leftarrow$ InitializationCMA(); // to optimize $Err(\alpha)$
repeat
  $\{\theta_{opt}, \mathcal{A}_{g+1}\} \leftarrow$ GenCMA(f,θ_{opt}, $\mathcal{A}_g$);
  $g \leftarrow g + 1$;
until $g = g_{start}$;
repeat
  $\widehat{f}(x) \leftarrow$ BuildSurrogateModel(α, $\mathcal{A}_g$, θ_{opt});
  $g_{prev} \leftarrow g$;
  for $i = 1, \ldots, \widehat{n}$ **do**
    $\{\theta_{opt}, \mathcal{A}_{g+1} = \mathcal{A}_g\} \leftarrow$ GenCMA($\widehat{f}$,θ_{opt}, $\mathcal{A}_g$);
    $g \leftarrow g + 1$;
  end for
  $\{\theta_{opt}, \mathcal{A}_{g+1}\} \leftarrow$ GenCMA(f,θ_{opt}, $\mathcal{A}_g$);
  $g \leftarrow g + 1$;
  Err(α) $\leftarrow$ MeasureSurrogateError($\widehat{f}$,θ_{opt});
  Err $\leftarrow (1 - \beta_{\mathrm{Err}})$Err $+ \beta_{\mathrm{Err}}$Err(α);
  $\widehat{n} \leftarrow \left\lfloor \frac{\tau_{err} - \mathrm{Err}}{\tau_{err}} \widehat{n_{max}} \right\rfloor$;
  // adjust surrogate hyper-parameters
  $\theta_{sur} \leftarrow$ GenCMA(Err,θ_{sur});
  $\alpha \leftarrow \theta_{sur}.m$; // detach the mean m of mutation distibution stored in θ_{sur}
until stopping criterion is met ;

Algorithm 4.3: Objective function Err(α) of surrogate model

given α
$\widehat{f}(x) \leftarrow$ BuildSurrogateModel(α, $\mathcal{A}_{g_{prev}}$, $\theta_{sur,g_{prev}}$);
Err(α) $\leftarrow$ MeasureSurrogateError($\widehat{f}$, $\theta_{opt,g_{prev}}$);

4.3.3 Experimental Validation

The experimental validation of the approach proceeds by comparing the performance of ^{s*}ACM-ES to the original CMA-ES and the active CMA-ES (aCMA-ES), considering IPOP and BIPOP restart scenarios with increasing population size (see Section 2.3.2 for a detailed description of CMA-ES variants).

The active IPOP-aCMA-ES [Hansen and Ros, 2010a] with the weighted negative covariance matrix update is found to perform equally well or better than IPOP-CMA-ES, which is explained as it more efficiently exploits the information of the worst $\lambda/2$ points. We use IPOP-aCMA-ES as challenging baseline, as it is a priori more difficult to speed up than the original IPOP-CMA-ES.

Parameter	Range for online tuning	Offline tuned value
ℓ=$N_{training}$	$\left[4n, 2(40 + \lfloor 4n^{1.7} \rfloor)\right]$	$40 + \lfloor 4n^{1.7} \rfloor$
C_{base}	$[0, 10]$	6
C_{pow}	$[0, 6]$	3
c_{sigma}	$[0.5, 2]$	1

Table 4.3: Surrogate hyper-parameters, default value and range of variation

Specifically, ^{s*}ACM-ES is validated on the noiseless BBOB testbed by comparing IPOP-aACM-ES with fixed hyper-parameters, and IPOP-^{s*}aACM-ES (also called IPOP-saACM-ES) with online adaptation of hyper-parameters of the surrogate model[4].

After detailing the experimental setting, this Section reports on the offline tuning of the number ℓ of points used to learn the surrogate model, and the online tuning of the surrogate hyper-parameters (line 21 of Algorithm 4.2).

4.3.3.1 Experimental Setting

The default BBOB stopping criterion is reaching target function value $f_{\mathrm{t}} = f_{\mathrm{opt}} + 10^{-8}$. Ranking SVM is trained using the ℓ most recently evaluated points; its stopping criterion is arbitrarily set to a maximum number of 1000ℓ iterations of the SMO optimization procedure (see Section 4.1.1).

After a few preliminary experiments, the Ranking SVM constraint violation weights (Eq. 4.1) are set to

$$C_i = 10^{C_{base}} (\ell - i)^{C_{pow}}$$

with $C_{base} = 6$ and $C_{pow} = 3$ by default; the cost of constraint violation is thus cubically higher for top-ranked samples. The σ parameter of the RBF kernel is set to $\sigma = c_{sigma}\sigma_x$, where σ_x is the dispersion of the training points (their average distance after translation, Eq. 4.12) and c_{sigma} is set to 1 by default. The number g_{start} of CMA-ES calls in the initial phase is set to 10, the maximum lifelength $\widehat{n_{max}}$ of a surrogate model is set to 20. The error threshold τ_{err} is set to 0.45 and the error relaxation factor β_{Err} is set to 0.2.

The surrogate hyper-parameters θ_{sur} are summarized in Table 4.3, with offline tuned value (default for IPOP-aACM-ES) and their range of variation for online tuning, (where n stands for the problem dimension). Surrogate hyper-parameters are optimized with a population size 20 ($\lambda_{hyp} = 20$ surrogate models), where the Err function associated to a hyper-parameter vector is measured on the λ most recently evaluated points in archive $\mathcal{A}$, λ being the current optimization population size.

[4] For the sake of reproducibility we used the Octave/MatLab source code of IPOP-CMA-ES with default parameters, available from its author's page, with the active flag set to 1. The ^{s*}ACM-ES source code is available at
`https://sites.google.com/site/acmesgecco/`.

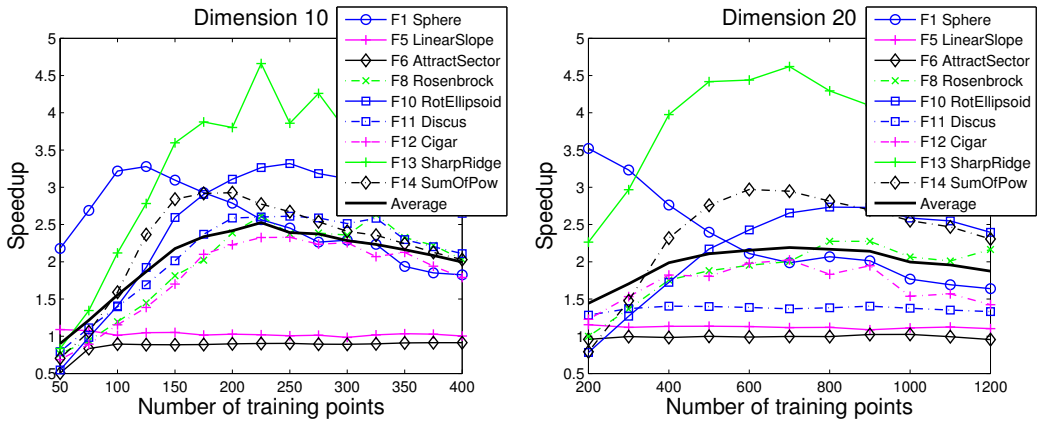

Figure 4.14: The speedup of IPOP-aACM-ES over IPOP-aCMA-ES w.r.t. *fixed* number of training points on **(Left)** 10-dimensional and **(Right)** 20-dimensional BBOB benchmark problems.

4.3.3.2 Offline Tuning: Number of Training Points

It is widely acknowledged that the selection of the training set is an essential ingredient of surrogate learning [Jin, 2005, Ingimundardottir and Runarsson, 2011]. After some alternative experiments the training set includes the most recent ℓ points in the archive (see Section 4.3.3.2 for a discussion of different training set selection strategies). The study thus focuses on the tuning of ℓ. Its optimal tuning is of course problem- and surrogate learning algorithm-dependent. Several tunings have been considered in the literature, for instance for 10-dimensional problems: 3λ for SVR [Ulmer *et al.*, 2004]; 30 for RBF [Ulmer *et al.*, 2003a]; $2n = 20$ for Kriging [Kruisselbrink *et al.*, 2010]; 50 for ANN [Jin, 2005]; $\lambda, 2\lambda$ for Ranking SVM [Runarsson, 2006, Ingimundardottir and Runarsson, 2011]; $\frac{n(n+1)}{2} + 1 = 66$ for LWR in the lmm-CMA-ES [Bouzarkouna *et al.*, 2010]; $\lfloor 30\sqrt{n} \rfloor = 95$ and $\lfloor 70\sqrt{n} \rfloor = 221$ for Ranking SVM in the ACM-ES (see Section 4.2.3).

In all above cases but ACM-ES, the surrogate models aim at local approximation. These approaches might thus be biased toward small ℓ values, as a small number of training points are required to yield good local models (e.g., in the case of the Sphere function), and small ℓ values positively contribute to the speedup. It is suggested however that the Sphere function might be misleading regarding the optimal adjustment of ℓ.

Let us consider the surrogate speedup of IPOP-aACM-ES w.r.t. IPOP-aCMA-ES depending on (fixed) ℓ, on unimodal benchmark problems from the BBOB noiseless testbed (Figure 4.14 for $n = 10, 20$). While the optimal speedup varies from 2 to 4, the actual speedup strongly depends on the number ℓ of training points.

Complementary experiments on n-dimensional problems with $n = 2, 5, 10, 20, 40$ yield to propose an average best tuning of ℓ depending on dimension n:

$$\ell = \lfloor 40 + 4n^{1.7} \rfloor \tag{4.16}$$

Eq. (4.16) is found to empirically outperform the one proposed for the original ACM-ES

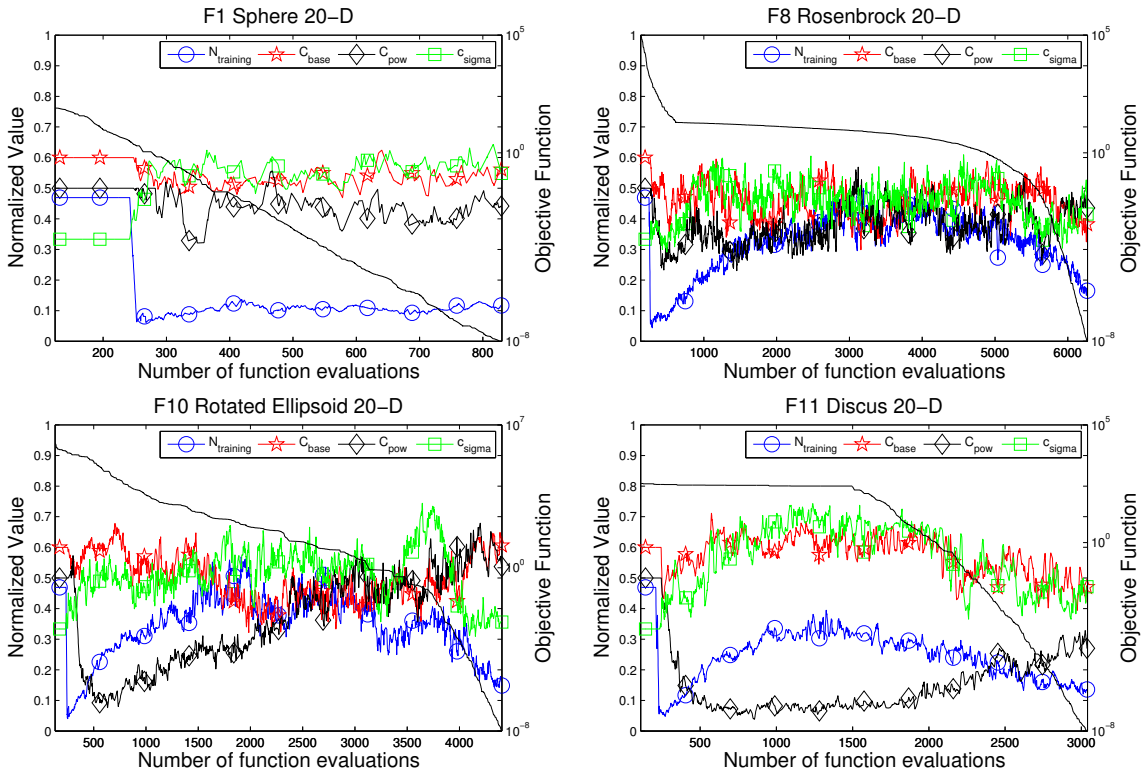

Figure 4.15: Median trajectories of normalized surrogate hyper-parameters estimated on 15 runs of the IPOP-^{s*}aACM-ES **with Ranking SVM** on Sphere, Rotated Ellipsoid, Discus and Rosenbrock 20-dimensional BBOB benchmark problems.

in Section 4.2.3 ($\ell = \lfloor 70\sqrt{n} \rfloor$), which appears to be biased to 10-dimensional problems, and underestimates the number of training points required in higher dimensions. Experimentally however, ℓ must increase super-linearly with n; Eq. (4.16) states that for large n the number of training points should triple when n doubles.

Further, Figure 4.14 shows that the optimal ℓ value is significantly smaller for the Sphere function than for other functions, which experimentally supports our conjecture that the Sphere function might be misleading with regard to the tuning of surrogate hyper-parameters.

4.3.3.3 Online Tuning: Surrogate Hyper-parameters

The IPOP-^{s*}ACM-ES achieves the online adaptation of the surrogate hyper-parameters within a specified range (Table 4.3), yielding the surrogate hyper-parameter values to be used in the next surrogate learning step.

Note that a surrogate hyper-parameter individual might be non-viable, i.e., if it does not enable to learn a surrogate model (e.g., the number of training points is negative).

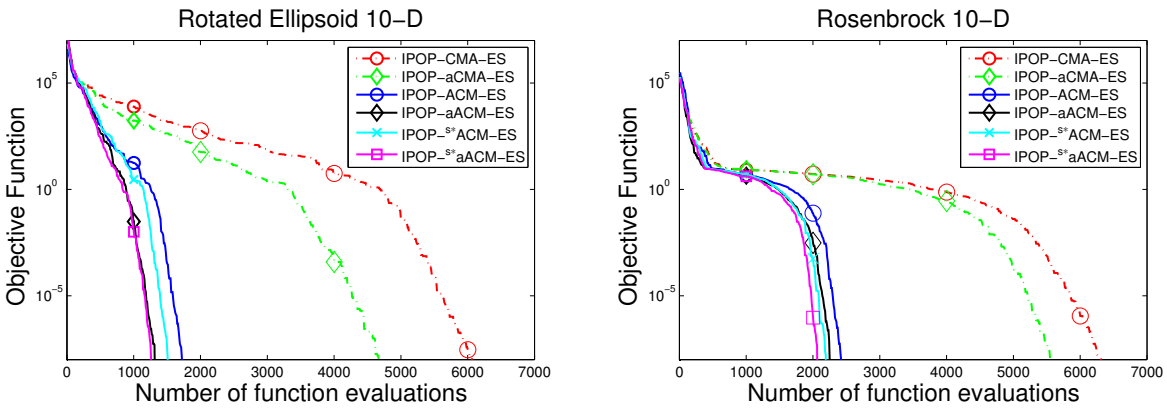

Figure 4.16: Comparison of the proposed surrogate-assisted versions of the original and active IPOP-CMA-ES algorithms on 10-dimensional Rotated Ellipsoid **(Left)** and Rosenbrock **(Right)** functions. The trajectories show the median of 15 runs.

Such non-viable individual is heavily penalized ($\mathrm{Err}(\alpha) > 1$). In case no usable hyper-parameter individual is found (which might happen in the very early generations as it is shown in Figure 4.15), θ_{sur} is set to its default value.

The online adaptation of surrogate hyper-parameters however soon reaches usable hyper-parameter values. The trajectory of the surrogate hyper-parameter values vs the number of generations is depicted in Figure 4.15, normalized in $[0, 1]$ and considering the median out of 15 runs optimizing 20-dimensional Sphere, Rosenbrock, Rotated Ellipsoid and Discus functions.

On Ellipsoid, Discus and Rosenbrock functions the trajectory of ℓ displays three stages. In a first stage, ℓ increases as the overall number of evaluated points (all points are required to build a good surrogate). In a second stage, ℓ reaches a plateau; its value is close to the one found by offline tuning (see Section 4.3.3.2). In a third stage, ℓ steadily decreases. This last stage is explained as CMA-ES approaches the optimum of f and gets a good estimate of the covariance matrix of the objective function. At this point the optimization problem is close to the Sphere function, and as can be seen from the results for the Sphere function, a good surrogate can be learned from comparatively few training points.

The trajectories of other surrogate hyper-parameters are more difficult to interpret, although they clearly show non-random patterns (e.g., C_{pow} on Ellipsoid and Discus functions).

4.3.3.4 Comparative Performances

The comparative performance of ^{s*}ACM-ES combined with the original and the active variants of IPOP-CMA-ES is depicted in Figure 4.16, on the 10-dimensional Rotated Ellipsoid (**Left**) and Rosenbrock (**Right**) functions. In both cases, the online adaptation of the surrogate hyper-parameters yields a quasi constant speedup, witnessing the robustness of ^{s*}ACM-ES. On the Ellipsoid function, the adaptation of the covariance matrix is much faster than for the baseline, yielding same convergence speed as for the original CMA-

ES on Sphere function. On the Rosenbrock function the adaptation is also much faster, although there is clearly room for improvements.

The performance gain of ^{s*}ACM-ES, explained from the online adjustment of the surrogate hyper-parameters, in particular ℓ, confirms the fact that the appropriate surrogate hyper-parameters vary along search, and can be adjusted based on the accuracy of the current surrogate model. Notably, IPOP-^{s*}ACM-ES almost always outperforms IPOP-ACM-ES, especially for $n > 10$ (in some cases, offline well-tuned hyper-parameters, indeed, may lead to better results).

4.3.3.5 Scalability w.r.t. Population Size

The default population size $\lambda_{default} = 4 + \lfloor 3\log n \rfloor$ is suggested to be the only CMA-ES parameter to possibly require manual tuning. Actually, $\lambda_{default}$ is well tuned for unimodal problems and only depends on the problem dimension. Increasing the population size usually does not decrease the overall number of function evaluations needed to reach an optimum. However, it allows one to reach the optimum faster in terms of number of generations. Increasing the population size and running the objective function computations in parallel is a source of speedup, which raises the question of ^{s*}ACM-ES scalability w.r.t. the population size.

Figure 4.17 shows the speedup of the IPOP-^{s*}aACM-ES compared to IPOP-aCMA-ES for unimodal 10-dimensional problems, when the population size λ is set to γ times the default population size $\lambda_{default}$ (the original IPOP-^{s*}aACM-ES is shown for $\gamma = 1$). In all experiments g_{start} was set to 2, because using large populations we may quickly store sufficiently many points in the training set. For F8 Rosenbrock, F12 Cigar and F14 Sum of Different Powers the speedup remains almost constant and independent of γ, while for F10 Rotated Ellipsoid, F11 Discus and F13 Sharp Ridge, it even increases with γ. With a larger population size, "younger" points are used to build the surrogate model, that is hence more accurate.

The experimental evidence suggests that ^{s*}ACM-ES can be applied on top of parallelized versions of IPOP-^{s*}aACM-ES, while preserving or even improving its speedup. Note that the same does not hold true for many surrogate-assisted methods; for instance in trust region methods, one needs to sequentially evaluate the points.

It is thus conjectured that further improvements of CMA-ES (e.g., refined parameter tuning, noise handling) will simultaneously be translated to ^{s*}ACM-ES, without degrading its speedup.

4.3.3.6 Ranking SVM vs Rank-based SVR

We also tested IPOP-^{s*}aACM-ES with Rank-based SVR surrogate models on 20-dimensional Sphere, Rosenbrock, Rotated Ellipsoid and Discus functions. In all experiments we used so-called '(1:N)' scheme, where fitness of each individual corresponds to its rank in the training set (see Section 4.1.4). While it was expected that adaptive scaling of rank-based fitness assignment should lead to better results (i.e., adding the scaling factor to the set of adapted model hyper-parameters), our preliminary experiments do

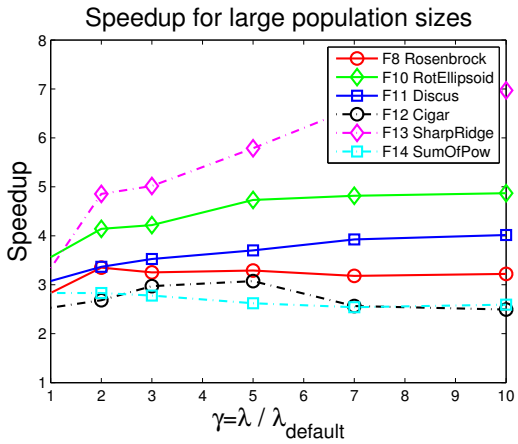

Figure 4.17: Speedup of the IPOP-^{s*}aACM-ES over IPOP-aCMA-ES for large population sizes $\lambda = \gamma\lambda_{default}$ on 10-D problems.

not confirm this hypothesis. The adaptation of ϵ of SVR also does not improve the results, therefore we set $\epsilon = 0$ for all experiments, that probably is a reasonable setting for noise-less problems (for a discussion of a dependency between the noise level and ϵ, see [Smola *et al.*, 1998]). The lack of improvements from the use of more hyper-parameters may be due to a larger space of hyper-parameters, which requires larger λ_{hyp} as well as λ for a better model quality estimation.

The results are shown in Figure 4.18 and can be directly comparable with the results of Ranking SVM, presented in Figure 4.15. It can be seen that SVR-based IPOP-^{s*}aACM-ES is about 3.2, 2.6, 2.8 and 2.6 times slower than Ranking SVM-based IPOP-^{s*}aACM-ES on Sphere, Rosenbrock, Rotated Ellipsoid and Discus functions, respectively. Thus, the use of SVR surrogate models insignificantly improves the original aCMA-ES. We suppose that the main reason for these results is that SVR learning is more constrained than Ranking SVM learning in the sense that f values in SVR learning are pre-defined, while in Ranking SVM they are variables under constraints that the ranking is correct. Thus, the space of satisfactory solutions of Ranking SVM model is larger than of SVR, and, moreover, includes the latter. Finally, the bad results of SVR are not that surprising if one closely looks at Figure 4.4, where it is shown that Rank-based SVR relatively badly approximates the Sphere function.

The number of iterations of SMO optimization was set to 1000ℓ for Ranking SVM and 10ℓ for SVR. These numbers are not directly comparable, because one iteration of SVR learning includes more simple numerical operations, and, therefore, computationally more expensive. If the number of training points is fixed, then the learning of SVR with the *given* number of iterations is faster than the one of Ranking SVM. However, in our experiments with hyper-parameters adaptation we found that the learning and the full run of SVR actually becomes more expensive than the one of Ranking SVM, because SVR usually requires (as suggested by the adaptation) more training points that quickly increases the computational complexity. Finally, the full run of SVR takes about 60,

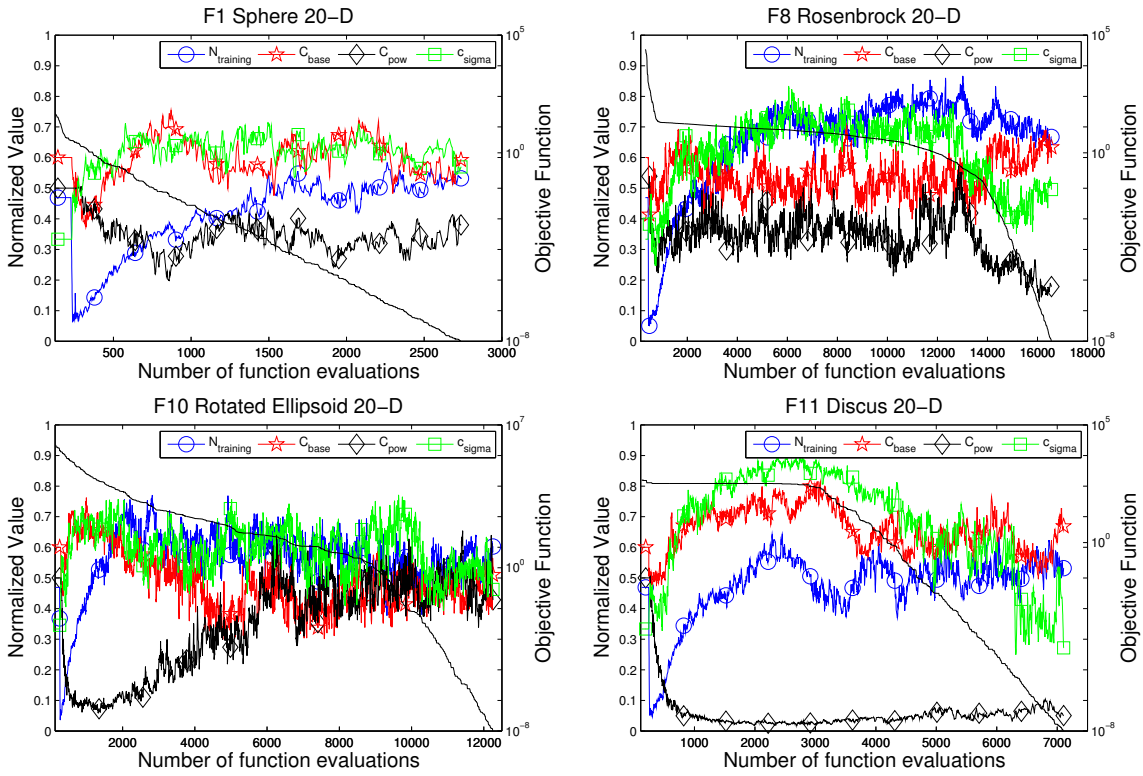

Figure 4.18: Median trajectories of normalized surrogate hyper-parameters estimated on 15 runs of the IPOP-^{s*}aACM-ES **with Rank-based SVR** on Sphere, Rotated Ellipsoid, Discus and Rosenbrock 20-dimensional BBOB benchmark problems. See Figure 4.15 for the results using **Ranking SVM**.

10, 10 and 15 times longer than the of Ranking SVM for Sphere, Rosenbrock, Rotated Ellipsoid and Discus functions, respectively. We also found that the use of larger than default population sizes improves the results for SVR, but it is still worse than Ranking SVM by a factor of about 2-3.

4.3.3.7 Benchmarking on Noiseless BBOB-2012 Testbed

For benchmarking on BBOB noiseless testbed (see Section 2.3.3 for a detailed description of BBOB framework) we consider four CMA-ES algorithms with restart scenario: IPOP-aCMA-ES [Hansen and Ros, 2010a], BIPOP-CMA-ES [Hansen, 2009], IPOP-^{s*}aACM-ES and BIPOP-^{s*}aACM-ES.

Results from experiments according to [Hansen *et al.*, 2012] on the benchmark functions given in [Hansen *et al.*, 2009a] are presented in Figures 4.20 and 4.21 and in Table 4.4. The **expected running time (ERT)**, used in the figures and table, depends on a given target function value, $f_\mathrm{t} = f_\mathrm{opt} + \Delta f$, and is computed over all relevant trials

(on the first 15 instances) as the number of function evaluations executed during each trial while the best function value did not reach f_t, summed over all trials and divided by the number of trials that actually reached f_t [Hansen *et al.*, 2012, Storn and Price, 1997]. **Statistical significance** is tested with the rank-sum test for a given target Δf_t (10^{-8} as in Figure 4.20) using, for each trial, either the number of needed function evaluations to reach Δf_t (inverted and multiplied by -1), or, if the target was not reached, the best Δf-value achieved, measured only up to the smallest number of overall function evaluations for any unsuccessful trial under consideration.

IPOP-^{s*}aACM-ES and BIPOP-^{s*}aACM-ES are the same algorithm (^{s*}aACM-ES) before the first restart occurs, therefore, the results are very similar for the unimodal functions, where the optimum can be found without restarts. The ^{s*}aACM-ES outperforms aCMA-ES usually by a factor from 2 to 4 on f_1, f_2, f_8, f_9, f_{10}, f_{11}, f_{12}, f_{13} and f_{14} for dimensions between 5 and 20. The speedup in dimension 2 is less pronounced for problems, where the running time is too short to improve the search. This is the case for f_5 Linear Slope function, where the speedup can be observed only for dimension 20, because the optimum can be found after about 200 function evaluations. To improve the search on functions with small budgets it would make sense to use the surrogate model right after the first ($g_{start} = 1$) generation of the CMA-ES, while in this study, this parameter g_{start} is conservatively set to 10 generations.

The good results on unimodal functions can be explained by the fact that, while using the same amount of information (all previously evaluated points), ^{s*}aACM-ES processes this information in a more efficient way by constructing the approximation model of the function. Similar effect of more efficient exploitation of the available information can be observed for aCMA-ES in comparison to CMA-ES.

The speedup on multi-modal functions is less pronounced, because they are more difficult to approximate and the final surrogate model often has a bad precision. In this case, the adaptation of the number of generations leads to an oscillation of $\hat{n}$ close to 0, such that the surrogate model is not used for optimization or used for small number of generations.

The BIPOP versions of CMA-ES usually perform better than IPOP on f_{23} and f_{24}, where the optimum is more likely to be found using small initial step-size. This leads to overall better performance of the BIPOP versions, and BIPOP-^{s*}aACM-ES in particular. The better performance of the latter in comparison with BIPOP-CMA-ES can be partially explained by the use of the active covariance matrix update. However, this is not the case for $f_{20} - f_{24}$ functions in 5-D and f_{15-19} in 20-D (see Figure 4.20).

The ^{s*}aACM-ES algorithms improve BBOB-2010 records in dimension 10 and 20 on f_7, f_{10}, f_{11}, f_{12}, f_{13}, f_{14}, f_{15}, f_{16}, f_{20}.

We also compared the proposed algorithms with 43 optimization algorithms tested during the BBOB-2009 and BBOB-2010. Figure 4.19 shows empirical runtime distributions of these algorithm on all noise-less functions ($f_1 - f_{24}$) with target values in $\{10^2, \ldots, 10^{-8}\}$ in dimension 20. The results for dimension 40 are not presented here, because they are incomplete due to extremely long runtime of surrogate-assisted versions on multi-modal functions, where generally millions of function evaluations are needed to reach the optimum.

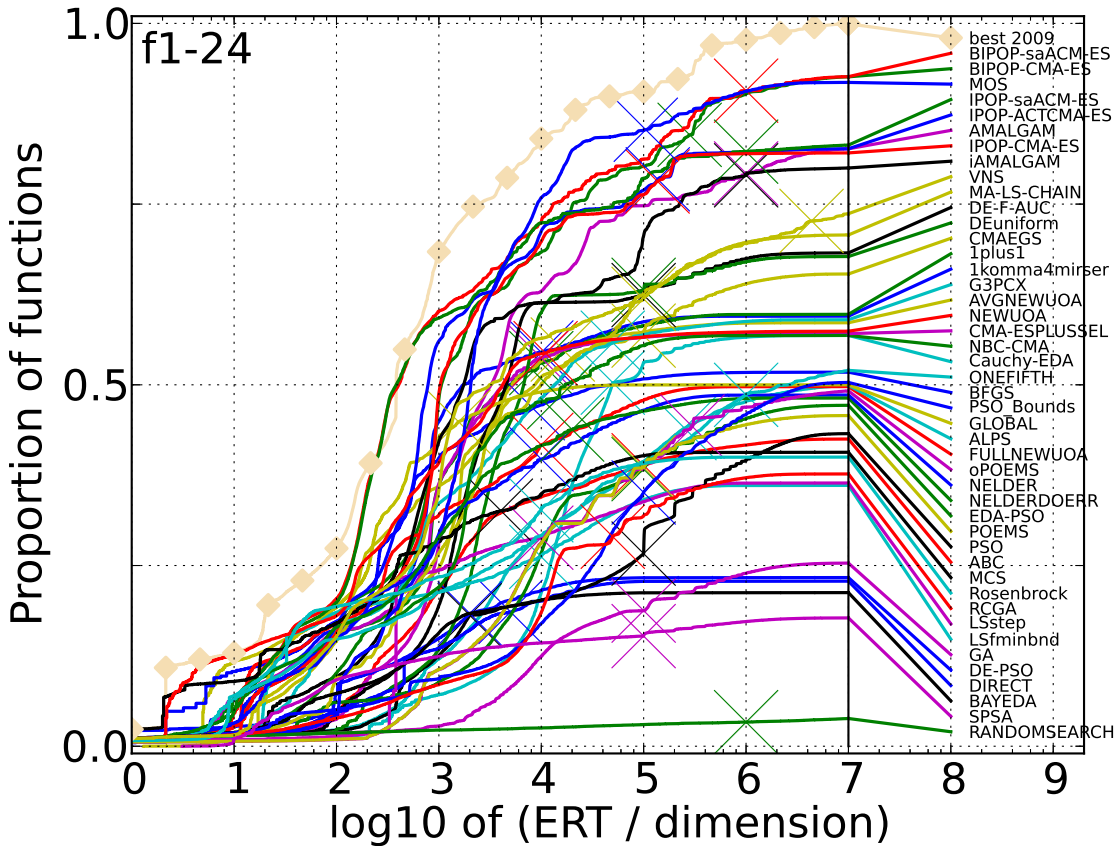

Figure 4.19: Performance of 45 optimization algorithms, including IPOP-^{s*}aACM-ES and BIPOP-^{s*}aACM-ES on 20-dimensional noiseless BBOB benchmark problems. For the interpretation of axis-x and axis-y see Section 2.3.3.

It may be difficult to recognize curves and corresponding algorithms, however, it can be clearly seen that IPOP-^{s*}aACM-ES and BIPOP-^{s*}aACM-ES dominate *all* other optimization algorithms in the range $[100n, 1000n]$ of functions evaluations used for optimization. In this range our surrogate-assisted algorithms outperform the closest competitor, IPOP-aCMA-ES, by a factor between 2 and 3. This speedup is due to the good performances on non-separable ill-conditioned problems (see Figure 4.20), where IPOP-^{s*}aACM-ES outperforms all tested on BBOB algorithms, including BFGS and NEWUOA. On original f_8 and rotated f_9 Rosenbrock functions IPOP-^{s*}aACM-ES is as fast as *derivative-based* BFGS and at most 2 times slower than NEWUOA algorithm with quadratic meta-models, which are indeed well suitable for the quadratic form of the Rosenbrock function, but may fail under certain transformations of f.

For a budget smaller than $100n$ function evaluations, the proposed algorithms are

among the best performing ones, while the latter often benefit from exploiting functions separability or very simple landscape (see, e.g., f_1 Sphere, f_2 Separable Ellipsoid, f_5 Linear slope).

For a budget larger than $5000n$ function evaluations, BIPOP-^{s*}aACM-ES outperforms all tested algorithm except MOS (a hybrid of DE and CMA-ES, [LaTorre *et al.*, 2010]) which exploits the separability and therefore performs well on f_3 Rastrigin and f_4 Skew-Rastrigin-Bueche functions. On multi-modal functions the advantages of using surrogate models are less significant because of difficult functions landscapes and limited number of training points together with high computational cost of surrogate learning. In this case, it might be more advantageous to use alternative restart strategies for CMA-ES which will lead to a comparable speedup but with a lower computational cost. We will investigate this question in the exploration part of this thesis, see Section 6.3.3.

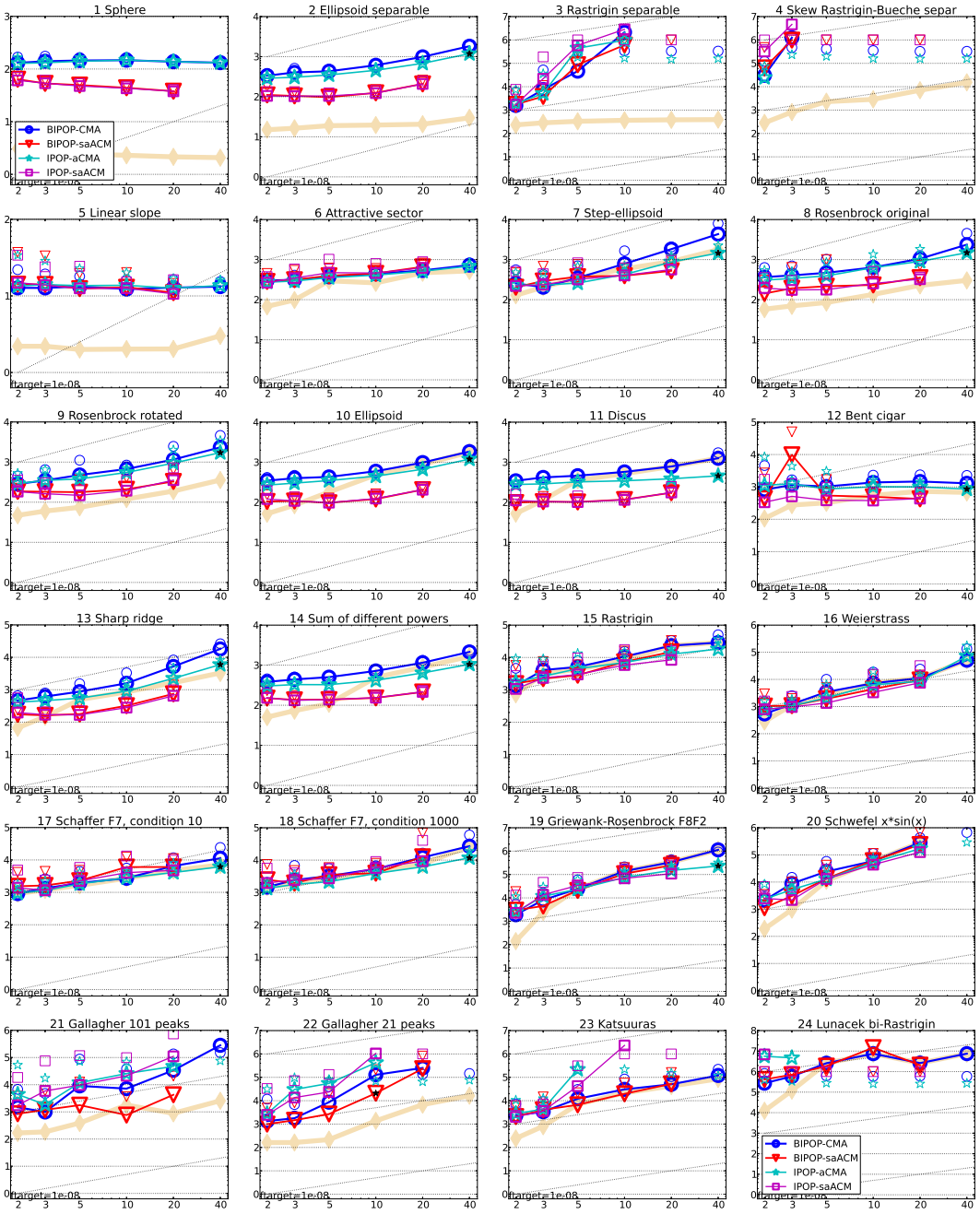

Figure 4.20: Expected running time (ERT in number of f-evaluations) divided by dimension for target function value 10^{-8} as $\log_{10}$ values versus dimension. Different symbols correspond to different algorithms given in the legend of f_1 and f_{24}. Light symbols give the maximum number of function evaluations from the longest trial divided by dimension. Horizontal lines give linear scaling, slanted dotted lines give quadratic scaling. Black stars indicate statistically better result compared to all other algorithms with $p < 0.01$ and Bonferroni correction number of dimensions (six). Legend: ○: BIPOP-CMA, ▽: BIPOP-saACM, ⋆: IPOP-aCMA, □: IPOP-saACM.

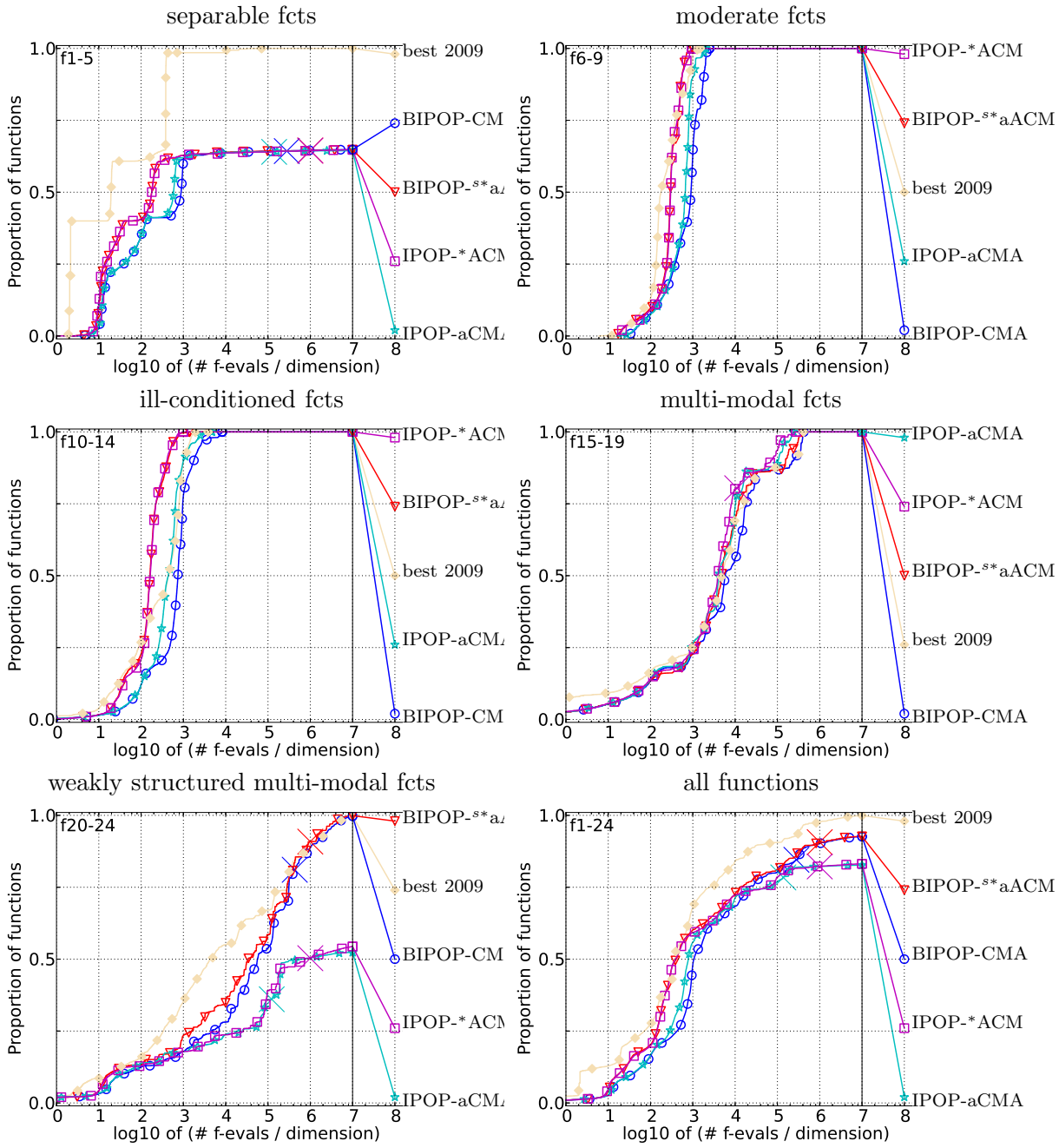

Figure 4.21: Bootstrapped empirical cumulative distribution of the number of objective function evaluations divided by dimension (FEvals/D) for 50 targets in $10^{[-8..2]}$ for all functions and subgroups in 20-D. The "best 2009" line corresponds to the best ERT observed during BBOB 2009 for each single target (generally with a different algorithm for different targets).

Δf_{opt}	1e1	1e0	1e-1	1e-3	1e-5	1e-7	#succ
f1	43	43	43	43	43	43	15/15
BIPOP-C	7.9(2)	14(3)	20(2)	33(4)	45(3)	57(3)	15/15
BIPOP-s	4.0(0.2)	5.1(0.4)	6.6(0.7)	10(0.7)	13(0.8)	16(1)	15/15
IPOP-aC	7.9(1)	14(1)	20(1)	33(2)	45(2)	58(2)	15/15
IPOP-sa	**3.9**(0.2)	**5.0**(0.4)	**6.5**(0.5)	**9.5**(0.7)	**13**(0.7)	**16**(0.8)	15/15
Δf_{opt}	1e1	1e0	1e-1	1e-3	1e-5	1e-7	#succ
f2	385	386	387	390	391	393	15/15
BIPOP-C	35(7)	40(4)	44(4)	47(2)	48(2)	50(2)	15/15
BIPOP-s	**6.8**(1)	**8.0**(1)	**8.9**(1)	10(1)	10(1)	10(1)	15/15
IPOP-aC	22(3)	27(2)	29(1)	31(2)	33(2)	34(2)	15/15
IPOP-sa	7.3(1)	8.3(2)	8.9(2)	**10**(2)	**10**(1)	**10**(1)	15/15
Δf_{opt}	1e1	1e0	1e-1	1e-3	1e-5	1e-7	#succ
f3	5066	7626	7635	7643	7646	7651	15/15
BIPOP-C	12(7)	∞	∞	∞	∞	∞ *6e6*	0/15
BIPOP-s	**10**(7)	∞	∞	∞	∞	∞ *2e7*	0/5
IPOP-aC	10(7)	∞	∞	∞	∞	∞ *3e6*	0/15
IPOP-sa	11(15)	∞	∞	∞	∞	∞ *2e7*	0/5
Δf_{opt}	1e1	1e0	1e-1	1e-3	1e-5	1e-7	#succ
f4	4722	7628	7666	7700	7758	1.4e5	9/15
BIPOP-C	∞	∞	∞	∞	∞	∞ *6e6*	0/15
BIPOP-s	∞	∞	∞	∞	∞	∞ *2e7*	0/5
IPOP-aC	∞	∞	∞	∞	∞	∞ *3e6*	0/15
IPOP-sa	**1.9e4**(2e4)	∞	∞	∞	∞	∞ *2e7*	0/5
Δf_{opt}	1e1	1e0	1e-1	1e-3	1e-5	1e-7	#succ
f5	41	41	41	41	41	41	15/15
BIPOP-C	5.1(0.8)	6.2(1)	6.3(1)	6.3(1)	6.3(1)	6.3(1)	15/15
BIPOP-s	4.7(0.7)	5.3(0.7)	5.4(0.7)	5.4(0.7)	5.4(0.7)	5.4(0.7)	15/15
IPOP-aC	5.1(1)	6.2(0.9)	6.2(1)	6.2(1)	6.2(1)	6.2(1)	15/15
IPOP-sa	**4.5**(0.7)	**5.1**(0.7)	**5.2**(0.8)	**5.2**(0.8)	**5.2**(0.8)	**5.2**(0.8)	15/15
Δf_{opt}	1e1	1e0	1e-1	1e-3	1e-5	1e-7	#succ
f6	1296	2343	3413	5220	6728	8409	15/15
BIPOP-C	1.5(0.4)	1.3(0.2)	1.2(0.2)	1.1(0.2)	1.2(0.1)	1.2(0.1)	15/15
BIPOP-s	**1.4**(0.3)	**1.2**(0.2)	1.1(0.2)	1.1(0.2)	1.3(0.3)	1.4(0.3)	15/15
IPOP-aC	1.6(0.3)	1.3(0.2)	1.1(0.2)	**1.1**(0.1)	**1.1**(0.1)	**1.1**(0.1)	15/15
IPOP-sa	1.5(0.4)	1.2(0.3)	**1.1**(0.2)	1.1(0.2)	1.2(0.2)	1.3(0.3)	15/15
Δf_{opt}	1e1	1e0	1e-1	1e-3	1e-5	1e-7	#succ
f7	1351	4274	9503	16524	16524	16969	15/15
BIPOP-C	**1**(0.5)	4.9(2)	3.5(0.6)	2.2(0.3)	2.2(0.3)	2.1(0.3)	15/15
BIPOP-s	1.0(0.9)	**1.6**(0.6)	**0.84**(0.3)	**0.61**$(0.1)_{\downarrow 3}$	**0.61**$(0.1)_{\downarrow 3}$	**0.60**$(0.1)_{\downarrow 3}$	15/15
IPOP-aC	1.6(2)	2.7(1)	1.6(0.5)	0.99(0.3)	0.99(0.3)	1.0(0.3)	15/15
IPOP-sa	1.0(1)	1.6(0.6)	0.92(0.6)	0.66$(0.3)_{\downarrow 2}$	0.66$(0.3)_{\downarrow 2}$	0.65$(0.3)_{\downarrow 2}$	15/15
Δf_{opt}	1e1	1e0	1e-1	1e-3	1e-5	1e-7	#succ
f8	2039	3871	4040	4219	4371	4484	15/15
BIPOP-C	4.0(1)	4.0(0.7)	4.3(0.6)	4.5(0.6)	4.6(0.6)	4.6(0.6)	15/15
BIPOP-s	**1.3**(0.2)	1.5(0.9)	1.5(0.9)	1.6(0.8)	1.6(0.8)	1.6(0.8)	15/15
IPOP-aC	3.5(0.8)	3.5(0.5)	3.7(0.6)	3.9(0.6)	3.9(0.5)	4.0(0.5)	15/15
IPOP-sa	1.4(0.2)	**1.3**(0.1)	**1.4**(0.1)	**1.4**(0.1)	**1.4**(0.1)	**1.4**(0.1)	15/15
Δf_{opt}	1e1	1e0	1e-1	1e-3	1e-5	1e-7	#succ
f9	1716	3102	3277	3455	3594	3727	15/15
BIPOP-C	4.7(2)	5.7(1)	6.0(1)	6.1(1)	6.1(1.0)	6.1(0.9)	15/15
BIPOP-s	**1.5**(0.3)	**1.7**(0.2)	**1.7**(0.2)	**1.8**(0.2)	**1.8**(0.2)	**1.7**(0.2)	15/15
IPOP-aC	4.1(0.7)	4.6(0.5)	4.9(0.5)	5.0(0.5)	5.0(0.5)	5.0(0.5)	15/15
IPOP-sa	1.6(0.4)	1.8(1)	1.9(1)	1.9(1)	1.9(1.0)	1.9(1.0)	15/15
Δf_{opt}	1e1	1e0	1e-1	1e-3	1e-5	1e-7	#succ
f10	7413	8661	10735	14920	17073	17476	15/15
BIPOP-C	1.9(0.2)	1.8(0.2)	1.6(0.1)	1.2(0.0)	1.1(0.0)	1.1(0.0)	15/15
BIPOP-s	0.36$(0.1)_{\downarrow 4}$	**0.35**$(0.0)_{\downarrow 4}$	**0.31**$(0.0)_{\downarrow 4}$	0.24$(0.0)_{\downarrow 4}$	0.23$(0.0)_{\downarrow 4}$	0.23$(0.0)_{\downarrow 4}$	15/15
IPOP-aC	1.2(0.2)	1.2(0.1)	1.0(0.1)	0.80$(0.0)_{\downarrow 4}$	0.73$(0.0)_{\downarrow 4}$	0.75$(0.0)_{\downarrow 4}$	15/15
IPOP-sa	**0.35**$(0.1)_{\downarrow 4}$	0.36$(0.1)_{\downarrow 4}$	0.31$(0.0)_{\downarrow 4}$	**0.24**$(0.0)_{\downarrow 4}$	**0.22**$(0.0)_{\downarrow 4}$	**0.23**$(0.0)_{\downarrow 4}$	15/15
Δf_{opt}	1e1	1e0	1e-1	1e-3	1e-5	1e-7	#succ
f11	1002	2228	6278	9762	12285	14831	15/15
BIPOP-C	10(0.5)	5.1(0.3)	1.9(0.1)	1.4(0.0)	1.2(0.0)	1.0(0.0)	15/15
BIPOP-s	**2.5**(0.4)	**1.2**(0.2)	**0.44**(0.1)	**0.30**$(0.0)_{\downarrow 4}$	**0.26**$(0.0)_{\downarrow 4}$	**0.23**$(0.0)_{\downarrow 4}$	15/15
IPOP-aC	4.5(0.2)	2.3(0.1)	0.87(0.1)	0.64$(0.0)_{\downarrow 4}$	0.56$(0.0)_{\downarrow 4}$	0.50$(0.0)_{\downarrow 4}$	15/15
IPOP-sa	2.5(0.5)	1.2(0.2)	0.45(0.1)	0.31$(0.1)_{\downarrow 4}$	0.26$(0.1)_{\downarrow 4}$	0.23$(0.0)_{\downarrow 4}$	15/15
Δf_{opt}	1e1	1e0	1e-1	1e-3	1e-5	1e-7	#succ
f12	1042	1938	2740	4140	12407	13827	15/15
BIPOP-C	3.0(2)	4.0(3)	4.5(3)	4.5(2)	1.9(0.7)	2.0(0.7)	15/15
BIPOP-s	0.99(0.9)	1.1(1)	1.2(0.9)	1.2(0.9)	**0.55**$(0.3)_{\downarrow}$	**0.59**$(0.3)_{\downarrow 2}$	15/15
IPOP-aC	2.6(1)	3.0(2)	3.2(2)	3.1(1)	1.3(0.4)	1.4(0.4)	15/15
IPOP-sa	**0.67**(0.1)	**0.88**(0.7)	**1.1**(0.7)	**1.2**(0.5)	0.56$(0.2)_{\downarrow 2}$	0.60$(0.2)_{\downarrow 2}$	15/15

Δf_{opt}	1e1	1e0	1e-1	1e-3	1e-5	1e-7	#succ
f13	652	2021	2751	18749	24455	30201	15/15
BIPOP-C	4.3(6)	2.7(2)	5.1(6)	1.5(0.8)	2.3(2)	3.0(2)	15/15
BIPOP-s	**1.1**(0.9)	**0.89**(0.7)	**1.4**(1.0)	0.38$(0.1)_{\downarrow 4}$	0.42$(0.2)_{\downarrow 4}$	**0.40**$(0.1)_{\downarrow 4}$	15/15
IPOP-aC	3.6(3)	3.4(3)	3.7(2)	0.80(0.4)	1.3(0.7)	1.3(0.7)	15/15
IPOP-sa	1.7(2)	1.7(0.8)	1.5(0.7)	**0.34**$(0.2)_{\downarrow 4}$	**0.37**$(0.1)_{\downarrow 4}$	0.41$(0.2)_{\downarrow 4}$	15/15
Δf_{opt}	1e1	1e0	1e-1	1e-3	1e-5	1e-7	#succ
f14	75	239	304	932	1648	15661	15/15
BIPOP-C	3.9(1)	2.9(0.4)	3.7(0.4)	4.1(0.3)	6.2(0.5)	1.2(0.1)	15/15
BIPOP-s	3.2(1)	1.8(0.6)	1.9(0.4)	1.5(0.2)	**1.4**(0.2)	**0.23**$(0.0)_{\downarrow 4}$	15/15
IPOP-aC	3.6(0.8)	2.7(0.3)	3.5(0.3)	3.2(0.3)	3.9(0.2)	0.67$(0.1)_{\downarrow 4}$	15/15
IPOP-sa	**3.0**(0.6)	**1.8**(0.3)	**1.9**(0.4)	**1.4**(0.2)	1.4(0.1)	0.23$(0.0)_{\downarrow 4}$	15/15
Δf_{opt}	1e1	1e0	1e-1	1e-3	1e-5	1e-7	#succ
f15	30378	1.5e5	3.1e5	3.2e5	4.5e5	4.6e5	15/15
BIPOP-C	1(0.4)	2.0(0.8)	1.4(0.5)	1.4(0.5)	1(0.3)	1(0.3)	15/15
BIPOP-s	0.65(0.6)	1.3(0.6)	0.91(0.7)	0.89(0.6)	0.66(0.5)	0.65(0.5)	15/15
IPOP-aC	0.82(0.3)	1.1(0.3)	0.71(0.2)	0.72(0.2)	0.53$(0.2)_{\downarrow 2}$	0.54$(0.2)_{\downarrow 2}$	15/15
IPOP-sa	**0.60**(0.5)	**0.92**(0.7)	**0.53**(0.4)	**0.52**(0.4)	**0.37**$(0.3)_{\downarrow 4}$	**0.37**$(0.3)_{\downarrow 4}$	15/15
Δf_{opt}	1e1	1e0	1e-1	1e-3	1e-5	1e-7	#succ
f16	1384	27265	77015	1.9e5	2.0e5	2.2e5	15/15
BIPOP-C	**1.7**(0.4)	1.0(0.7)	1.2(0.7)	1(0.7)	1(0.7)	1(0.7)	15/15
BIPOP-s	1.9(0.6)	0.74(0.4)	**0.51**(0.3)	0.60(0.5)	0.84(0.5)	0.83(0.5)	15/15
IPOP-aC	2.8(5)	1.1(0.5)	0.88(0.7)	0.80(0.5)	0.82(0.5)	0.76(0.5)	15/15
IPOP-sa	1.8(0.8)	**0.55**(0.4)	0.77(0.8)	**0.52**(0.4)	**0.55**(0.4)	**0.50**$(0.3)_{\downarrow}$	15/15
Δf_{opt}	1e1	1e0	1e-1	1e-3	1e-5	1e-7	#succ
f17	63	1030	4005	30677	56288	80472	15/15
BIPOP-C	**2.2**(2)	1(0.3)	1(1)	1.2(1)	1.3(0.6)	1.4(0.7)	15/15
BIPOP-s	3.2(2)	1.2(0.4)	2.7(3)	1.2(0.7)	1.2(0.5)	1.4(0.8)	15/15
IPOP-aC	2.3(2)	**0.89**(0.2)	**0.50**(0.1)	**0.82**(0.3)	**0.83**(0.5)	**0.87**(0.3)	15/15
IPOP-sa	2.5(2)	0.91(0.3)	0.98(1)	1.2(0.5)	1.2(0.4)	1.1(0.5)	15/15
Δf_{opt}	1e1	1e0	1e-1	1e-3	1e-5	1e-7	#succ
f18	621	3972	19561	67569	1.3e5	1.5e5	15/15
BIPOP-C	1.0(0.4)	2.4(2)	1.2(0.9)	1.1(0.6)	1.7(0.7)	1.6(0.6)	15/15
BIPOP-s	1.0(0.3)	1.5(1)	0.92(0.4)	0.96(0.4)	1.6(0.6)	1.6(0.5)	15/15
IPOP-aC	1.2(0.4)	1.5(2)	**0.75**(0.4)	0.91(0.4)	**0.78**(0.4)	**0.83**(0.3)	15/15
IPOP-sa	**0.96**(0.5)	**1.4**(2)	0.91(0.6)	**0.78**(0.5)	0.88(0.4)	1.3(0.8)	15/15
Δf_{opt}	1e1	1e0	1e-1	1e-3	1e-5	1e-7	#succ
f19	1	1	3.4e5	6.2e6	6.7e6	6.7e6	15/15
BIPOP-C	169(74)	**2.4e4**(1e4)	1.2(0.6)	1(0.3)	1(0.3)	1(0.3)	15/15
BIPOP-s	**143**(52)	2.5e4(1e4)	**0.42**(0.3)	0.72$(0.4)_{\downarrow}$	0.73(0.4)	0.73(0.4)	15/15
IPOP-aC	166(60)	2.9e4(2e4)	0.63(0.4)	0.43$(0.2)_{\downarrow 3}$	0.44$(0.2)_{\downarrow 3}$	0.44$(0.2)_{\downarrow 3}$	15/15
IPOP-sa	154(50)	3.0e4(2e4)	0.61(0.5)	**0.33**(0.1)	**0.32**(0.2)	**0.32**(0.2)	14/15
Δf_{opt}	1e1	1e0	1e-1	1e-3	1e-5	1e-7	#succ
f20	82	46150	3.1e6	5.5e6	5.6e6	5.6e6	14/15
BIPOP-C	4.3(1)	9.2(4)	1(0.5)	1(0.3)	1(0.3)	1(0.3)	14/15
BIPOP-s	2.9(0.5)	2.1(1)	0.97(0.7)	0.87(0.4)	0.86(0.4)	0.85(0.4)	15/15
IPOP-aC	4.7(1)	3.2(1)	0.83(0.4)	0.58(0.2)	0.59(0.2)	0.60(0.2)	15/15
IPOP-sa	**2.8**(0.5)	**1.7**(0.8)	**0.49**$(0.2)_{\downarrow 3}$	**0.45**$(0.2)_{\downarrow}$	**0.45**$(0.2)_{\downarrow}$	**0.45**$(0.2)_{\downarrow}$	15/15
Δf_{opt}	1e1	1e0	1e-1	1e-3	1e-5	1e-7	#succ
f21	561	6541	14103	14643	15567	17589	15/15
BIPOP-C	3.2(6)	55(48)	48(86)	46(84)	43(84)	39(77)	13/15
BIPOP-s	2.6(4)	**1.5**(1)	**6.0**(11)	**5.8**(11)	**5.5**(10)	**4.8**(9)	15/15
IPOP-aC	**1.9**(4)	81(109)	66(94)	64(88)	60(85)	54(77)	9/15
IPOP-sa	2.6(4)	53(94)	157(308)	151(297)	142(279)	126(247)	15/15
Δf_{opt}	1e1	1e0	1e-1	1e-3	1e-5	1e-7	#succ
f22	467	5580	23491	24948	26847	1.3e5	12/15
BIPOP-C	**6.8**(13)	**13**(21)	215(267)	202(247)	188(227)	37(48)	5/15
BIPOP-s	7.7(9)	100(96)	**178**(320)	**173**(301)	**168**(274)	**35**(54)	15/15
IPOP-aC	462(1351)	264(443)	∞	∞	∞	∞ *1e6*	0/15
IPOP-sa	175(98)	978(1807)	∞	∞	∞	∞ *2e7*	0/15
Δf_{opt}	1e1	1e0	1e-1	1e-3	1e-5	1e-7	#succ
f23	3.2	1614	67457	4.9e5	8.1e5	8.4e5	15/15
BIPOP-C	4.3(5)	32(33)	1(0.8)	2.0(1)	**1.2**(0.9)	**1.2**(0.9)	15/15
BIPOP-s	**3.0**(6)	**21**(13)	**0.61**(0.3)	**1.4**(1)	1.3(1)	1.3(1)	15/15
IPOP-aC	4.1(6)	2.3e4(3e4)	∞	∞	∞	∞ *3e6*	0/15
IPOP-sa	4.3(6)	2.9e4(3e4)	906(1022)	∞	∞	∞ *2e7*	0/15
Δf_{opt}	1e1	1e0	1e-1	1e-3	1e-5	1e-7	#succ
f24	1.3e6	7.5e6	5.2e7	5.2e7	5.2e7	5.2e7	3/15
BIPOP-C	1(0.9)	1(0.9)	1(1.0)	1(1)	1(1)	1(1.0)	3/15
BIPOP-s	**0.99**(1)	**0.88**(0.7)	**0.80**(0.9)	**0.80**(0.9)	**0.80**(0.8)	**0.79**(0.8)	6/15
IPOP-aC	25(32)	4.5(5)	∞	∞	∞	∞ *5e6*	0/15
IPOP-sa	28(30)	38(43)	∞	∞	∞	∞ *2e7*	0/15

Table 4.4: Expected running time (ERT in number of function evaluations) divided by the respective best ERT measured during BBOB-2009 (given in the respective first row) for different Δf values of *noise-less* functions in dimension 20. The central 80% range divided by two is given in braces. The median number of conducted function evaluations is additionally given in *italics*, if $\text{ERT}(10^{-7}) = \infty$. #succ is the number of trials that reached the final target $f_{\text{opt}} + 10^{-8}$. Best results are printed in bold.

4.3.3.8 Benchmarking on Noisy BBOB-2012 Testbed

For benchmarking we consider ^{s*}ACM-ES in IPOP restart scenario (IPOP-^{s*}aACM-ES) using default parameters and termination criteria as given in [Hansen and Ros, 2010b]. The only one parameter of the surrogate part of IPOP-^{s*}aACM-ES different from the default one is the index of generation g_{start} when we start to use the surrogate model. For noisy case we set $g_{start} = 5(i_{restart} + 1)$ instead of the default $g_{start} = 10$. We found that sometimes it makes sense to postpone the surrogate-assisted search if several restarts ($i_{restart}$) were performed.

Results from experiments according to [Hansen *et al.*, 2012] on the benchmark functions given in [Hansen *et al.*, 2009b] are presented in Figures 4.22, 4.23. Table 4.5 gives the Expected Running Time (ERT) for targets $10^{1,\,-1,\,-3,\,-5,\,-7}$ divided by the best ERT obtained during BBOB-2009 (given in the $\mathrm{ERT}_{\mathrm{best}}$ row) in 20-D.

The IPOP-^{s*}aACM-ES outperforms IPOP-^{s*}aACM-ES usually by a factor from 2 to 3 on functions with moderate noisy. This is the case for Sphere (f_{101}, f_{102}, f_{103}) and Rosenbrock (f_{104}, f_{105}, f_{106}) functions with Gaussian, Uniform and Cauchy noise models. It seems that the moderate noise only slightly affects the quality of the surrogate model and allows to have a speedup comparable to the one of the noise-less case.

On most functions with severe noise the surrogate model usually is not used ($\hat{n}$ oscillates around zero), because it gives a very imprecise prediction of the objective function. An exception is the 20-dimensional f_{124} Schaffer function with Cauchy noise, where IPOP-^{s*}aACM-ES requires about 7 times more functions evaluations to reach the optimum with $\Delta f_{opt} = 10^{-7}$ than IPOP-aCMA-ES (see Figure 4.22). However, according to Table 4.5, the performance for $\Delta f_{opt} = 10^{-5}$ is exactly the same for both algorithms, therefore, we suppose that the loss of performance for $\Delta f_{opt} = 10^{-7}$ can be explained by some influence of surrogate-assisted search on restart conditions. We also found that if default coefficients c_1 and c_μ for the covariance matrix update are used instead of noisy settings of $c_1/5$ and $c_\mu/5$, then IPOP-^{s*}aACM-ES performs as well as IPOP-aCMA-ES on *this* function. However, the use of default coefficients worsen the results of IPOP-aCMA-ES and IPOP-^{s*}aACM-ES on other functions.

We also observe some loss in performance of f_{125} Griewank-Rosenbrock and f_{128} Gallagher functions for $n \leq 5$. For f_{115} we observe the speedup for $n = 5$ and loss for $n = 20$, probably because of the same reasons as for f_{124}.

The IPOP-^{s*}aACM-ES improves (sometimes insignificantly) the BBOB-2010 records in dimension 20 on f_{101}, f_{102}, f_{103}, f_{104}, f_{105}, f_{106}, f_{107}, f_{109}, f_{112}, f_{114}, f_{117}, f_{118}, f_{120}, f_{122}, f_{123}, f_{127}, f_{129}.

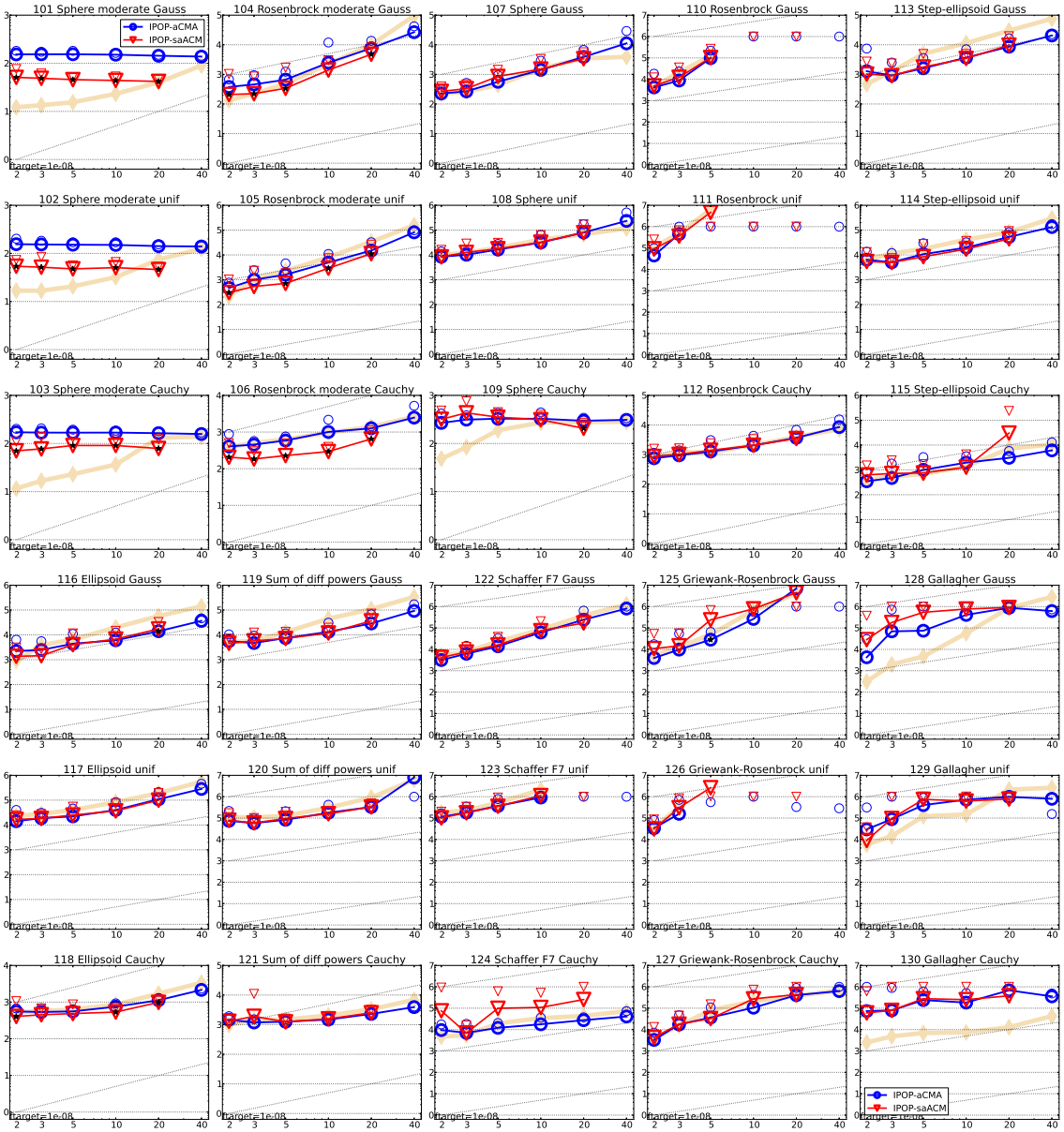

Figure 4.22: Expected running time (ERT) divided by dimension for target function value 10^{-8} as $\log_{10}$ values versus dimension. Different symbols correspond to different algorithms given in legend of f_{101} and f_{130}. Light symbols give the maximum number of function evaluations from all trials divided by the dimension. Horizontal lines give linear scaling, the slanted dotted lines give quadratic scaling. Legend: ○: IPOP-aCMA, ▽: IPOP-saACM

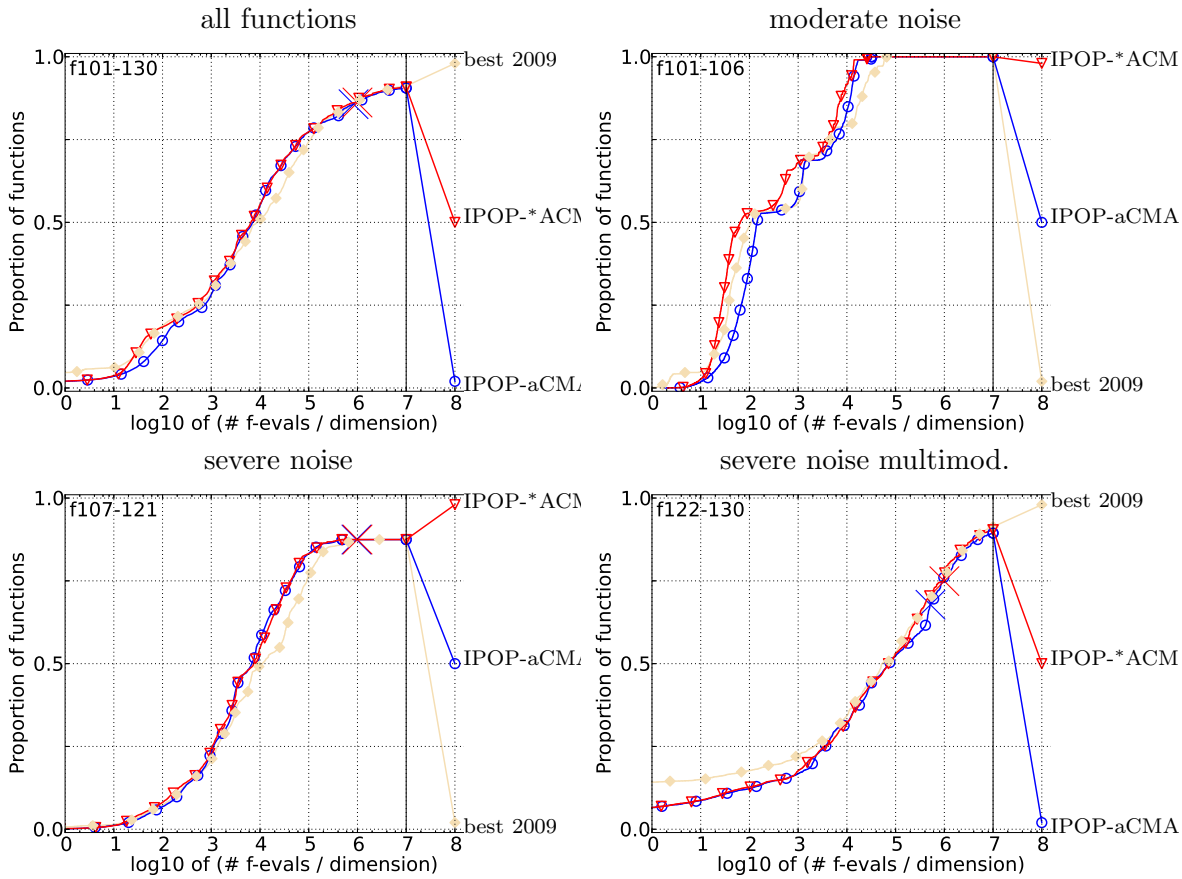

Figure 4.23: Bootstrapped empirical cumulative distribution of the number of objective function evaluations divided by dimension (FEvals/D) for 50 targets in $10^{[-8..2]}$ for all functions and subgroups in 20-D. The "best 2009" line corresponds to the best ERT observed during BBOB 2009 for each single target.

Δf_{opt}	1e1	1e0	1e-1	1e-3	1e-5	1e-7	#succ
f101	59	425	571	700	739	783	15/15
IPOP-aC	6.1(1.0)	1.5(0.1)	1.6(0.1)	2.1(0.2)	2.7(0.1)	3.3(0.2)	15/15
IPOP-sa	**4.7**(1)*	**0.86**(0.2)$^{\star 4}$	**0.73**(0.1)$^{\star 4}_{\downarrow 2}$	**0.78**(0.1)$^{\star 4}_{\downarrow 3}$	**0.88**(0.1)$^{\star 4}_{\downarrow 4}$	**0.99**(0.1)$^{\star 4}$	15/15
Δf_{opt}	1e1	1e0	1e-1	1e-3	1e-5	1e-7	#succ
f102	231	399	579	921	1157	1407	15/15
IPOP-aC	1.5(0.4)	1.6(0.2)	1.6(0.2)	1.6(0.1)	1.7(0.1)	1.8(0.1)	15/15
IPOP-sa	**1.2**(0.2)	**0.93**(0.2)$^{\star 4}$	**0.75**(0.1)$^{\star 4}_{\downarrow 3}$	**0.61**(0.1)$^{\star 4}_{\downarrow 4}$	**0.60**(0.0)$^{\star 4}_{\downarrow 4}$	**0.60**(0.0)$^{\star 4}_{\downarrow 4}$	15/15
Δf_{opt}	1e1	1e0	1e-1	1e-3	1e-5	1e-7	#succ
f103	65	417	629	1313	1893	2464	14/15
IPOP-aC	5.4(0.9)	1.5(0.1)	1.5(0.1)	1.2(0.1)	1.2(0.1)	1.2(0.1)	15/15
IPOP-sa	**3.9**(0.8)$^{\star 2}$	**0.83**(0.2)$^{\star 4}_{\downarrow 2}$	**0.66**(0.1)$^{\star 4}$	**0.52**(0.1)$^{\star 4}_{\downarrow 4}$	**0.55**(0.1)$^{\star 4}_{\downarrow 4}$	**0.58**(0.1)$^{\star 4}_{\downarrow 3}$	15/15
Δf_{opt}	1e1	1e0	1e-1	1e-3	1e-5	1e-7	#succ
f104	23690	85656	1.7e5	1.8e5	1.9e5	2.0e5	15/15
IPOP-aC	4.9(3)	1.6(1.0)	0.82(0.5)	0.80(0.5)	0.79(0.5)	0.77(0.4)	15/15
IPOP-sa	**3.5**(2)	**1.1**(0.6)	**0.55**(0.3)	**0.52**(0.3)	**0.50**(0.3)	**0.49**(0.3)	15/15
Δf_{opt}	1e1	1e0	1e-1	1e-3	1e-5	1e-7	#succ
f105	1.9e5	6.1e5	6.3e5	6.5e5	6.6e5	6.7e5	15/15
IPOP-aC	1.2(0.3)	0.43(0.1)$_{\downarrow 3}$	0.43(0.1)$_{\downarrow 3}$	0.44(0.1)$_{\downarrow 3}$	0.44(0.1)$_{\downarrow 3}$	0.44(0.1)$_{\downarrow 3}$	15/15
IPOP-sa	**1.0**(0.4)	**0.36**(0.1)$_{\downarrow 3}$	**0.35**(0.1)$_{\downarrow 3}$	**0.34**(0.1)$_{\downarrow 3}$	**0.34**(0.1)$_{\downarrow 3}$	**0.33**(0.1)$_{\downarrow 3}$	15/15
Δf_{opt}	1e1	1e0	1e-1	1e-3	1e-5	1e-7	#succ
f106	11480	21668	23746	25470	26492	27360	15/15
IPOP-aC	0.77(0.2)	0.76(0.2)$_{\downarrow 3}$	0.84(0.2)$_{\downarrow 2}$	0.89(0.1)	0.91(0.1)	0.91(0.1)	15/15
IPOP-sa	**0.28**(0.1)$^{\star 4}_{\downarrow 4}$	**0.37**(0.3)$^{\star 2}_{\downarrow 4}$	**0.39**(0.2)$^{\star 3}_{\downarrow 4}$	**0.45**(0.2)$^{\star 3}_{\downarrow 4}$	**0.46**(0.2)$^{\star 3}_{\downarrow 4}$	**0.47**(0.2)$^{\star 3}_{\downarrow 4}$	15/15
Δf_{opt}	1e1	1e0	1e-1	1e-3	1e-5	1e-7	#succ
f107	8571	13582	16226	27357	52486	65052	15/15
IPOP-aC	**0.81**(0.4)	**0.97**(0.4)	**1.3**(0.6)	1.5(0.9)	1.3(0.7)	1.1(0.5)	15/15
IPOP-sa	0.83(0.5)	1.3(0.8)	1.4(0.7)	**1.3**(0.8)	**1.0**(0.5)	**0.94**(0.4)	15/15
Δf_{opt}	1e1	1e0	1e-1	1e-3	1e-5	1e-7	#succ
f108	58063	97228	2.0e5	4.5e5	6.3e5	9.0e5	15/15
IPOP-aC	0.74(0.3)	**0.98**(0.5)	**1.0**(0.6)	**1.1**(0.6)	**1.5**(0.4)	1.5(0.3)	15/15
IPOP-sa	**0.72**(0.3)	1.2(0.6)	1.1(0.6)	1.2(0.7)	1.6(0.3)	**1.4**(0.3)	15/15
Δf_{opt}	1e1	1e0	1e-1	1e-3	1e-5	1e-7	#succ
f109	333	632	1138	2287	3583	4952	15/15
IPOP-aC	1.1(0.2)	1.2(0.1)	1.2(0.2)	1.2(0.1)	1.1(0.1)	1.1(0.1)	15/15
IPOP-sa	**0.93**(0.3)	**0.78**(0.2)$^{\star 3}_{\downarrow}$	**0.78**(0.2)$^{\star 3}_{\downarrow 2}$	**0.89**(0.3)*	**0.79**(0.2)$^{\star 3}_{\downarrow}$	**0.75**(0.2)$^{\star 3}_{\downarrow 2}$	15/15
Δf_{opt}	1e1	1e0	1e-1	1e-3	1e-5	1e-7	#succ
f110	∞	∞	∞	∞	∞	∞	0
IPOP-aC	.	.	.	.	.	.	0/15
IPOP-sa	.	.	.	.	.	.	0/15
Δf_{opt}	1e1	1e0	1e-1	1e-3	1e-5	1e-7	#succ
f111	∞	∞	∞	∞	∞	∞	0
IPOP-aC	.	.	.	.	.	.	0/15
IPOP-sa	.	.	.	.	.	.	0/15
Δf_{opt}	1e1	1e0	1e-1	1e-3	1e-5	1e-7	#succ
f112	25552	64124	69621	73557	76137	78238	15/15
IPOP-aC	**0.84**(0.2)	0.84(0.5)	0.89(0.5)	0.93(0.5)	0.94(0.5)	0.93(0.4)	15/15
IPOP-sa	0.89(0.3)	**0.79**(0.1)	**0.84**(0.1)	**0.88**(0.1)	**0.88**(0.1)	**0.88**(0.1)	15/15
Δf_{opt}	1e1	1e0	1e-1	1e-3	1e-5	1e-7	#succ
f113	50123	3.6e5	5.6e5	5.9e5	5.9e5	5.9e5	15/15
IPOP-aC	0.60(0.4)	**0.27**(0.1)$_{\downarrow 3}$	**0.27**(0.1)$_{\downarrow 4}$	**0.29**(0.1)$_{\downarrow 4}$	**0.29**(0.1)$_{\downarrow 4}$	**0.29**(0.1)$_{\downarrow 4}$	15/15
IPOP-sa	**0.54**(0.2)	0.35(0.2)$_{\downarrow 2}$	0.31(0.1)$_{\downarrow 4}$	0.32(0.1)$_{\downarrow 4}$	0.32(0.1)$_{\downarrow 4}$	0.32(0.1)$_{\downarrow 4}$	15/15
Δf_{opt}	1e1	1e0	1e-1	1e-3	1e-5	1e-7	#succ
f114	2.1e5	1.1e6	1.4e6	1.6e6	1.6e6	1.6e6	15/15
IPOP-aC	**0.64**(0.5)	**0.35**(0.1)$_{\downarrow 4}$	0.53(0.3)$_{\downarrow}$	0.62(0.3)	0.62(0.3)	0.63(0.3)	15/15
IPOP-sa	0.71(0.3)	0.39(0.3)$_{\downarrow 3}$	**0.40**(0.2)$_{\downarrow 3}$	**0.50**(0.3)$_{\downarrow 2}$	**0.50**(0.3)$_{\downarrow 2}$	**0.55**(0.3)$_{\downarrow}$	15/15
Δf_{opt}	1e1	1e0	1e-1	1e-3	1e-5	1e-7	#succ
f115	2405	30268	91749	1.3e5	1.3e5	1.3e5	15/15
IPOP-aC	1.4(2)	1.2(0.6)	0.54(0.1)	**0.45**(0.0)$_{\downarrow 4}$	**0.45**(0.0)$_{\downarrow 4}$	**0.45**(0.1)$_{\downarrow 4}$	15/15
IPOP-sa	**0.75**(2)	**0.67**(0.3)	**0.31**(0.2)$^{\star 2}$	4.8(15)	4.8(15)	4.7(14)	15/15

Δf_{opt}	1e1	1e0	1e-1	1e-3	1e-5	1e-7	#succ
f116	5.0e5	6.9e5	8.9e5	1.0e6	1.1e6	1.1e6	15/15
IPOP-aC	**0.36**(0.1)	**0.28**(0.1)$_{\downarrow}$	**0.23**(0.0)$_{\downarrow 2}$	**0.22**(0.0)$_{\downarrow 4}$	**0.23**(0.0)$_{\downarrow 4}$	**0.24**(0.0)$_{\downarrow 4}$	15/15
IPOP-sa	0.46(0.1)	0.35(0.1)	0.30(0.1)	0.28(0.1)$_{\downarrow 4}$	0.29(0.1)$_{\downarrow 4}$	0.30(0.1)$_{\downarrow 4}$	15/15
Δf_{opt}	1e1	1e0	1e-1	1e-3	1e-5	1e-7	#succ
f117	1.8e6	2.5e6	2.6e6	2.9e6	3.2e6	3.6e6	15/15
IPOP-aC	0.37(0.2)$_{\downarrow 2}$	0.35(0.2)$_{\downarrow 4}$	0.41(0.3)$_{\downarrow 3}$	0.45(0.2)$_{\downarrow 3}$	0.47(0.2)$_{\downarrow 3}$	0.56(0.3)$_{\downarrow 3}$	15/15
IPOP-sa	**0.29**(0.1)$_{\downarrow 3}$	**0.26**(0.1)$_{\downarrow 4}$	**0.29**(0.1)$_{\downarrow 4}$	**0.35**(0.2)$_{\downarrow 4}$	**0.42**(0.2)$_{\downarrow 3}$	**0.48**(0.4)$_{\downarrow 2}$	15/15
Δf_{opt}	1e1	1e0	1e-1	1e-3	1e-5	1e-7	#succ
f118	6908	11786	17514	26342	30062	32659	15/15
IPOP-aC	0.82(0.1)	0.78(0.2)	0.71(0.2)	0.63(0.1)$_{\downarrow 3}$	0.64(0.1)$_{\downarrow 4}$	0.66(0.1)$_{\downarrow 3}$	15/15
IPOP-sa	**0.42**(0.2)$^{\star 3}_{\downarrow 4}$	**0.49**(0.1)$^{\star 3}_{\downarrow 4}$	**0.54**(0.1)$^{\star}_{\downarrow 3}$	**0.54**(0.2)$_{\downarrow 4}$	**0.56**(0.1)$_{\downarrow 4}$	**0.58**(0.1)$^{\star}_{\downarrow 4}$	15/15
Δf_{opt}	1e1	1e0	1e-1	1e-3	1e-5	1e-7	#succ
f119	2771	29365	35930	4.1e5	1.4e6	1.9e6	15/15
IPOP-aC	1.6(1)	**0.62**(0.4)	**0.83**(0.4)	0.42(0.3)$_{\downarrow 2}$	**0.25**(0.1)$_{\downarrow 4}$	**0.28**(0.1)$_{\downarrow 4}$	15/15
IPOP-sa	**1.5**(2)	0.74(0.3)	0.88(0.3)	**0.33**(0.1)$_{\downarrow 3}$	0.25(0.1)$_{\downarrow 4}$	0.37(0.3)$_{\downarrow 3}$	15/15
Δf_{opt}	1e1	1e0	1e-1	1e-3	1e-5	1e-7	#succ
f120	36040	1.8e5	2.8e5	1.6e6	6.7e6	1.4e7	13/15
IPOP-aC	**0.62**(0.3)	**0.64**(0.2)	**0.79**(0.4)	**0.78**(0.4)	0.44(0.2)$_{\downarrow 3}$	0.40(0.2)$_{\downarrow 3}$	15/15
IPOP-sa	0.65(0.5)	0.80(0.4)	1.2(0.6)	0.87(0.5)	**0.42**(0.1)$_{\downarrow 3}$	**0.39**(0.2)$_{\downarrow 3}$	15/15
Δf_{opt}	1e1	1e0	1e-1	1e-3	1e-5	1e-7	#succ
f121	249	769	1426	9304	34434	57404	15/15
IPOP-aC	1.2(0.3)	1.0(0.2)	1.1(0.2)	0.77(0.1)$_{\downarrow 3}$	**0.56**(0.1)$_{\downarrow 4}$	**0.64**(0.1)$_{\downarrow 4}$	15/15
IPOP-sa	**1.2**(0.4)	**0.85**(0.2)	**0.92**(0.3)	**0.69**(0.1)$_{\downarrow 3}$	0.58(0.1)$_{\downarrow 4}$	0.71(0.1)$_{\downarrow 3}$	15/15
Δf_{opt}	1e1	1e0	1e-1	1e-3	1e-5	1e-7	#succ
f122	692	52008	1.4e5	7.9e5	2.0e6	5.8e6	15/15
IPOP-aC	**2.3**(3)	**0.81**(0.3)	0.97(0.6)	0.56(0.3)	0.66(0.1)	0.81(0.9)	15/15
IPOP-sa	2.5(3)	0.94(0.6)	**0.81**(0.3)	**0.53**(0.1)$_{\downarrow}$	**0.51**(0.2)$_{\downarrow}$	**0.57**(0.3)	15/15
Δf_{opt}	1e1	1e0	1e-1	1e-3	1e-5	1e-7	#succ
f123	1063	5.3e5	1.5e6	5.3e6	2.7e7	1.6e8	0
IPOP-aC	**6.4**(4)	**0.72**(0.4)	0.88(0.8)	**0.94**(0.7)	**0.50**(0.1)	1.9(2)	0/15
IPOP-sa	7.6(8)	0.77(0.5)	**0.81**(0.5)	1.1(0.7)	0.63(0.4)	**0.92**(1)	0/15
Δf_{opt}	1e1	1e0	1e-1	1e-3	1e-5	1e-7	#succ
f124	192	1959	40840	1.3e5	3.9e5	8.0e5	15/15
IPOP-aC	1.1(0.5)	3.9(11)	**1.0**(0.7)	**0.91**(0.6)	0.76(0.4)	**0.62**(0.3)	15/15
IPOP-sa	**0.86**(0.4)	**3.0**(0.8)	2.2(2)	1.4(0.5)	**0.76**(0.3)	4.0(5)	14/15
Δf_{opt}	1e1	1e0	1e-1	1e-3	1e-5	1e-7	#succ
f125	1	1	1	2.5e7	8.0e7	8.1e7	4/15
IPOP-aC	1(0)	**827**(912)	3.8e6(4e6)	1.1(1)	1.7(2)	1.7(2)	2/15
IPOP-sa	1(0)	1083(1766)	**3.3e6**(2e6)	**0.61**(0.5)	**1.1**(1)	**1.1**(1)	3/15
Δf_{opt}	1e1	1e0	1e-1	1e-3	1e-5	1e-7	#succ
f126	1	1	1	∞	∞	∞	0
IPOP-aC	1(0)	**6417**(3982)	∞	.	.	.	0/15
IPOP-sa	1(0)	7156(4580)	∞	.	.	.	0/15
Δf_{opt}	1e1	1e0	1e-1	1e-3	1e-5	1e-7	#succ
f127	1	1	1	4.4e6	7.3e6	7.4e6	15/15
IPOP-aC	1(0)	**193**(102)	**2.8e5**(4e5)	1.0(0.9)	1.1(1)	1.1(1.0)	15/15
IPOP-sa	1(0)	238(106)	3.3e5(4e5)	**0.75**(0.6)	**0.93**(0.5)	**0.97**(0.6)	14/15
Δf_{opt}	1e1	1e0	1e-1	1e-3	1e-5	1e-7	#succ
f128	1.4e5	1.3e7	1.7e7	1.7e7	1.7e7	1.7e7	9/15
IPOP-aC	**0.51**(0.6)	0.72(1)	**1.0**(2)	**1.0**(2)	**1.0**(1)	**1.0**(1)	7/15
IPOP-sa	1.3(2)	**0.59**(0.8)	1.1(1)	1.1(2)	1.1(1)	1.1(2)	8/15
Δf_{opt}	1e1	1e0	1e-1	1e-3	1e-5	1e-7	#succ
f129	7.8e6	4.1e7	4.2e7	4.2e7	4.2e7	4.2e7	5/15
IPOP-aC	**0.16**(0.2)$_{\downarrow}$	**0.27**(0.3)	0.46(0.6)	0.46(0.6)	0.46(0.6)	0.46(0.6)	6/15
IPOP-sa	0.41(0.9)	0.28(0.5)	**0.36**(0.5)	**0.36**(0.5)	**0.36**(0.5)	**0.36**(0.5)	9/15
Δf_{opt}	1e1	1e0	1e-1	1e-3	1e-5	1e-7	#succ
f130	4904	93149	2.5e5	2.5e5	2.6e5	2.6e5	7/15
IPOP-aC	1.5(2)	66(99)	54(71)	54(71)	54(72)	53(70)	6/15
IPOP-sa	**0.55**(1)	**27**(34)	**30**(43)	**30**(49)	**30**(39)	**30**(41)	12/15

Table 4.5: Expected running time (ERT in number of function evaluations) divided by the respective best ERT measured during BBOB-2009 (given in the respective first row) for different Δf values of *noisy* functions in dimension 20. The central 80% range divided by two is given in braces. The median number of conducted function evaluations is additionally given in *italics*, if $\text{ERT}(10^{-7}) = \infty$. #succ is the number of trials that reached the final target $f_{\text{opt}} + 10^{-8}$. Best results are printed in bold.

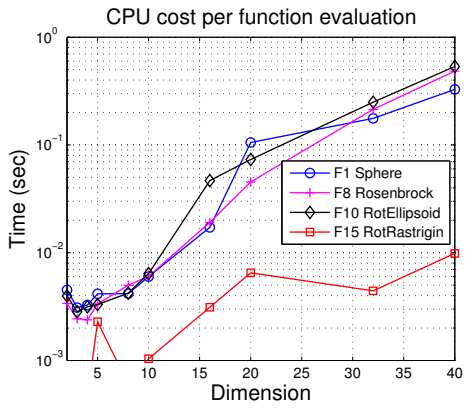

Figure 4.24: CPU cost per function evaluation of IPOP-aACM-ES with *fixed* hyper-parameters.

4.3.3.9 CPU Timing Experiment

For the timing experiment the IPOP-^{s*}aACM-ES was run on noiseless f_1, f_8, f_{10} and f_{15} functions *without* self-adaptation of surrogate model hyper-parameters. The crucial hyper-parameter for CPU time measurements, the number of training points, was set to $\ell = \lfloor 40 + 4n^{1.7} \rfloor$ as a function of dimension n.

These experiments have been conducted on a single core with 2.4 GHz under Windows XP using Matlab R2006a.

On unimodal functions the time complexity of surrogate model learning usually increases cubically in the search space dimension (see Figure 4.24) and quadratically in the number of training points. For small dimensions ($n < 10$) the overall time complexity increases super-linearly in the dimension. The time complexity per function evaluation depends on the population size, because one model is used to estimate the ranking of all points of the population. This leads to a smaller computational complexity on multi-modal functions, e.g., f_{15} Rastrigin function, where the population becomes much larger after several restarts. The time complexity on noisy functions is more similar to the one of Rastrigin function, because in both cases the large populations are used.

The results presented here do not take into account the optimization of model hyper-parameters, where λ_{hyp} surrogate models should be build at each iteration, which leads to an increase of CPU time per function evaluation by a factor of λ_{hyp}. For IPOP-^{s*}aACM-ES λ_{hyp} was set to 20.

4.3.3.10 Quadratic Programming Problem Optimization

The number of iterations n_{iter} used to optimized the QP problem 4.3 is left fixed to 1000ℓ in the hyper-parameters optimization procedure. However, it can also be adapted by setting $\text{Min}(n_{iter}) = 100\ell$ and $\text{Max}(n_{iter})$=1500ℓ (this would complement Table 4.3). Thus, the procedure of hyper-parameters adaptation could, if necessary, reduce the CPU

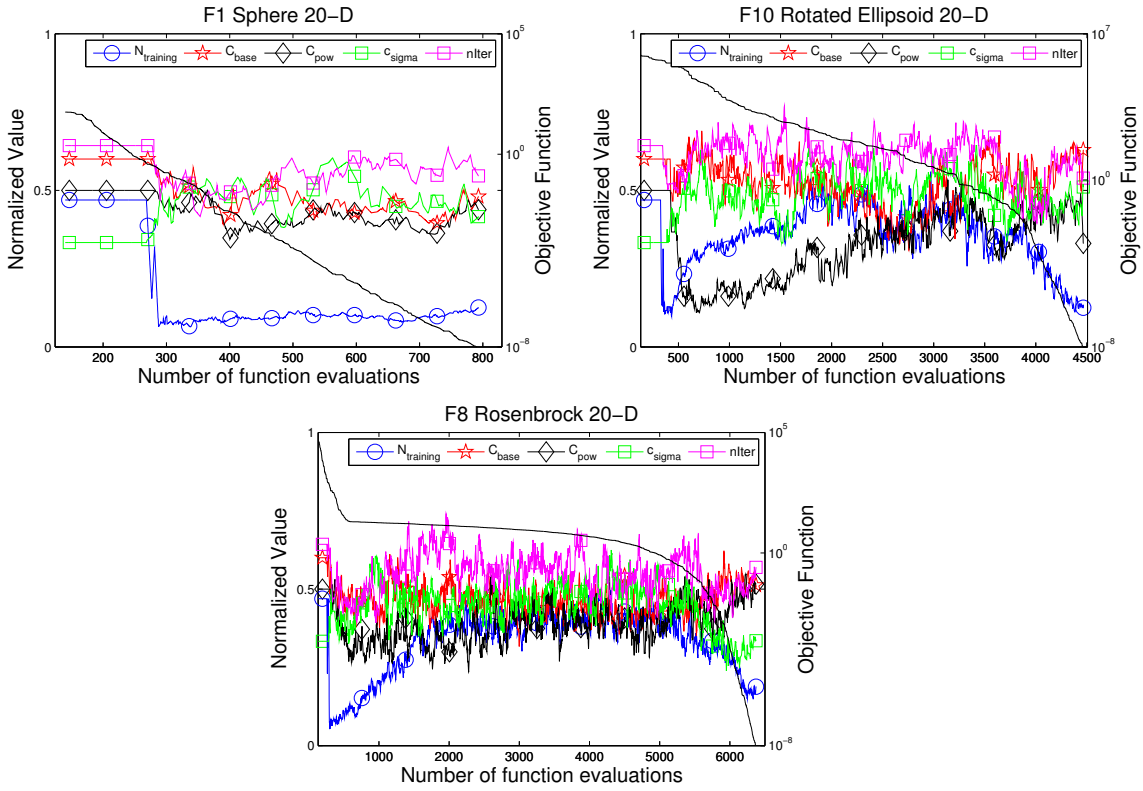

Figure 4.25: Median trajectories of normalized surrogate hyper-parameters (including n_{iter}) from 15 runs of the IPOP-^{s*}aACM-ES with Ranking SVM on Sphere, Rotated Ellipsoid and Rosenbrock 20-dimensional BBOB benchmark problems.

cost from 1000ℓ (default setting) to 100ℓ iterations (i.e., by a factor of 10) or on the opposite allocate 1500ℓ iterations in total to obtain a more precise solution. Figure 4.25 illustrates the results of IPOP-^{s*}aACM-ES on 20-dimensional Sphere, Rotated Ellipsoid and Rosenbrock functions (see also Figure 4.15 for similar results without adaptation of n_{iter}). The results show that the adapted n_{iter} often lies quite close to its default value 1000ℓ, at least for these objective functions and given procedures of surrogate learning and exploitation. Therefore, it is likely that more precise solutions of QP will not improve the results on these test problems. However, a complete analysis of the adaptation of n_{iter} should be performed on large dimension (i.e., 20-D and 40-D), for both noiseless and noisy BBOB functions in order to investigate whether the results are improved or not.

The surrogate learning step involves a trade-off between the computational effort and the accuracy of the QP resolution. This trade-off can be controlled through adapting the number n_{iter} of iterations, and/or selecting the α_{i_x}s (see Section 4.1.1), e.g., selecting a working set selection based on gradient information of the Lagrangian L. In practice, the selection proceeds by computing ΔL for all α_{i_x} at each iteration of the algorithm, to

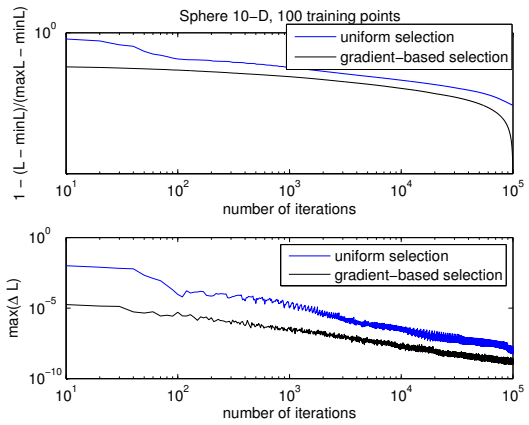

Figure 4.26: Cumulative normalized improvements of Lagrangian (**Top**, lower values are better) and maximal local improvements of Lagrangian (**Bottom**) vs number of iterations of Ranking SVM surrogate learning of 10-dimensional Sphere function for both uniform and gradient-based selection of Lagrangian multipliers.

update the α_{i_x} which leads to the largest increase of the Lagrangian and ΔL.

This trade-off has been empirically investigated, comparing the uniform and gradient-based selection strategies on 10-dimensional Sphere and Rosenbrock functions with 100 training points and 40-dimensional Sphere and Rosenbrock functions with 2000 training points. The training points, uniformly randomly drawn from $[-0.5, 0.5]^n$, are used to build Ranking SVM surrogate model with RBF kernel, where σ parameter is defined as the average distance between the points. The constant C of Ranking SVM is set to 10^6 in all experiments. For both selection strategies the maximum number of iterations is 1000ℓ, for gradient-based selection an additional stopping criterion is used: the algorithm also stops if $\frac{Max(\Delta L)}{C^2} < 10^{-20}$.

The results are displayed in Figure 4.26, showing the cumulative increase of Lagrangian L and observed $Max(\Delta L)$ for uniform and gradient-based selection on 10-dimensional Sphere function. As expected, gradient-based selection converges faster to the optimum of the QP problem by selecting at each iteration the most promising α_{i_x} Lagrangian multiplier. The speedup w.r.t. uniform selection is of order 100 for small number of iterations (e.g., 10) and of order smaller than 10 for relatively large number of iterations (e.g., $10^4 - 10^5$). Indeed, these speedup factors are problem- and SVM hyper-parameters dependent. However, an important aspect that should be taken into account is that one operation of gradient-based selection is numerically more expensive than random or periodic selection. Therefore, the overall CPU time of the gradient selection-based surrogate learning might be longer than the one of the uniform selection-based learning. In order to investigate the time complexity of both approaches, we re-plotted the results with, on the x-axis, the "time" metric, where "time" is equal to the number of iterations for uniform selection and the number of iterations times a factor of how much one gradient

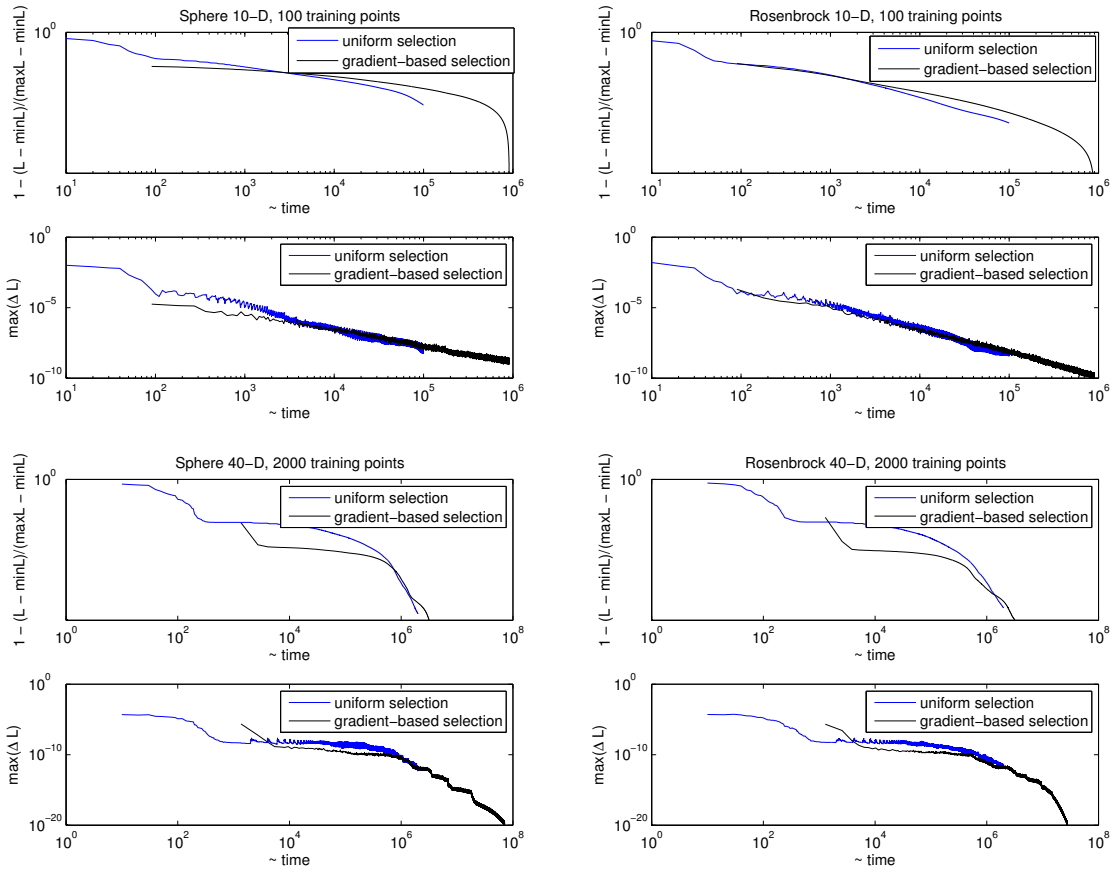

Figure 4.27: Convergence to the optimum of QP problems vs "time" of Ranking SVM surrogate learning for 10-dimensional Sphere and Rosenbrock functions with 100 training points and for 40-dimensional Sphere and Rosenbrock functions with 2000 training points. See text for details.

selection-based iteration is more expensive than uniform selection-based iteration.

Figure 4.27 shows the convergence to the optimum of the QP problem versus "time" for uniform selection and gradient selection-based strategies. As can be seen, the advantages of gradient-based selection becomes less obvious by taking into account the CPU time instead of the number of iterations. Moreover, uniform selection outperforms gradient-based selection on 10-dimensional Sphere and Rosenbrock functions in the sense of the cumulative increase of the Lagrangian at the typical stopping point of $n_{iter} = 1000\ell$. This was observed in our earlier experiments and has been discussed in Section 4.1.1. The results for 2000 training points suggest that both approaches are quite comparable at $500\ell \ldots 1000\ell$ iterations of uniform selection-based learning. However, at early stages of QP problem optimization, gradient-based selection clearly outperforms uniform selection. Thus, if the accuracy of QP problem solution at these early stages is sufficient for accurate

predictions of $f(x)$, then the CPU time complexity of surrogate model learning can be reduced by a factor of 10-100 by considering a gradient-based selection. Unfortunately, our preliminary experiments, as well as the results shown in Figure 4.25 (the adaptation of n_{iter}), suggest that a much lower accuracy of QP problem solutions is not sufficient to build accurate surrogate models. These preliminary findings, however, should be very carefully verified considering more objective functions and larger dimensions, since the gradient-based selection is one of the most straightforward ways to reduce the time complexity of surrogate learning procedure and scale the algorithm to larger problem dimensions. Another possibility, to be considered in further work, might be to leave the decision of gradient-based versus uniform selection, to the hyper-parameter optimization step.

4.3.4 Conclusion and Perspectives

In this Section, we have presented a generic framework for adaptive surrogate-assisted optimization, which can in principle be combined with any iterative population-based optimization and surrogate learning algorithms. This framework has been instantiated on top of surrogate-assisted ACM-ES, using CMA-ES as optimization algorithm and Ranking SVM as surrogate learning algorithm. The resulting algorithm, ^{s*}ACM-ES, inherits from CMA-ES and ACM-ES the property of invariance w.r.t. monotonous transformations of the objective function and orthogonal transformations of the search space.

The main contribution of the ^{s*}ACM-ES regards the online adjustment of i). the number $\widehat{n}$ of generations a surrogate model is used, called surrogate lifelength; ii). the surrogate hyper-parameters controlling the surrogate learning phase. The surrogate lifelength is adapted depending on the quality of the current surrogate model; the higher the quality, the longer the next surrogate model will be used. The adjustment of the surrogate hyper-parameters is likewise handled by optimizing them w.r.t. the quality of the surrogate model, without requiring any prior knowledge on the optimization problem at hand.

IPOP-^{s*}aACM-ES (respectively, BIPOP-^{s*}aACM-ES) was found to improve on IPOP-aCMA-ES (respectively, BIPOP-CMA-ES) with a speedup ranging from 2 to 3 on unimodal n-dimensional functions from the BBOB-2012 noiseless testbed, with dimension n ranging from 2 to 20. On multi-modal functions, IPOP-^{s*}aACM-ES is equally good or sometimes better than IPOP-aCMA-ES, although the speedup is less significant than for unimodal problems. Further, IPOP-^{s*}aACM-ES also improves on IPOP-aCMA-ES on problems with moderate noise from BBOB-2012 noisy testbed. BIPOP-^{s*}aACM-ES usually outperforms IPOP-^{s*}aACM-ES and BIPOP-CMA-ES on multi-modal functions (note that an active version of BIPOP-CMA-ES, BIPOP-aCMA-ES, will be presented in Section 6.3.3).

A long term perspective for further research is to better handle multi-modal (see Section 6.3.3) and noisy functions. A shorter-term perspective is to consider a more comprehensive surrogate learning phase, involving a portfolio of learning algorithms and using the surrogate hyper-parameter optimization phase to achieve portfolio selection. Another perspective is to design a tighter coupling of the surrogate learning phase, and the CMA-ES optimization, e.g., using the surrogate model $\widehat{f}$ to adapt the CMA-ES hyper-parameters

during the optimization of the expensive objective f.

4.4 Discussion

In this Chapter, we focused on single-objective surrogate-assisted CMA-ES algorithms for optimization of expensive problems of small to medium dimension. In the following, we analyze alternatives which may be considered for further research:

Core Optimization Algorithm CMA-ES seems to be a good candidate baseline optimizer, the only competitive algorithms are i). BFGS and NEWUOA algorithms which now perform not better than ^{s*}ACM-ES even on well suitable (for them) functions such as Rosenbrock, being sensitive to rank-preserving transformations of f; ii). Differential Evolution algorithms which are based on alternative strategies of optimization and have attracted a lot of attention in the last years (see, e.g., several DE algorithms in BBOB-2012), but are about one order of magnitude slower than ^{s*}ACM-ES.

Surrogate Modeling Approach We strongly believe that the ordinal regression should be preferred to the metric regression, because the invariance of the former allows to reduce the problem of hyper-parameters tuning. We also suppose that Ranking SVM definitely should be used as a baseline surrogate technique for comparison-based optimization algorithms, at least on unimodal optimization problems. For multi-modal and/or noisy problems the use $\ell - 1$ constraints seems to be too optimistic and additional selection of constraints (e.g., the most violated ones) should be considered. As an alternative to Ranking SVM, Gaussian Processes for ordinal regression can be used [Chu and Ghahramani, 2005a], however, our preliminary experiments showed that the surrogate learning is computationally more expensive and numerically instable.

Surrogate Model Control Alternative approaches to the simple surrogate model based control used in this Chapter were discussed in Section 4.3.1.4. The lifelength-based control strategy is used because it can be parallelized on λ CPUs and is simple to interpret. This strategy may be improved by using more sophisticated $\hat{n}(Err(\hat{f}))$ functions (dotted curves in Figure 4.12) instead of the linear one (bold curve). A more meaningful estimation of the model error can be obtained if use weights for different points in Eq. (4.9). We suppose that the two ideas described above may significantly improve the results. However, we intentionally avoided their further analysis to prevent the algorithm from a potential overfitting to the testbed and to keep the strategy in the simple and interpretable form.

Surrogate Model Hyper-parameters Adaptation In addition to already adapted hyper-parameters, we may also learn which Kernel function is the most suitable in the current state of the search [Tenne and Armfield, 2007]. Apart from the computational complexity, there is no reason not to use different surrogate modeling techniques with hyper-parameters adaptation for each technique independently, then

use the best model or an aggregation of the models for the exploitation phase. It is also suggested to use larger λ_{hyp} if the computational of the model is relatively cheap.

The main limitations of the ^{s*}ACM-ES which should be addressed in further research:

Space complexity Ranking SVM with non-linear Kernels needs to store Kernel matrix of size ℓ^2. The number of training points usually scales super-linearly with n such that for $n > 100$ it is very likely that all required training points cannot be stored in memory. However, ^{s*}ACM-ES still can be used for say $n = 1000$ by setting upper bound for ℓ, but this will lead to a smaller speedup (see Figure 4.9 for a similar effect for the original ACM). To reduce the space complexity, ensembles of surrogate models can be used, such that each surrogate model is responsible for $\ell' < \ell$ training points. In this case, an aggregation procedure of different surrogates should be used.

Time complexity The algorithm scales with $O(\ell^2)$. To drastically reduce the time complexity, one should not use non-linear Kernels. Recent results show that large-scale linear classification can be extremely fast (see LIBLINEAR [Fan *et al.*, 2008]). We suppose that the use of ensembles of linear Ranking SVM is an attractive *long term* direction of research.

Small Speedup on Noisy and/or Multi-modal Functions The simple reason why the speedup may be relatively small on noisy and multi-modal functions is that these functions are difficult to approximate and usually more training points are required to build their accurate model. To better deal with this problem, one should closely look at the model learning on simplest 2-dimensional instances of the multi-modal and noisy problems at hand.

We suppose that the performance of ^{s*}ACM-ES on unimodal functions can be further improved by more carefully developing surrogate model control and adaptation procedures, taking inspiration from the prospective directions of research that have been discussed. On multi-modal functions, however, it seems more prospective to look at alternative restart strategies for CMA-ES which potentially may bring a comparable speedup at a lower computational cost. We will address this issue in detail in Section 6.3.3. Another interesting observation that we made during the development of ^{s*}ACM-ES is that if transformation (4.11) allows to decorrelate all the variables as well as possible such that the transformed space resembles the Sphere function, then why not use some very simple optimization algorithm which exploits the separability of this space? To answer this question we propose and investigate in Section 6.1 Adaptive Coordinate Descent method, a non-evolutionary and non-stochastic algorithm that has a comparable performance with CMA-ES on unimodal functions and may have *linear* time complexity.

Chapter 5

Multi-Objective Surrogate-Assisted CMA-ES

Multi-objective optimization problems are usually difficult to solve, because they inherit properties of individual objectives and a set of Pareto optimal solutions is the primal goal, rather than one single solution (see Section 2.4 for a review of multi-objective optimization). Mainstream surrogate approaches for multi-objective problems, with the notable exception of [Yun *et al.*, 2004], often extend surrogate-based standard EAs, building one surrogate for each objective function and replacing the objective by its surrogate (see Section 3.3.3). The main limitation of such approaches is due to the approximation noise as the number of objectives increases. The learning cost indeed increases linearly with the number of objectives; but the Pareto dominance test, checking whether one individual is dominated by another one, requires comparing their surrogate values over all objectives; the error thus exponentially increases in the worst case with the number of objectives. Alternative single-model approaches based on the notion of expected improvement in multi-objective optimization in terms of hypervolume indicator have been proposed by [Emmerich *et al.*, 2006a, Ponweiser *et al.*, 2008] (see Section 3.3.3). These approaches, however, usually assume the evaluation of only one candidate solution per iteration that may lead to a loss of efficiently in the scenario with parallel evaluations.

Addressing the limitations described above, we propose a mono surrogate approach based on Aggregated Surrogate Models (ASM) aiming at building a global surrogate model in decision space, characterizing whether an individual belongs to i). the current Pareto set, or ii). the dominated region, or iii). the rest of the decision space (not yet visited, and containing the *true* Pareto set). This surrogate model, providing an aggregated perspective on all objective functions simultaneously, is then used to guide the search in the vicinity of the current Pareto set, and speed up the population move toward the true Pareto set. ASM is constructed by combining ideas from Regression and One-class SVMs and is described in detail in Section 5.1.

The formulation of ASM has been found to be over-constrained in Section 5.4.3.1, and, similarly to Chapter 4, we propose a relaxed version inspired from Ranking SVM, rank-based ASM model (RASM). RASM only requires to locally approximate the Pareto dominance relation, enabling to rank neighbor points within the objective space. Thanks to the flexibility of Ranking SVM, RASM is able to learn any kind of preference relations defined for solutions of multi-objective problem, e.g., based on Pareto dominance, Quality Indicator and Decision Maker preferences. The description of RASM is presented in Section 5.2.

As for surrogate model exploitation, we employ a simple pre-selection scheme in order

to investigate basic properties of ASM models (see Section 5.3). In Section 5.4, we experimentally validate both ASM and RASM models on a relatively simple two-objective benchmark testbed, demonstrating a significant reduction of the number of evaluations of the actual objective functions both for ASM-assisted NSGA-II and MO-CMA-ES algorithms. Finally, Section 5.5 concludes the Chapter and presents some perspectives for further research.

The results presented in this Chapter have been published as [Loshchilov *et al.*, 2010a, Loshchilov *et al.*, 2010b, Loshchilov *et al.*, 2010d].

5.1 Aggregated Surrogate Model

In mono surrogate approach, the goal is to build an Aggregated Surrogate Model which *aggregates* the informations about preferences among training points in the *objective space*, usable to drive the population toward the *true* Pareto set. In this Section, a surrogate model $\hat{f}$ of a multi-objective problem f is learned from i). points belonging to the current Pareto set, and ii). dominated points.

5.1.1 Rationale and Assumption

At any given time during the EMOA run, the relative position of the Pareto set and the dominated points can be schematically depicted as follows. The situation might be simple in the objective space (Figure 5.1-a), with the true Pareto front and the dominated region located on the two opposite sides of the current Pareto front. It can be much more intricate in the decision space; Figure 5.1-b illustrates the case where the true Pareto set (respectively, the dominated region) lies within (respectively, outside) the convex hull of the current Pareto set. Furthermore, the Pareto set can include many disjoint regions in the decision space. The assumption made is that the Pareto region includes a small number of connected components; note that this assumption holds for most classical multi-objective optimization benchmarks (e.g., IHR1, see Figure 5.5-c and -d).

While ASM expectedly discriminates the Pareto set and the dominated region, a binary classification approach is ill-suited, as it would not give any precise indication about where the *true* Pareto set is located. More generally, the Pareto set (true or current) and the dominated points cannot be handled in a symmetrical way: dominated points span over a subspace whereas the Pareto set should better be viewed as a manifold.

It thus comes to map all Pareto points onto a single value ρ (up to some tolerance ϵ); meanwhile, the dominated points would be mapped onto the half space $]-\infty, \rho-\epsilon[$. Such a mapping might actually provide useful indications: expectedly, points mapped onto the half space $[\rho+\epsilon, +\infty[$ would belong to the yet unexplored region, which is bound to contain the *true* Pareto set, and these points could thus be considered promising.

The above constraints on the ASM mapping can be expressed by combining the Support Vector Regression formulation ([Smola and Schölkopf, 2004], see Section 3.2.2), mapping each point $\boldsymbol{x}$ onto some target value $f(\boldsymbol{x})$ up to some tolerance ϵ, and the One-class SVM ([Schölkopf *et al.*, 2001], see Section 3.2.3), mapping a set of points onto a connected interval and thus characterizing the support of the underlying sample distribution. The

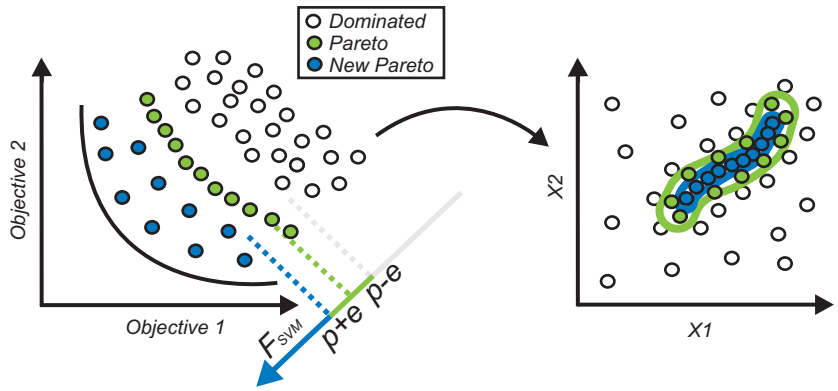

(a) Objective space (b) Decision space

Figure 5.1: An *idealistic* schematic view of the Pareto front, depicting dominated points (white), current Pareto (green) and new Pareto (blue) respectively in objective and decision space.

main difference is that the target value ρ associated to the Pareto points is free in the ASM problem.

5.1.2 Lagrangian formulation

Let the training set be defined as $\mathcal{D} = \{\boldsymbol{x}_1, \dots \boldsymbol{x}_\ell, \boldsymbol{x}_{\ell+1}, \dots \boldsymbol{x}_m\}$ where the first ℓ points belong to the current Pareto front and the following points $\boldsymbol{x}_{\ell+1}, \dots \boldsymbol{x}_m$ are dominated ones. As discussed above, the ASM is obtained from the following learning constraints:

- All Pareto points $\boldsymbol{x}_1 \dots \boldsymbol{x}_\ell$ are mapped on some value ρ up to tolerance ϵ (regression constraints);
- All dominated points are mapped onto $(-\infty, \rho - \epsilon[$ (one-class constraints).

Let C and ϵ be two positive constants, and ξ_i^{up}, ξ_i^{low} are slack variables measuring constraints violations, the *primal* ASM learning problem is:

$$\underset{\{w,\, \xi^{(*)},\, \rho\}}{\text{Minimize}} \frac{1}{2}||w||^2 + C\sum_{i=1}^{\ell}(\xi_i^{up} + \xi_i^{low}) + C\sum_{i=\ell+1}^{m}\xi_i^{up} + \rho \tag{5.1}$$

subject to

$$< w, \Phi(\boldsymbol{x}_i) > \leq \rho + \epsilon + \xi_i^{up} \quad (i = 1 \dots \ell) \tag{5.2}$$
$$< w, \Phi(\boldsymbol{x}_i) > \geq \rho - \epsilon - \xi_i^{low} \quad (i = 1 \dots \ell) \tag{5.3}$$
$$< w, \Phi(\boldsymbol{x}_i) > \leq \rho - \epsilon + \xi_i^{up} \quad (i = \ell + 1 \dots m) \tag{5.4}$$
$$\xi_i^{up} \geq 0 \quad (i = 1 \dots \ell) \tag{5.5}$$
$$\xi_i^{low} \geq 0 \quad (i = 1 \dots \ell) \tag{5.6}$$
$$\xi_i^{up} \geq 0 \quad (i = \ell + 1 \dots m) \tag{5.7}$$

The formulation of dual form of ASM learning problem and its resolution using SMO method is described in Appendix B.

In some cases the set of non-dominated points is too small to build accurate surrogate models or the preference relations between training points are only partially known, then it would be reasonable to directly learn preference relations as will be discussed in the next Section.

5.2 Rank-based Aggregate Surrogate Model

This Section gives an overview of the Rank-based Aggregate Surrogate Model (RASM), a Ranking SVM-based approach for learning preference information with a relatively small number of constraints.

5.2.1 Learning Preference Information in Multi-objective Space

To build a mono surrogate model $\hat{f}$ of a multi-objective problem f, one can use preference information defined on a set of training points $\mathcal{D} = \{\boldsymbol{x}_1, \ldots, \boldsymbol{x}_\ell\}$ to satisfy $\hat{f}(\boldsymbol{x}_a) > \hat{f}(\boldsymbol{x}_b)$ whenever $\boldsymbol{x}_a$ is preferred to $\boldsymbol{x}_b$. All preference pairs (a, b) can be stored in a set of preference constraints $\mathcal{P}$. Thus, one can formalize the learning of $\hat{f}$ using Ranking SVM approach (see Sections 3.2.4) as follows:

$$\text{Minimize}_{\{w,\xi\}} \ \frac{1}{2}||w||^2 + \sum_{i=1}^{|\mathcal{P}|} C_i \xi_i \tag{5.8}$$

$$\text{subject to} \begin{cases} \langle w, \boldsymbol{x}_a \rangle - \langle w, \boldsymbol{x}_b \rangle \geq \epsilon_i - \xi_i, & i = 1, \ldots, |\mathcal{P}|; (a, b) \leftarrow \mathcal{P}_i \\ \xi_i \geq 0, & i = 1, \ldots, |\mathcal{P}| \end{cases} \tag{5.9}$$

The mentioned above problem can be solved using SMO method as described in Section 4.1.1. The crucial question is how to fill $\mathcal{P}$ such that the final surrogate $\hat{f}$ would be *ideal* for a given algorithm $\mathcal{A}$. Any kind of preference information can be used to fill $\mathcal{P}$, however, one should look at the following sources, relevant for the multi-objective context, to decide whether a preference pair (a, b) should be added to $\mathcal{P}$:

Pareto Dominance Check whether $\boldsymbol{x}_a$ dominates $\boldsymbol{x}_b$.

Quality Indicator Check whether $I(\boldsymbol{x}_a)$ is preferred to $I(\boldsymbol{x}_b)$ w.r.t. a given Quality Indicator I, e.g., hypervolume contribution indicator (see Section 2.4.1).

Decision Maker Check whether the Decision Maker prefers $\boldsymbol{x}_a$ to $\boldsymbol{x}_b$.

When $\boldsymbol{x}_a$ is preferred to $\boldsymbol{x}_b$ ((a, b) is the i-th preference constraint $\mathcal{P}_i$) we learn such $\hat{f}$ that $\hat{f}(\boldsymbol{x}_a) - \hat{f}(\boldsymbol{x}_b) = \langle w, \boldsymbol{x}_a \rangle - \langle w, \boldsymbol{x}_b \rangle \geq \epsilon_i - \xi_i$, where ϵ_i is usually set to 1. Such definition corresponds to the preference constraint in its usual sense, referred to as ">"-constraint. We also may define equality of $\boldsymbol{x}_a$ and $\boldsymbol{x}_b$ setting ϵ_i to a relatively small value, say 10^{-3}, and adding two pairs of constraints: i). $\langle w, \boldsymbol{x}_a \rangle - \langle w, \boldsymbol{x}_b \rangle \geq 10^{-3}$, and ii).

$\langle w, \boldsymbol{x}_b \rangle - \langle w, \boldsymbol{x}_a \rangle \geq 10^{-3}$. Thus, the learning algorithm will try to satisfy both constraints, mapping $\boldsymbol{x}_a$ and $\boldsymbol{x}_b$ to the same value of $\hat{f}$ with a small fluctuation in the order of 10^{-3}. Such "="-constraint pairs can be especially useful to define equality of points belonging to the same non-dominated front.

It should be noted that for a training set of size ℓ we may have at most $n_{alpha} = \ell^2 - \ell$ constraints ($\frac{\ell^2-\ell}{2}$ if use only ">"-constraints). Let us recall that the computational complexity of Ranking SVM scales with $O(n_{alpha}^2)$, i.e., $O(\ell^4)$ if all constraints are used. Moreover, from the the single-objective surrogate-assisted search, we know that ℓ may scale with $O(n^{1.7})$ that would lead to $O(n^7)$ complexity of learning full model. This is clearly an unsatisfactory computational complexity, therefore we should find a way to build reasonably good $\hat{f}$ using much less constraints, preferably $O(\ell)$ number of constraints.

5.2.2 Dominance-based Preference Learning

For the sake of tractability of RASM model learning we propose the following simple procedure (see, e.g., [Vapnik, 1979] for "chunking" procedure and [Joachims, 2005] for a recent review of the idea of selection of the most violated constraint):

1. Initialize a set of *active* constraints Ω_{active} by *primary* constraints and a set of *passive* constraints $\Omega_{passive}$ by *secondary* constraints.
2. Optimize Eq. (5.8) with $\mathcal{P} = \Omega_{active}$.
3. Remove the most violated constraint from $\Omega_{passive}$ and add it to Ω_{active}. Optimize Eq. (5.8) with $\mathcal{P} = \Omega_{active}$. Repeat this step until stopping criterion is met.

Figure 5.2-**Left** illustrates a set of solutions in the objective space for which one should find a suitable set of constraints to learn $\hat{f}$. For fast model learning the size of the set of constraints should be linear in number of solutions. *Primary* constraints are constraints which best describe the model and should be learnt in the first place. *Secondary* constraints are all other constraints which represent a source of the information about f, but cannot be learnt all together due to limited computational resources. Let *primary dominance constraints* be associated to pairs $(\boldsymbol{x}_i, \boldsymbol{x}_j)$ such that $\boldsymbol{x}_j$ is the nearest neighbor of $\boldsymbol{x}_i$ conditionally to the fact that $\boldsymbol{x}_i$ dominates $\boldsymbol{x}_j$ (continuous arrow, Figure 5.2-**Left**, Algorithm 5.1, lines 4-10), and let **secondary dominance constraints** be associated to pairs $(\boldsymbol{x}_i, \boldsymbol{x}_j)$ such that $\boldsymbol{x}_i$ belongs to the current Pareto front and $\boldsymbol{x}_j$ belongs to another front from non-dominated sorting (dotted arrow, Figure 5.2-**Left**, Algorithm 5.1, lines 17-22).

After optimization of Eq. (5.8) for $N_{IterActive} = 1000 \times |\Omega_{active}|$ iterations (Algorithm 5.2, line 3), the model $\hat{f}$ still may incorrectly predict some (test) preference relations from $\Omega_{passive}$. We may identify the *most violated constraint* $constr_{mv}$ from $\Omega_{passive}$ (lines 6-13) and add it to Ω_{active} (line 17) to continue learning the model for $N_{IterPerPassive} = 10 \times |\Omega_{active}|$. After adding $N_{ConstrToAdd}$ such constraints (typically 10% the number of primary constraints in the presented experiments, see Section 5.4), a robust $\hat{f}$ can be obtained with relatively cheap learning.

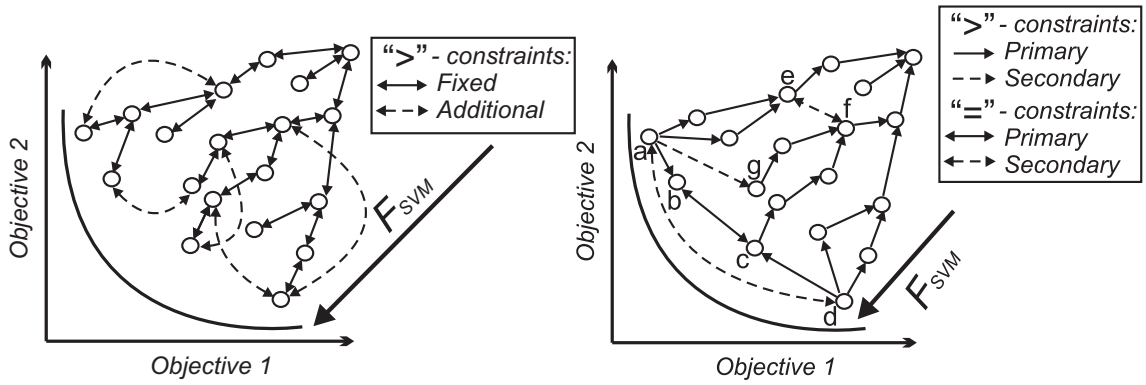

Figure 5.2: Constraints involved in Rank-based Aggregated Surrogate Models. Left: The current RASM. Right: possible extensions with "=" constraints, see Section 5.5.

5.3 ASM-assisted MOEAs with Pre-selection

This Section describes the Pareto-SVM algorithm, exploiting the ASM and RASM mono surrogates (ASMs) to speed up Evolutionary Multi-Objective Optimization. The terms ASM and RASM will be used interchangeably in this Section.

5.3.1 Discussion

As mentioned earlier, surrogate-assisted multi-objective optimization most commonly proceeds by replacing the objective function with the surrogate model, computing the true objective on carefully selected points, and retraining the model from time to time using recently evaluated individuals.

The situation here is different as the optimization problem is a multi-objective one, and the single ASM surrogate model is being built. The most natural idea, optimizing directly the ASM model, raises the following two issues. Firstly, the true Pareto set expectedly lies away from the dominated points and beyond the current Pareto set; the ASM would thus be used to explore yet unexplored regions, i.e., for extrapolation. Secondly and more importantly, identifying the Pareto set critically relies on the population diversity. While all individuals in the current Pareto set are equally mapped on the same $\hat{f}$ value, some will be 'more equal than others', in the sense that they will get a higher ASM value by chance. Optimizing *ex abrupto* the ASM model would thus favor some regions of the Pareto set and hinder the population diversity.

For these reasons, the ASM model will be used to implement the pre-selection (aka informed operators) approach (see Section 3.3.1.4). Next Sections respectively outline the full algorithm, and describe the two specific modules of the Pareto-SVM algorithm, the surrogate model update and its use within informed operators.

Algorithm 5.1: Selection of Constraints for RASM model

```
1: given (x_1, y_1), ..., (x_ℓ, y_ℓ), C
2: initialize Ω_active, Ω_passive ← ∅
3: Rank_{1,...,ℓ} ← NonDominatedSorting((x_1, y_1), ..., (x_ℓ, y_ℓ))
4: for i = 1, ..., ℓ do
5:    Δy_min ← ∞
6:    for j = 1, ..., n do
7:       if ((x_i ≻ x_j) AND (i ≠ j)) then
8:          Δy ← ‖y_i − y_j‖
9:          if Δy < Δy_min then
10:            Δy_min ← Δy; j_min ← j          // nearest neighbor in objective space
11:         end if
12:      end if
13:   end for
14:   constr.α ← random ∈ [0, C]; constr.a ← i; constr.b ← j_min; constr.ϵ ← 1.0
15:   Ω_active ← Ω_active ∪ {constr}
16: end for
17: for i = 1, ..., ℓ do
18:   for j = 1, ..., ℓ do
19:      if ((Rank_i < Rank_j) AND (Rank_i = 1)) then
20:         constr.α ← random ∈ [0, C]; constr.a ← i; constr.b ← j; constr.ϵ ← 1.0
21:         if constr ∉ Ω_active then
22:            Ω_passive ← Ω_passive ∪ {constr}
23:         end if
24:      end if
25:   end for
26: end for
27: return Ω_active, Ω_passive
```

5.3.2 The Algorithm

The general description of MOEA (Algorithm 5.3) is based on the usual parent-selection → variation → survival selection loop, with optionally some archive maintenance (line 5), as many popular MOEAs need to maintain some archive of the non-dominated individuals encountered during the search [Deb *et al.*, 2000]. Note that line 4 describes both the parent selection and the application of the variation operators; it implicitly accounts for any choice procedure among multiple operators.

The Pareto-SVM algorithm is described likewise in Algorithm 5.4. The main differences are the model update (line 5) and the call to the informed operators (line 7) that replaces the standard call to variation operators, with the surrogate model $\hat{f}$ as additional argument. The archive maintenance is limited to storing all newborn offspring (line 8). Actual update, including the ASM update, takes place every K_{learn} generations (line 4).

Algorithm 5.2: SVM Optimization

1: **given** Ω_{active}, $\Omega_{passive}$, $N_{IterActive}$, $N_{IterPerPassive}$, $N_{ConstrToAdd}$
2: **for** $i = 1, \ldots, N_{IterActive}$ **do**
3: $\quad \Omega_{active} \leftarrow$ SVMOptimizationIteration(Ω_{active})
4: **end for**
5: **for** $i = 1, \ldots, N_{ConstrToAdd}$ **do**
6: $\quad constr_{mv} \leftarrow \Omega_{passive_1}$
7: $\quad \xi_{max} \leftarrow 0$
8: $\quad$ **for** $j = 1, \ldots, |\Omega_{passive}|$ **do**
9: $\quad\quad constr \leftarrow \Omega_{passive_j}$
10: $\quad\quad \xi_j \leftarrow \hat{f}(\boldsymbol{x}_{constr.i}) + \epsilon_{constr.\epsilon}$ - $\hat{f}(\boldsymbol{x}_{constr.j})$
11: $\quad\quad$ **if** $\xi_{max} > \xi_j$ **then**
12: $\quad\quad\quad \xi_{max} \leftarrow \xi_j$
13: $\quad\quad\quad constr_{mv} \leftarrow constr$ // find the most violated constraint
14: $\quad\quad$ **end if**
15: $\quad$ **end for**
16: $\quad$ **if** $\xi_{max} > 0$ **then**
17: $\quad\quad \Omega_{active} \leftarrow \Omega_{active} \cup \{constr_{mv}\}$
18: $\quad\quad \Omega_{passive} \leftarrow \Omega_{passive} \setminus \{constr_{mv}\}$
19: $\quad\quad$ **for** $j = 1, \ldots, N_{IterPerPassive}$ **do**
20: $\quad\quad\quad \Omega_{active} \leftarrow$ SVMOptimizationIteration(Ω_{active})
21: $\quad\quad$ **end for**
22: $\quad$ **end if**
23: **end for**
24: **return** Ω_{active}

Algorithm 5.3: Standard MOEA

1: **initialize** Archive $\leftarrow \emptyset$
2: Pop $\leftarrow$ MOEA.Init()
3: **while** NOT Stopping Criterion **do**
4: $\quad$ Offspring $\leftarrow$ VarOp(ParentSelect(Pop))
5: $\quad$ UpdateArchive(Pop,Offspring)
6: $\quad$ Pop $\leftarrow$ SurvivalSelect(Pop,Offspring)
7: **end while**
8: **return** Pop.BestIndividual

5.3.2.1 Model Update

The model update (Algorithm 5.5) starts from the current archive (as produced from the previous update) augmented by all newborn offspring (line 8 of Algorithm 5.4) and first removes the possible duplicates (line 1 of Algorithm 5.5). In most cases (depending on K_{learn} and the number of offspring generated per generation), the size of the archive

Algorithm 5.4: PARETO-SVM

```
1:  initialize Archive ← ∅
2:  Pop ← MOEA.Init()
3:  while NOT Stopping Criterion do
4:    if #generation ≡ 0 [K_learn] then
5:      f̂ = UpdateModel(Archive, Pop)          // every K_learn generation
6:    end if
7:    Offspring ← InfOp(ParentSelect(Pop), f̂)
8:    Archive ← Archive ∪ Offspring
9:    Pop ← SurvivalSelect(Pop, Offspring)
10: end while
11: return Pop.BestIndividual
```

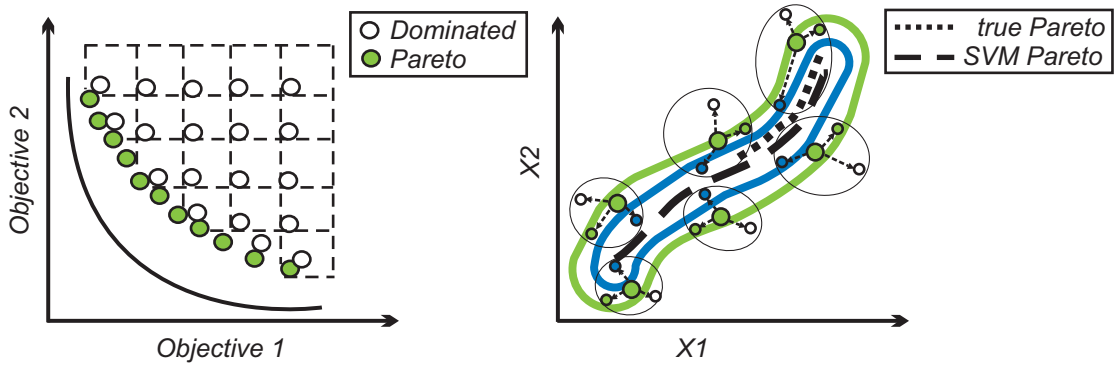

Figure 5.3: A schematic view of the training data selection in objective space (**Left**) and SVM-informed selection of children from the pool of pre-children in decision space (**Right**).

increases far too much to make it possible to efficiently apply the Pareto-SVM learning. Furthermore, pruning the archive should not be done solely based on Pareto dominance, as in most standard MOEAs where only the best Pareto points are of interest. We need instead to ensure a good coverage of the dominated region that has been visited in the past, to make sure that the ASM will label these regions as 'dominated'. Borrowing ideas from PESA [Corne *et al.*, 2001], the objective space is equally partitioned into $N_{archive}$ boxes, and the archive keeps one point per box. Boxes are computed in lines 2 and 3, points are put in their respective boxes in line 5, and all boxes are pruned (line 8), keeping a uniformly chosen point among the non-dominated points of the box if any.

ASM is learned from a training set made of one point per box (line 10), plus the current population that is likely to contain non-dominated points (line 11). The training set is pruned to remove the duplicates and thereafter sorted using non-dominated sort to distinguish between current Pareto and dominated points (line 13). Finally it is passed to the ASM learning algorithm that returns the new ASM surrogate model to the main

Algorithm 5.5: UpdateModel(Archive, Pop)

```
1: EliminateDuplicates(Archive)
2: ComputeObjectiveBounds(Archive)
3: PartitionObjectiveSpace(N_Archive)
4: for all P ∈ Archive do
5:    FindBox(P)                          // Assign P to the box it belongs to
6: end for
7: for all Boxes B do
8:    Ind[B] ← Random(NonDominated(B))    // Select one point per box
9: end for
10: Archive ← ⋃_B Ind[B]                  // at most N_Archive points
11: TrainingData ← Archive ∪ Pop
12: EliminateDuplicates(TrainingData)
13: NonDominatedSort(TrainingData)
14: return Pareto-SVM(Training Data)      // returns f̂
```

Algorithm 5.6: InfOp(Parents, F)

```
Require: OP(s)                            // variation operator(s)
1: Offspring ← ∅
2: for iOff = 1 to RequiredSize do
3:    Choose variation operator Op        // Eventually
4:    GainBest ← 0
5:    for i = 1 to λ_Pre do
6:       Ind ← Op(Parents)
7:       IndPop ← NearestNeighbor(Ind,ND-Parents)
8:       Gain ← f̂(IndPop) - f̂(Ind)
9:       if Gain > GainBest then
10:         GainBest ← Gain
11:         Best ← Ind
12:      end if
13:   end for
14:   Offspring ← Offspring ∪ {Best}
15: end for
16: return Offspring
```

algorithm (line 14).

5.3.2.2 Informed Operators

The Pareto-SVM algorithm uses the ASM to yield *informed operators* [Rasheed and Hirsh, 2000]. Upon calling a variation operator, λ_{Pre} *pre-children* are generated and ordered according to their quality estimate on $\hat{f}$; a probabilistic selection attached

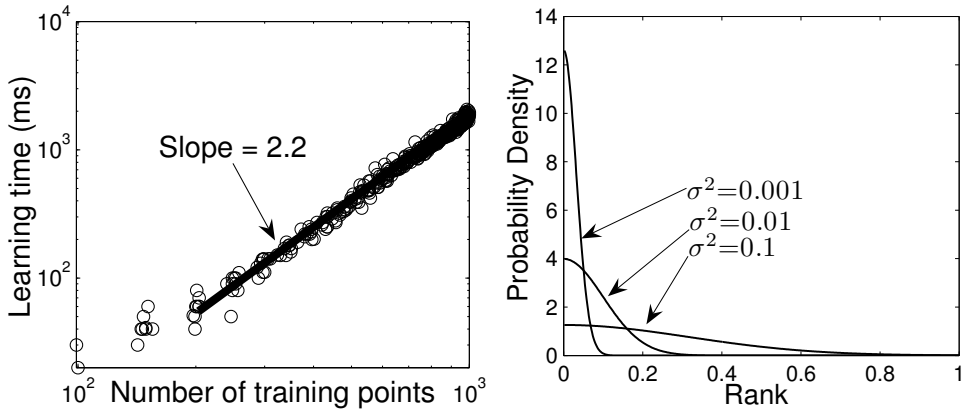

Figure 5.4: **Left**: Learning time of the proposed dominance-based RASM on ZDT1 function. **Right**: Mapping the ranks of pre-children to a normal distribution.

to the offspring indices is achieved, using a normal distribution with variance σ^2_{sel} (Figure 5.4-**Right**). Granted that the number of offspring is sufficiently large, parameter σ^2_{sel} thus controls the selection pressure and the exploration vs exploitation trade-off. However we use at the moment a small value $\sigma^2_{sel} = 0.001$ for the normal distribution for the ranked point to be chosen (Figure 5.4-**Right**) to simulate the situation when new offspring always has the first rank.

An additional difficulty is raised in the multi-objective context, as a better surrogate value does not imply a smaller distance from the Pareto set. Quite the contrary, a child that is far from its parent can have a better ASM value than its parent while being nevertheless farthest from the Pareto front than some other points, because of the errors in the surrogate model, and/or the ϵ tolerance in the ASM and RASM formulations. In order to handle this issue, confirmed from preliminary experiments, the pre-children filtering is based on their ASM gain with respect to the closest point in the current Pareto set.

Formally, Algorithm 5.6 describes how all offspring are generated from the current parent population. For each offspring to be generated (outer loop, lines 2 to 15), a variation operator is chosen (line 3) if more than one are available (depending on the type of MOEA) and applied λ_{Pre} times (line 6). To each pre-child thus obtained, is associated its nearest neighbor among current non-dominated parents (line 7), and the ASM improvement of the pre-child compared to its nearest neighbor determines whether the pre-child is kept (line 9). An example for $\lambda_{Pre} = 3$ is shown in Figure 5.3-**Right**.

5.4 Experimental Validation

5.4.1 Experimental Setting

Two state-of-the-art EMOA algorithms are considered: (100+100)-NSGA-II (see Section 2.4.3) and $100 \times (1+1)$-MO-CMA-ES (see Section 2.4.4). Both algorithms use the hypervolume indicator as second-level sorting criterion to rank individuals on the same level of non-dominance.

The PARETO-SVM approach is assessed by comparing the original algorithms with their ASM and RASM enhanced versions, considering the widely used ZDT1:3-6 [Zitzler *et al.*, 2000] and their rotated variants IHR1:3-6 [Igel *et al.*, 2007b] benchmark problems. The dimension is set to 30 (resp. to 10) for ZDT1-3 problems (resp. for all other problems). As the true Pareto front of all ZDT problems lies on the boundary of the decision space, and for the sake of an unbiased assessment (to prevent MO-CMA-ES from exploiting this specificity), the penalization term is set to $\alpha = 1$ instead of the original 10^{-6} [Igel *et al.*, 2007b] (see Section 6.2.2.2 for a discussion).

Both ASM and RASM are based on the RBF kernel, where the bandwidth σ is set as the average distance between all pairs of training points. The SVM penalization constant C is set to 1000 after few preliminary experiments.

The training set $\mathcal{D}$ that is used at each generation to build the RASM model is an archive that contains at most $N_{archive} = 1000$ points. The current population is added to the archive at each generation. When this archive gets larger than $N_{archive}$, it is pruned by removing the worst individuals after non-dominated sorting. Furthermore, in order to improve the diversity of the training set (many points too close together can lead to poor surrogate model), an additional filtering procedure is applied to the archive. The 2-objective space has been divided into 100×100 boxes, and at most one point among the archived non-dominated points of each box is retained in the archive (see Figure 5.3).

The parameters of ASM models have been calibrated using a few preliminary experiments (their automatic tuning will be considered in further work):

ASM The allowed deviation ϵ of non-dominated points on $\hat{f}$ is set to 10^{-5}. The ASM learning was stopped after 300,000 iterations, corresponding to circa 0.5 – 1.0 sec. on a 2.26 GHz processor for ZDT1.

RASM As detailed in Section 5.2, RASM maintains the set Ω_{active} of active constraints, initialized to the set of primary dominance constraints. After an initial round of $N_{IterActive} = 1000\,|\Omega_{active}|$ iterations, Ω_{active} is incrementally enriched every $N_{IterPerPassive} = 10\,|\Omega_{active}|$ iterations with the most violated constraint among the secondary dominance constraints, until a total of at most $N_{ConstrToAdd} = 0.1\,|\Omega_{active}|$ secondary the most violated constraints have been added.

The $\hat{f}$ update frequency K_{learn} is set to 10. The ASM-enhanced operators were computed as described in Algorithm 5.4. In the MO-CMA-ES case, in order to introduce an additional diversity, the global mutation step size of pre-selected offspring was modified to $\sigma' = \sigma \exp^{(-d+2dk)}$ where $d = 0.7$ and k is uniformly distributed in $[0, 1]$.

5.4.2 Performance Measures

Many ways of measuring the performance of EMO algorithms have been proposed. After [Knowles *et al.*, 2006], this study uses Pareto-compliant quality indicators, more particularly the widely used hypervolume indicator I_H. Let P be a μ-size approximation of Pareto front and let P^* be the approximate μ-optimal distribution of optimal Pareto points [Auger *et al.*, 2009]. Several algorithms proposed in [Auger *et al.*, 2009] can be used for approximation of μ-optimal distribution. The approximation error of the Pareto front is defined by $\Delta H(P^*, P) = I_H(P^*) - I_H(P)$. All reported results are averaged over 10 independent runs with at most 100,000 fitness evaluations.

In the case of IHR problems, the arbitrary rotation matrix $\mathbf{O} \in \mathbb{R}^{n \times n}$ must be fixed.

5.4.3 Model Validation

The goal of the first experiments is to empirically evaluate the accuracy of ASM and RASM models.

5.4.3.1 ASM model

In order to evaluate its accuracy on ZDT1 and IHR1 problems, the ASM model was trained using calibrated training data set A: 20000 points were generated at a given distance from the (known) nearly-optimal Pareto points, and non-dominated sorting was applied to rank those points. Front $ndom_1(A)$ denotes the closest front from the true Pareto front, $ndom_2(A)$ denotes the second one and so forth.

Figure 5.5 illustrates the distribution of $\hat{f}$ values for training and test data in decision and objective spaces, where the training set respectively includes $ndom_{80}(A)$ and $ndom_{100}(A)$ as non-dominated and dominated points. As shown in Figure 5.5, $\hat{f}$ correctly approximates the Pareto-dominance in the sense that for all k, $\hat{f}(ndom_k(A)) > \hat{f}(ndom_{k+20}(A))$ on average.

As seen for the IHR1 problem, although the $\hat{f}$ value usually lies in an ϵ-width tube for training Pareto points, the new Pareto front may be non-linear. This behavior is quite normal when we deal with difficult problems. It may lead to premature convergence if we use very selective $\hat{f}$ -based filter (λ_{Pre} is large), as high $\hat{f}$-based selection pressure may accelerate the exploration of the prospective regions of Pareto front and entail some loss of diversity. Note that, as Pareto-SVM was devised to speed up the EMOA convergence and does not specifically take into account the Pareto diversity, it may be inefficient with regard to the approximation of the μ-optimal distribution of nearly-optimal Pareto points.

As mentioned in the introduction, the ASM problem is over-constrained as all Pareto points must be mapped on a narrow interval $]\rho - \epsilon, \rho + \epsilon[$; in such cases, it results in a poor generalization error of the ASM (visible, e.g., from its errors on the rest of the Pareto archive). This problem was fixed using an additional k factor, replacing ρ by $k\rho$ in Eq. (5.1). The best k value w.r.t. the ASM generalization error was determined in original algorithm from a preliminary trial, leading to $k = 1$ for one set of problems and $k = -1$

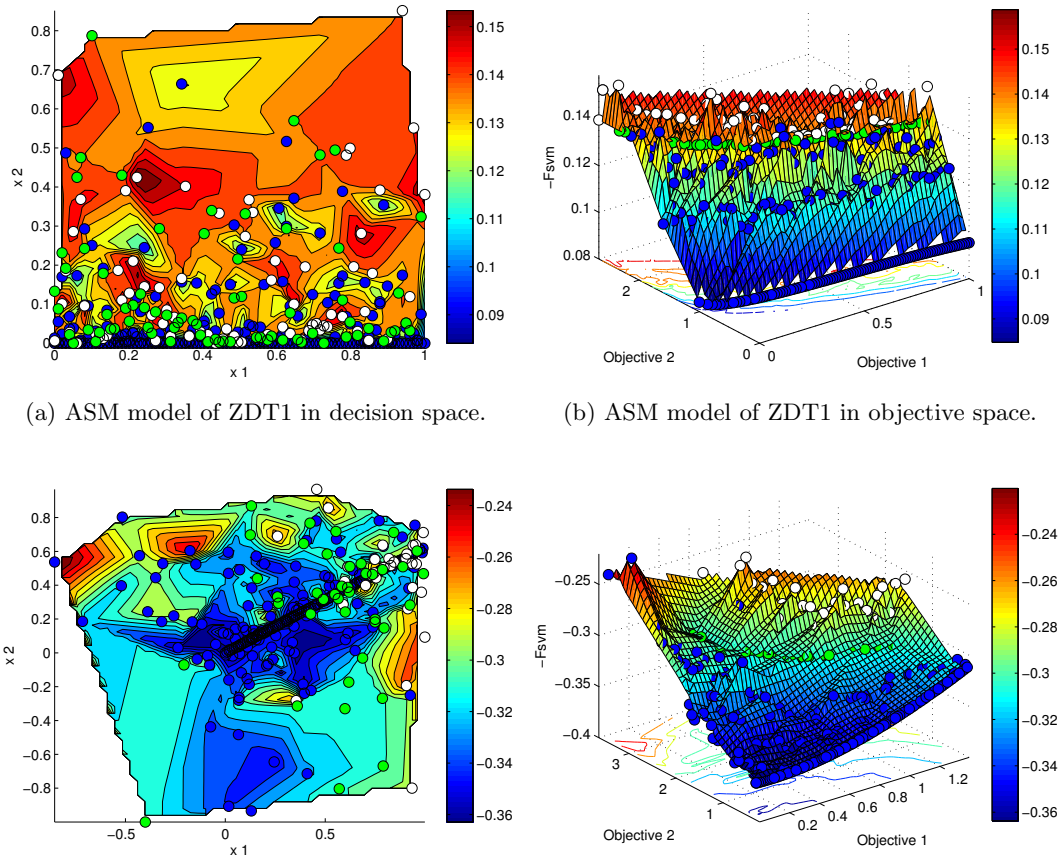

(a) ASM model of ZDT1 in decision space.

(b) ASM model of ZDT1 in objective space.

(c) ASM model of IHR1 in decision space.

(d) ASM model of IHR1 in objective space.

Figure 5.5: ASM model for 30-dimensional ZDT1 and IHR1 problems.Non-dominated fronts $ndom_{80}(A)$ (white circles) $\prec ndom_{100}(A)$ (green circles) form the training data, while $ndom_k(A)$ (blue circles) for $k < 80$ represent the test data. See text for details.

for another set. Probably, a better solution is to reformulate Eq. (5.1) as follows:

$$\underset{\{w,\, \xi^{(*)},\, \rho\}}{\text{Minimize}}\ \frac{1}{2}||w||^2 + C\sum_{i=1}^{\ell}(\xi_i^{up} + \xi_i^{low}) + C\sum_{i=\ell+1}^{m}\xi_i^{up} + \frac{1}{2}D\rho^2$$

In the new formulation, D is an additional problem-dependent parameter, which in some sense makes the learning problem harder. On-going work aims at understanding this phenomenon +/-ρ, and relating it to the structure of the multi-objective landscape.

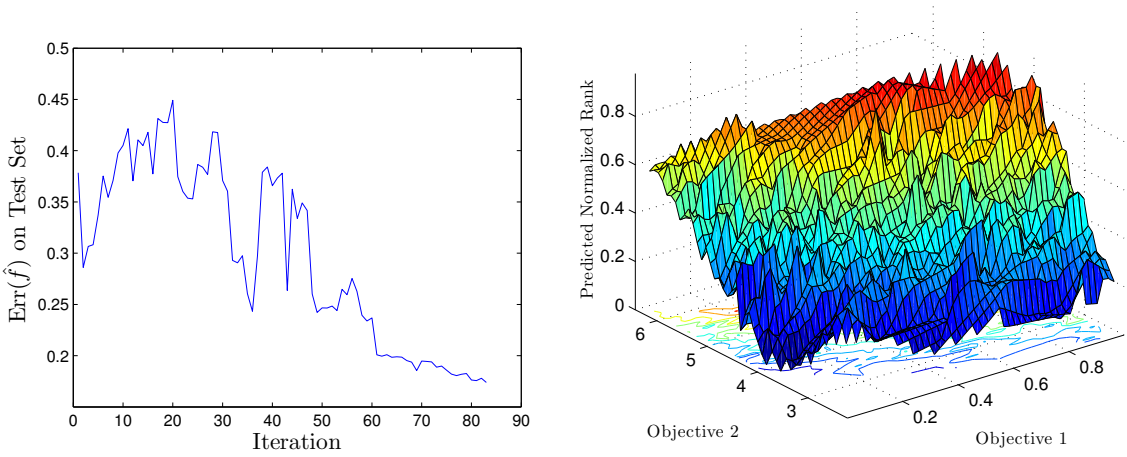

Figure 5.6: **Left**: at each iteration of RASM model learning procedure the most violated *secondary* constraint is added and model quality $\hat{f}$ is estimated on 1000 test points. **Right**: normalized Pareto rank predicted by RASM model for 1000 test points on 30-dimensional ZDT1 functions.

5.4.3.2 RASM model

Some experiments are first conducted to estimate the complexity of RASM model training on 30-dimensional ZDT1 problem. The empirical complexity with respect to the number of training points is circa 2.2 (slope in Figure 5.4-**Left** in log scale). The fact that the complexity is super-quadratic is not surprising since the computational complexity of SMO optimization procedure is quadratic in number of constraints and the number of constraints is up to 10% larger than the number of training points. The complexity however remains bounded as the size of the training set (extracted from the archive) is less than 1,000, limiting *de facto* the computational cost of the RASM learning.

Figure 5.6-**Left** shows RASM model learning for 30-dimensional ZDT1 problem using 500 training points, uniformly randomly generated in $[0, 1]^{30}$ search space. We sorted all training points using non-dominated sorting procedure and filled the sets of primary and secondary constraints as described in Section 5.2.2. After the initial learning of RASM model with primary constraints, we iteratively add the most violated secondary constraint and continue to learn the model. Figure 5.6-**Left** shows that the model error estimated at each iteration on 1000 (hidden from the learning part) test points decreases. The learning stops when the most violated constraint does not violate preference relations anymore. In the following we limit the number of the most violated constraints to be added by 10% of the number of primary constraints (e.g., would be 50 the most violated constraint for this example). Figure 5.6-**Right** shows normalized Pareto Rank, predicted by RASM model. The prediction, indeed, is not perfect but seems to be suitable to direct the search toward the Pareto front.

5.4.4 Benchmarking of ASM and RASM assisted MOEAs

The second set of experiments investigates the effect of using ASM and RASM model within existing MOEAs on different benchmark functions.

The first experiments with ASM and RASM-based MOEAs show that Pareto-SVM indeed speeds up both *S*-NSGA-II and MO-CMA-ES on most problems. Figure 5.7 shows the on-line behavior of the algorithms for ZDT1 and IHR1 with ASM models (the results for RASM are quite similar).

For the ZDT1 problem, the optimal Pareto front is linear and lies on the boundary of the decision space. Therefore, dominated points often lie at the decision space center, while Pareto points go toward the boundary, making the ASM model fairly simple: the One-Class SVM for dominated points covers the internal region of the decision space, while a small subspace of the Pareto points is covered by SVM-Regression with a given ϵ value.

ASM-based *S*-NSGA-II (*ASM*-NSGA) works nearly 1.5 times faster with $\lambda_{Pre} = 2$ and more than 2 times faster with $\lambda_{Pre} = 10$ than the original version with regard to the ΔH value and the number of function evaluations. The value $\Delta H = 0.001$ for ZDT problems corresponds to the situation when all points are non-dominated.

The IHR problems, rotated variants of ZDT problems, are non-separable and thus significantly more difficult for the MOEAs with variation operators which use separability. The Pareto set of IHR1 for a given rotation matrix is shown in Figure 5.5-c. The MO-CMA-ES inherits invariance properties from the CMA-ES (though the hypervolume indicator is not invariant w.r.t. rank-preserving transformations of objectives, the invariance can be achieved by an approach described in Section 6.4.3), therefore it is also efficient on these rotated problems, while *S*-NSGA-II can approximate only a small part of optimal Pareto front which corresponds to the center of decision space.

The variance of results on ZDT1 problem is small because this problem is very simple for surrogate modeling and even if some premature convergence initially leads to sample only a small part of the Pareto set, the algorithm quickly explores the rest of the set thanks to separability. On rotated IHR1 problem, such quick moving is difficult, hence the higher variance of results which corresponds to slowly moving along the Pareto front. A high selection pressure also accelerates this effect.

Both MO-CMA-ES and *S*-NSGA-II only approximate a small part of the Pareto front of IHR1 in first generations, but in contrast to *S*-NSGA-II, MO-CMA-ES can gradually approximate the whole front. This can be seen clearly in Figure 5.7-b, witnessed by the flat line between 10000 and 40000 evaluations. In this case, while the ASM model helps MO-CMA-ES to converge faster to the Pareto front, it can not give any preference to the extreme points which in fact help to move along the Pareto front.

This observation sustains the idea that quality indicators should probably be taken into account during the ASM learning. The hypervolume indicator may provide useful additional information, especially because extreme points usually have the highest importance. Also, hypervolume or epsilon indicators are well suited for many-objective optimization, when most points are non-dominated.

Table 5.1 shows the comparative results of all baselines, ASM and RASM-based EMOs; in the latter cases, both $\lambda_{Pre} = 2$ and $\lambda_{Pre} = 10$ pre-offspring are considered. Different

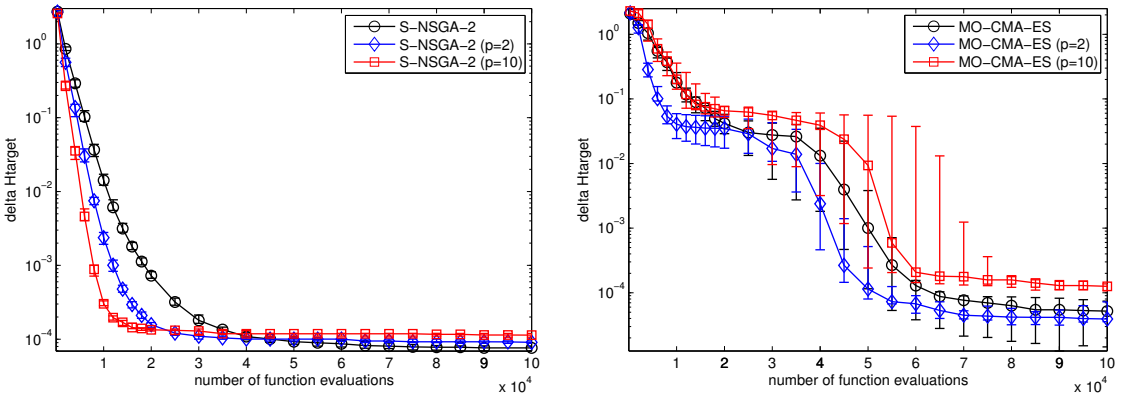

Figure 5.7: On-line performances of original and ASM-informed *S*-NSGA-II on ZDT1 (left) and MO-CMA-ES on IHR1 (right) problems with different values of number of pre-children $p = \lambda_{Pre}$. Error bars indicate the 20% and 80% percentiles (almost indistinguishable for ZDT1).

target values for ΔH have been set, and the number of evaluation needed to reach those values are reported - normalized by the smallest value of the table (recalled on the top row, legend "Best"). Hence 1 indicates the best result, while e.g., 2 indicates that this algorithm needed twice the number of evaluations of the best algorithm to reach the target ΔH value. These results first confirm that *S*-NSGA-II performs best on separable functions ZDTx and *MO*-CMA-ES on non-separable functions IHRx. They also show that both *RASM*-NSGA and *RASM*-MO-CMA work nearly 1.5 times faster with $\lambda_{Pre} = 2$ and more than 2 times faster with $\lambda_{Pre} = 10$ than the baseline versions with regards to the ΔH value and the number of function evaluations.

ASM-NSGA and *RASM*-NSGA yield comparable performances. A more thorough analysis shows that *RASM*-MO-CMA is usually faster at the beginning (up to 10000-15000 function evaluations) though it might suffer from a premature convergence thereafter: experiments on concave IHR2 (and to some extent, also on ZDT2) show that *RASM*-MO-CMA converges to the value $\Delta H = 0.1$ nearly 1.5 times faster than with ASM model, and fails to go further. This failure is blamed on the fact that the diversity of the population is hardly preserved; a small part of the optimal Pareto front is sampled. A general trend is observed, that increasing the selection pressure leads to a faster convergence. However, increasing the number of pre-children can also lead to premature convergence, like for MO-CMA-ES on IHR problems with $\lambda_{Pre} = 10$. This happens because the filter prefers the points which are possibly better than their parents according to $\hat{f}$ though they might be farther from the true Pareto front than other parents. The comparison of the pre-children with the closest parent in decision space (Algorithm 5.6, line 7) addresses this drawback to some extent. Indeed, RASM learning and the RASM-based offspring selection only aim at speeding up the convergence; further work will be required to extend the approach and

approximate the μ-optimal distribution of nearly-optimal Pareto points.

Table 5.1: Comparative results of two baseline EMOAs, namely *S*-NSGA-II and *MO*-CMA-ES and their ASM and RASM variants. Median number of function evaluations (out of 10 independent runs) to reach ΔHtarget values, normalized by Best: a value of 1 indicates the best result, a value $X > 1$ indicates that the corresponding algorithm needed X times more evaluations than the best to reach the same precision.

ΔHtarget	1	0.1	0.01	1e-3	1e-4	1	0.1	0.01	1e-3	1e-4
			ZDT1					ZDT2		
Best	1100	3000	5300	7800	38800	1400	4200	6600	8500	32700
S-NSGA-II	1.6	2	2	2.3	1.1	1.8	1.7	1.8	2.3	1.2
ASM-NSGA λ_{Pre}=2	1.2	1.5	1.4	1.5	1.5	1.2	1.2	1.2	1.4	**1**
ASM-NSGA λ_{Pre}=10	**1**	**1**	**1**	**1**	.	**1**	**1**	**1**	**1**	.
RASM-NSGA λ_{Pre}=2	1.2	1.4	1.4	1.6	**1**	1.3	1.2	1.2	1.5	**1**
RASM-NSGA λ_{Pre}=10	**1**	1.1	1.1	1.5	.	1.1	**1**	**1**	1.2	.
MO-CMA-ES	16.5	14.4	12.3	11.3	.	14.7	10.7	10	10.1	.
ASM-MO-CMA λ_{Pre}=2	6.8	8.5	8.3	8	.	5.9	8.2	7.7	7.5	.
ASM-MO-CMA λ_{Pre}=10	6.9	10.1	10.4	12.1	.	5	.	.	.	.
RASM-MO-CMA λ_{Pre}=2	5.1	7.7	7.6	7.4	.	5.2	.	.	.	.
RASM-MO-CMA λ_{Pre}=10	3.6	4.3	4.9	7.2	.	3.2	.	.	.	.
			ZDT3					ZDT6		
Best	1300	3500	7100	10100	15200	2500	3600	5200	12300	.
S-NSGA-II	1.4	1.9	1.6	1.9	2.2	2.1	3.4	3.8	2.7	.
ASM-NSGA λ_{Pre}=2	1.1	1.3	1.1	1.2	1.3	1.4	2.4	2.6	2	.
ASM-NSGA λ_{Pre}=10	**1**	**1**	**1**	**1**	**1**	1.1	1.8	2.3	2.3	.
RASM-NSGA λ_{Pre}=2	1.1	1.3	1.2	1.4	1.6	1.5	2.4	2.8	2.1	.
RASM-NSGA λ_{Pre}=10	**1**	1.1	1.1	2	.	1.4	2	2.3	1.8	.
MO-CMA-ES	15.4	17.8	.	.	.	2.5	2.6	2.5	2	.
ASM-MO-CMA λ_{Pre}=2	9	.	.	.	.	1.1	1.2	1.1	**1**	.
ASM-MO-CMA λ_{Pre}=10	8	25.6	.	.	.	**1**	1.1	1.3	2.5	.
RASM-MO-CMA λ_{Pre}=2	8.5	.	.	.	.	1.5	1.2	1.2	**1**	.
RASM-MO-CMA λ_{Pre}=10	8.1	.	.	.	.	**1**	**1**	**1**	1.6	.
			IHR1					IHR2		
Best	500	2000	35300	41200	50300	1700	7000	12900	52900	.
S-NSGA-II	1.6	1.5	.	.	.	1.1	3.2	6.2	.	.
ASM-NSGA λ_{Pre}=2	1.2	1.3	.	.	.	**1**	3.9	4.9	.	.
ASM-NSGA λ_{Pre}=10	**1**	1.5	.	.	.	1.4	6.4	4.6	.	.
RASM-NSGA λ_{Pre}=2	1.2	1.2	.	.	.	1.5	.	.	.	.
RASM-NSGA λ_{Pre}=10	**1**	**1**	.	.	.	1.2	5.1	4.8	.	.
MO-CMA-ES	8.2	6.5	1.1	1.2	1.2	5.8	2.7	2.1	**1**	.
ASM-MO-CMA λ_{Pre}=2	4.6	2.9	**1**	**1**	**1**	3.1	1.6	1.4	1.1	.
ASM-MO-CMA λ_{Pre}=10	9.2	6.1	1.3	1.2	.	5.9	2.6	2.4	.	.
RASM-MO-CMA λ_{Pre}=2	2.6	2.3	2.4	2.1	.	2.2	**1**	**1**	.	.
RASM-MO-CMA λ_{Pre}=10	1.8	1.9	.	.	.	.	.	.	.	.
			IHR3					IHR6		
Best	800	.	.	.	.	.	16500	.	.	.	.
S-NSGA-II	1.5	.	.	.	.	5.4	.	.	.	.
ASM-NSGA λ_{Pre}=2	1.1	.	.	.	.	3.8	.	.	.	.
ASM-NSGA λ_{Pre}=10	**1**	.	.	.	.	.	.	.	.	.
RASM-NSGA λ_{Pre}=2	1.3	.	.	.	.	2.2	.	.	.	.
RASM-NSGA λ_{Pre}=10	1.1	.	.	.	.	2.6	.	.	.	.
MO-CMA-ES	9.6	.	.	.	.	2	.	.	.	.
ASM-MO-CMA λ_{Pre}=2	7.2	.	.	.	.	2	.	.	.	.
ASM-MO-CMA λ_{Pre}=10	12.1	.	.	.	.	.	.	.	.	.
RASM-MO-CMA λ_{Pre}=2	3.3	.	.	.	.	**1**	.	.	.	.
RASM-MO-CMA λ_{Pre}=10	2.6	.	.	.	.	**1**	.	.	.	.

5.5 Discussion

In this Chapter, we investigated two Aggregated Surrogate Models, ASM and RASM, for surrogate-assisted multi-objective optimization with pre-selection of promising offspring.

The original ASM model is built by combining One-class and regression SVMs; thanks to the non-linear kernel, ASM can be learned efficiently in non-linear functional spaces. ASM learning problem, however, was found to be over-constrained; in such cases, it results in a poor generalization error. In contrast, using a *Learning to Rank* framework in RASM, the resulting surrogate model does not require that all Pareto points are mapped onto the same value. It is thus both more constrained in the dominated region, and less constrained on the Pareto front, than ASM.

Furthermore, RASM approach opens new and interesting perspectives for real world multi-objective problems, enabling for instance to account for the user's preferences in a flexible way by simply adding user-defined constraints to the order-based SVM formulation. Most importantly, the rank constraint formalization enables to accommodate conflicting preferences: to the best of our knowledge, this corresponds to a significant advance on the state of the art.

The experimental validation of the proposed approach shows that RASM-EMO usually converges faster than ASM-EMO, with the caveat that it sometimes leads to premature convergence (e.g., on ZDT2 and IHR2 problems). This premature convergence was blamed on the selection pressure and the adjustment of parameter σ^2_{sel}. A further work will explore the adjustment of σ^2_{sel} and λ_{Pre} depending on the model error $\hat{f}$ in a similar way to $\hat{n}$ in the case of single-objective surrogate-assisted optimization (see Section 4.3.1.3).

It is emphasized that RASM might incorporate additional specific constraints in each generation. Some possible constraints are described in Figure 5.2-Right: such **non-dominance** constraints involved points on the current Pareto front, and include inequality constraints from the extremal points over their neighbors (continuous arrows), and equality constraints for all neighbor pairs on the Pareto front (continuous double arrow), as well as between extremal points (dotted double arrows). Along the same lines, constraints could be weighted, e.g., the weight of constraints related to points with the largest hypervolume contributions can be increased online. We already tested several strategies for primary and secondary constraints selection and found that the following simple strategy for primary constraints selection often shows better results: select a pair (a, b) with probability p (e.g., 10%) if $\boldsymbol{x}_b$ is located in the following Pareto front to the front of $\boldsymbol{x}_a$. The main drawback of this strategy is its computational complexity which is growing faster than for the proposed in this Chapter approach due to usually larger number of constraints needed to learn the model. However, the strategy seems to be prospective and should be further investigated.

Historically, most of the work presented in this Chapter was done in 2009 and 2010, before the introduction of surrogate model control and hyper-parameters adaptation for single-objective surrogate-assisted optimization in Chapter 4. Thus, the extension of these approaches to the multi-objective case will be in the focus of future research. Preliminary results for direct optimization of SVR-based surrogate models (one model per objective)

and an analysis of offline tuning of $\hat{n}$ are presented in [Yagoubi, 2012], where NSGA-II surrogate-assisted algorithm was successfully applied for real-world multi-objective optimization of Diesel combustion. [Pilát and Neruda, 2011] proposed Multiobjective Memetic Algorithm with Aggregate Surrogate Model (ASM-MOMA), where ASM model is used for direct local optimization and the best found individual during the optimization is placed back to the population. The authors combine direct optimization with pre-selection in [Pilát and Neruda, 2012] and suggest to use Evolution Strategy for ASM model optimization. The speedup between a factor of 2 and 10 is reported for optimization of ZDT problems. Thus, the question whether individual surrogates per objective or ASM models are better for surrogate-assisted search remains open. The answer on this question may become clearer when self-adaptation mechanisms investigated in Chapter 4 will be translated to the multi-objective case and assessed on a rich set of benchmark problems, organized in a kind of BBOB for multi-objective optimization.

Chapter 6

Exploring new frontiers using CMA-like algorithms

In this Chapter, we explore and expand frontiers of the Evolutionary Computation domain, and CMA-ES in particular, motivated by pure curiosity and answering questions, which have arisen in the exploitation part of the thesis in Chapters 4, 5. The discussed questions and corresponding approaches are presented in chronological order.

In Chapter 3 (see Section 4.2.1), we showed that the use of the decorrelated coordinate system, provided by the covariance matrix of CMA-ES, may drastically improve the results of surrogate-assisted CMA-ES on non-separable and ill-conditioned functions. Given the fact that CMA-ES can be viewed as CSA-ES performing in this decorrelated space [Hansen, 2008], we wondered whether there is a simpler algorithm which is competitive to CSA-ES in this space? As candidate algorithm we take one of the simplest derivative-free optimizer, Coordinate Descent method, and combine it with the Adaptive Encoding procedure proposed in [Hansen, 2008] to design Adaptive Coordinate Descent (ACiD), a method, which has a competitive performance to CMA-ES on unimodal functions and, to the best of our knowledge, is the only linear time algorithm with a reasonably good performance on non-separable ill-conditioned problems. This algorithm is investigated in Section 6.1. Some of the results have been published in [Loshchilov *et al.*, 2011a].

In Chapter 5, we observed that the multi-objective optimization may significantly slow down when only few individuals of the population are able to improve the current Pareto front approximation. This is the case for IHR1 problem (see Figure 5.7), where a sub-part of the Pareto front can be relatively quickly found, while the rest of the front is approximated slowly and substantially thanks to the extreme (right) point in the objective space which generates new (hopefully) extreme point. We wondered whether there is a way to improve the search allowing the most successful individuals to generate offspring more often? To answer this question we introduce *reward-based* parent selection schemes for multi-objective optimization in Section 6.2 and demonstrate that a significant speedup can be obtained by carefully looking at the dynamic of successful individuals. Some of the results have been published in [Loshchilov *et al.*, 2011b].

In our recent experiments with ^{s*}aACM-ES in Chapter 4 we found that the speedup obtained on multi-modal functions is much less significant than on unimodal ones. This is mainly due to the difficulty to learn the landscapes of these functions, which typically require a very large number of training points. The latter requirement is usually difficult to satisfy because i). we simply do not have enough training points around the actual region of search, and ii). the computational complexity of learning grows quickly (usually quadratically) with the number of training points, given that the runtime is usually very

large on multi-modal functions. In this case, rather than build computationally expensive surrogate models, it might be reasonable to look at alternative restart strategies for CMA-ES to improve the search without any increase of the computational cost. We address this idea in Section 6.3, where we propose two new alternatives to the original IPOP and BIPOP restart strategies, that have also been published in [Loshchilov *et al.*, 2012a, Loshchilov *et al.*, 2012d].

In Section 6.4, we briefly discuss other prospective approaches that we investigated during the thesis. Finally, Section 6.5 concludes the Chapter and presents some perspectives for further research.

6.1 Adaptive Coordinate Descent

Independence from the coordinate system is one source of efficiency and robustness for the Covariance Matrix Adaptation Evolution Strategy (CMA-ES). The recently proposed Adaptive Encoding (AE) [Hansen, 2008] procedure generalizes CMA-ES adaptive mechanism, and can be used together with any optimization algorithm. Adaptive Encoding gradually builds a transformation of the coordinate system such that the new coordinates are as decorrelated as possible with respect to the objective function. But any optimization algorithm can then be used together with Adaptive Encoding, and this Section proposes to use one of the simplest of all, that uses a dichotomy procedure on each coordinate in turn. The resulting algorithm, termed Adaptive Coordinate Descent (ACiD), is analyzed on the Sphere function, and experimentally validated on BBOB testbed where it is shown to outperform the standard $(1 + 1)$-CMA-ES, and is found comparable to other state-of-the-art CMA-ES variants on unimodal functions.

In this Section, we present an extended version of ACiD, originally published in [Loshchilov *et al.*, 2011a], with a more detailed discussion of i). Adaptive Encoding parametrization in Section 6.1.3.1; ii). extension to noisy optimization in Section 6.1.3.5; iii). extension to large-scale optimization in Section 6.1.3.6.

6.1.1 Introduction

Separable continuous optimization problems are problems in which the objective function can be optimized coordinate-wise. Finding the global optimum of a separable function in $\mathbb{R}^n$ amounts to perform n simple *line searches* along each of the n coordinates. Unfortunately, interesting problems are usually not separable. Nevertheless, many optimization methods implicitly assume some form of separability of the objective function, or at least are much more efficient on separable functions as they explicitly use the coordinate system in their search. A well-known exception is the CMA-ES that performs a rotation-invariant search, and is thus independent of any coordinate system. The basic idea of CMA-ES is to evolve, besides a population of solutions to the optimization problem at hand, a "Covariance Matrix" that can be viewed as a coordinate transform: in case of a quadratic objective function, CMA-ES Covariance Matrix has been empirically demonstrated to gradually converge to a matrix which is proportional to the inverse Hessian matrix of the objective function. In the coordinate system defined by this inverse Hessian, the quadratic

objective function has become separable, and the optimization problem, almost trivial. Of course, CMA-ES covariance matrix is only, in the quadratic case, an approximation of the inverse Hessian. And many interesting problems are not quadratic indeed (and if they were, they would be easy to solve directly). Nevertheless, twice continuously differentiable objective functions can be viewed as close-to-quadratic around their optima (local or global), and adapting the coordinate system with respect to the "cumulative path" of the search makes it easier and faster to find the optimum.

The basic principles of this adaptive coordinate transformation have been generalized to general search strategies, under the name of *Adaptive Encoding* in [Hansen, 2008], and experimented with Cauchy mutations in a stochastic search framework. The original Cauchy-based ES is heavily coordinate-dependent, and its results deteriorate when the degree of non-separability of the objective function increases. However, this limitation of Cauchy mutation almost vanishes with Adaptive Encoding, demonstrating the usefulness of a well-designed adaptive coordinate system.

Putting things together, a natural idea is then to couple with Adaptive Encoding some simple optimization method, i.e., some successive coordinate-wise line searches: coordinate line-searches only work well for separable functions, but Adaptive Encoding should gradually lead the search toward a transformed coordinate system where the objective function resembles more a separable function than in the original system, paving the road for the coordinate line-searches. Though the resulting algorithm has little to do with Evolutionary Computation, it heavily relies on Adaptive Encoding, the backbone of CMA-ES algorithms. The idea of adapting the coordinate system during the search can be attributed to the famous Rosenbrock's method [Rosenbrock, 1960].

This Section is organized the following way: Section 6.1.2 first introduces the algorithmic background, namely Adaptive Encoding and some Coordinate Descent Method, before detailing their coupling into the Adaptive Coordinate Descent algorithm. Section 6.1.3 presents the experiments that validate Adaptive Coordinate Descent first on the Sphere function, the well-known separable test function, establishing performance bounds for the proposed approach. Extensive experiments on the BBOB testbed are then presented and discussed. Finally, Section 6.1.4 concludes the Section and sketches directions for further research.

6.1.2 Algorithms

6.1.2.1 Adaptive Encoding

Though historically introduced as a derandomization of self-adaptive Evolution Strategies [Hansen *et al.*, 2003], CMA-ES was only recently revisited as a hybrid between some ES with adaptive step-size and some *Adaptive Encoding* (AE) procedure [Hansen, 2008]. AE can be applied to any continuous domain search algorithm, in order to make it independent from any given coordinate system. As a result, some search algorithms that performed rather poorly on non-separable functions can be tremendously boosted (e.g., by a factor up to 3 orders of magnitude for Evolution Strategy with Cauchy mutation [Hansen, 2008]).

An iteration of CMA-ES, decomposed into Adaptive Encoding and Evolution Strategy

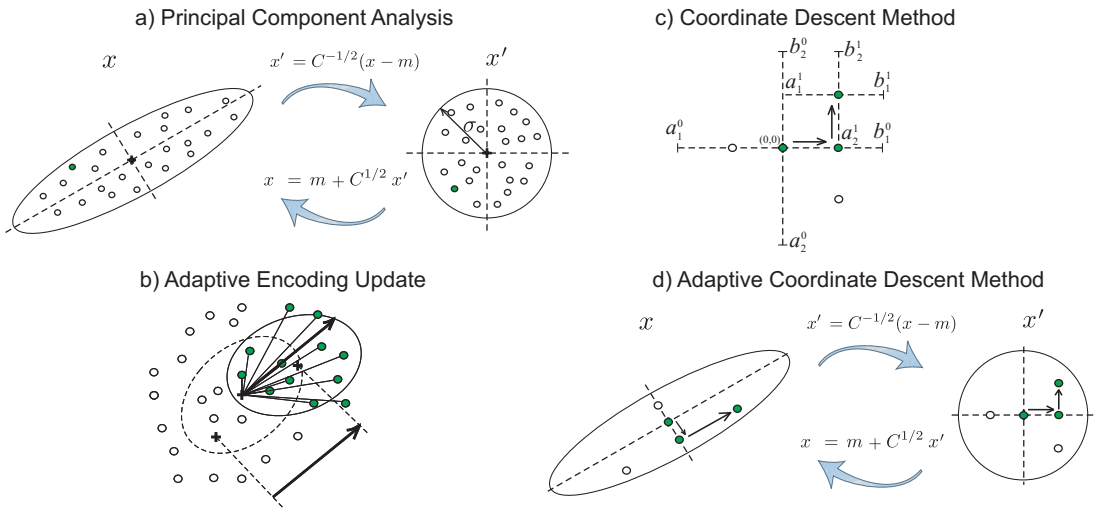

Figure 6.1: AE_{CMA}-like Adaptive Encoding Update (**b**) mostly based on Principal Component Analysis (**a**) is used to extend some Coordinate Descent method (**c**) to the optimization of non-separable problems (**d**). See text for details.

Algorithm 6.1: CMA-ES = Adaptive Encoding + ES

1: $\boldsymbol{x}_i \leftarrow m + \sigma\mathcal{N}_i(0, \boldsymbol{I})$, for $i = 1 \ldots \lambda$
2: $f_i \leftarrow f(\mathbf{B}\boldsymbol{x}_i)$, for $i = 1 \ldots \lambda$
3: **if** Evolution Strategy (ES) with 1/5th success rule **then**
4: $\quad \sigma \leftarrow \sigma\, \boldsymbol{exp}^{\propto(\frac{\texttt{success rate}}{\texttt{expected success rate}} - 1)}$
5: **end if**
6: **if** Cumulative Step-Size Adaptation ES (CSA-ES) **then**
7: $\quad \sigma \leftarrow \sigma\, \boldsymbol{exp}^{\propto(\frac{\|\texttt{evolution path}\|}{\|\texttt{expected evolution path}\|} - 1)}$
8: **end if**
9: $\mathbf{B} \leftarrow$AdaptiveEncoding$(\mathbf{B}\boldsymbol{x}_1, \ldots, \mathbf{B}\boldsymbol{x}_\mu)$

with step-size adaptation, is described in Algorithm 6.1. In standard Evolution Strategy, λ offspring are sampled (line 1) from a normal distribution with step-size σ and mean $\boldsymbol{m}$, where $\boldsymbol{m}$ is the centroid of best μ individuals of the previous iteration. The λ offspring are evaluated (line 2 with $\mathbf{B} = \boldsymbol{I}$ the identity matrix). Depending on the choice of the step-size adaptation rule, the step-size is then adapted, either by some rule similar to the one-fifth rule [Rechenberg, 1973] (line 4), or using the Cumulative Step-size Adaptation [Hansen and Ostermeier, 1996] (line 7).

CMA-ES differs from standard ES on lines 2 and 9, that describe the use of the Adaptive Encoding procedure. CMA-ES maintains a coordinate system transformation matrix $\boldsymbol{B}$, and though it evaluates the individuals in the original coordinate system of $\mathbb{R}^n$ (line 2), it generates the offspring, using some isotropic normal distribution, in some transformed

coordinate system (line 1). The $n \times n$ matrix $\boldsymbol{B}$ is the matrix of the transformation. In Algorithm 6.1, offspring $\boldsymbol{x}_i$ are represented in this transformed coordinate system, and $\boldsymbol{B}\boldsymbol{x}_i$ are their images in the original coordinate system. Matrix $\boldsymbol{B}$ is iteratively adapted by the AE procedure using information from the most successful μ offspring (line 9).

The CMA update rule for $\boldsymbol{B}$, denoted as AE_{CMA}, derived from the original Covariance Adaptation rule of the (μ, λ)-CMA-ES [Hansen and Ostermeier, 2001, Hansen *et al.*, 2003], is detailed in Algorithm 6.2. The Adaptive Encoding update is similar to some Principal Component Analysis (PCA) of the successful search steps. The goal of PCA is to find an orthogonal transformation to convert the set of possibly correlated variables into a set of uncorrelated variables, called principal components, that are the eigenvectors of the covariance matrix of the data. However, while PCA is usually used to reduce the dimensionality of the data by taking into account only the main principal components (corresponding to the largest eigenvalues), CMA retains all principal components. These components are determined at each iteration by the eigendecomposition of the current covariance matrix $\boldsymbol{C}$ (line 16 of Algorithm 6.2). The transformation matrix $\boldsymbol{B}$ is the square-root of the covariance matrix $\boldsymbol{C}$ (line 17). An illustration of Principal Components Analysis is shown in Figure 6.1-a, where the principal components are depicted as the dotted lines, such that the largest variance by any projection of the data comes to lie on the first principal component, the second largest variance on the second, and so on. The idea of such a transformation is to make the objective function in the transformed space as similar as possible to the Sphere function, which is known to be simple for analysis and optimization.

Figure 6.1-b illustrates an Adaptive Encoding Update iteration, where only the μ (green/bold) best among λ generated offspring are used to compute a partial covariance matrix $\boldsymbol{C}_\mu$ (line 14), which replaces a fraction c_μ of the current covariance matrix $\boldsymbol{C}$ (line 15). Additionally, the path of the mean of distribution (evolution path $\boldsymbol{p}$) is recorded in order to increase the variance of favorable directions (line 13, and bold arrow in Figure 6.1-b). A fraction c_1 of the current covariance matrix $\boldsymbol{C}$ is also replaced by the rank-one matrix of eigendirection $\boldsymbol{p}$ (line 15). However, the update in line 15 might become instable if $c_\mu + c_1 > 1$. Hence the parameter setting (line 3) needs to be chosen specifically for the algorithm at hand.

It has been shown in [Hansen, 2008] that the AE_{CMA}-update applied to Evolution Strategy with Cauchy distribution improves the performance on some non-separable functions by a factor of roughly one thousand. These results and the fact that the Sphere-like transformed space is usually simpler to analyze than the original one, make it reasonable to explicitly exploit this property in search.

6.1.2.2 Coordinate Descent by Dichotomy

Coordinate Descent (CD) is probably one of the oldest multidimensional optimization method. It became especially popular in numerical linear algebra under the name of Gauss-Seidel method for solving systems of linear equations. In Evolutionary Computation community, when used for optimization, this method is called Coordinate Strategy [Schwefel, 1993]. CD is based on the idea that an n-dimensional optimization problem

Algorithm 6.2: Adaptive Encoding

given $\boldsymbol{x}_1, \ldots, \boldsymbol{x}_\mu$
if *Initialize* **then**
  $w_i \leftarrow \frac{1}{\mu}$; $c_p \leftarrow \frac{1}{\sqrt{n}}$; $c_1 \leftarrow \frac{0.5}{n}$; $c_\mu \leftarrow \frac{0.5}{n}$
  $\mathbf{p} \leftarrow 0$
  $\mathbf{C} \leftarrow \boldsymbol{I}$; $\mathbf{B} \leftarrow \boldsymbol{I}$
  $\boldsymbol{m} \leftarrow \sum_{i=1}^{\mu} \boldsymbol{x}_i w_i$
  return.
end if
$\boldsymbol{m}^- \leftarrow \boldsymbol{m}$
$\boldsymbol{m} \leftarrow \sum_{i=1}^{\mu} \boldsymbol{x}_i w_i$
$z_0 \leftarrow \frac{\sqrt{n}}{\left\|\mathbf{B}^{-1}(\boldsymbol{m}-\boldsymbol{m}^-)\right\|}(\boldsymbol{m}-\boldsymbol{m}^-)$
$z_i \leftarrow \frac{\sqrt{n}}{\left\|\mathbf{B}^{-1}(\boldsymbol{x}_i-\boldsymbol{m}^-)\right\|}(\boldsymbol{x}_i-\boldsymbol{m}^-)$
$\mathbf{p} \leftarrow (1-c_p)\mathbf{p} + \sqrt{c_p(2-c_p)}z_0$ // evolution path update
$\mathbf{C}_\mu \leftarrow \sum_{i=1}^{\mu} w_i z_i z_i^T$ // rank-μ update covariance matrix
$\mathbf{C} \leftarrow (1-c_1-c_\mu)\mathbf{C} + c_1\mathbf{p}\mathbf{p}^T + c_\mu\mathbf{C}_\mu$ // covariance matrix update
$\mathbf{B}^\circ\mathbf{D}\mathbf{D}\mathbf{B}^{\circ T} \leftarrow$ `eigendecomposition`$(\mathbf{C})$
$\mathbf{B} \leftarrow \mathbf{B}^\circ\mathbf{D}$
return B

can be decomposed into n one-dimensional sub-problems. Each variable is updated in turn, while all other variables remain fixed, by solving a one-dimension optimization sub-problem using any suitable one-dimension optimization algorithm. Note that CD can be viewed as a special case of Block Coordinate Descent, that partitions the coordinates into N blocks: f is iteratively optimized with respect to one of the coordinate block while other coordinates are fixed [Tseng, 2001]. Obviously, it is reasonable to use CD when dealing with unimodal separable problems.

Adaptive Dichotomy

One of the simplest one-dimension optimization algorithm to use is a dichotomy method (inspired by the bisection method to find a zero of a given function). Let us consider an interval $[a, b]$ where the optimum is known to lie, and assume that the value of the objective function f is known at the center $\boldsymbol{m} = \frac{a+b}{2}$ of the interval. Evaluate the two points $\boldsymbol{x}_1 = \boldsymbol{m} - \frac{(b-a)}{4}$ and $\boldsymbol{x}_2 = \boldsymbol{m} + \frac{(b-a)}{4}$, centers of the left and right parts of $[a, b]$. If f is unimodal, only three cases are possible: $\boldsymbol{x}_1$ is better than $\boldsymbol{m}$ and x_2, $\boldsymbol{x}_2$ is better than $\boldsymbol{m}$ and $\boldsymbol{x}_1$, or both $\boldsymbol{x}_1$ and $\boldsymbol{x}_2$ are worse than $\boldsymbol{m}$ (if $\boldsymbol{x}_1$ and $\boldsymbol{x}_2$ are both better than $\boldsymbol{m}$, then the problem is multi-modal).

If $\boldsymbol{x}_1$ is better than $\boldsymbol{m}$ and $\boldsymbol{x}_2$, then the optimum lies in the interval $[a, \boldsymbol{m})$: replace b with $\boldsymbol{m}$ and $\boldsymbol{x}$ with $\boldsymbol{x}_1$. Similarly, if $\boldsymbol{x}_2$ is better than $\boldsymbol{m}$ and $\boldsymbol{x}_1$, replace a with $\boldsymbol{m}$ and $\boldsymbol{m}$ with $\boldsymbol{x}_2$. Finally, if $\boldsymbol{x}_1$ and $\boldsymbol{x}_2$ are worse than $\boldsymbol{m}$, then the optimum lies in the interval $(\boldsymbol{x}_1, \boldsymbol{x}_2)$: replace a with $\boldsymbol{x}_1$ and b with $\boldsymbol{x}_2$. In all 3 cases, we end up with a new interval $[a, b]$ which contains the optimum, whose length is half that of the original $[a, b]$, and for which

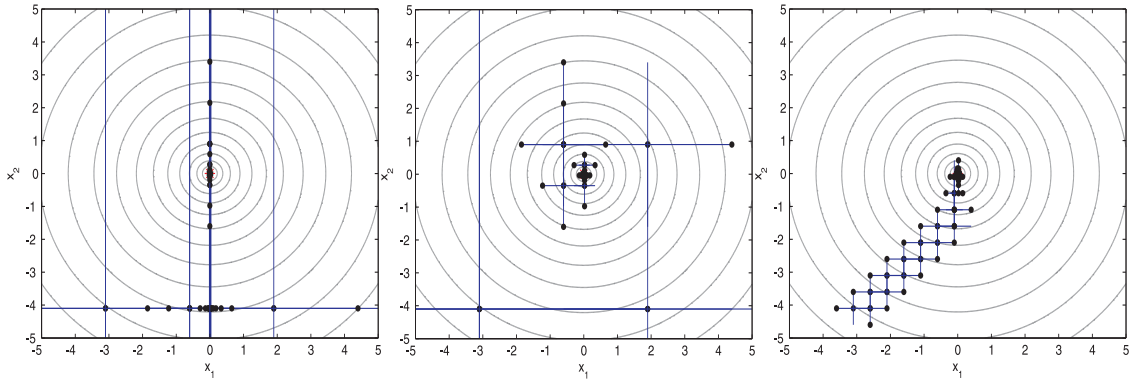

(a) CD k_{succ}=0.5, 80 evaluations. (b) CD k_{succ}=0.5, 80 evaluations. (c) CD k_{succ}=1.0, 117 evaluations.

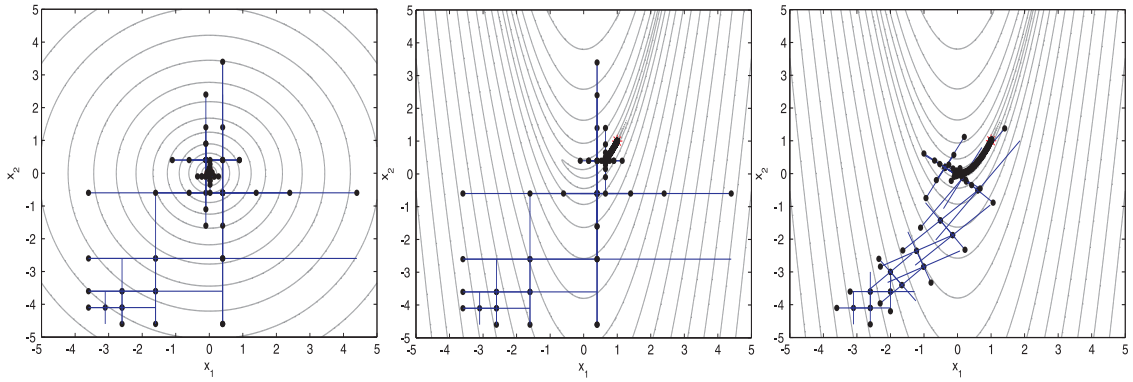

(d) CD k_{succ}=2.0, 149 evaluations. (e) CD k_{succ}=2.0, 22231 evaluations. (f) ACiD k_{succ}=1.2, 325 evaluations.

Figure 6.2: Coordinate Descent (CD) (**a-e**) and Adaptive Coordinate Descent (ACiD) (**f**) on Sphere (**a-d**) and Rosenbrock (**e,f**) functions. The initial point $\boldsymbol{x}_0$=(-3.1,-4,1) and the target point $\boldsymbol{x}_{target}$ with $f(\boldsymbol{x}_{target}) < 10^{-10}$. While the CD with the dichotomy (**a,b**) performs best on the Sphere function cyclically dividing by two the step size for the corresponding coordinate (depicted as the line), the increasing of the step size by factor k_{succ} in the case of successful sampling leads to a better but still slow convergence on non-separable Rosenbrock function (**e**). The adaptation of the coordinate system allows significantly speed up the search (**f**).

we know the value of f at its center, thus closing the loop, and ready for next iteration.

When dealing with multi-dimensional problems, dichotomy steps can be achieved on each coordinate successively: Figure 6.1-c illustrates the 2-dimensional case and displays an example of one dichotomy step in each direction.

Another point of view on the dichotomy method is to consider it as a derandomized $(1+2)$-EA algorithm with step-size adaptation: Assuming the current step-size is σ and current solution is $\boldsymbol{m}$, the basic step of the dichotomy method described above generates 2 offspring $\boldsymbol{x}_1$ and $\boldsymbol{x}_2$ in a deterministic way. The best of $\boldsymbol{m}$, $\boldsymbol{x}_1$, and $\boldsymbol{x}_2$ becomes the next parent, and σ is divided by 2. In the case of one-dimensional unimodal problems, if the initial interval contains the global optimum, this algorithm will get an approximation as wanted of. Similarly, in the case of multi-dimensional unimodal problems, if the initial rectangle contains the global optimum, the algorithm will find it, either by running the dichotomy method on each coordinate up to a given precision (see Figure 6.2-a), or by alternating one step of the dichotomy method in each direction in turn (see Figure 6.2-b). Figure 6.2-a shows the result of such an optimization of the Sphere function $f(\boldsymbol{x}) = \sum_{i=1}^{n} x_i^2$ starting from the initial point $\boldsymbol{x}_0 = (-3.1, -4.1)$. Dichotomy proceeds for 20 iterations for the first coordinate and then for 20 iterations for the second coordinate, reaching the target function value 10^{-10} after 80 evaluations. Exactly the same result is obtained by cyclically repeating this procedure over each coordinate in turn, as shown in Figure 6.2-b. The second variant, however, seems to be more robust if the problem is not perfectly separable, exploring a larger region of the search space rather than rapidly reducing one dimension to a single value.

However, if the optimum lies outside the initial interval, or if the interval is somehow transformed after a rotation of the coordinate system (e.g., due to Adaptive Encoding, see Section 6.1.2.3), it might be necessary to allow more exploration in case of successful sampling (one offspring was better than the parent $\boldsymbol{m}$). Such dichotomy method with step-size (interval) adaptation will be called Adaptive Dichotomy (AD), and works as follows: Generate two offspring $\boldsymbol{x}_1$ and $\boldsymbol{x}_2$ as above. If at least one of these two offspring is better than its parent $\boldsymbol{m}$, then $\sigma \leftarrow \sigma k_{succ}$, otherwise $\sigma \leftarrow \sigma k_{unsucc}$. In the case of standard dichotomy, $k_{succ} = k_{unsucc} = 0.5$, which is suitable for the unimodal separable problems, when initial interval contains the optimum. However, whereas $k_{unsucc} = 0.5$ seems a good choice for all situations, and will be used in the following, $k_{succ} > 0.5$ is mandatory in most cases (otherwise, even on the Sphere function, the algorithm will not converge if the initial domain does not contain the optimum). Figure 6.2-c and Figure 6.2-d illustrate runs where the optimum does not lie in the initial rectangle. However, with $k_{succ} = 1.0$ and $k_{succ} = 2.0$ respectively, the Coordinate Descent with Adaptive Dichotomy converges, though at the price of additional functions evaluations.
A more formal description of CD with Adaptive Dichotomy will be given in Section 6.1.2.3 (Algorithm 6.3).

Convergence Rates Before turning to Adaptive Encoding and non-separable functions, let us analyze the convergence rate of CD with Adaptive Dichotomy on the Sphere function, and compare it that of standard Evolution Strategies, whose behavior is well studied in this context.

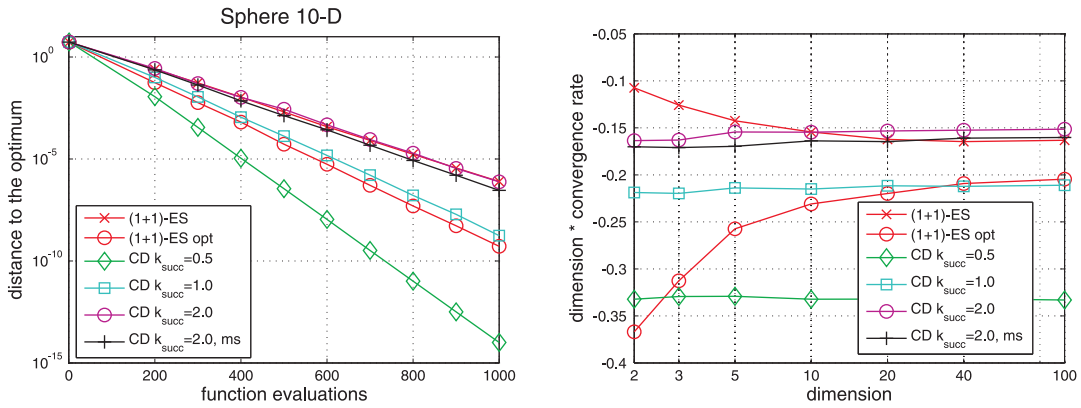

Figure 6.3: **Left**: Evolution of distance to the optimum versus number of function evaluations for the (1+1)-ES, (1+1)-ES opt, CD k_{succ}=0.5, CD k_{succ}=1.0, CD k_{succ}=2.0 and CD k_{succ}=2.0 ms on $f(x) = \|x\|^2$ in dimension **10**. **Right**: Convergence rate c (the lower the better) multiplied by the dimension n for different algorithms depending on the dimension n. The convergence rates have been estimated for the median of 101 runs.

Linear convergence to the optimal point $\boldsymbol{x}^*$ takes place if there is a constant $c \neq 0$, such that

$$\frac{1}{T_k} \ln \frac{\|\boldsymbol{x}_k - \boldsymbol{x}^*\|}{\|\boldsymbol{x}_0 - \boldsymbol{x}^*\|} \to c, \tag{6.1}$$

where $\boldsymbol{x}_0$ is the initial point and $\boldsymbol{x}_k$ the best point found after k iterations for a cost of T_k fitness function evaluations.

The empirical convergence rate on the Sphere function of the proposed CD with $k_{succ} = 0.5$, 1.0 and 2.0, as well as that of two variants of (1+1)-Evolution Strategy, as estimated from the median of 101 independent runs, is shown in Figure 6.3. The algorithm denoted as "(1+1)-ES" corresponds to the (1+1)-Evolution Strategy with the initial step-size $\sigma_0 = 1.8$, while the search interval is $[-3; 3]^n$. The "(1+1)-ES opt" algorithm is the (1+1) Evolution Strategy with the scale-invariant step-size: the optimal step-size for ES on Sphere function is proved to be $\sigma = \frac{1.2}{n} \|\boldsymbol{x} - \boldsymbol{x}^*\|$, i.e., proportional to the distance to the optimum.

It is clear that the convergence rate of the CD with (standard) dichotomy ($k_{succ} = 0.5$) is linear with dimension n, and is equal to $-\ln(2)/2n = -0.3465/n$. The rates for CD with Adaptive Dichotomy, with $k_{succ} = 1.0$ and $k_{succ} = 2.0$ are 1.5 and 2.0 times slower, respectively, than with $k_{succ} = 0.5$.

The recently proposed technique of *mirrored sampling* (ms) and *sequential selection* for Evolution Strategy [Brockhoff *et al.*, 2010], can also be used with the CD method proposed here, because the sampled points are symmetric by definition. We hence propose a modified version of the CD with Adaptive Dichotomy algorithm, called "CD k_{succ}=2.0 ms ", in which the second offspring is not evaluated if the first one is better than the

parent. This does reduce the number of fitness function evaluations, though marginally, as can be seen in Figure 6.3 (line with label "ms").

It is important to note that the optimal convergence rate of "(1+1)-ES opt" is not achievable in practice, because the optimal step-size is unknown for a given black-box function. In the case of CD, parameter k_{succ}, which controls the exploration rate, can be used to implicitly tune the target convergence rate.

A final remark on one-dimensional algorithms: Obviously, any other one-dimensional optimization method could be used instead of the Dichotomy method. The Golden Section method (also called Fibonacci method) is known to have a better convergence rate $c = -\ln(\frac{1+\sqrt{5}}{2})/n = -0.4812/n$. However, the Golden Section generates new points with respect to two evaluated points on a line. Therefore, after a change of coordinate (due to Adaptive Encoding, see next Section) it will require to recompute the fitness of these rotated point whereas dichotomy only requires the fitness value of the center of the current domain, that is preserved by the change of coordinate.

6.1.2.3 Adaptive Coordinate Descent

The Adaptive Encoding procedure (Section 6.1.2.1) iteratively learns the coordinate systems in which the objective function is "as close to separable as possible". The Coordinate Descent method (Section 6.1.2.2) takes advantage of the separability of the problem at hand, iteratively optimizing n independent one-dimensional problems. Combining both approaches leads to propose Adaptive Coordinate Descent (ACiD), which benefits from these two ideas, interleaving CD and AE, learning the same coordinate transform than the original AE, and performing CD steps in the transformed space.

Figure 6.1-d illustrates how AE acts on the iterations of one-dimensional search steps of Figure 6.1-c. The advantages of ACiD over CD become obvious on non-separable functions. Figure 6.2-e and Figure 6.2-f show sample runs of CD and ACiD respectively, on Rosenbrock function in 2-D: ACiD (with $k_{succ} = 2.0$) quickly adapts an appropriate coordinate system and finds the optimum 70 times faster than CD.

Algorithm 6.3 describes the proposed ACiD algorithm. Note that it also describes the non-adaptive CD method by taking $\boldsymbol{B} = \boldsymbol{I}$ and removing the call to AdaptiveEncoding (line 30). Algorithm starts by randomly initializing the current parent $\boldsymbol{m}$ uniformly in the given rectangle domain $\Pi_i[x_i^{min}, x_i^{max}]$, and evaluating it. Initial step-sizes σ_i are set to $\frac{1}{4}$ of the corresponding interval length. i_x is the index of the current coordinate, going from 1 to n cyclically (line 8)[1]. The two offspring $\boldsymbol{x}_1$ and $\boldsymbol{x}_2$ are generated from $\boldsymbol{m}$ with offset $\pm\sigma_{i_x}$ on coordinate i_x (lines 9-11). If one of them has better fitness value than $\boldsymbol{m}$ (minimization assumed here), $\boldsymbol{m}$ and f_{best} are updated accordingly (line 14 or 17). The i_x step-size σ_{i_x} is then updated multiplicatively depending on the success indicator (line 21 or 23). The coordinates and fitness of both offspring are then stored (lines 25 and 26). At the end of the coordinate loop (i.e., when $i_x = n$, line 29), the Adaptive Encoding procedure is called to update the transformation matrix $\boldsymbol{B}$, using information from the μ best offspring encountered during the n coordinate steps (line 30).

[1]Random cycles were also tried, but no significant impact on performance was ever observed, so only the cyclic variant is shown here for the sake of simplicity.

Algorithm 6.3: ACiD

$\boldsymbol{m} \leftarrow x^{min}_{i:d} + \mathbb{U}_{i:d}(x^{max}_{i:n} - x^{min}_{i:d})$
$f_{best} \leftarrow evaluate(m)$
$\sigma_{i:d} \leftarrow (x^{max}_{i:d} - x^{min}_{i:d})/4$
$\mathbf{B} \leftarrow \boldsymbol{I}$
$i_x \leftarrow 0$
$impr \leftarrow 1$
while NOT Stopping Criterion **do**
  $i_x \leftarrow i_x + 1$ mod. n // Cycling over $[1, n]$
  $\boldsymbol{x}'_{1:d} \leftarrow 0$
  $\boldsymbol{x}'_{i_x} \leftarrow -\sigma_{i_x}$; $\boldsymbol{x}_1 \leftarrow \boldsymbol{m} + \mathbf{B}\boldsymbol{x}'$; $f_1 \leftarrow evaluate(\boldsymbol{x}_1)$
  $\boldsymbol{x}'_{i_x} \leftarrow +\sigma_{i_x}$; $\boldsymbol{x}_2 \leftarrow \boldsymbol{m} + \mathbf{B}\boldsymbol{x}'$; $f_2 \leftarrow evaluate(\boldsymbol{x}_2)$
  $succ \leftarrow 0$
  if $f_1 < f_{best}$ **then**
    $f_{best} \leftarrow f_1$; $\boldsymbol{m} \leftarrow \boldsymbol{x}_1$; $succ \leftarrow 1$
  end if
  if $f_2 < f_{best}$ **then**
    $f_{best} \leftarrow f_2$; $\boldsymbol{m} \leftarrow \boldsymbol{x}_2$; $succ \leftarrow 1$
  end if
  if $succ = 1$ **then**
    $impr \leftarrow 1$
    $\sigma_{i_x} \leftarrow k_{succ} \cdot \sigma_{i_x}$
  else
    $\sigma_{i_x} \leftarrow k_{unsucc} \cdot \sigma_{i_x}$
  end if
  $\boldsymbol{x}^a_{(2i_x-1)} \leftarrow \boldsymbol{x}_1$; $f^a_{(2i_x-1)} \leftarrow f_1$
  $\boldsymbol{x}^a_{2i_x} \leftarrow \boldsymbol{x}_2$; $f^a_{2i_x} \leftarrow f_2$
  if $(i_x = n)$ and $(impr = 1)$ **then**
    $impr \leftarrow 0$
    $\boldsymbol{x}^a \leftarrow \left\{\boldsymbol{x}^a_{<:i} | 1 \leq i \leq 2n\right\}$
    $\mathbf{B} \leftarrow AdaptiveEncoding(\boldsymbol{x}^a_1, \ldots, \boldsymbol{x}^a_\mu)$
  end if
end while

The proposed algorithm is deterministic, therefore the resulting solution for the noiseless functions only depends on the starting point.

6.1.3 Experimental Validation

Adaptive Coordinate Descent has been benchmarked on the noiseless BBOB testbed. Thanks to the publically available results of many algorithms on the same testbed, and to automatic comparison procedures provided by this framework, ACiD results will be compared to those of the state-of-the-art algorithms: BIPOP-CMA-ES, IPOP-CMA-ES,

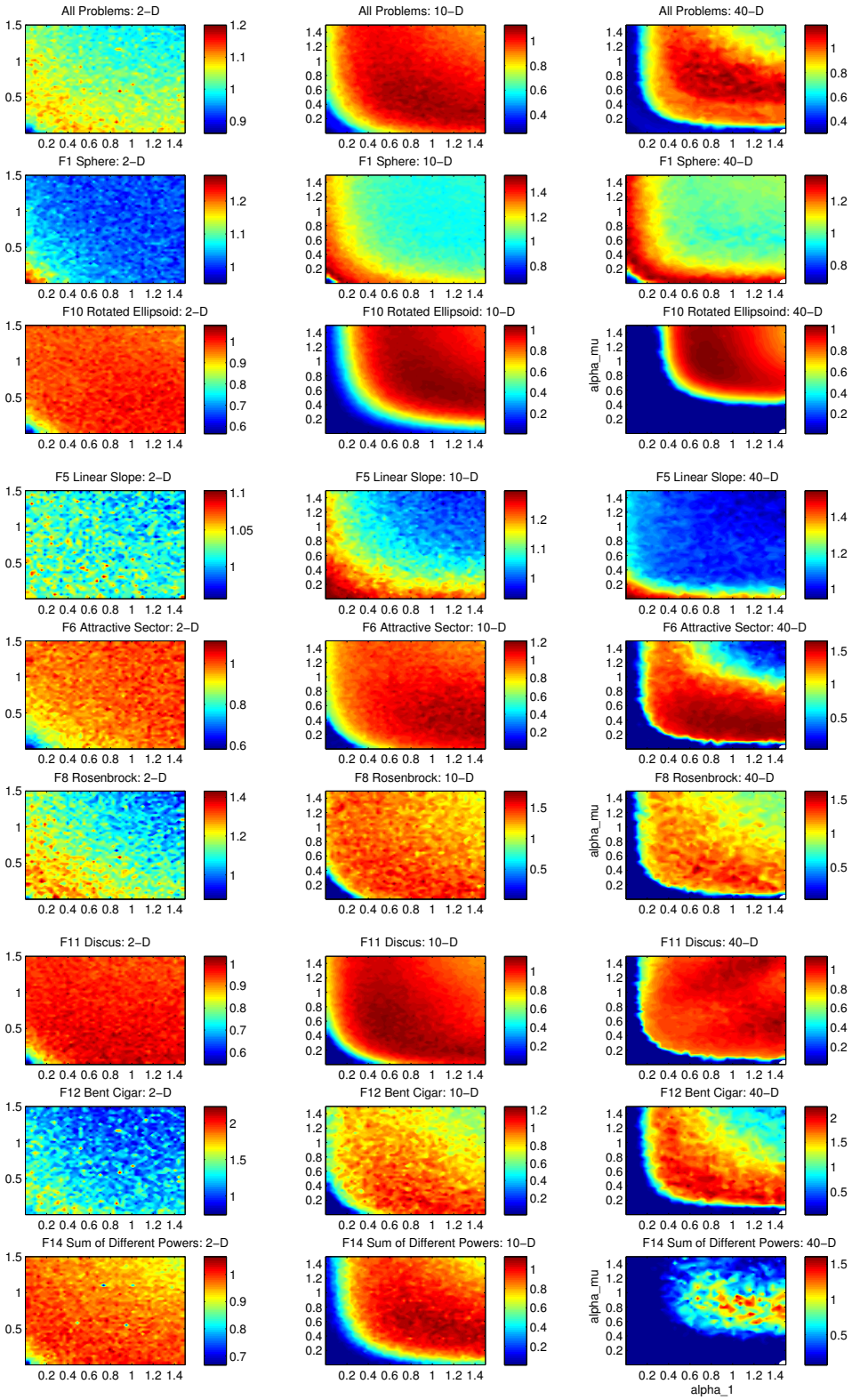

Figure 6.4: Performance analysis of ACiD in $\alpha_{ccov} \times \alpha_{cpath}$ space. All colorscales are different. See text for details.

IPOP-aCMA-ES, (1+1)-CMA-ES and $(1 + 2^s_m)$-CMA-ES [Auger *et al.*, 2010].

6.1.3.1 Adaptive Encoding Calibration

The main parameters in Adaptive Encoding procedure that [Hansen, 2008] suggested to calibrate are c_1 and c_μ. To scale them with the dimension we can define: $c_1 \leftarrow \frac{0.5}{n^{\alpha_1}}$ and $c_\mu \leftarrow \frac{0.5}{n^{\alpha_\mu}}$ (with $k_{succ} = 2$). Figure 6.4 illustrates the potential speedup for different values of α_1 and α_μ w.r.t. to the baseline algorithm ($\alpha_1 = 1.0$ and $\alpha_\mu = 1.0$). First, for each of 8 benchmark problems the baseline SP1 value to reach the target value 1e-10 is calculated (30 runs, $\alpha_1 = 1.0$ and $\alpha_\mu = 1.0$). Then this procedure is repeated for 10000, 4000 and 1500 times with random values of α_1 (x-axis) and α_μ (y-axis) on 2-, 10- and 40-dimensional problems respectively (left, center, right). The average speedup for 8 tested problems is plotted on top. It should be noted that the bottom left corner (respectively, top right corner) of each small plot corresponds to *large* values of c_1 and c_μ (respectively, *small* values of c_1 and c_μ).

It can be clearly seen that optimal parameters of α_1 and α_μ depend very much both on the problem and its dimension. In 2-D the results are somewhat difficult to interpret, while in 10-D and 40-D, they are much more illustrative. Some general observations:

- very large α_1 and α_μ (bottom left corner) slow down the search, because the performed PCA takes into account only local information, obtained from few recent individuals, and, therefore is not sufficiently correct.
- very small α_1 and α_μ (top right corner) also slow down the search, because the covariance matrix stores a lot of outdated information.
- the optimal α_1 and α_μ are located somewhere in the middle, but often close to the "bad" region, where the performance quickly drops.
- on some problems the Pareto shape is observed in the sense that a set of α_1 and α_μ from the same "front" leads to the same performance.

The baseline results (for $\alpha_1 = 1$ and $\alpha_\mu = 1$) on Sphere and Linear Slope functions can be improved by using quite large c_1 and c_μ. On Sum of Different Powers, the results are very sensitive to c_1 and c_μ and the optimal region is quite small. It would be interesting to note that while the region of average speedup (top) seems to be quite large, the actual region of choice is rather constrained by the region of Rotated Ellipsoid function, where the speedup quickly drops if α_1 or α_μ is smaller than 0.8 (in 40-D). Another important observation is that α_1-α_μ hyper-parameters optimization problem sometimes is multi-modal (let us forget about noise) as can be clearly observed for 40-dimensional Discus function, where two peaks are located symmetrically to each other! This is rather unexpected observation.

In overall, the baseline results can be improved by 10-70% by choosing optimal α_1 and α_μ parameters for each problem.

6.1.3.2 Coordinate Descent Calibration

Next experiment is concerned with the **sensitivity of parameter** k_{succ}. Figure 6.5-**Left** shows the performance of ACiD (in terms of BBOB-SP1) depending on k_{succ}, for several problems in 10-D. k_{succ} determines how fast the step-size will increase for a given coordinate if the last step along that coordinate was successful. There is a strong link between k_{succ} and the covariance matrix learning coefficients c_1 and c_μ, since they both determine the comparative impact of the new steps.

The experiments show that ACiD does not converge for $k_{succ} \leq 1$ on non-separable problems, whereas on the Sphere function, ACiD obtains nearly the same results than CD with $0.5 \leq k_{succ} < 1.0$. The reason for this is easy to understand on a small example: if $k_{unsucc} = 0.5$ and $k_{succ} = 1.1$, then in the case of 2 consecutive unsuccessful steps, the step-size σ is divided by 4; so in order to come back to initial step size, 13 consecutive successful steps are needed! The optimal pair k_{succ}, k_{unsucc} of course depends on the problem, and on the other parameters of the ACiD, too. But $k_{succ} = \frac{1}{k_{unsucc}} = 2.0$ seems to be both robust and simple, at least for the BBOB problems.

6.1.3.3 Experimental Settings

In order to validate ACiD with a robust version, a value of $k_{succ} = 2$ will be used as a baseline (while $k_{unsucc} = 0.5$). Indeed, while other values for $k_{succ} \in [0.5, 2.0]$ may lead to faster convergence, they also sometimes result in premature convergence on some problems, even on the Sphere function, as demonstrated by preliminary experiments. Also note that the basic rates for the covariance matrix update are set to the simple values $c_1 = \frac{0.5}{n}$ and $c_\mu = \frac{0.5}{n}$ rather than the default ones ($c_1 = \alpha_c \frac{0.2}{(n+1.3)^2+\mu_w}, c_\mu = \alpha \frac{0.2(\mu_w - 2 + \frac{1}{\mu_w})}{(n+2)^2+0.2\mu_w}$, where $\alpha_c = 10$ for CMA-ES, leading to $c_1 \approx \frac{2}{n^2}$, $c_\mu \approx \frac{\mu_w}{n^2}$, [Hansen, 2008]). A total of 4 variants will be tested in the following: the baseline described above is denoted *ACiD*; *ACiD-k_succ1.5* is the same variant, but with $k_{succ} = 1.5$; *ACiD-ms* uses the value $k_{succ} = 2$, but implements mirrored sampling and sequential selection (Section 6.1.2.2); finally, *ACiD-a_cmu0.8* uses $c_\mu = \frac{0.5}{n^{0.8}}$ rather than the default value, as our experiments in Section 6.1.3.1 have shown that c_μ is a sensitive parameter indeed, and the value of $\frac{0.5}{n^{0.8}}$ can bring up to 10-70% improvement on some problems.

Because ACiD can be considered as $(1 + 2)$-EA, a restart procedure is necessary to improve the performance on multi-modal functions. Similarly to the other $(1 + 1)$-CMA-ES that ACiD will be compared to within BBOB testbed, the algorithm is restarted if the improvements of the best solution is smaller than 10^{-25} during the last $10 + \lfloor 20n^{1.5} \rfloor$ function evaluations. The maximum number of function evaluations is $10^4 n$, and the initial interval is $[-3, 3]^n$. All results are statistics over 15 independent runs, one run per BBOB problem instance (e.g., 15 runs on different instances of the Sphere functions).

The MatLab source code of ACiD is available online at
`http://sites.google.com/site/acdgecco/`.

6.1.3.4 Results on Noiseless BBOB Testbed

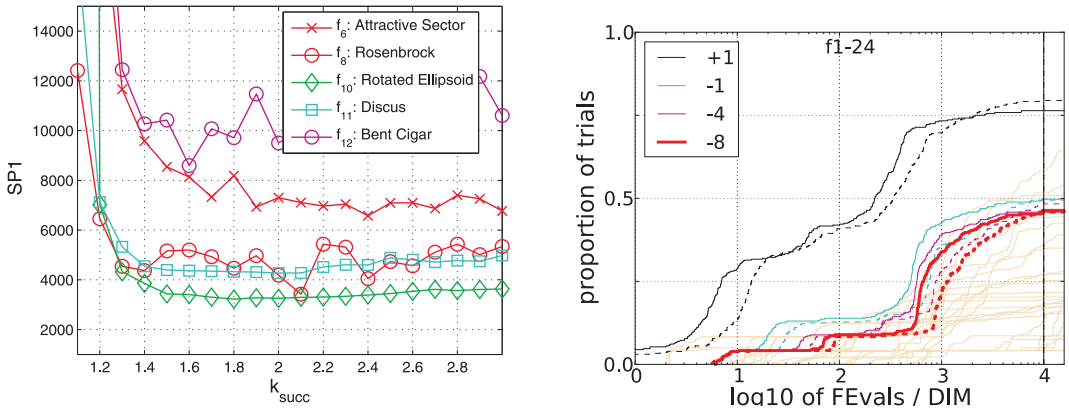

Figure 6.5: **Left**: The performance of ACiD in **10-D**: BBOB-SP1 (the average number of function evaluations to reach target value 10^{-8} divided by success rate) versus step-size multiplier k_{succ}. **Right**: BBOB-like results for noiseless functions in **20-D**: ECDF for ACiD (continuous lines) and $(1+1)$-CMA-ES (dashed lines), of the running time, normalized by dimension n, needed to reach target precision $f_{\text{opt}} + 10^k$ (for $k = +1, -1, -4, -8$). The vertical black line indicates the maximum number of function evaluations. Light yellow (or gray in b&w) lines in the background show similar ECDFs for target value 10^{-8} of all algorithms benchmarked during BBOB 2009.

Figure 6.5-**Right** presents the ECDFs of both ACiD and $(1+1)$-CMA-ES aggregated over the 24 noiseless benchmark problems in 20-D. A closer look at the results (details not shown here) reveals that for 50% of the solved functions, ACiD is faster about by 40% than $(1+1)$-CMA-ES. ACiD converges on Attractive Sector function f_6, while $(1+1)$-CMA-ES does not. On Rosenbrock f_8 and f_9, Ellipsoid f_2 and f_{10} and Discus f_{11}, some ACiD algorithms are up to 2 times faster than (1+1)-CMA. Furthermore, with a budget of $1000n$ function evaluations, ACiD performs best in 20-D among all algorithms that entered BBOB-2009 competition.

Figure 6.6 gives a more general view of similar experiments in 10-D and 40-D – but here experiments with 50 different target values are aggregated. Overall, the functions are not easy to solve. Even the best CMA-ES algorithm, BIPOP-CMA-ES, can solve less than 90% of the problems using maximum number of function evaluations (the large crosses). Furthermore, the elitist algorithms (ACiD, $(1+1)$-CMA-ES, $(1+2^s_m)$-CMA-ES) are more likely to get stuck in a local optimum than the generational algorithms (BIPOP-CMA-ES, IPOP-CMA-ES and IPOP-aCMA-ES), especially in the case where the step-size decreases after each unsuccessful step. The increase of the population size after restart in the case of the premature convergence is the main tool, which leads to a superior performance of the generational CMA-ES algorithms over the single-population algorithms on the multimodal problems. Indeed, only 10 out of 24 problems are unimodal and this 42% threshold can be seen in Figure 6.6. However, the good news is that all ACiD algorithms have at least

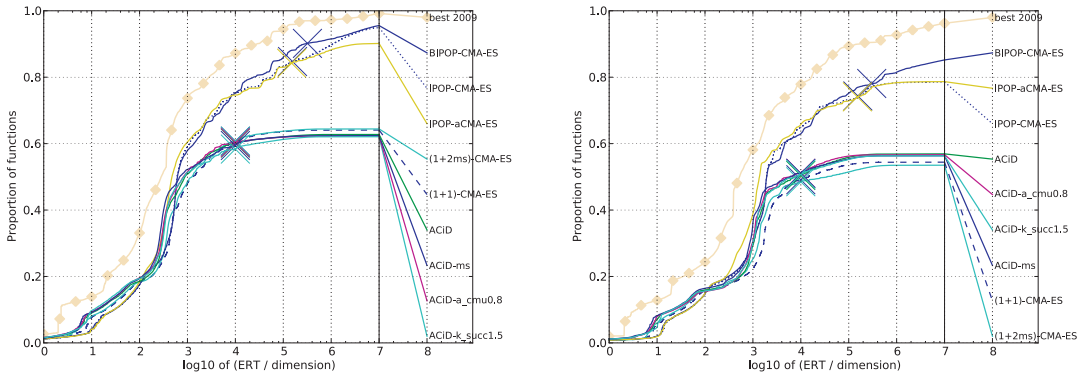

Figure 6.6: Empirical cumulative distribution of the bootstrapped distribution of ERT vs dimension for 50 targets in $10^{[-8..2]}$ for all functions and subgroups in **10-D** (**Left**) and **40-D** (**Right**). The "best 2009" line corresponds to the best result obtained by at least one algorithm from BBOB 2009 for each of the targets.

comparable performance with $(1+1)$-CMA-ES and $(1+2^s_m)$-CMA-ES: they outperform one another depending on the problem, but the differences are not significant.

6.1.3.5 Extension to Noisy Optimization

The original ACiD is an elitist algorithm, where offspring replaces the parent only if it is better on f. This approach seems to be too "greedy" if f is noisy and the algorithm may suffer from premature convergence. To reduce this effect we propose here a very simple modification: i). we manually set or check online whether f is noisy or not; ii). if f is noisy, at each iteration we re-evaluate the best solution found so far before the line 8 of Algorithm 6.3. This simple modification increases the budget of evaluations by 50% per iteration, but according to our (not shown here) preliminary experiments, drastically improves the results on functions with moderate noise. We omit these preliminary experiments for brevity.

6.1.3.6 Extension to Large-Scale Optimization

The original ACiD algorithm performs n dichotomy steps and evaluates 2 individuals iteratively on n principal components (overall $2n$ evaluations), then calls the Adaptive Encoding procedure in line 30 of Algorithm 6.3. The computation complexity of the Adaptive Encoding procedure is defined by the eigendecomposition of the covariance matrix C and scales with $O(n^3)$. Thus, performing the eigendecomposition every n iterations or $2n$ function evaluations, the computational complexity of ACiD per function evaluation becomes quadratic. The computational complexity is also quadratic for i). (μ, λ)-CMA-ES, where the eigendecomposition of C is postponed, and ii). the recently proposed version of (1+1)-CMA-ES [Suttorp *et al.*, 2009] thanks to the use of Cholesky factor update. However, it

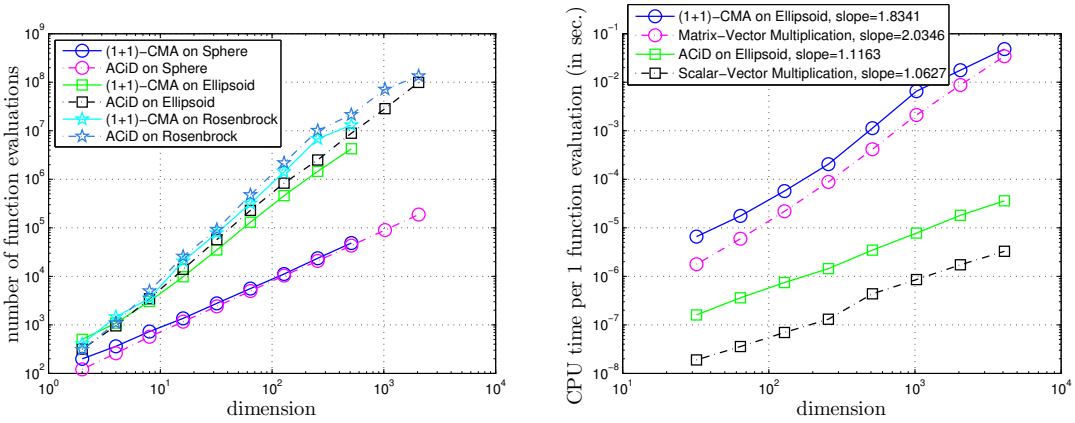

Figure 6.7: Results for ACiD with linear time complexity (LACiD) on Sphere, Ellipsoid and Rosenbrock functions for different problem dimensions. **Left**: SP1 to reach 10^{-8}. **Right**: CPU time per function evaluation.

should be noted that **there is no** version of CMA-ES which can be linear in time **and** at the same time be able to learn the full covariance matrix (SEP-CMA-ES learns only the diagonal of $\mathbf{C}$ [Ros and Hansen, 2008]). This is due to the procedure of sampling of new offspring, which involves matrix-vector multiplication which is already quadratic in n .

In order to reduce the computational complexity of ACiD we may replace $\boldsymbol{x}'_{i_x} \leftarrow -\sigma_{i_x}$; $\boldsymbol{x}_1 \leftarrow \boldsymbol{m} + \mathbf{B}\boldsymbol{x}'$ in line 10 of Algorithm 6.3 by $\boldsymbol{x}_1 \leftarrow \boldsymbol{m} - \sigma_{i_x}\mathbf{B}(:, i_x)^T$. Thus, we replace quadratic in n matrix-vector multiplication by linear in time multiplication of vector (i_x-th eigenvector) and scalar. In contrast, in (full covariance matrix based) CMA-ES in order to generate an offspring we first should multiply its randomly generated pre-image vector $\boldsymbol{x}'_1$ by $\mathbf{B}$, that is quadratic in n. However, we still have overall quadratic complexity of ACiD due to eigendecompostion of $\mathbf{C}$. To reduce the complexity to be *linear* we postpone the eigendecomposition (lines 16-17 of Algorithm 6.2) and perform it only every n iterations. We also should remove rank-μ update (remove lines 12 and 14, set $c_\mu = 0$) which would lead to quadratic complexity of ACiD. We additionally simplify rank-one update such that $\boldsymbol{m}$ equals to the best solution $\boldsymbol{x}_{best}$ found so far. We call this modified version of ACiD, linear time ACiD (LACiD).

Figure 6.7-**Left** shows the results of (1+1)-CMA-ES and LACiD on Sphere, Ellipsoid and Rosenbrock function for different problem dimensions. It should be noted that the LACiD usually performs worse than the original ACiD because of described above simplifications. However, as can be seen from the results, LACiD performs as well as (1+1)-CMA-ES on Sphere function and slightly slower on Ellipsoid and Rosenbrock. The loss of ACiD in comparison with (1+1)-CMA-ES is growing with dimension and is about a factor of 1.5-2 for $n = 512$ (the results for (1+1)-CMA-ES are incomplete for large n due to large required time of computations).

Figure 6.7-**Right** shows CPU time complexity per function evaluation (in seconds) for (1+1)-CMA-ES and LACiD, estimated on Ellipsoid problem. While ACiD is invariant

to orthogonal transformations of the search space, we generate a *random* initial coordinate system defined by matrix B to imitate the optimization of Rotated Ellipsoid function (otherwise, the computation of fitness function would be very expensive itself). For our experiments we use fast version of (1+1)-CMA-ES proposed by [Suttorp *et al.*, 2009], where the Cholesky factor of C is used for sampling new solutions. The Cholesky factor (and its inverse) is iteratively updated, thus, requiring only matrix-vector multiplication operations. It can be seen from the Figure that (1+1)-CMA-ES scales almost quadratically with n and very closely to the computational complexity of one matrix-vector multiplication operation. In contrast, LACiD scales almost linearly with n and is only by a factor of 10 slower than one scalar-vector multiplication. Thus, the complexity of LACiD is about $10n$ operations.

In overall, the LACiD is about n times faster in terms of time and is about 2 times slower in terms of number of function evaluations for $n > 1000$. If the objective function is relatively cheap to compute, then the overall speedup for $n = 1000$ is about a factor of 500.

The LACiD can be compared to SEP-CMA-ES, proposed by [Ros and Hansen, 2008]. However, the latter is not suitable for learning the full covariance matrix, and, therefore, does not solve Rotated Ellipsoid function in a reasonable number of function evaluations [Ros and Hansen, 2008]. The same is also true for the elegant Rank-One NES (linear time Natural Evolution Strategy), recently proposed by [Sun *et al.*, 2011]. While CPU time experiments performed on different platforms and languages are hardly comparable, it should be noted that CPU cost of Rank-One NES is about 10^{-3} for $n = 512$, that is about a factor of 100 slower than LACiD. As well as SEP-CMA-ES, Rank-One NES can be used for non-separable optimization, but is efficient if only one (or few) principal components are sufficient to reach the optimum quickly. However, it is not able to benefit from learning all principal components.

6.1.4 Conclusion and Perspectives

The very powerful Covariance Matrix Adaptation part of the state-of-the-art CMA-ES algorithm has been generalized into the Adaptive Encoding procedure that can be used in conjunction with any optimization algorithm, gradually learning an optimal coordinate system where the objective function at hand is (in the best case, and at least locally) separable. Simple yet powerful algorithms can be used to optimize separable functions, as for instance the Coordinate Descent (CD), that performs up to 2 times faster than the $(1 + 1)$-ES on the Sphere function. The Adaptive Coordinate Descent algorithm (ACiD) uses AE coupled with adaptive CD. ACiD has been shown to be competitive with the CMA-ES algorithms and even up to 2 times faster than $(1 + 1)$-CMA-ES on several functions of the BBOB test suite.

The superiority of the ACiD as an absolutely deterministic algorithm was not obvious a priori. These experiments confirm the hypothesis that the efficiency of CMA-ES is greatly due to the Adaptive Encoding procedure, and that the second component of the algorithm (Evolution Strategies, and Gaussian mutations) can be replaced without significant (or even any) loss of performance, at least in the case of the single-individual algorithms.

The IPOP-aCMA-ES is the only algorithm among the ones presented here that uses all λ offspring in its covariance matrix update. While the best μ points are used to increase the variance along the successful directions, the worst $\lambda - \mu = \mu$ points are used with negative sign to exclude irrelevant directions of search. It is clear that such kind of negative update can be applied to ACiD too. This will be the subject of further work.

Of course, the generational versions of CMA-ES outperform the single-individual ones like $(1 + 1)$-CMA-ES and ACiD, on most multi-modal problems. But this is essentially due to the restarts with increasing population size. Some further work will be concerned with designing a generational extension of ACiD.

Partial experiments indicate that the off-line tuning of the covariance matrix learning rates c_1 and c_μ can lead to 10-70% speedup depending on the problem and dimension: more detailed experiments must be made in this direction. However, CMA-ES algorithms would of course also profit from tuning their parameters for the BBOB benchmark.

Borrowing ideas from [Pošík, 2004], an extension of the Adaptive Encoding procedure to the non-linear case using Kernel Principal Component Analysis (KPCA) [Scholkopf *et al.*, 1996] is envisioned. Such extension should for instance make it feasible to sample the non-linear distribution along the parabolic shaped optimal valley of the Rosenbrock function (see Section 6.4.1).

In ACiD, the evolution path somehow approximates the gradient of the fitness function, and this information is used in the Adaptive Encoding update. However, the line search along the gradient could also be performed explicitly, as in quasi-Newton methods (e.g., BFGS method [Shanno, 1970]) and Pattern Search methods (e.g., Hooke and Jeeves method [Hooke and Jeeves, 1961]).

We anticipate successful applications of ACiD algorithm to constrained problems. For CMA-ES in large dimensions, resampling the infeasible points does not work, and leads to a rapid decrease of the step-size that further limits the exploration [Arnold and Hansen, 2012]. Within ACiD, the resampling on a line is easy, both in the transformed and in the original spaces.

Another possible extension of ACiD is concerned with surrogate models: the computationally cheap meta-model assisted one-dimensional search becomes favorable even with some budget of 3 to 5 function evaluations, at least for unimodal problems. Furthermore, in order to preserve the invariance properties of the ACiD, comparison-based surrogate models can be used (see Chapter 4).

Finally, the one-dimensional search procedure used in ACiD could be replaced by some k-dimensional search ($k \leq d$). For $k = 2$, the budget is $2k = 4$ function evaluations to find the best of 8 possible states (see Figure 6.1-c). By taking into account all available information, such as the projection of the evolution path on 2-D, we could increase the chances to directly find new best points, for example in the corner. In this case, by simply increasing both step-sizes, the resulting speedup would increase to 4. We suppose that even such simple strategies, together with sequential selection, can make ACiD significantly faster.

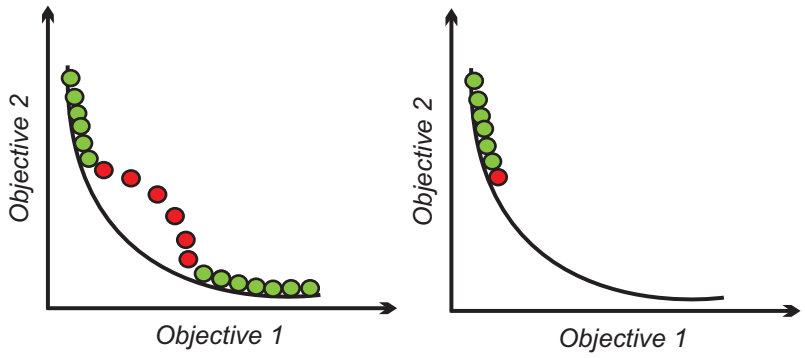

Figure 6.8: Two examples when some parents (red points) might be preferred to other parents (green points) for parent selection in multi-objective optimization, and MO-CMA-ES in particular.

6.2 Reward-based Parent Selection

In Steady State variants of Multi-Objective CMA-ES (SS-MO-CMA-ES, see Section 2.4.4) an offspring is generated from a uniformly selected parent. In our own experiments (see Section 5.4.4) we observed that such selection may be inefficient if only few parents may significantly improve current optimal Pareto front approximation. Figure 6.8 illustrates two examples where this may be the case. A common case is when some non-dominated points are already relatively close to the optimal Pareto front (Figure 6.8-**Left**), while other non-dominated points are quite far but their mating selection might lead to a faster convergence. A less common case we observed on IHR1 problem (a similar behaviour is shown in Figure 6.8-**Right**, see also Section 5.4.4) when one offspring typically has better chances to improve the overall quality of the population. In both cases it might be reasonable to encourage parents which best contribute to the convergence toward the optimal Pareto front.

In this Section, we investigate some alternative parent selection schemes for SS-MO-CMA-ES, based on the conjecture that not all (non-dominated) parents are equal. The new schemes involve the definition of multi-objective rewards, estimating the expectation of the offspring survival and its hypervolume contribution. Two selection modes, respectively using tournament, and inspired from the Multi-Armed Bandit framework [Auer *et al.*, 2002], are used on top of these rewards.

This Section provides a more detailed description of the work published in [Loshchilov *et al.*, 2011b]. Section 6.2.1 details the proposed parent selection operators and how they fit in the generic scheme of MO-CMA-ES. In Section 6.2.2, the resulting algorithms are experimentally assessed on some well-known benchmark unimodal functions, comparatively to the previous versions of MO-CMA-ES. Section 6.2.3 provides a discussion with some perspectives for further research.

6.2.1 New Parent Selections for Steady-State MO-CMA-ES

The original generational and steady-state versions of MO-CMA-ES are described in Section 2.4.4.

After [Igel *et al.*, 2007a], the more "greedy" variant $(\mu_{\prec}+1)$-MO-CMA outperforms all other variants on unimodal problems. In contrast, on multi-modal problems such as ZDT4 and IHR4, $(\mu+1)$-MO-CMA performs better than $(\mu_{\prec}+1)$-MO-CMA [Igel *et al.*, 2007a], but it does not perform too well, and neither does the generational version of MO-CMA-ES, comparatively to other MOEAs (see, e.g., [Igel *et al.*, 2007b] for a comparison of the generational MO-CMA-ES with NSGA-II on ZDT4).

These remarks naturally lead to propose more "greedy" parent selection operators within SS-MO-CMA-ES (line 4 of Algorithm 6.4), in order to further improve its performances on unimodal problems, leaving aside at the moment the multi-modality issue. A parent selection operator is based on i). a selection mechanism (line 4 of Algorithm 6.4, and Algorithm 6.5), and ii). a rewarding procedure (line 16 of Algorithm 6.4, and Algorithm 6.6). A family of such operators is presented in this Section; the selection procedure either is based on a standard tournament selection (Section 6.2.1.1), or inspired from the Multi-Armed Bandit paradigm (Section 6.2.1.2). The rewarding procedures are described in Section 6.2.1.3.

6.2.1.1 Tournament Selection

Standard tournament selection is parameterized from a tournament size $t_{size} \in \mathbb{N}$. Given a set $\boldsymbol{Q}$, t_{size}-tournament selection proceeds by uniformly selecting t_{size} individuals (with or without replacement) from $\boldsymbol{Q}$ and returning the best one according to the criterion at hand (here, the $\prec_{\boldsymbol{Q}^t}$ criterion, see Section 2.4.1). The parent selection procedure (line 4 of Algorithm 6.4) thus becomes tournament selection (line 11 of Algorithm 6.5). The rewarding procedure (line 16 of Algorithm 6.4) only computes for each parent its Pareto rank and hypervolume contribution.

The Steady-State MO-CMA-ES using t_{size}-size Tournament Selection is denoted $(\mu +_{t_{size}} 1)$-MO-CMA in the following, or $(\mu +_{t_{size}} 1)$ for short. Parameter t_{size} thus controls the selection greediness; the larger t_{size}, the more often points with high hypervolume contribution will be selected on average.

6.2.1.2 Multi-Armed Bandit Selection

Another parent selection procedure (line 4 of Algorithm 6.4) inspired from the Multi-Armed Bandit (MAB) paradigm is described here. How to define the underlying rewards (line 16 of Algorithm 6.4) will be detailed in next Section.

The standard MAB setting considers several options, also called arms, each one with an (unknown but fixed) reward distribution [Auer *et al.*, 2002]. The MAB problem is to find a selection strategy, selecting an arm $i, \overline{t}$ in each time step $\overline{t}$ and getting an instance of the corresponding reward distribution, such that this strategy optimizes the cumulative reward.

Algorithm 6.4: $(\mu+\lambda)$-MO-CMA-ES Reward-based Parent Selection

initialize $t \leftarrow 0$, random parent population $\boldsymbol{Q}^{t=0}$
repeat
  for $k = 1, \ldots, \lambda$ **do**
    $i_k \leftarrow ParentSelection(\boldsymbol{Q}^t, k)$
    Generate offspring $\boldsymbol{a}_k'^{t+1}$ using parent $\boldsymbol{a}_{i_k}^t$
    $\boldsymbol{Q}^t \leftarrow \boldsymbol{Q}^t \cup \{\boldsymbol{a}_k'^{t+1}\}$
  end for
  for $k = 1, \ldots, \lambda$ **do**
    Update CMA-ES parameters of $\boldsymbol{a}_k'^{t+1}$ and $\boldsymbol{a}_{i_k}^t$
  end for
  $\boldsymbol{Q}^{t+1} \leftarrow \{\boldsymbol{Q}^t_{\prec:i} | 1 \leq i \leq \mu\}$ // Deterministic Selection according to $\prec_{\boldsymbol{Q}^t}$
  for $k = 1, \ldots, \lambda$ **do**
    $i^t_{parent} \leftarrow i_k$
    $i^{t+1}_{parent} \leftarrow \left\{ i_{\boldsymbol{a}_i^{t+1} = \boldsymbol{a}_{i_k}^t} | 1 \leq i \leq \mu + \lambda \right\}$
    $i^{t+1}_{offspring} \leftarrow \left\{ i_{\boldsymbol{a}_i^{t+1} = \boldsymbol{a}_k'^{t+1}} | 1 \leq i \leq \mu + \lambda \right\}$
    $\boldsymbol{Q}^{t+1} \leftarrow ComputeRewards(\boldsymbol{Q}^t, \boldsymbol{Q}^{t+1}, i^t_{parent}, i^{t+1}_{parent}, i^{t+1}_{offspring}, \overline{t}, W)$
  end for
  $t \leftarrow t + 1$
until stopping criterion is met.

The Upper Confidence Bound (UCB) algorithm yielding an optimal result has been proposed by [Auer *et al.*, 2002]; this algorithm proceeds by selecting the arm which maximizes

$$\hat{q}_{i,\overline{t}} + C\sqrt{\frac{2log\sum_k n_{k,\overline{t}}}{n_{i,\overline{t}}}}, \tag{6.2}$$

the sum of an exploitation term $\hat{q}_{i,\overline{t}}$ (the empirical quality, or average of rewards the arm has ever actually received) and an exploration term $\sqrt{\frac{2log\sum_k n_{k,\overline{t}}}{n_{i,\overline{t}}}}$ (ensuring that non-optimal arms will be selected sufficiently often to enforce the identification of the truly optimal arm). The constant C defines the trade-off between these two terms.

Considering that our setting is a dynamic one (as evolution proceeds toward the Pareto front), no algorithm with theoretical guarantees is available, and some heuristic adaptation of the above MAB algorithm is used:

1. The average reward of an arm (a parent) is replaced by its average reward $\hat{q}_{i,\overline{t}}$ along a time window of size w;

Algorithm 6.5: ParentSelection

1: **given** $\boldsymbol{Q}^t$, k;
2: **if** $SelectionScheme = (\mu + \mu)$ **then**
3: $i_k \leftarrow k$;
4: **end if**
5: **if** $SelectionScheme = (\mu + 1)$ **then**
6: $i_k \leftarrow U\left(1, \left|Q^t\right|\right)$;
7: **end if**
8: **if** $SelectionScheme = (\mu_{\prec} + 1)$ **then**
9: $i_k \leftarrow U\left(1, \left|\texttt{ndom}(Q^t\right|\right)$;
10: **end if**
11: **if** $SelectionScheme = (\mu +_{t_{size}} 1)$ **then**
12: $i_k \leftarrow U\left(1, \left|Q^t\right|\right)$;
13: **for** $k = 2, \ldots, t_{size}$ **do**
14: $i_{cur} \leftarrow U\left(1, \left|Q^t\right|\right)$;
15: **if** $i_{cur} < i_k$ **then**
16: $i_k \leftarrow i_{cur}$;
17: **end if**
18: **end for**
19: **end if**
20: **if** $SelectionScheme = (\mu + 1_{succ})$or $(\mu + 1_{rank})$or $(\mu + 1_{\Delta H_1})$or $(\mu + 1_{\Delta H_i})$ **then**
21: $i_k \leftarrow argmax_i\left(\hat{q}_{i_k,\bar{t}}\right)$;
22: **end if**
23: **return** i_k;

2. The exploration is enforced by selecting once every arm which i). occurs only once in the time window, and ii). is about to disappear from the time window (it was selected w time steps ago);

3. In all other cases, the selection is on the exploitation side, and the arm with best average reward along the last w time steps is selected. The constant factor C of Eq. (6.2) is set to 0.

In summary, the MAB-like selection always selects the parent with best average reward in the last w time steps, except for case 2 (a current parent is about to disappear from the time window). Parameter w thus controls the exploration strength of the selection. Experimentally however, the sensitivity of the algorithm w.r.t. w seems to be rather low, and w was set to 500 in all experiments (Section 6.2.2).

Figure 6.9 illustrates simple steps of MAB-based parent selection.

6.2.1.3 Defining Rewards

This Section describes the rewards underlying the MAB-like selection mechanism (Algorithm 6.6). A key related issue is how to share the reward between parents and offspring.

Algorithm 6.6: ComputeRewards

given $\boldsymbol{Q}^t, \boldsymbol{Q}^{t+1}, i^t_{parent}, i^{t+1}_{parent}, i^{t+1}_{offspring}, \overline{t}, W$
$r^{\overline{t}} \leftarrow 0$
if $i^{t+1}_{offspring} \leq \mu$ **then**
  // offspring will be inserted in population
  if $SelectionScheme = (\mu + 1_{succ})$ **then**
    $r^{\overline{t}} \leftarrow 1.0$
  end if
  if $SelectionScheme = (\mu + 1_{rank})$ **then**
    $r^{\overline{t}} \leftarrow 1.0 - \frac{i^t_{offspring}{}^{-1}}{\mu}$
  end if
  if $SelectionScheme = (\mu + 1_{\Delta H_1})$or $(\mu + 1_{\Delta H_i})$ **then**
    $\boldsymbol{F}^{t+1} \leftarrow NomDomFronts(\boldsymbol{Q}^{t+1})$
    $\boldsymbol{F}^{t} \leftarrow NomDomFronts(\boldsymbol{Q}^{t})$
    for $i = 1, \ldots, min(\left|\boldsymbol{F}^{t+1}\right|, \left|\boldsymbol{F}^{t}\right|)$ **do**
      $H_i \leftarrow \sum_{a^{t+1} \in \boldsymbol{F}^{t+1}_i} \Delta H(a^{t+1}, \boldsymbol{F}^{t+1}_i) - \sum_{a^t \in \boldsymbol{F}^t_i} \Delta H(a^t, \boldsymbol{F}^t_i)$
    end for
    if $SelectionScheme = (\mu + 1_{\Delta H_1})$ **then**
      $r^{\overline{t}} \leftarrow H_1$
    end if
    if $SelectionScheme = (\mu + 1_{\Delta H_i})$ **then**
      $r^{\overline{t}} \leftarrow \left\{ \frac{H_i}{2^{i-1}} | argmin_i(H_i > 0), 1 \leq i \leq |H_i| \right\}$
    end if
  end if
  $r^*_{i^{t+1}_{offspring}} \leftarrow r^*_{i^{t+1}_{offspring}} \cup \left\{ r^{\overline{t}} \right\}$
end if
if $i^{t+1}_{parent} \leq \mu$ **then**
  // parent remains in population
  $r^*_{i^{t+1}_{parent}} \leftarrow r^*_{i^{t+1}_{parent}} \cup \left\{ r^{\overline{t}} \right\}$
end if
for $i = 1, \ldots, \mu$ **do**
  if $r^{\overline{t}-W} \in r^*_i$ **then**
    $r^*_i \leftarrow r^*_i \backslash \left\{ r^{\overline{t}-W} \right\}$
  end if
  $n_{i,\overline{t}} \leftarrow |r^*_i|$
  if $n_{i,\overline{t}} = 0$ **then**
    $n_{i,t} \leftarrow 1$
    $\widehat{q}_{i,\overline{t}} \leftarrow 1.0$
  else
    $\widehat{q}_{i,\overline{t}} \leftarrow \frac{1}{n_{i,\overline{t}}} \sum_{r \in r^*_i} r$
  end if
end for

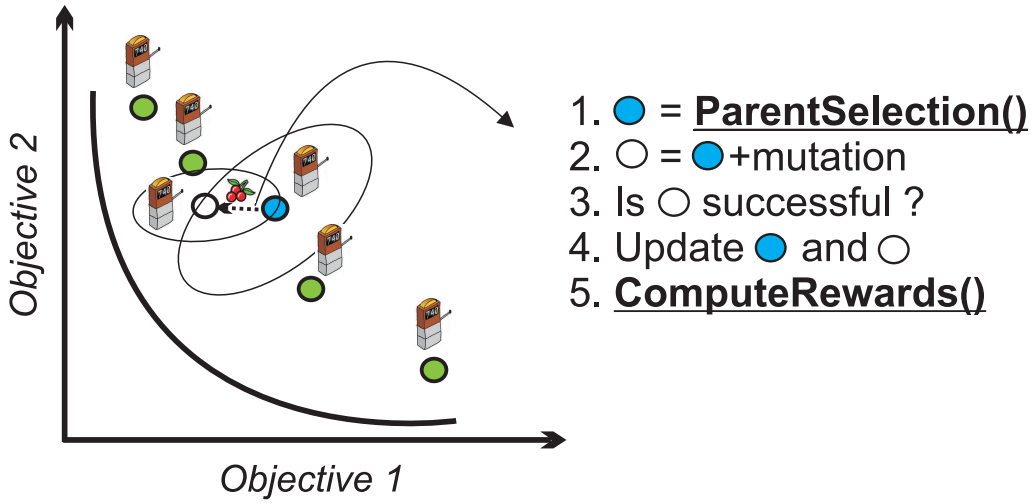

Figure 6.9: Multi-Armed Bandits-based parent selection.

On the one hand, if an offspring survives, it is better that some old parents and might thus be a good starting point for further advances toward the Pareto front. The offspring must thus inherit a sufficient fraction of its parent reward, to enable its exploitation. On the other hand, the reward of a parent should be high when it yields good-performing offspring, and in particular no reward should be awarded to the parent if the newborn offspring does not survive. Several reward indicators have been considered.

$(\mu + 1_{succ})$

A first possibility is to consider boolean rewards. If an offspring makes it to the next generation, both the offspring and the parent receive reward 1 (line 6 of Algorithm 6.6). Formally:

$$r^{\overline{t}} = 1.0 \text{ if } \boldsymbol{a}_1'^{t+1} \in \boldsymbol{Q}^{t+1}$$

Such boolean rewards entail a very "greedy" behavior. The newborn offspring, receiving 1 as instant reward, gets 1 as average reward over the time window; it will thus very rapidly (if not immediately) be selected at next parent. Likewise, its parent which already had a top average reward (it was selected), will improve its average reward and tend to be selected again.

$(\mu + 1_{rank})$

A smoother reward is defined by taking into account the rank of the newly inserted offspring (line 9):

$$r^{\overline{t}} = 1.0 - \frac{rank(\boldsymbol{a}_1'^{t+1}) - 1}{\mu} \text{ if } \boldsymbol{a}_1'^{t+1} \in \boldsymbol{Q}^{t+1}$$

where $rank(\boldsymbol{a}_1'^{t+1})$ is the rank of the newly inserted offspring in population $\boldsymbol{Q}^{t+1}$ (using comparison operator $\prec_{\boldsymbol{Q}^t}$ defined by Eq. (2.9); the top individual gets rank 0). Along this line, the reward ranges linearly from 1 (for a non-dominated individual with best hypervolume contribution) to 0. A newborn offspring will here be selected rapidly only if

it makes it into the top-ranked individuals of the current population. The average reward of the parent can decrease if its offspring gets a poor rank, even if the offspring survives.

$(\mu + 1_{\Delta H_1})$

Another way of getting smooth rewards is based on the hypervolume contribution of the offspring. Let us set the reward to 0 for dominated offspring (noting that most individuals are non-dominated at the end of evolution); for non-dominated offspring, one sets the reward to the increase of the total hypervolume contribution from generation t to $t+1$ (line 18):

$$r^{\overline{t}} = \sum_{a \in \boldsymbol{Q}^{t+1}} \Delta H(a, \boldsymbol{Q}^{t+1}) - \sum_{a \in \boldsymbol{Q}^{t}} \Delta H(a, \boldsymbol{Q}^{t})$$

$(\mu + 1_{\Delta H_i})$

In the early stages of evolution, many offspring are dominated and the above hypervolume-based reward thus gives little information. A relaxation of the above reward, involving a rank-based penalization is thus defined. Formally, if k denote the Pareto rank of the current offspring, the reward is (line 21):

$$r^{\overline{t}} = \frac{1}{2^{k-1}} \left(\sum_{a \in ndom_k(\boldsymbol{Q}^{t+1})} \Delta H(a, ndom_k(\boldsymbol{Q}^{t+1})) - \sum_{a \in ndom_k(\boldsymbol{Q}^{t})} \Delta H(a, ndom_k(\boldsymbol{Q}^{t})) \right)$$

After the reward $r^{\overline{t}}$ is estimated using one of the described above strategies, it should be added to a list of rewards $r^*_{i^{t+1}_{offspring}}$ of offspring $i^{t+1}_{offspring}$ (line 24) and to a list of rewards $r^*_{i^{t+1}_{parent}}$ of parent i^{t+1}_{parent}. Of course, adding the reward makes sense only if the parent survives ($i^{t+1}_{parent} \leq \mu$) and/or offspring survives ($i^{t+1}_{offspring} \leq \mu$). Note that the newly created offspring inherits its parent's list of rewards. For each individual i the list of rewards r^*_i should be shrinked to a size of time window W (line 32). If the new size $n_{i,t}$ (line 34) of the list is 0 (i.e., i-th individual was checked last time at least W time steps ago), then we reward i-th individual by 1 (lines 36-37) to be very likely selected in the next generation. If the list of rewards is not null, then the average reward $\widehat{q}_{i,\overline{t}}$ is computed in line 39 to be used later in parent selection in line 21 of Algorithm 6.5.

6.2.1.4 Discussion

The difficulty of associating a reward to a pair (parent, offspring) in Multi-Objective optimization is twofold. On the one hand, defining absolute indicators (e.g., reflecting some aggregation of the objective values) goes against the very spirit of MO. On the other hand, relative indicators such as above-defined must be taken with care: they give a snapshot of the current situation, which evolves along the population progresses toward the Pareto front. The well-founded Multi-Armed Bandit setting, and its trade-off between exploration and exploitation, must thus be modified to account for non-stationarity.

Another difficulty is related to the finiteness of the population: while new arms appear, some old arms must disappear. The parent selection, e.g., based on the standard deterministic selection ($\prec_{\boldsymbol{Q}^t}$) is biased toward exploitation as it does not offer any way of "cooling

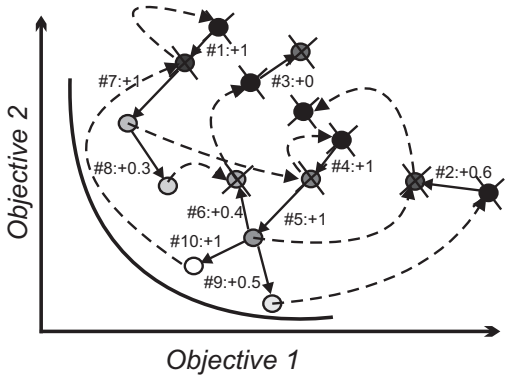

Figure 6.10: Reward-based multi-objective optimization with bounded population. "#6:+0.4" means reward 0.4 on 6th iteration.

down" the process. Such a bias is illustrated in Figure 6.10. Let the population size of a steady-state EMOA be 5, and consider a sequence of 10 evolution steps, generating 10 new points oldest (respectively, newest) points are black (respectively, white). At each iteration the parent with best reward generates an offspring, then 6 points are compared using $\prec_{Q^t}$, and the worst point (crossed out) is eliminated. The instant parent reward reflects the quality of the offspring. Along evolution, some prospective points/arms are thus eliminated because they progress more slowly than others, although they do progress, due to the fixed population size. Expectedly, this bias toward exploitation adversely affects the discovery of multi-modal and/or disconnected Pareto front. We will also discuss this issue in Section 6.2.3.

6.2.2 Experimental Validation

This Section reports the experimental validation of the proposed schemes, comparatively to the baseline MO-CMA-ES algorithms, detailing the experimental setting in Section 6.2.2.1 before discussing the experimental evidence in Section 6.2.2.3.

6.2.2.1 Experimental Setting

Algorithms.

The experiments involve:

- The steady-state MO-CMA-ES with tournament-based parent selection, where the tournament size t_{size} is set to 2 or 10 (respectively noted $(\mu +_2 1)$ and $(\mu +_{10} 1)$);
- The steady-state MO-CMA-ES with MAB-based parent selection, considering the four rewards described in Section 6.2.1.2 (respectively noted $(\mu + 1_{succ})$, $(\mu + 1_{rank})$, $(\mu + 1_{\Delta H_1})$ and $(\mu + 1_{\Delta H_i})$);

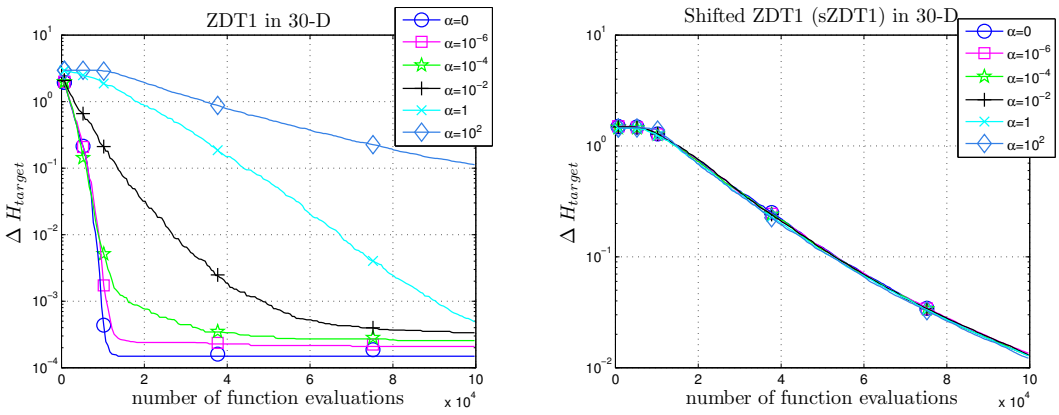

Figure 6.11: MO-CMA-ES on 30-dimensional **(Left)** ZDT1 problem and **(Right)** Shifted ZDT1 (sZDT1) problem for different settings of the penalty parameter α.

- The baseline algorithms include the generational $(\mu + \mu)$-MO-CMA and its steady-state variants $(\mu + 1)$-MO-CMA and $(\mu_{\prec} + 1)$-MO-CMA (see Section 2.4.4).

All parameters of MO-CMA-ES are set to their default values [Igel *et al.*, 2007b] (in particular, $\mu = 100$); all algorithms only differ by their parent selection procedure. All reported results are based on 31 independent runs with at most 200,000 fitness evaluations. Median results are reported when the target precision was reached.

Problems.

The well-known bi-criteria ZDT1:3-6 and their rotated variants IHR1:3-6 have been considered. Note however that the true Pareto front of all ZDT problems lies on the boundary of the decision space, which might make it easier to discover. For the sake of an unbiased assessment, the true Pareto front is thus shifted in decision space: $\boldsymbol{x}'_i \leftarrow |\boldsymbol{x}_i - 0.5|$ for $2 \leq i \leq n$, where n is the problem dimension. The shifted ZDT problems are denoted sZDT.

The set of recently proposed benchmark problems LZ09-1:5 [Li and Zhang, 2009] have also been used for their complicated Pareto front in decision space (Figure 6.14).

The performance assessment procedure described in Section 2.4.5 is used.

6.2.2.2 Constraints Handling in MO-CMA-ES

In the original paper on MO-CMA-ES ([Igel *et al.*, 2007b]) the following box-constraints handling procedure was used. Consider an optimization problem with m objectives $f_1, \ldots, f_m : X \mapsto \mathbb{R}$ with $X = [x_1^l, x_1^u] \times \ldots \times [x_n^l, x_n^u] \subset \mathbb{R}^n$. For $\boldsymbol{x} \in \mathbb{R}^n$ let feasible($\boldsymbol{x}$)= $(\min(\max(x_1, x_1^l), x_1^u), \ldots, \min(\max(x_n, x_n^l), x_n^u))^T$. The penalized fitness is defined as follows:

$$f_m^{penalty}(\boldsymbol{x}) = f_m(feasible(\boldsymbol{x})) + \alpha||\boldsymbol{x} - feasible(\boldsymbol{x})||_2^2, \tag{6.3}$$

where $\alpha > 0$ is a penalty parameter. [Igel *et al.*, 2007b] suggest to set $\alpha = 10^{-6}$.

In order to investigate the performance of MO-CMA-ES depending on the choice of α we run the algorithm on ZDT1 problem. The results shown in Figure 6.11-**Left** confirms that MO-CMA-ES is very sensitive to the value of α. MO-CMA-ES demonstrates almost identical behaviour for $\alpha = 10^{-6}$ and $\alpha = 0$ which can be interpreted as follows. (1+1)-CMA-ES algorithm of the initial population relatively often samples offspring outside of the box-constraint due to a relatively large step-size σ. The objective values of these offspring are computed and penalized by a small location-based value proportional to α. For a particular case of ZDT problems, where the Pareto front lies on the boundary of the decision space, each box-outlier x_i translates back in the feasible region, i.e., directly on the Pareto front for x_1 (given that ZDT problems are separable). In other words, MO-CMA-ES samples points outside of the box and translates them back on the Pareto front without significant penalization. This process can be clearly seen for small α in Figure 6.11-**Left**. In order to make penalization "more realistic" we may increase α, and as can be seen, it significantly worsen the results. Roughly speaking, there are different types of constraint handling techniques, depending on whether the constraints tend to "repel" candidate solutions (that corresponds to large α), or to "attract" candidate solutions (that corresponds to small α). We argue that a reasonable value for α for ZDT1 problem (α is problem-dependent) should be in the order of 1 rather than in order of 10^{-6}. Indeed, in this case, some trade-off of "repel"/"attract" effects can be achieved such that the influence of both is relatively negligible and the solution of ZDT1 can be found almost as fast as the one of sZDT1 (a shifted variant of ZDT1). This is visible when looking at the evolution of the hypervolume indicator for MO-CMA-ES with $\alpha = 1$ on ZDT1 and MO-CMA-ES with different α on sZDT1 at the point of 40.000 functions evaluations on Figure 6.11-**Right**. As can be seen, the results of MO-CMA-ES on shifted ZDT1 function (sZDT1) (as well as on IHR functions) are insensitive to α ... and the case $\alpha = 1$ for ZDT1 corresponds to a very similar behavior (though this is by no mean a proof).

We argue that the results of MO-CMA-ES on ZDT problems presented in [Igel *et al.*, 2007b] and several following papers should be reviewed and/or interpreted w.r.t. the choice of α.

Note that a better box-constraints handling may be obtained by replacing the original (1+1)-CMA-ES by the recently proposed prospective version of (1+1)-CMA-ES for constrained optimization [Arnold and Hansen, 2012], and this will be a part of our further work.

6.2.2.3 Result Analysis

All empirical results are displayed in Table 6.1. These results show that the proposed algorithms generally outperform the baseline MO-CMA-ES approaches, with the exception of problems sZDT3, IHR6 and LZ09-5. A first general remark is that the steady-state variants of MO-CMA-ES outperform the generational one on unimodal benchmark problems; as already noted in [Igel *et al.*, 2007a], the greedier $(\mu_{\prec} + 1)$-MO-CMA is usually faster than the original steady-state on sZDT and IHR problems; in counterpart, it is too "greedy" on LZ09 problems (see below). Another general remark is that $(\mu + 1_{\Delta H_i})$-MO-CMA is usually more robust and faster than $(\mu+1_{\Delta H_1})$-MO-CMA; this fact is explained as

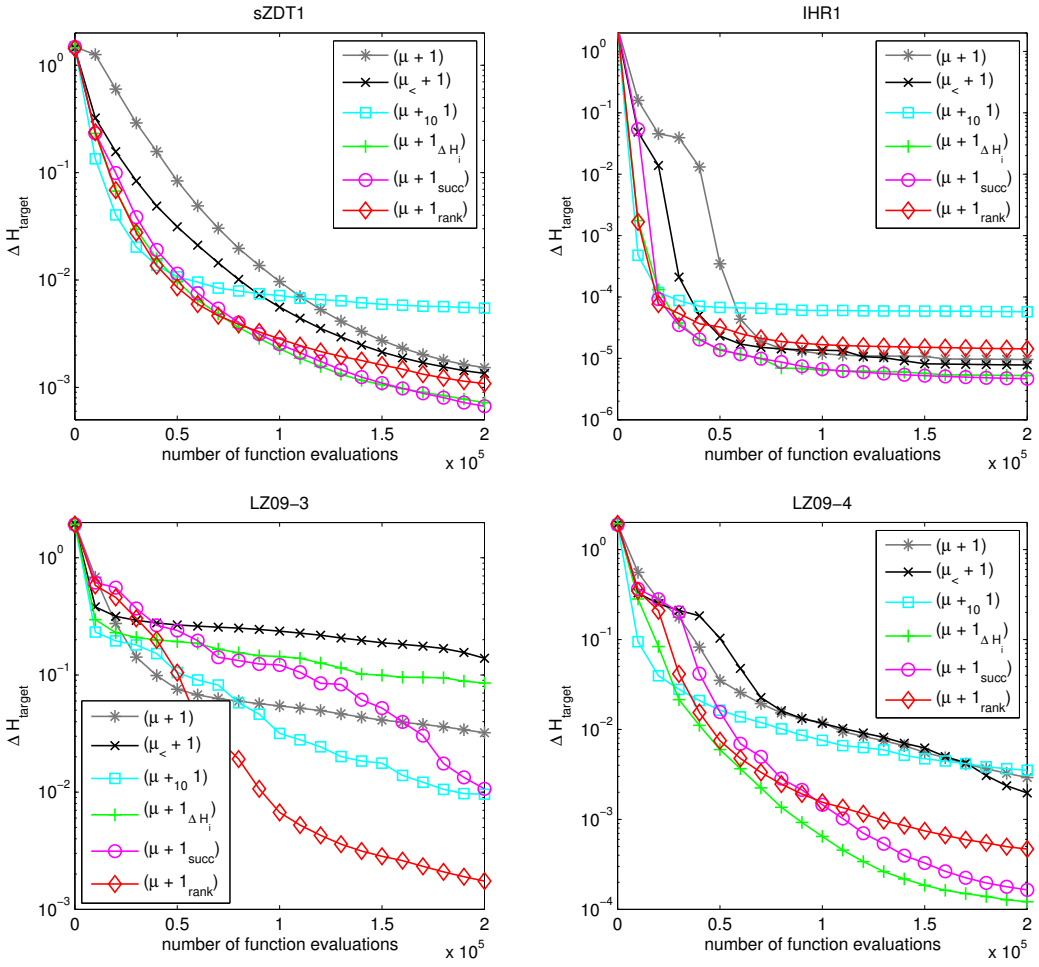

Figure 6.12: On-line performances of baseline and proposed variants of steady-state MO-CMA-ES on sZDT1, IHR1, LZ09-3 and LZ09-4 problems (median out of 31 runs).

the former exploit a better informed hypervolume contribution-based reward, considering also the contribution of dominated points.

The on-line performance of most considered algorithms on sZDT1, IHR1, LZ09-3 and LZ09-4 shows the general robustness of $(\mu + 1_{rank})$-MO-CMA (Figure 6.12, displaying $\Delta H(P^*, P)$ versus the number of function evaluations). The comparatively disappointing results of $(\mu+1)$-MO-CMA on IHR1 are explained from the structure of the Pareto front, which includes an easy-to-find segment. This segment can be discovered by selecting the extreme parent (in objective space), thus with probability $1/\mu$ within a uniform selection scheme. Quite the contrary, reward-based selection schemes quickly catch the fruitful directions of search.

The price to pay for this is depicted in Figure 6.13, showing $(\mu + 1_{succ})$-MO-CMA

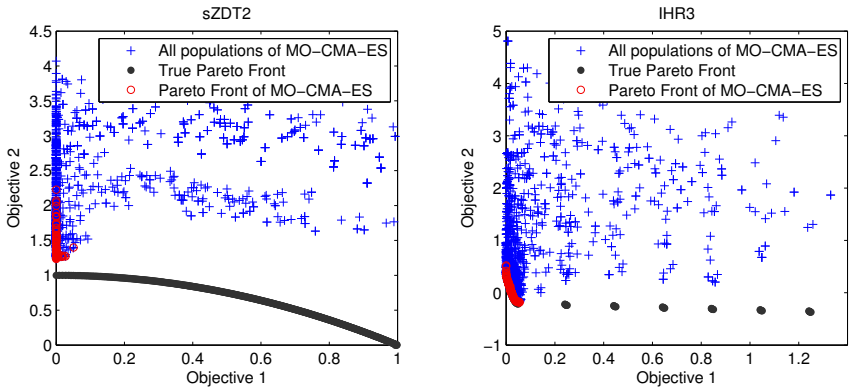

Figure 6.13: Typical behavior of $(\mu+1_{succ})$-MO-CMA on sZDT2 (**Left**) and IHR3 (**Right**) problems: premature convergence after 5,000 fitness function evaluations.

on sZDT2 and IHR3 problems. On these problems, a premature convergence toward a small segment of the Pareto front is observed after circa 5,000 function evaluations. The interpretation provided for this premature convergence goes as follows. As one part of the Pareto front is easier to find than others, points aiming at this part quickly reach their goal; due to non-dominated sorting (and to the fixed population size), these eliminate other points, resulting in a very poor diversity (in objective space) of the population. This remark suggests that some additional diversity preserving technique should be used together with MO-CMA-ES; note that, even in the original MO-CMA-ES, a premature convergence is observed on IHR3.

LZ09 problems have also been considered because of their non-linear Pareto front in decision space (Figure 6.14), contrasting with the linear Pareto front of all sZDT and IHR problems. The results depicted in Figure 6.14 show that $(\mu + 1_{rank})$-MO-CMA better approximates the Pareto front than $(\mu + 1)$ and $(\mu +_{10} 1)$-MO-CMA, for all problems except LZ09-5. It is interesting to note that the results of $(\mu + 1_{rank})$-MO-CMA after 100,000 fitness evaluations match those of MOEA/D-DE after 150,000 fitness evaluations [Li and Zhang, 2009].

Overall (see also Table 6.1), $(\mu + 1_{rank})$-MO-CMA and $(\mu +_{10} 1)$-MO-CMA perform best on most problems, while $(\mu+1_{\Delta H_i})$-MO-CMA is slightly more robust. Most generally, all "greedy" versions of MO-CMA-ES get better results on problems with a convex Pareto front; on problems with a concave or disconnected Pareto front, they suffer from premature convergence, entailed by a loss of diversity, due to non-dominated sorting and bounded population size.

6.2.3 Conclusion and Perspectives

The goal and main contribution of the Section is to speed up MO-CMA-ES using new parent selection schemes, based on tournament and reward-based approaches inspired from the Multi-Armed Bandit framework, in order to quickly identify the most fruitful directions

Table 6.1: Comparative results of two baseline EMOAs, namely generational and steady-state MO-CMA-ES and several versions of steady-state MO-CMA-ES with different parent selection schemes. Median number of function evaluations (out of 31 independent runs) to reach ΔHtarget values, normalized by Best: a value of 1 indicates the best result, a value $X > 1$ indicates that the corresponding algorithm needed X times more evaluations than the best to reach the same precision.

ΔHtarget	1	0.1	0.01	1	0.1	0.01	1	0.1	0.01	1	0.1	0.01
	sZDT1			sZDT2			sZDT3			sZDT6		
Best	2500	12000	47000	2500	15000	59000	3000	18500	70000	4500	141200	.
$(\mu+\mu)$	7.3	4.3	2.2	8.6	4.3	2.1	5.5	3	1.5	8.2	**1**	.
$(\mu+1)$	6.5	3.9	2.1	7.6	3.9	2	5.1	2.8	1.4	7.2	1.1	.
$(\mu_{\prec}+1)$	1.5	2.2	1.7	**1**	2	1.5	1.3	1.8	1.2	**1**	.	.
$(\mu+_2 1)$	3.7	2.4	1.5	4.4	2.4	1.4	3.1	1.7	**1**	4.3	.	.
$(\mu+_{10} 1)$	1.2	**1**	1.1	1.4	**1**	1.3	**1**	**1**	.	1.3	.	.
$(\mu+1_{\Delta H_1})$	3.5	1.5	**1**	3.4	1.6	**1**	2.5	.	.	1.7	.	.
$(\mu+1_{\Delta H_i})$	1.7	1.3	**1**	1.8	1.3	**1**	1.1	.	.	1.5	.	.
$(\mu+1_{succ})$	1.2	1.7	1.1	1.6	.	.	**1**	.	.	2.1	.	.
$(\mu+1_{rank})$	**1**	1.4	**1**	1.4	.	.	**1**	.	.	1.7	.	.
	IHR1			IHR2			IHR3			IHR6		
Best	500	1500	6000	1500	4000	8500	1000	.	.	6000	.	.
$(\mu+\mu)$	8.4	8.8	6.9	6.4	4.8	3.3	8.2	.	.	5.6	.	.
$(\mu+1)$	7	7.3	6.7	5.6	4.1	2.9	7	.	.	5	.	.
$(\mu_{\prec}+1)$	**1**	**1**	3	**1**	1.6	1.7	**1**	.	.	**1**	.	.
$(\mu+_2 1)$	4	4.3	4	3.3	2.5	1.9	4	.	.	3	.	.
$(\mu+_{10} 1)$	2	1.6	1.1	**1**	**1**	**1**	**1**	.	.	**1**	.	.
$(\mu+1_{\Delta H_1})$	2	1.6	**1**	2	1.5	1.2	2.5	.	.	1.4	.	.
$(\mu+1_{\Delta H_i})$	2	2.3	**1**	1.3	1.3	1.1	1.5	.	.	1.2	.	.
$(\mu+1_{succ})$	2	2.3	2	5.3	2.7	1.7	1.5	.	.	1.9	.	.
$(\mu+1_{rank})$	2	2	1.5	1.6	1.7	1.3	1.5	.	.	1.6	.	.
	LZ09-1			LZ09-2			LZ09-3			LZ09-4		
Best	500	6000	17000	3500	144000	.	1500	35000	120500	1000	10000	40500
$(\mu+\mu)$	11.4	5.1	3.2	3.6	.	.	4.1	1.2	.	5.7	3.2	2.4
$(\mu+1)$	9	4.7	3	3.2	.	.	3.6	**1**	.	5	3.9	2.5
$(\mu_{\prec}+1)$	2	2.5	2.2	**1**	.	.	**1**	.	.	**1**	4.3	2.3
$(\mu+_2 1)$	6	2.8	1.9	2.2	.	.	2.3	1.7	.	3.5	2.7	1.9
$(\mu+_{10} 1)$	2	**1**	**1**	**1**	.	.	**1**	1.4	1.4	1.5	**1**	2
$(\mu+1_{\Delta H_1})$	9	2.1	1.5	2	.	.	1.6	5.6	.	2	1.8	**1**
$(\mu+1_{\Delta H_i})$	2	1.5	1.3	2.1	**1**	.	2	4.2	.	2.5	1.5	**1**
$(\mu+1_{succ})$	**1**	2.1	1.4	3.5	.	.	1.3	3.6	.	2	3.5	1.3
$(\mu+1_{rank})$	**1**	1.9	1.3	5.8	1.1	.	1.3	1.6	**1**	1.5	2.4	**1**
	LZ09-5											
Best	1500	19000	.									
$(\mu+\mu)$	3.4	1.6	.									
$(\mu+1)$	3.3	1.4	.									
$(\mu_{\prec}+1)$	**1**	.	.									
$(\mu+_2 1)$	2	**1**	.									
$(\mu+_{10} 1)$	**1**	1.7	.									
$(\mu+1_{\Delta H_1})$	1.3	.	.									
$(\mu+1_{\Delta H_i})$	1.6	1.9	.									
$(\mu+1_{succ})$	1.3	.	.									
$(\mu+1_{rank})$	**1**	.	.									

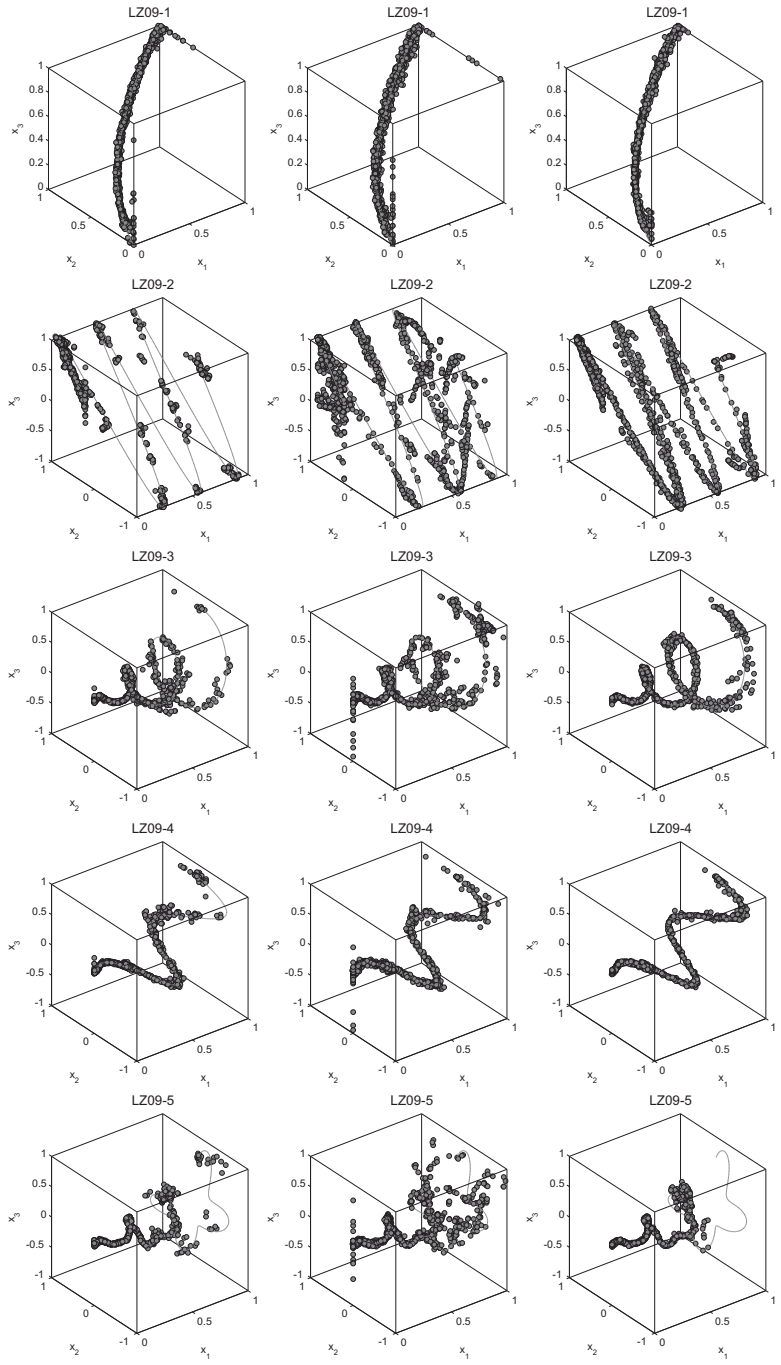

Figure 6.14: Plots of all 10 populations found by $(\mu+1)$-MO-CMA (**Left**), $(\mu+_{10}1)$-MO-CMA (**Center**) and $(\mu+1_{rank})$-MO-CMA (**Right**) in the $x_1 - x_2 - x_3$ space on LZ09-1:5 after 100,000 function evaluations.

of search. Experiments on several bi-objective problems have shown a significantly speedup of MO-CMA-ES on unimodal problems (for both generational and previous steady-state variants). However, the proposed approach results in a poor convergence on multi-modal multi-objective problems, or problems where some parts of the Pareto front are much easier to reach than others, such as IHR3 (Figure 6.13, and discussion in Sections 6.2.1.4 and 5.4.3).

These remarks open some perspectives for further research, aimed at preserving the benefits of parent selection schemes while addressing the premature convergence on multi-modal landscapes. A first perspective is to maintain the points located at the border of the already visited region, and to give them some chance to produce offspring as well although they are dominated. The question thus becomes to handle yet another exploration vs exploitation dilemma, and distribute the fitness evaluations between the current population and the borderline points; it also remains to extend the reward definition for the borderline points. Such an approach is similar in spirit to the so-called BIPOP-CMA-ES designed to overcome premature convergence within single-objective evolutionary optimization [Hansen *et al.*, 2010b]; BIPOP-CMA-ES proceeds by maintaining one large population for exploration purposes, and a small one for fast and accurate convergence, for exploitation purposes.

A second perspective is to design a more integrated multi-objective CMA-ES based algorithm, by linking the reward mechanism used in the parent selection and the internal update rules of CMA-ES. Indeed, the success rate used to control the $(1+1)$-ES evolution and the empirical success expectation used in $(\mu + 1_{succ})$-MO-CMA are strongly related. Further work will consider how to use the success rate *in lieu* of reward for parent selection, expectedly resulting in a more consistent evolution progress. Meanwhile, the CMA update rules might want to consider the discarded offspring (possibly weighting their contribution depending on their hypervolume contribution), since they might contain useful information even though they are discarded.

Last but not least, the MO-CMA-ES and the proposed parent selection schemes must be analyzed and compared with other state-of-the art MOEAs, specifically SMS-EMOA [Emmerich *et al.*, 2005], the first algorithm, to our best knowledge, to advocate the use of steady state within EMO; it also proposed separable variation operators, resulting in excellent results comparatively to MO-CMA-ES on separable problems. How to extend these variation operators in the non-separable case, following ideas of Adaptive Encoding will also be investigated.

6.3 Alternative Restart Strategies for CMA-ES

This Section focuses on analyzing and improving the restart strategy of CMA-ES (IPOP and BIPOP), viewed as a noisy hyper-parameter optimization problem in a 2-dimensional space (population size, initial step-size). Two restart strategies are defined. The first one, NIPOP-aCMA-ES (for *New* IPOP-aCMA-ES), differs from IPOP-CMA-ES as it simultaneously increases the population size and decreases the step size. The second one, NBIPOP-aCMA-ES, allocates computational power to different restart settings de-

pending on their current results. While these strategies have been designed with the BBOB benchmarks in mind [Hansen *et al.*, 2012], their generality is also demonstrated on an independent real-world problem suite related to spacecraft trajectory optimization [Vinko and Izzo, 2008].

The Section is organized as follows. The original restart strategies and their analysis are presented in Sections 6.3.1 and 6.3.2, respectively. The proposed restart schemes are described in Section 6.3.3. Section 6.3.4 reports on their experimental validation. The Section concludes with a discussion and some perspectives for further research.

6.3.1 The CMA-ES with Restarts: IPOP and BIPOP CMA-ES

CMA-ES has been extended with restart strategies to accommodate multi-modal fitness landscapes, and to specifically handle objective functions with many local optima. As observed by [Hansen and Kern, 2004], the probability of reaching the optimum (and the overall number of function evaluations needed to do so) is very sensitive to the population size. The default population size $\lambda_{default}$ has been tuned for unimodal functions; it is hardly large enough for multi-modal functions. Accordingly, [Auger and Hansen, 2005] proposed a "doubling trick" restart strategy to enforce global search: the restart $(\mu/\mu_w, \lambda)$-CMA-ES with increasing population, called IPOP-CMA-ES, is a multi-restart strategy where the population size of the run is doubled at each restart until meeting a stopping criterion.

The BIPOP-CMA-ES instead considers two restart regimes. The first one, which corresponds to IPOP-CMA-ES, doubles the population size at every restart $i_{restart}$ ($\lambda_{large} = 2^{i_{restart}} \lambda_{default}$) and uses an initial step-size $\sigma^0_{large} = \sigma^0_{default}$.
The second regime uses a small population size λ_{small} and initial step-size σ^0_{small}, which are randomly drawn in each restart as:

$$\lambda_{small} = \left\lfloor \lambda_{default} \left(\frac{1}{2} \frac{\lambda_{large}}{\lambda_{default}} \right)^{U[0,1]^2} \right\rfloor, \quad \sigma^0_{small} = \sigma^0_{default} \times 10^{-2U[0,1]} \tag{6.4}$$

where $U[0,1]$ stands for the uniform distribution in $[0,1]$. Population size λ_{small} thus varies in $[\lambda_{default}, \lambda_{large}/2]$. BIPOP-CMA-ES launches the first run with default population size and initial step-size. In each restart, it selects the restart regime with less function evaluations used so far. Clearly, the second regime consumes less function evaluations than the doubling regime; it is therefore launched more often.

6.3.2 Preliminary Analysis

The restart strategies of IPOP- and BIPOP-CMA-ES can be viewed as a search in the hyper-parameter space.

IPOP-CMA-ES only aims at adjusting population size λ. It is motivated by the results observed on multi-modal problems [Hansen and Kern, 2004], suggesting that the population size must be sufficiently large to handle problems with global structure. In such cases, a large population size is needed to uncover this global structure and to lead the algorithm to discover the global optimum. IPOP-CMA-ES thus increases the population size in each

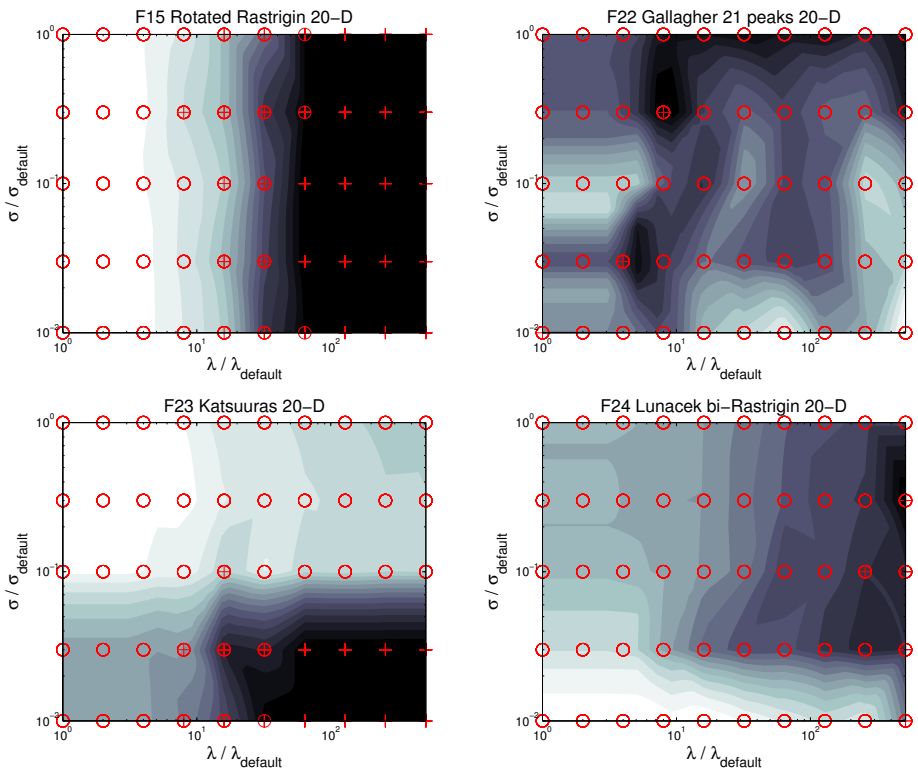

Figure 6.15: Restart performances in the 2-dimensional hyper-parameter space (population size and initial mutation step size in log. coordinates). For each 20-dimensional objective function (Rastrigin - **Top-Left**, Gallagher 21 peaks - **Top-Right**, Katsuuras - **Bottom-Left** and Lunacek bi-Rastrigin **Bottom-Right**), the median best function value out of 15 runs is indicated. Legends indicate that the optimum of the objective function up to precision $f(x) = 10^{-10}$ is found always ($+$), at least once ($\oplus$) or never ($\circ$). Black regions are better than white ones.

restart, irrespective of the results observed so far; at each restart, it launches a new CMA-ES with population size $\lambda = \rho_{inc}^{i_{restart}} \lambda_{default}$ (see $\circ$ in Figure 6.15). Factor ρ_{inc} must be not too large to avoid "overjumping" some possibly optimal population size λ^*; it must also be not too small in order to reach λ^* in a reasonable number of restarts. The use of the doubling trick ($\rho_{inc} = 2$) guarantees that the loss in terms of function evaluations (compared to the "oracle" restart strategy which would directly set the population size to the optimal value λ^*) is at most about a factor of 2.

On the Rastrigin 20-D function, IPOP-CMA-ES performs well and always finds the optimum after about 5 restarts (Figure 6.15, **Top-Left**). The Rastrigin function displays indeed a global structure where the optimum is the minimizer of this structure. For such functions, IPOP-CMA-ES certainly is the method of choice. For some other functions such as the Gallagher function, there is no such global structure; increasing the population size

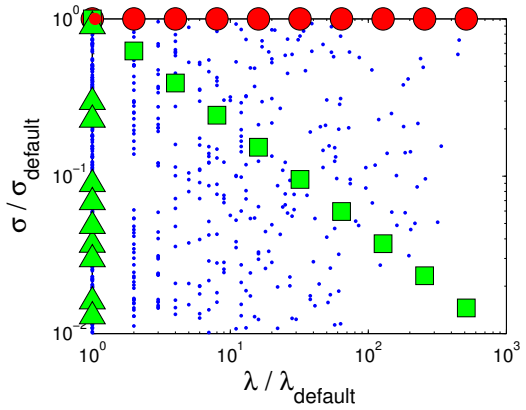

Figure 6.16: An illustration of λ and σ hyper-parameters distribution for 9 restarts of IPOP-aCMA-ES ($\circ$), BIPOP-aCMA-ES ($\circ$ and $\cdot$ for 10 runs), NIPOP-aCMA-ES ($\square$) and NBIPOP-aCMA-ES ($\square$ and many $\triangle$ for $\lambda/\lambda_{default} = 1$, $\sigma/\sigma_{default} \in [10^{-2}, 10^{0}]$). The first run of all algorithms corresponds to the point with $\lambda/\lambda_{default} = 1$, $\sigma/\sigma_{default} = 1$.

does not improve the results. On Katsuuras and Lunacek bi-Rastrigin functions, the optimum can only be found with small initial step-size (lesser than the default one); this explains why it can be solved by BIPOP-CMA-ES, sampling the two-dimensional (λ, σ) space.

Actually, the optimization of a multi-modal function by CMA-ES with restarts can be viewed as the optimization of the function $h(\theta)$, which returns the optimum found by CMA-ES defined by the hyper-parameters θ=(λ, σ). Function $h(\theta)$, graphically depicted in Figure 6.15 can be viewed as a black box, computationally expensive and stochastic function (reflecting the stochasticity of CMA-ES). Both IPOP-CMA-ES and BIPOP-CMA-ES are based on implicit assumptions about $h(\theta)$: IPOP-CMA-ES achieves a deterministic uni-dimensional trajectory, and BIPOP-CMA-ES randomly samples the 2-dimensional search space.

Function $h(\theta)$ also can be viewed as a multi-objective fitness, since in addition to the solution found by CMA-ES, $h(\theta)$ could return the number of function evaluations needed to find that solution. $h(\theta)$ could also return the computational effort SP1 (i.e., the average number of function evaluations of all successful runs, divided by proportion of successful runs). However, SP1 can only be known for benchmark problems where the optimum is known; as the empirical optimum is used in lieu of true optimum, SP1 can only be computed *a posteriori*.

6.3.3 Alternative Restart Strategies

Two new restart strategies for CMA-ES, respectively referred to as NIPOP-aCMA-ES and NBIPOP-aCMA-ES, are presented.

If the restart strategy is restricted to the case of increasing population size (IPOP),

we propose to use NIPOP-aCMA-ES, where we additionally decrease the initial step-size by some factor $\rho_{\sigma dec}$. The rationale behind this approach is that the CMA-ES with relatively small initial step-size is able to explore small basins of attraction (see Katsuuras and Lunacek bi-Rastrigin functions in Figure 6.15), while with initially large step-size and population size, it will neglect the local structure of the function, but converge to the minimizer of the global structure. Moreover, initially, relatively small step-size will quickly increase if it makes sense, and this will allow the algorithm to recover the same global search properties than with initially large step-size (see Rastrigin function in Figure 6.15).

NIPOP-aCMA-ES thus explores the two-dimensional hyper-parameter space in a deterministic way (see □ symbols in Figure 6.16). For $\rho_{\sigma dec} = 1.6$ used in this study, NIPOP-aCMA-ES thus reaches the lower bound ($\sigma = 10^{-2}\sigma_{default}$) used by BIPOP-CMA-ES after 9 restarts, expectedly reaching the same performance as BIPOP-CMA-ES albeit using only a large population.

The second restart strategy, NBIPOP-aCMA-ES, addresses the case where the probability to find the global optimum does not much vary in the (λ, σ) space. Under this assumption, it makes sense to have many restarts for a fixed budget (number of function evaluations). Specifically, NBIPOP-aCMA-ES implements the competition of the NIPOP-aCMA-ES strategy (increasing λ and decreasing initial σ^0 in each restart) and a uniform sampling of the σ space, where λ is set to $\lambda_{default}$ and $\sigma^0 = \sigma^0_{default} \times 10^{-2U[0,1]}$ The selection between both regimes (NIPOP-aCMA-ES and the uniform sampling) depends on the allowed budget, like in BIPOP-aCMA-ES. The difference is that NBIPOP-aCMA-ES adaptively sets the budget allowed to each restart strategy, where the restart strategy leading to the overall best solution found so far is allowed twice ($\rho_{budget} = 2$) the budget given to the other strategy.

6.3.4 Experimental Validation

The experimental validation of NIPOP-aCMA-ES and NBIPOP-aCMA-ES investigates the performance of the approach comparatively to IPOP-aCMA-ES and BIPOP-aCMA-ES on BBOB noiseless problems and one black-box real-world problem related to spacecraft trajectory optimization. The default parameters of CMA-ES [Hansen and Ros, 2010a, Hansen, 2009] are used. This Section also presents the first experimental study of BIPOP-aCMA-ES[2], the active version of BIPOP-CMA-ES [Hansen, 2009].

6.3.4.1 Performance on Rastrigin Function

Figure 6.17 shows one run of NIPOP-aCMA-ES on 20-dimensional Rastrigin function, where 6 restart were performed before reaching the target objective function (cyan curve) value 10^{-8}. It should be noted that NIPOP-aCMA-ES finds the optimum even with each restart smaller and smaller initial step-sizes (green curve), and it can be clearly seen that the initially small step-size quickly increases and reaches an "appropriate" value. This is

[2]For the sake of reproducibility, the source code for NIPOP-aCMA-ES and NBIPOP-aCMA-ES is available at `https://sites.google.com/site/ppsnbipop/`

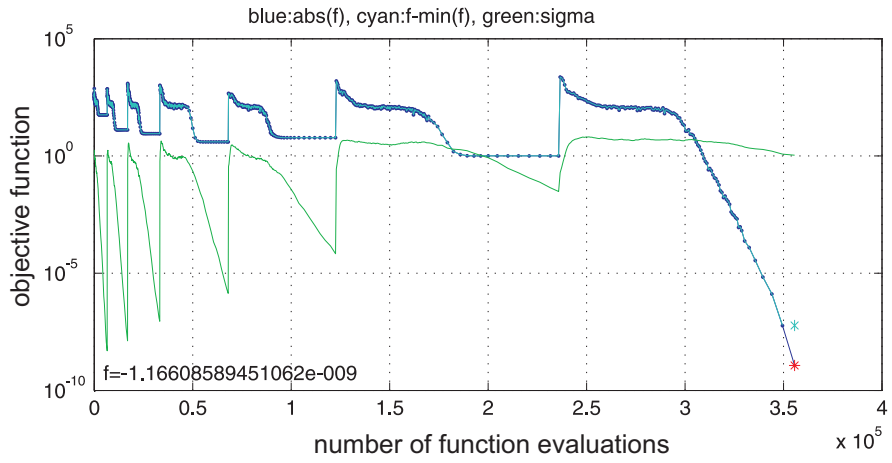

Figure 6.17: One run of NIPOP-aCMA-ES on 20-dimensional Rastrigin function.

due to the fact that i). the multi-modality of Rastrigin function is hardly observable far away from the optimum, and ii). relatively large population reinforces the latter effect. At the same time, the performance is not surprising and corresponds to the results illustrated in Figure 6.15.

To summarize, a smaller than default initial step-size does not necessarily lead to a premature convergence, but can be adapted by CMA-ES to an "appropriate" step-size.

6.3.4.2 Benchmarking with BBOB Framework

The BBOB framework is made of 24 noiseless and 30 noisy functions (see Section 2.3.3). Only the noiseless case has been considered here. Furthermore, only the 12 multi-modal functions among these 24 noiseless functions are of interest for this study, as CMA-ES can solve the 12 other functions without any restart.

With same experimental methodology as in [Hansen *et al.*, 2012], the results obtained on these benchmark functions are presented in Figure 6.18 and Table 6.2. The results are given for dimension 40, because the differences are larger in higher dimensions. The **expected running time (ERT)**, used in the figures and table, depends on a given target function value, $f_t = f_{opt} + \Delta f$. It is computed over all relevant trials as the number of function evaluations required in order to reach f_t, summed over all 15 trials, and divided by the number of trials that actually reached f_t [Hansen *et al.*, 2012].

NIPOP-aCMA-ES. On 6 out of 12 test functions (f_{15}, f_{16}, f_{17}, f_{18}, f_{23}, f_{24}) NIPOP-aCMA-ES obtains the best known results for BBOB-2009 and BBOB-2010 workshops. On f_{23} Katsuuras and f_{24} Lunacek bi-Rastrigin, NIPOP-aCMA-ES has a speedup of a factor from 2 to 3, as could have been expected. It performs unexpectedly well on f_{16} Weierstrass functions, 7 times faster than IPOP-aCMA-ES and almost 3 times faster than BIPOP-aCMA-ES. Overall, according to Figure 6.18, NIPOP-aCMA-ES performs as well as BIPOP-aCMA-ES, while restricted to only one regime of increasing population size.

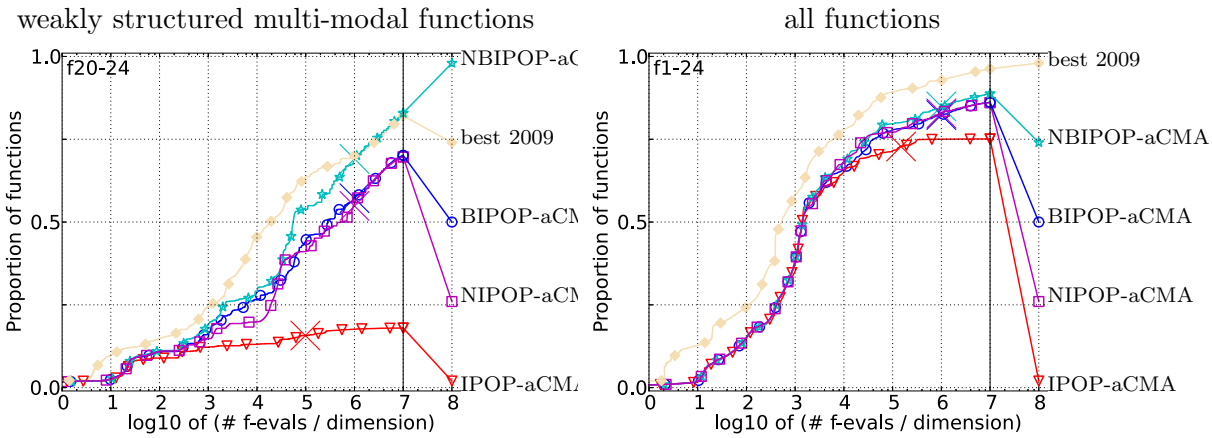

Figure 6.18: Bootstrapped empirical cumulative distribution of the number of objective function evaluations divided by dimension (FEvals/D) for 50 targets in $10^{[-8..2]}$ for all functions and weakly structured multi-modal subgroup in 40-D. The "best 2009" line corresponds to the best ERT observed during BBOB 2009 for each single target.

NBIPOP-aCMA-ES. Thanks to the first regime of increasing population size, NBIPOP-aCMA-ES inherits some results of NIPOP-aCMA-ES. However, on functions where the population size does not play any important role, it performs significantly better than BIPOP-aCMA-ES. This is the case for f_{21} Gallagher 101 peaks and f_{22} Gallagher 21 peaks functions, where NBIPOP-aCMA-ES has a speedup of a factor of 6. It seems that the adaptive choice between two regimes works efficiently on all functions except on f_{16} Weierstrass. In this last case, NBIPOP-aCMA-ES mistakingly prefers small populations, with a loss factor 4 compared to NIPOP-aCMA-ES. According to Figure 6.18, NBIPOP-aCMA-ES performs better than BIPOP-aCMA-ES on weakly structured multi-modal functions, showing overall best results for BBOB-2009 and BBOB-2010 workshops in dimensions 20 (results not shown here) and 40.

6.3.4.3 Interplanetary Trajectory Optimization

The NIPOP-aCMA-ES and NBIPOP-aCMA-ES strategies, designed for the BBOB benchmark functions, can possibly *overfit* this benchmark suite. In order to test the generality of these strategies, a real-world black-box problem is considered, pertaining to a completely different domain: Advanced Concepts Team of European Space Agency is making available several difficult spacecraft trajectory optimization problems as black box functions to invite the operational research community to compare different derivative-free solvers on these test problems [Vinko and Izzo, 2008].

The following results consider the 18-dimensional bound-constrained black- box function "TandEM-Atlas501", that defines an interplanetary trajectory to Saturn from the Earth with multiple fly-bys, launched by the rocket Atlas 501. The final goal is to maximize the mass $f(\boldsymbol{x})$, which can be delivered to Saturn using one of 24 possible fly-by

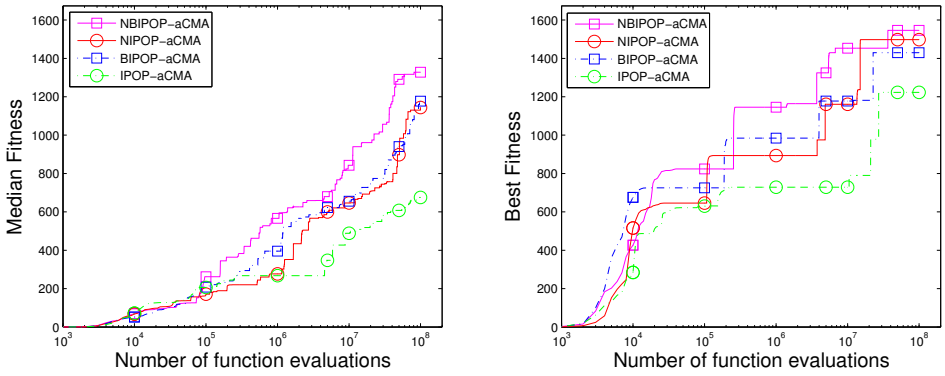

Figure 6.19: Comparison of all CMA-ES restart strategies on the Tandem fitness function (mass): median (left) and best (right) values out of 30 runs.

sequences with possible maneuvers around Venus, Mars and Jupiter.

The first best results was found for a sequence Earth-Venus-Earth-Earth-Saturn ($f_{max} = 1533.45$) in 2008 by [Addis *et al.*, 2008]. The best results so far ($f_{max} = 1673.88$) was found in 2011 by [Stracquadanio *et al.*, 2011].

All versions of CMA-ES with restarts have been launched with a maximum budget of 10^8 function evaluations. All variables are normalized in the range $[0, 1]$. In the case of sampling outside of boundaries, the fitness is penalized and becomes $f(\boldsymbol{x}) = f(\boldsymbol{x}_{feasible}) - \alpha \|\boldsymbol{x} - \boldsymbol{x}_{feasible}\|^2$, where $\boldsymbol{x}_{feasible}$ is the closest feasible point from point $\boldsymbol{x}$ and α is a penalty factor, which was arbitrarily set to 1000.

As shown in Figure 6.19, the new restart strategies NIPOP-aCMA-ES and NBIPOP-aCMA-ES respectively improve on the former ones (IPOP-aCMA-ES and BIPOP-aCMA-ES); further, NIPOP-aCMA-ES reaches same performances as BIPOP-aCMA-ES.

The best solution found by NBIPOP-aCMA-ES [3] improves on the best solution found in 2008, while it is worse than the current best solution, which is blamed on the lack of problem specific heuristics [Addis *et al.*, 2008, Stracquadanio *et al.*, 2011], on the possibly insufficient time budget (10^8 fitness evaluations), and also on the lack of appropriate constraint handling heuristics (that might be improved using the technique proposed in [Arnold and Hansen, 2012]).

6.3.5 Conclusion and Perspectives

This contribution of this Section regards two new restart strategies for CMA-ES. NIPOP-aCMA-ES is a deterministic strategy simultaneously increasing the population size *and* decreasing the initial step-size of the Gaussian mutation. NBIPOP-aCMA-ES implements a competition between NIPOP-aCMA-ES and a random sampling of the initial mutation

[3] $\boldsymbol{x}$ =[0.83521, 0.45092, 0.50284, 0.65291, 0.61389, 0.75773, 0.43376, 1, 0.89512, 0.77264, 0.11229, 0.20774, 0.018255, 6.2057e-09, 4.0371e-08, 0.2028, 0.36272, 0.32442]; fitness($\boldsymbol{x}$) = mass($\boldsymbol{x}$) = 1546.5

step-size, adaptively adjusting the computational budget of each one depending on their current best results. Besides the extensive validation of NIPOP-aCMA-ES and NBIPOP-aCMA-ES on the BBOB benchmark, the generality of these strategies has been tested on a new problem, related to interplanetary spacecraft trajectory planning.

The main limitation of the proposed restart strategies is to quasi implement a deterministic trajectory in the θ space. Further work will consider $h(\theta)$ as yet another expensive noisy black-box function, and the use of a CMA-ES in the hyper-parameter space will be studied. The critical issue is naturally to keep the overall number of fitness evaluations beyond reasonable limits. A surrogate-based approach will be investigated, learning and exploiting an estimate of the (noisy and stochastic) $h(\theta)$ function.

Δf_{opt}	1e1	1e0	1e-1	1e-3	1e-5	1e-7	#succ
f3	15526	15602	15612	15646	15651	15656	15/15
BIPOP-a	**2395**(2759)	∞	∞	∞	∞	∞ *4e7*	0/15
IPOP-aC	∞	∞	∞	∞	∞	∞ *6e6*	0/8
NBIPOP-	8177(9018)	∞	∞	∞	∞	∞ *4e7*	0/15
NIPOP-a	4615(5541)	∞	∞	∞	∞	∞ *4e7*	0/15
Δf_{opt}	1e1	1e0	1e-1	1e-3	1e-5	1e-7	#succ
f4	15536	15601	15659	15703	15733	2.8e5	6/15
BIPOP-a	∞	∞	∞	∞	∞	∞ *4e7*	0/15
IPOP-aC	∞	∞	∞	∞	∞	∞ *6e6*	0/8
NBIPOP-	∞	∞	∞	∞	∞	∞ *4e7*	0/15
NIPOP-a	∞	∞	∞	∞	∞	∞ *4e7*	0/15
Δf_{opt}	1e1	1e0	1e-1	1e-3	1e-5	1e-7	#succ
f15	1.9e5	7.9e5	1.0e6	1.1e6	1.1e6	1.1e6	15/15
BIPOP-a	1.2(0.5)	1.1(0.5)	1.1(0.4)	1.1(0.4)	1.1(0.4)	1.1(0.4)	15/15
IPOP-aC	**0.72**(0.3)	**0.43**(0.1)$_{\downarrow 2}$	0.60(0.4)	0.61(0.4)	0.62(0.5)	0.63(0.5)	8/8
NBIPOP-	1.0(0.4)	0.71(0.3)$_{\downarrow 2}$	0.75(0.3)	0.76(0.3)	0.77(0.3)	0.77(0.3)	15/15
NIPOP-a	0.92(0.3)	0.61(0.2)$_{\downarrow}$	**0.55**(0.2)	**0.56**(0.2)	**0.57**(0.2)	**0.58**(0.2)	15/15
Δf_{opt}	1e1	1e0	1e-1	1e-3	1e-5	1e-7	#succ
f16	5244	72122	3.2e5	1.4e6	2.0e6	2.0e6	15/15
BIPOP-a	1.3(0.4)	0.96(0.3)	0.80(0.4)	0.54(0.3)	0.50(0.3)	0.51(0.3)	15/15
IPOP-aC	**0.91**(0.3)	1.1(0.5)	1.0(0.9)	0.51(0.7)	1.4(1)	1.4(1)	8/8
NBIPOP-	0.97(0.3)	0.78(0.4)	0.34(0.1)$_{\downarrow 3}$	0.38(0.3)$_{\downarrow 2}$	0.46(0.4)	0.74(1)	15/15
NIPOP-a	1.2(0.4)	**0.65**(0.2)	**0.23**(0.1)$^{\star}_{\downarrow 4}$	**0.21**(0.2)$_{\downarrow 3}$	**0.16**(0.1)$^{\star}_{\downarrow 3}$	**0.18**(0.1)$_{\downarrow 3}$	15/15
Δf_{opt}	1e1	1e0	1e-1	1e-3	1e-5	1e-7	#succ
f17	399	4220	14158	51958	1.3e5	2.7e5	14/15
BIPOP-a	1.1(0.3)	0.64(0.2)	1.6(1)	1.1(0.4)	1.4(1)	0.87(0.4)	15/15
IPOP-aC	1.0(0.4)	0.52(0.2)	1.3(1)	1.3(0.9)	**0.97**(0.2)	0.83(0.3)	8/8
NBIPOP-	1.0(0.4)	0.57(0.2)	1.2(1)	1.2(0.5)	1.0(0.3)	0.81(0.3)	15/15
NIPOP-a	**0.97**(0.3)	**0.52**(0.1)	**0.97**(1)	**1.00**(0.4)	1.1(0.6)	**0.70**(0.2)$_{\downarrow}$	15/15
Δf_{opt}	1e1	1e0	1e-1	1e-3	1e-5	1e-7	#succ
f18	1442	16998	47068	1.9e5	6.7e5	9.5e5	15/15
BIPOP-a	**0.94**(0.2)	**0.51**(0.8)	1.0(0.4)	0.98(0.4)	0.88(0.7)	0.67(0.5)	15/15
IPOP-aC	0.96(0.4)	0.68(0.9)	1.0(0.4)	**0.66**(0.2)$_{\downarrow}$	**0.45**(0.4)	0.48(0.2)	8/8
NBIPOP-	1.0(0.2)	0.97(1)	1.1(0.6)	0.93(0.4)	0.57(0.4)	0.53(0.3)	15/15
NIPOP-a	0.95(0.2)	0.58(0.8)	**0.75**(0.1)	0.71(0.2)$_{\downarrow}$	0.50(0.3)	**0.42**(0.2)	15/15

Δf_{opt}	1e1	1e0	1e-1	1e-3	1e-5	1e-7	#succ
f19	1	1	1.4e6	2.6e7	4.5e7	4.5e7	8/15
BIPOP-a	**396**(82)	6.7e4(5e4)	0.87(0.7)	1.2(1)	1.0(0.9)	1.0(1.0)	9/15
IPOP-aC	462(122)	**4.4e4**(2e4)	**0.57**(0.5)	**0.34**(0.1)$_{\downarrow 2}$	**0.20**(0.1)$_{\downarrow 2}$	**0.20**(0.1)$_{\downarrow 2}$	8/8
NBIPOP-	424(90)	8.3e4(6e4)	0.97(0.6)	0.81(0.5)	1.1(0.9)	1.1(0.9)	9/15
NIPOP-a	436(102)	8.2e4(4e4)	1.9(6)	0.48(0.3)$_{\downarrow}$	0.32(0.2)$_{\downarrow}$	0.32(0.2)$_{\downarrow}$	15/15
Δf_{opt}	1e1	1e0	1e-1	1e-3	1e-5	1e-7	#succ
f20	222	1.3e5	1.6e8	∞	∞	∞	0
BIPOP-a	4.0(0.4)	9.0(4)	0.34(0.4)	.	.	.	0/15
IPOP-aC	**3.9**(0.8)	8.1(5)	**0.18**(0.2)	.	.	.	0/8
NBIPOP-	4.0(0.8)	8.5(3)	0.39(0.4)	.	.	.	0/15
NIPOP-a	4.0(0.6)	**6.5**(2)	0.32(0.3)	.	.	.	0/15
Δf_{opt}	1e1	1e0	1e-1	1e-3	1e-5	1e-7	#succ
f21	1044	21144	1.0e5	1.0e5	1.0e5	1.0e5	26/30
BIPOP-a	7.5(11)	60(19)	37(56)	37(56)	37(56)	37(55)	15/15
IPOP-aC	7.1(11)	421(491)	∞	∞	∞	∞ *3e6*	0/8
NBIPOP-	**4.9**(6)	**10**(20)	**5.1**(8)	**5.1**(8)	**5.1**(8)	**5.1**(8)	15/15
NIPOP-a	14(22)	440(890)	173(228)	172(227)	171(226)	171(201)	12/15
Δf_{opt}	1e1	1e0	1e-1	1e-3	1e-5	1e-7	#succ
f22	3090	35442	6.5e5	6.5e5	6.5e5	6.5e5	8/30
BIPOP-a	**12**(20)	343(565)	201(223)	200(222)	200(201)	199(214)	4/15
IPOP-aC	144(492)	**93**(127)	∞	∞	∞	∞ *3e6*	0/8
NBIPOP-	12(6)	112(120)	**32**(41)	**32**(39)	**32**(40)	**32**(40)	12/15
NIPOP-a	179(468)	583(914)	∞	∞	∞	∞ *4e7*	0/15
Δf_{opt}	1e1	1e0	1e-1	1e-3	1e-5	1e-7	#succ
f23	7.1	11925	75453	1.3e6	3.2e6	3.4e6	15/15
BIPOP-a	8.4(9)	**7.8**(7)	**1.3**(1)	1.9(1)	1.00(0.4)	0.99(0.4)	15/15
IPOP-aC	9.2(13)	∞	∞	∞	∞	∞ *4e6*	0/8
NBIPOP-	8.6(11)	10(12)	1.6(2)	1.3(0.4)	0.58(0.2)	0.59(0.2)	15/15
NIPOP-a	**5.9**(7)	61(18)	11(3)	**0.72**(0.2)	**0.36**(0.2)*	**0.38**(0.2)*	15/15
Δf_{opt}	1e1	1e0	1e-1	1e-3	1e-5	1e-7	#succ
f24	5.8e6	9.8e7	3.0e8	3.0e8	3.0e8	3.0e8	1/15
BIPOP-a	3.6(4)	1.4(1)	∞	∞	∞	∞ *4e7*	0/15
IPOP-aC	∞	∞	∞	∞	∞	∞ *1e7*	0/8
NBIPOP-	2.1(3)	0.19(0.2)	0.97(1)	0.97(1.0)	0.97(1)	0.97(1.0)	2/15
NIPOP-a	**1.2**(1)	**0.15**(0.2)	**0.44**(0.5)	**0.44**(0.5)	**0.44**(0.5)	**0.44**(0.5)	4/15

Table 6.2: Overall results on multi-modal functions $f3-4$ and $f15-24$ in dimension $n = 40$: Expected running time (ERT in number of function evaluations) divided by the respective best ERT measured during BBOB-2009 for precision Δf ranging in 10^i, $i = 1 \ldots -7$. The median number of conducted function evaluations is additionally given in *italics*, if $\text{ERT}(10^{-7}) = \infty$. #succ is the number of trials that reached the final target $f_{\text{opt}} + 10^{-8}$. Best results are printed in bold.

6.4 Other Approaches

In this Section, we very briefly describe several approaches that we investigated, but whose detailed description is omitted.

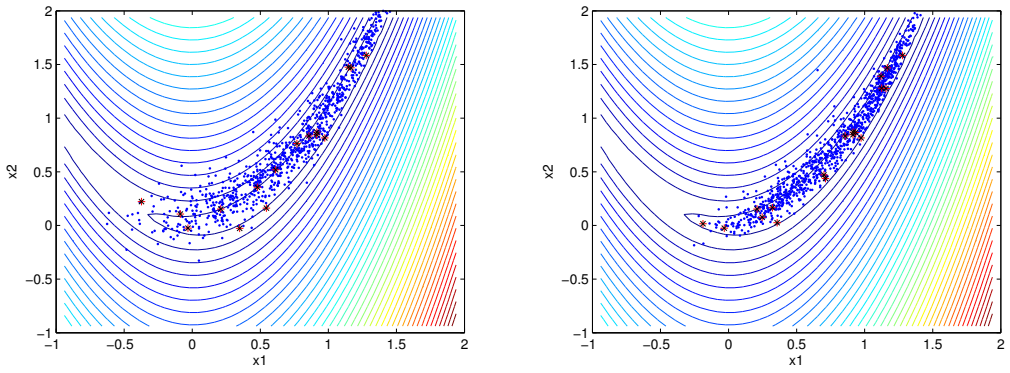

Figure 6.20: Kernel PCA-based CMA-ES on 2-dimensional Rosenbrock function. Kernel PCA was built using 20 red training points and tested (without evaluation) on 1000 blue test points to demonstrate the learned distribution. **Left**: generation k. **Right:** generation $k + 2$.

6.4.1 Kernel PCA-based CMA-ES

Kernel Principal Component Analysis (Kernel PCA or KPCA) is an extension of PCA to non-linear PCA using kernel methods [Scholkopf *et al.*, 1996]. The original PCA can be formulated in terms of dot product between data points, therefore, it can be extended to non-linear case by replacing dot product in the original space by kernel function to compute dot product in a reproduced kernel Hilbert space [Aronszajn, 1950].

We implemented a version of CMA-ES decomposed into CSA-ES and Adaptive Encoding procedure, replacing the original PCA by KPCA in the latter. Thus, instead of sampling new points on principal components in the original search space, we sample new points on principal components found in some feature space. However, finding pre-images of sampled points in the original space for their further evaluation of f is not straightforward, but can be done solving so-called pre-image problem [Kwok and Tsang, 2004]. Another difficulty is to reformulate step-size adaptation rule to be adequate to metrics of the feature space, we did not find any elegant solution for this problem, and, therefore, use CSA-ES adaptation for points in the original space.

Figure 6.20 illustrates generations k (**Left**) and $k + 2$ (**Right**) of the KPCA-based CMA-ES on 2-dimensional Rosenbrock, where KPCA was built using 20 best (red) points found so far and tested to illustrate the sampling distribution using 1000 (blue) test points. It can be seen that KPCA clearly can catch non-linear landscape of Rosenbrock function and sample accordingly, in contrast to the original CMA-ES which would sample on 2 principal components (some ellipsoid). We suppose that the extension of CMA-ES to non-linear case, in the sense of learning non-linear principal components, is a prospective direction of research. However, for robustness of the algorithm several issues should be addressed: step-size control, pre-image problem, computational complexity. Some of these issues were already discussed in [Pošık, 2007], where a KPCA-based GA was proposed.

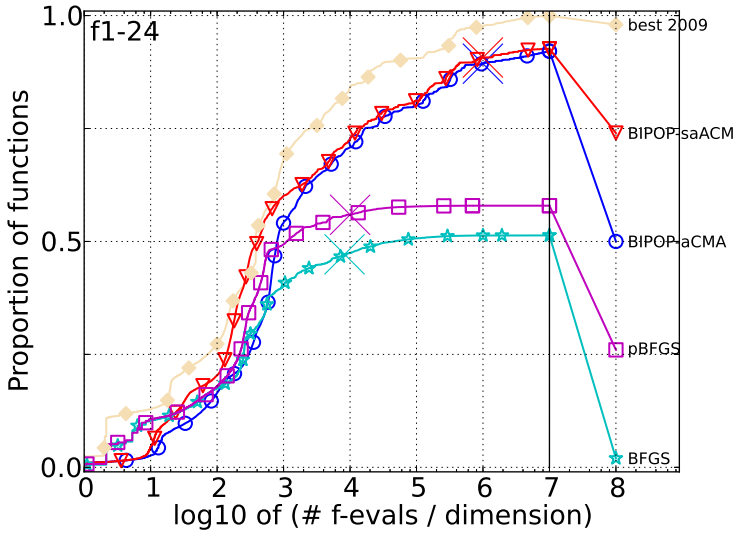

Figure 6.21: Bootstrapped empirical cumulative distribution of the number of objective function evaluations divided by dimension (FEvals/D) for 50 targets in $10^{[-8..2]}$ for all noise-less functions in 20-D. The "best 2009" line corresponds to the best ERT observed during BBOB 2009 for each single target.

6.4.2 High-precision BFGS

In Section 4.3.3.7, we showed that IPOP-^{s*}aACM-ES and BIPOP-^{s*}aACM-ES algorithms outperform BFGS on a set of 24 noise-less BBOB benchmark problems. A more detailed analysis of the results of BFGS [Ros, 2009] demonstrates that the algorithm performs quite well in the beginning of the optimization of ill-conditioned problems (5 problems out of 24), i.e., reaches target objective values $10^1, 10^0, 10^{-2}$ relatively quickly in comparison with other algorithms, but then slows down and hardly finds better target objective values. We suppose that this happens mainly due to a of loss of precision of estimation of gradient of f (and as a consequence, of Hessian of f) and its cumulation during the optimization. A discussion about updating BFGS formula in ill-conditioned environment can be found in [Powell, 1987].

In order to check whether the performance of BFGS degrades because of numerical/rounding problems or some other reasons, we implemented a version of BFGS with high-precision arithmetic, referred to as pBFGS. The MatLab implementation of BFGS was rewritten in C++ and integrated with a software packages for high-precision arithmetic called ARPREC [Bailey *et al.*, 2002]. ARPREC supports arbitrary high level of numerical precision (up to approximately ten million decimal digits). In our experiments we found that double-double precision with about 32 decimal digits (double precision has about 16 digits) is sufficient to overcome numerical problems observed on BBOB benchmark problems. Having more decimal digits we may benefit from using a deviation

value $\epsilon = 10^{-12}$ (estimating the gradient as $f'(\boldsymbol{x}) = \frac{f(\boldsymbol{x}+\epsilon)-f(\boldsymbol{x})}{\epsilon}$), smaller than the default $\epsilon = 10^{-8}$ used for gradient estimation in the finite difference method.

Figure 6.21 shows the results of benchmarking pBFGS and BFGS in comparison with BIPOP-^{s*}aACM-ES and BIPOP-aCMA-ES on noise-less BBOB testbed. It can be clearly seen that the results for pBFGS are much better than for BFGS, and high-precision computation indeed leads to a faster and more robust convergence. However, the results of pBFGS with restarts are still worse than the ones of BIPOP-^{s*}aACM-ES.

An important remark is that in order to demonstrate the performance of pBFGS without loss of precision, we implemented not only the high-precision version of BFGS, but also a high-precision version of BBOB framework. The loss of performance occurs not only on the side of BFGS which computes the finite difference, but also on the side of BBOB framework which evaluates objective values for candidates, different in the decision space by a small ϵ value. It should be noted that a double-double version of some programming code is usually computationally more expensive, thus, the speedup from the use of pBFGS should be larger than the loss (typically a factor of 2) because of slower computations of f. Moreover, in a black-box scenario the source code of f is unavailable.

Despite the uncovered difficulties of using the high-precision arithmetic within BFGS, we now have a better estimation of its "best case" performance. It would be also interesting to find a better implementation of BFGS with pBFGS-like performance, a promising candidate might be an implementation suggested in [Voglis *et al.*, 2012] with an adaptable ϵ (see also [Voglis *et al.*, 2009]). However, given that pBFGS is already outperformed by BIPOP-^{s*}aACM-ES, it also may completely fail under certain rank-preserving transformations of f.

6.4.3 Comparison-based Multi-objective Optimization and Comparison-based Hypervolume Indicator

A natural extension of ^{s*} to surrogate-assisted multi-objective optimization would be to build individual $\hat{f}_i$ surrogates for each of f_i objectives (i is the index of objective). The use of ordinal regression-based surrogate models will lead to their invariance w.r.t. rank-preserving transformation of $\hat{f}_i$. Surprisingly, this is a new feature for multi-objective optimization in the sense that most of MOEAs are not invariant w.r.t. rank-preserving transformations of f_i, because they use value-based metrics in the environmental selection (e.g., crowding distance, hypervolume indicator, epsilon indicator). Before going into details of the extension of ^{s*}, we wondered whether we could make MOEAs invariant w.r.t. rank-preserving transformations of f_i. We propose the following simple solution to this problem.

During the optimization we evaluate ℓ candidate solutions $\boldsymbol{x}_j, j = 1, \ldots, \ell$, on f and store corresponding objective values $f_i(\boldsymbol{x}_j)$ in archives $\mathcal{A}_i$. Finally we have m such archives (m is the number of objectives) containing ℓ objective values of evaluated points. Then, objective values can be sorted such that we can associate to each candidate solution $\boldsymbol{x}_j$ not only its *raw* objective value $f_i(\boldsymbol{x}_j)$, but also its *rank-based* objective value $f_i^{rank}(\boldsymbol{x}_j)$ which corresponds to the rank of its solution among other solutions on objective f_i. Thus, we may simply replace the raw objective values by rank-based values, and this does not change any

Pareto dominance relations among the points. We may use such intermediate procedure within *any* MOEAs, making them invariant w.r.t. rank-preserving transformations of f_i.

Our preliminary experiments within *rank-based* NSGA-II showed quite similar results to the original NSGA-II. Two important aspect should be noted: i). the fact of using *rank-based* objectives values does not change position of optimal Pareto front in the decision space, but ii). it may change the final Pareto front approximation, because the objectives now are differently scaled. The described above aspects mean that it is rather unlikely to have the same Pareto front approximation from the rank-based and value-based versions of the same MOEA, because their objectives are different.

Using the proposed rank-based framework, Quality Indicators also become rank-based. We anticipate interesting theoretical and practical results from rank-based hypervolume indicator. The fact that all objective values are integers and that adding a new point into a set we shift objective values of some points by +1 or -1 may bring some interesting results on computational complexity of hypervolume indicator computation. It should be noted, that the sorting of points in archives $\mathcal{A}_i$ is actually not required, since the operation of insertion, deletion and access can be performed in $O(log(\ell))$ operations by representing archives as trees.

6.5 Discussion

In this Chapter, we investigated a set of algorithms based on CMA-ES for continuous optimization problems with different properties: single-objective (ACiD, NBIPOP-aCMA-ES, NIPOP-aCMA-ES), multi-objective (MO-CMA-ES with reward-based parent selection), large scale (ACiD, LACiD with linear time complexity) and multi-modal (NBIPOP-aCMA-ES, NIPOP-aCMA-ES).

We showed that simple deterministic coordinate descent method, performed on principal components of an adaptive coordinated system is at least as efficient as (1+1)-CMA-ES algorithm which operates by adapting multi-variate normal distribution in a stochastic way. The proposed Adaptive Coordinate Descent (ACiD) was also extended to LACiD, which requires only about $10n$ elementary operations per function evaluation in contrast to the fastest version of (1+1)-CMA-ES with $O(n^2)$ computational complexity. The overall speedup of LACiD in comparison with (1+1)-CMA-ES is in the order of n. To further improve the original ACiD in terms of number of function evaluations one should consider alternative strategies for search on principal components. A more extreme modification would be to replace PCA by Kernel PCA and perform the search on kernel principal components, which might be beneficial for highly non-linear optimization problems. A possible solution to further reduce the number of operations per function evaluation of LACiD would be to call the eigendecomposition even less often; this, however, may increase the overall number of function evaluations to reach the optimum. To reduce the $O(n^2)$ space complexity of LACiD, one should consider iterative search on principal components of a smaller dimension $n_{small} << n$. This may allow to extend the algorithm to $n > 10000$, but should be carefully done to prevent the explosion of overall number of function evaluations on fully non-separable ill-conditioned problems.

As was shown for MO-CMA-ES, not all parent individuals are equally interesting for generating offspring, and the proposed reward-based parent selection schemes may significantly speedup the convergence toward the optimal Pareto front. These schemes are efficient not only during the convergence phase of the search, but also for optimal μ-distribution approximation before all points become equally prospective. While the schemes were tested for MO-CMA-ES where (1+1) selection scenario is applied, they also can be extended to multi-parent scenario (e.g., for NSGA-II) by sharing the reward between the parents.

The proposed alternative restart strategies for CMA-ES, NIPOP and NBIPOP, improve the results on multi-modal functions, especially in larger dimensions, thanks to a different principles of search in (λ, σ)-space of hyper-parameters of CMA-ES and the adaptive allocation of budgets of function evaluations for different regimes of restarts depending on their performance. We envision that the results can be further improved if the restarts of CMA-ES are viewed as individual evaluations in (λ, σ)-space: perform some surrogate-assisted search in this space. While the use of restarts of CMA-ES is currently a dominating approach to deal with multi-modal optimization, we suppose that the population size can be adapted during the search depending on the observed landscape. Our preliminary results suggests that a speedup of a factor of about 2 can be achieved by adjusting the population size during the search depending on the fitness-distance correlation metric. The latter can be be translated to the rank-based fitness distance correlation by using ranks of fitnesses and distances of individuals. Further research should also consider alternative niching methods [Shir and Bäck, 2006].

It also would be interesting to incorporate the Multi-Armed Bandits approach into CMA-ES for adaptive selection of different regimes, e.g., different regimes of uncertainty handling, parameters adaptation, etc.

Part IV

General Conclusion

Chapter 7

Conclusion

In this thesis, we have explored a wide range of approaches to the problem of efficient continuous optimization. What have we learned about continuous optimization, and what are the most promising direction for future research? This final Chapter seeks to answer these questions.

7.1 Summary of Contributions

In this thesis, we followed the strategy described in Chapter 1 and searched for optimal approaches to continuous optimization by first performing an exploitation step (Chapters 4 and 5) aiming at improvements with respect to "greedy" indicators of performance (e.g., number of function evaluations to reach the optimum), and then an exploration step (Chapter 6) aiming at introducing new prospective paradigms and approaches that would keep the diversity on a sufficiently rich level for further improvements. We applied our strategy to CMA-ES as a candidate algorithm with a relatively good performance at least in single-objective case (see Section 2.3.3).

In the exploitation part of the thesis we proposed to use ordinal regression-based (comparison-based) surrogate (approximate) models for expensive continuous optimization within CMA-ES.

In Chapter 4, we first showed why ordinal regression-based surrogates should be preferred to metric regression-based surrogates in the black-box scenario, when the landscape of the objective function is unknown. The most important reason is that the ordinal regression-based (comparison-based) surrogate models are invariant with respect to rank preserving transformations of the objective function. This, indeed, represents a source of robustness. Another source of such robustness is the invariance with respect to orthogonal transformations of the search space, which can be obtained from the information about correlations between the variables, provided by the covariance matrix adapted by CMA-ES. We showed that the approach of Support Vector Machines can be efficiently used to build surrogates models for surrogate-assisted CMA-ES such that the described above invariance properties, inherent to CMA-ES, can be preserved. When the surrogate model is built using a set of hyper-parameters and a set training points, it can be directly optimized by CMA-ES for a given number of generations, which is a function (e.g., linear function) of the estimated model quality. An important contribution of this thesis is the proposed surrogate model hyper-parameters adaptation procedure: the user is only needed to define the range of controlling hyper-parameters of the surrogate learning, and the procedure will optimize them automatically during the optimization of the objective function, such that the surrogate model is (optimized to be) best suited to the

current search region. The proposed framework ^{s*} and its CMA-ES instances IPOP-^{s*}aACM-ES and BIPOP-^{s*}aACM-ES were extensively benchmarked on BBOB noiseless and noisy benchmark problems, where they improved (often by a factor of 2-3) the best know results for certain problems obtained from more than 40 other classical and Evolutionary Algorithms. The aggregated results for noiseless problems are best illustrated in Figure 4.19. We also showed that the approach can be efficiently parallelized: this is, indeed, not the case for many surrogate-assisted algorithms (e.g., some trust-region based algorithms).

In Chapter 5, we investigated surrogate-assisted multi-objective search within MO-CMA-ES and NSGA-II using a relatively simple model exploitation procedure based on offspring pre-selection. We proposed to build Aggregated Surrogate Model of the original multi-objective problem in order to aggregate the information about the preferences between solutions in the objective space. Different sources of preference information can be used: Pareto dominance, Quality Indicators or Decision Maker based preferences. In contrast to "multi-surrogate" approaches, the proposed ASM model represents a single objective which imitates an aggregated preference which the optimization algorithm should follow. In the procedure of model exploitation, λ_{Pre} offspring per one parent are generated for pre-selection of the best candidate for its later evaluation on the expensive function. The experimental validation of ASM-assisted MO-CMA-ES and NSGA-II algorithms showed that ASM models significantly speedup the search (by a factor of about 2) in the phase of convergence toward the optimal Pareto front, but tends to lack of diversity in the phase of the optimal Pareto front approximation.

In the exploration part of the thesis, we presented a set of approaches which we developed in order to explore and extend the frontiers of Evolutionary Computation, and CMA-ES in particular, answering some questions which have arisen in the exploitation part of the thesis.

In Chapter 5, we proposed Adaptive Coordinate Descent answering the question whether we could efficiently exploit a potential separability of the decorrelated search space provided by Adaptive Encoding procedure. The final algorithm was shown to be competitive with (1+1)-CMA-ES, while being deterministic and based on simple dichotomy method. The extension of ACiD to large scale optimization, linear time ACiD (LACiD), demonstrated slightly worse performance than (1+1)-CMA-ES in terms of number of function evaluations (a loss of about a factor of 2 for $n = 512$ on Ellipsoid and Rosenbrock functions), but linear time complexity in contrast to quadratic time complexity of the fastest version of (1+1)-CMA-ES. In fact, LACiD scales with $10n$ elementary operations that is about $10^{-8}n$ seconds per function evaluation (see Figure 6.7). Thus, with this algorithm we explored the extreme opposite of surrogate-assisted search for expensive optimization - large scale optimization with cheap function evaluations.

Answering the question whether we could improve the results of multi-objective optimizers without using surrogate models, we proposed to look more carefully at the dynamic of success of parent individuals in offspring sampling. We showed that reward-based parent selection schemes can be highly beneficial for MO-CMA-ES allowing the algorithm to quickly catch fruitful directions of search.

Our observations of a relatively small speedup of BIPOP-^{s*}aACM-ES on multi-modal problems (due to difficult to learn the fitness landscapes) motivated the development of

simple restarts strategies for CMA-ES, NIPOP and NBIPOP, which were found to be competitive to the original restart schemes, IPOP and BIPOP. The new schemes are often faster than the original restarts schemes especially in higher dimensions, where the alternative exploration of (λ, σ)-space and the adaption of computational budgets of regimes of restarts are especially beneficial. In order to check against overfitting to BBOB benchmark problems, the proposed restarts schemes were tested on the real-world problem of interplanetary trajectory optimization, where they also showed good performance.

7.2 Future Directions

Here we would like to mention several directions of future research which look the most promising, of course, without pretending to cover everything that is important for EC, and CMA-ES in particular. Some of these ideas were already discussed in the corresponding Chapters and Sections.

There is a global goal to find an extremely cheap and fast (in terms of computational complexity *and* memory requirements *and* number of functions evaluations) optimization algorithm, suitable for different classes of optimization problems. It seems difficult to find such algorithm in a near future (if it exists) and we rather should think of a Pareto set of algorithms which better or worse satisfy the described above objectives.

A subspace of computationally cheap algorithms is covered by SEP-CMA-ES, Rank-One NES and linear time ACiD. They, however, have different performance and memory requirements. For example, the linear time ACiD is suitable for learning the full covariance matrix and performs well on Rotated Ellipsoid problem, but requires $O(n^2)$ memory space in order to store the covariance matrix. Thus, the primary interest in this direction would be to further explore these algorithms to find i). a version of linear time ACiD with linear space complexity; ii). a version of the original CMA-ES which uses linear time offspring sampling procedure and, thus, can be linear in time; iii). versions of SEP-CMA-ES and Rank-One NES which may learn few more principal components and, thus, performs better on fully non-separable problems.

Our preliminary results show that ^{s*}aACM-ES algorithms can be further improved by a factor of up to 2 by more carefully looking at the surrogate model exploitation procedure. This would further shift to the left the curves of ^{s*}aACM-ES algorithms presented in Figure 4.19. We also anticipate good results from the use of different surrogate learning techniques and their simultaneous adaptation to the current region of search. The primary interest in surrogate-assisted search would be to i). reduce the time and space complexity of the used surrogate learning procedure; ii). improve the accuracy of surrogates on multi-modal functions.

A natural perspective for ^{s*}aACM-ES would be its extension to multi-objective optimization. This would require the rank-based formulation of multi-objective optimization and *rank-based Hypervolume indicator* (i.e., invariant with respect to the rank-preserving transformations of objectives) as discussed in Section 6.4.3. The surrogate model exploitation procedure, however, might be more complicated and less efficient since the accuracy of models for different objectives may differ significantly (e.g., from ideal to random pre-

diction). Alternatively, if we succeed to carefully replace PCA by Kernel PCA in Adaptive Encoding part of CMA-ES, then the use of ASM surrogate models for multi-objective optimization seems to be prospective. In this case, Kernel PCA-based ^{s*}aACM-ES would learn the distribution of non-dominated points and sample offspring according to this distribution. We may evaluate these offspring on ASM model learned from the preference information, thus, unifying the single-objective and multi-objective surrogate-assisted optimization.

Bibliography

[Abbass *et al.*, 2001] Hussein A. Abbass, Ruhul Sarker, and Charles Newton. PDE: A Pareto-frontier Differential Evolution Approach for Multi-objective Optimization Problems. In *IEEE Congress on Evolutionary Computation*, pages 971–978. IEEE Press, 2001. (Cited on page 41)

[Abboud and Schoenauer, 2002] K. Abboud and Marc Schoenauer. Surrogate Deterministic Mutation: Preliminary Results. In *Selected Papers from the 5th European Conference on Artificial Evolution*, pages 104–116, London, UK, UK, 2002. Springer-Verlag. (Cited on page 68)

[Acar and Rais-Rohani, 2009] E. Acar and M. Rais-Rohani. Ensemble of metamodels with optimized weight factors. *Structural and Multidisciplinary Optimization*, 37(3):279–294, January 2009. (Cited on page 67)

[Addis *et al.*, 2008] B. Addis, A. Cassioli, M. Locatelli, , and F. Schoen. Global optimization for the design of space trajectories. *Optimization On Line*, 11, 2008. (Cited on page 191)

[Aizerman *et al.*, 1964] A. Aizerman, E.M. Braverman, and LI Rozoner. Theoretical foundations of the potential function method in pattern recognition learning. *Automation and remote control*, 25:821–837, 1964. (Cited on page 59)

[Akimoto and Ollivier, 2013] Y. Akimoto and Y. Ollivier. Objective Improvement in Information-Geometric Optimization. In Frank Neumann and Kenneth De Jong, editors, *Foundations of Genetic Algorithms, 12th International Workshop, FOGA 2013, Adelaide, Australia, January 16-20, 2013, Proceedings*, page to appear. ACM, 2013. (Cited on page 4)

[Alander, 1994] Jarmo T. Alander. *An Indexed Bibliography of Genetic Algorithms: Years 1957–1993*. Art of CAD ltd, Vaasa, Finland, 1994. (Cited on page 11)

[Amari, 1998] S. Amari. Natural Gradient Works Efficiently in Learning. *Neural Computation*, 10(2):251–276, 1998. (Cited on page 29)

[Anderson and Hsu, 1999] Kurt S. Anderson and YuHung Hsu. Genetic Crossover Strategy using an Approximation Concept. In Peter J. Angeline, Zbyszek Michalewicz, Marc Schoenauer, Xin Yao, and Ali Zalzala, editors, *Proceedings of the Congress on Evolutionary Computation*, volume 1, pages 527–533. IEEE Press, 6-9 July 1999. (Cited on page 68)

[Antonisse, 1989] J. Antonisse. A new interpretation of schema notation that overtums the binary encoding constraint. In *Proceedings of the 3rd International Conference on Genetic Algorithms*, pages 86–91. Morgan Kaufmann Publishers Inc., 1989. (Cited on page 15)

[Applegate *et al.*, 2009] David L. Applegate, Robert E. Bixby, Vašek Chvátal, William Cook, Daniel G. Espinoza, Marcos Goycoolea, and Keld Helsgaun. Certification of an optimal TSP tour through 85,900 cities. *Operations Research Letters*, 37(1):11 – 15, 2009. (Cited on page 17)

[Arnold and Beyer, 2002] Dirk V. Arnold and Hans-Georg Beyer. Random Dynamics Optimum Tracking with Evolution Strategies. In *In Parallel Problem Solving from Nature*, pages 3–12. Springer, 2002. (Cited on pages 23 and 27)

[Arnold and Beyer, 2008] Dirk V. Arnold and Hans-Georg Beyer. Evolution strategies with cumulative step length adaptation on the noisy parabolic ridge. *Natural Computing*, 7(4):555–587, December 2008. (Cited on page 27)

[Arnold and Hansen, 2012] D.V. Arnold and N. Hansen. A (1+1)-CMA-ES for constrained optimisation. In *Proceedings of the fourteenth international conference on Genetic and evolutionary computation conference*, pages 297–304. ACM, 2012. (Cited on pages 169, 179, and 191)

[Arnold *et al.*, 2011] L. Arnold, A. Auger, N. Hansen, and Y. Ollivier. Information-Geometric Optimization Algorithms: A Unifying Picture via Invariance Principles. *ArXiv e-prints*, June 2011. (Cited on pages 4 and 30)

[Aronszajn, 1950] N. Aronszajn. Theory of reproducing kernels. *Trans. Amer. Math. Soc*, 68(3):337–404, 1950. (Cited on page 193)

[Atkeson *et al.*, 1997] C.G. Atkeson, A.W. Moore, and S. Schaal. Locally weighted learning. *Artificial intelligence review*, 11(1):11–73, 1997. (Cited on pages 51 and 71)

[Auer *et al.*, 2002] P. Auer, N. Cesa-Bianchi, and P. Fischer. Finite-time Analysis of the Multi-armed Bandit Problem. *Machine Learning*, 47(2-3):235–256, 2002. (Cited on pages 170, 171, and 172)

[Auger and Hansen, 2005] A Auger and N Hansen. A Restart CMA Evolution Strategy With Increasing Population Size. In *IEEE Congress on Evolutionary Computation*, pages 1769–1776. IEEE Press, 2005. (Cited on pages 29, 31, and 185)

[Auger and Hansen, 2006] Anne Auger and Nikolaus Hansen. Reconsidering the progress rate theory for evolution strategies in finite dimensions. In *Proceedings of the 8th annual conference on Genetic and evolutionary computation*, GECCO 2006, pages 445–452, New York, NY, USA, 2006. ACM. (Cited on page 14)

[Auger *et al.*, 2009] Anne Auger, Johannes Bader, Dimo Brockhoff, and Eckart Zitzler. Theory of the Hypervolume Indicator: Optimal μ-Distributions and the Choice of the Reference Point. In *FOGA*, pages 87–102. ACM, 2009. (Cited on pages 46 and 143)

[Auger *et al.*, 2010] A. Auger, S. Finck, N. Hansen, and R. Ros. BBOB 2010: Comparison Tables of All Algorithms on All Noiseless Functions. Technical Report RR-7215, INRIA, 2010. (Cited on page 163)

[Auger, 2009] Anne Auger. Benchmarking the (1+1) Evolution Strategy with one-fifth success rule on the BBOB-2009 function testbed. In *Proceedings of the 11th Annual Conference Companion on Genetic and Evolutionary Computation Conference: Late Breaking Papers*, GECCO 2009, pages 2447–2452, New York, NY, USA, 2009. ACM. (Cited on page 15)

[Bäck and Schütz, 1995] Thomas Bäck and Martin Schütz. Evolution Strategies for Mixed-Integer Optimization of Optical Multilayer Systems. In *Evolutionary Programming*, pages 33–51, 1995. (Cited on page 17)

[Bader and Zitzler, 2011] Johannes Bader and Eckart Zitzler. Hype: An algorithm for fast hypervolume-based many-objective optimization. *Evolutionary Computation*, 19(1):45–76, March 2011. (Cited on page 42)

[Bailey *et al.*, 2002] D.H. Bailey, H. Yozo, X.S. Li, and B. Thompson. ARPREC: An arbitrary precision computation package. Technical report, Ernest Orlando Lawrence Berkeley National Laboratory, Berkeley, CA (US), 2002. (Cited on page 194)

[Barricelli, 1954] N. Barricelli. Esempi numerici di processi di evoluzione. *Methodos*, pages 45–68, 1954. (Cited on page 13)

[Barricelli, 1957] N. Barricelli. Symbiogenetic evolution processes realized by artificial methods. *Methodos*, pages 143–182, 1957. (Cited on page 13)

[Büche *et al.*, 2004] Dirk Büche, Nicol N. Schraudolph, and Petros Koumoutsakos. Accelerating Evolutionary Algorithms with Gaussian Process Fitness Function Models. *IEEE Transactions on Systems, Man and Cybernetics*, 35:183–194, 2004. (Cited on page 52)

[Bersini *et al.*, 1996] Hugues Bersini, Marco Dorigo, Stefan Langerman, Gregory Seront, and Luca Maria Gambardella. Results of the First International Contest on Evolutionary Optimisation (1st ICEO). In *International Conference on Evolutionary Computation*, pages 611–615, 1996. (Cited on page 31)

[Beyer and Finck, 2012] Hans-Georg Beyer and Steffen Finck. HappyCat – A Simple Function Class Where Well-Known Direct Search Algorithms Do Fail. In *12th International Conference on Parallel Problem Solving From Nature - PPSN*, 2012. (Cited on page 35)

[Bickel *et al.*, 1997] P. J. Bickel, F. ötze, and W. R. Van Zwet. Resampling fewer than n observations: gains, losses, and remedies for losses. *STATIST. SINICA*, 7:1–32, 1997. (Cited on page 66)

[Bischl *et al.*, 2012] B. Bischl, O. Mersmann, H. Trautmann, and C. Weihs. Resampling methods for meta-model validation with recommendations for evolutionary computation. *Evolutionary Computation*, 20(2):249–275, June 2012. (Cited on pages 66 and 67)

[Bishop, 2006] C.M. Bishop. *Pattern recognition and machine learning*, volume 4. springer New York, 2006. (Cited on pages 53 and 54)

[Blum and Merkle, 2008] C. Blum and D. Merkle. *Swarm intelligence: introduction and applications*. Springer, 2008. (Cited on page 19)

[Bosman and Thierens, 2005] P. Bosman and D. Thierens. The Naive MIDEA: A Baseline Multi–objective EA. In *Evolutionary Multi-Criterion Optimization*, pages 428–442. Springer, 2005. (Cited on page 41)

[Bouzarkouna *et al.*, 2010] Zyed Bouzarkouna, Anne Auger, and Didier Yu Ding. Investigating the Local-Meta-Model CMA-ES for Large Population Sizes. In *EvoApplications (1)*, pages 402–411, 2010. (Cited on pages 5, 71, 73, 74, 95, 97, and 108)

[Bouzarkouna *et al.*, 2011] Zyed Bouzarkouna, Anne Auger, and Didier Yu Ding. Local-meta-model CMA-ES for partially separable functions. In *GECCO*, pages 869–876, 2011. (Cited on pages 71 and 73)

[Box and Hunter, 1959] G. E. P. Box and J. S. Hunter. Condensed Calculations for Evolutionary Operation Programs. *Technometrics*, 1:77–95, 1959. (Cited on page 12)

[Box and Wilson, 1951] G.E.P. Box and KB Wilson. On the experimental attainment of optimum conditions. *Journal of the Royal Statistical Society. Series B (Methodological)*, 13(1):1–45, 1951. (Cited on pages 5, 12, and 51)

[Box, 1957] G. E. P. Box. Evolutionary Operation: A Method for Increasing Industrial Productivity. *Applied Statistics*, 6(2):81–101, June 1957. (Cited on page 12)

[Branke, 2001] Jürgen Branke. Evolutionary Approaches to Dynamic Optimization Problems-Updated Survey. In Jürgen Branke and Thomas Bäck, editors, *Proceedings of the GECCO Workshop on Evolutionary Algorithms for Dynamic Optimization Problems*, pages 27–30, San Francisco, California, USA, July 2001. (Cited on page 23)

[Bremermann, 1962] H.J. Bremermann. Optimization through evolution and recombination. *Self-organizing systems*, pages 93–106, 1962. (Cited on page 13)

[Bremmerman, 1958] H. J. Bremmerman. *The evolution of intelligence: The nervous system as a model of its environment*. University of Washington, 1958. (Cited on page 13)

[Brest *et al.*, 2006] J. Brest, S. Greiner, B. Boskovic, M. Mernik, and V. Zumer. Self-Adapting Control Parameters in Differential Evolution: A Comparative Study on Numerical Benchmark Problems. *Evolutionary Computation, IEEE Transactions on*, 10(6):646–657, December 2006. (Cited on page 19)

[Brockhoff *et al.*, 2010] D. Brockhoff, A. Auger, N. Hansen, D. V. Arnold, and T. Hohm. Mirrored Sampling and Sequential Selection for Evolution Strategies. In R. Schaefer et al., editor, *PPSN XI*, pages 11–20. LNCS 5199, Springer Verlag, 2010. (Cited on page 159)

[Brockhoff *et al.*, 2012] Dimo Brockhoff, Tobias Wagner, and Heike Trautmann. On the properties of the R2 indicator. In *Proceedings of the fourteenth international conference on Genetic and evolutionary computation conference*, GECCO '12, pages 465–472, New York, NY, USA, 2012. ACM. (Cited on page 38)

[Bryson and Ho, 1975] Arthur E. Jr. Bryson and Yu-Chi Ho. *Applied Optimal Control-Optimization, Estimation, and Control*. Taylor and Francis, 1975. (Cited on page 53)

[Buche *et al.*, 2005] D. Buche, N. N. Schraudolph, and P. Koumoutsakos. Accelerating evolutionary algorithms with Gaussian process fitness function models. *Systems, Man and Cybernetics, Part C, IEEE Transactions on*, 35(2):183–194, 2005. (Cited on page 71)

[Burges, 1998] C.J.C. Burges. A tutorial on support vector machines for pattern recognition. *Data mining and knowledge discovery*, 2(2):121–167, 1998. (Cited on page 59)

[Burjorjee, 2008] Keki M. Burjorjee. The Fundamental Problem with the Building Block Hypothesis. *CoRR*, abs/0810.3356, 2008. (Cited on page 15)

[Chang and Lin, 2001] C.C. Chang and C.J. Lin. Training v-support vector classifiers: Theory and algorithms. *Neural Computation*, 13(9):2119–2147, 2001. (Cited on page 60)

[Chaput and Szostak, 2004] J.C. Chaput and J.W. Szostak. Evolutionary optimization of a nonbiological ATP binding protein for improved folding stability. *Chemistry & biology*, 11(6):865–874, 2004. (Cited on page 3)

[Charnes and Cooper, 1961] A. Charnes and W.W. Cooper. *Management models and industrial applications of linear programming*. Management Models and Industrial Applications of Linear Programming. Wiley, 1961. (Cited on page 39)

[Chiong *et al.*, 2011] R. Chiong, T. Weise, and Z. Michalewicz. *Variants of evolutionary algorithms for real-world applications*. Springer-Verlag New York Inc, 2011. (Cited on page 4)

[Chotard *et al.*, 2012] Alexandre Adrien Chotard, Anne Auger, and Nikolaus Hansen. Cumulative Step-size Adaptation on Linear Functions. *CoRR*, abs/1206.1208, 2012. (Cited on page 27)

[Chu and Ghahramani, 2005a] W. Chu and Z. Ghahramani. Gaussian Processes for Ordinal Regression. *Journal of Machine Learning Research*, 6:1019–1041, 2005. (Cited on page 129)

[Chu and Ghahramani, 2005b] W. Chu and Z. Ghahramani. Preference learning with Gaussian processes. In *Proceedings of the 22nd international conference on Machine learning*, pages 137–144. ACM, 2005. (Cited on page 79)

[Chu and Keerthi, 2005] W. Chu and S.S. Keerthi. New approaches to support vector ordinal regression. In *Proceedings of the 22nd international conference on Machine learning*, pages 145–152. ACM, 2005. (Cited on page 80)

[Coello and Lamont, 2004] C.A.C. Coello and G.B. Lamont. *Applications of multi-objective evolutionary algorithms*, volume 1. World Scientific Pub Co Inc, 2004. (Cited on page 4)

[Corne *et al.*, 2001] David W. Corne, Nick R. Jerram, Joshua D. Knowles, and Martin J. Oates. PESA-II: Region-based Selection in Evolutionary Multiobjective Optimization. In Lee Spector et al., editor, *GECCO 2001*, pages 283–290. Morgan Kaufmann, 2001. (Cited on page 139)

[Coulom, 2007] R. Coulom. Computing Elo ratings of move patterns in the game of Go. In *Computer games workshop*, 2007. (Cited on page 102)

[Cramer, 1985] N.L. Cramer. A representation for the adaptive generation of simple sequential programs. In *Proceedings of the First International Conference on Genetic Algorithms*, volume 183, page 187, 1985. (Cited on page 18)

[Dangauthier *et al.*, 2007] P. Dangauthier, R. Herbrich, T. Minka, T. Graepel, et al. Trueskill through time: Revisiting the history of chess. *Advances in Neural Information Processing Systems*, 20:337–344, 2007. (Cited on page 102)

[Darwin, 1859] Charles Darwin. *On the Origin of Species by Means of Natural Selection*. Murray, London, 1859. or the Preservation of Favored Races in the Struggle for Life. (Cited on page 12)

[Deb and Goyal, 1996] Kalyanmoy Deb and Mayank Goyal. A Combined Genetic Adaptive Search (GeneAS) for Engineering Design. *Computer Science and Informatics*, 26:30–45, 1996. (Cited on page 43)

[Deb and Kalyanmoy, 2001] Kalyanmoy Deb and Deb Kalyanmoy. *Multi-Objective Optimization Using Evolutionary Algorithms*. Wiley, 1 edition, June 2001. (Cited on page 39)

[Deb *et al.*, 2000] Kalyanmoy Deb, Amrit Pratap, Sameer Agarwal, and T. Meyarivan. A Fast Elitist Multi-Objective Genetic Algorithm: NSGA-II. *IEEE Transactions on Evolutionary Computation*, 6:182–197, 2000. (Cited on pages 38, 41, 42, and 137)

[Deb *et al.*, 2001] K. Deb, L. Thiele, M. Laumanns, and E. Zitzler. Scalable Test Problems for Evolutionary Multi-Objective Optimization. TIK Report 112, Computer Engineering and Networks Laboratory (TIK), ETH Zurich, 2001. (Cited on pages 37 and 46)

[Deb *et al.*, 2002] Kalyanmoy D. Deb, Amrit Pratap, Sameer Agarwal, and T. Meyarivan. A fast and elitist multiobjective genetic algorithm : NSGA-II. *IEEE Transactions on Evolutionary Computation*, 6(2):182–197, April 2002. (Cited on page 17)

[Deb, 2005] K. Deb. A population-based algorithm-generator for real-parameter optimization. *Soft Comput.*, 9(4):236–253, April 2005. (Cited on page 16)

[Dorigo and Stützle, 2003] M. Dorigo and T. Stützle. The Ant Colony Optimization Metaheuristic: Algorithms, Applications, and Advances. In Fred Glover and Gary Kochenberger, editors, *Handbook of Metaheuristics*, volume 57 of *International Series in Operations Research & Management Science*, chapter 9, pages 250–285–285. Springer, New York, 2003. (Cited on page 17)

[Dorigo, 1992] M. Dorigo. *Optimization, Learning and Natural Algorithms*. PhD thesis, Politecnico di Milano, Italy, 1992. (Cited on page 17)

[Droste *et al.*, 1998] Stefan Droste, Thomas Jansen, and Ingo Wegener. On the optimization of unimodal functions with the (1+1) evolutionary algorithm. In Agoston Eiben, Thomas Back, Marc Schoenauer, and Hans-Paul Schwefel, editors, *Parallel Problem Solving from Nature 1998 PPSN V*, volume 1498 of *LNCS*, pages 13–22. Springer, 1998. (Cited on page 13)

[Efron and Tibshirani, 1979] B. Efron and R Tibshirani. Improvements on cross-validation: The 0.632 + bootstrap method. *Journal of the American Statistical Association*, 92:548–560, 1979. (Cited on page 66)

[Efron, 1979] B. Efron. Bootstrap methods: another look at the jackknife. *Ann. Statistics*, 7:1–26, 1979. (Cited on page 66)

[Elshamy *et al.*, 2007] Wesam Elshamy, Hassan M. Emara, and A. Bahgat. Clubs-based Particle Swarm Optimization. In *Swarm Intelligence Symposium, 2007*, pages 289–296, 2007. (Cited on page 19)

[Emmerich and Fonseca, 2011] Michael T. M. Emmerich and Carlos M. Fonseca. Computing hypervolume contributions in low dimensions: asymptotically optimal algorithm and complexity results. In *Proceedings of the 6th international conference on Evolutionary multi-criterion optimization*, EMO'11, pages 121–135, Berlin, Heidelberg, 2011. Springer-Verlag. (Cited on page 42)

[Emmerich and Naujoks, 2004] Michael Emmerich and Boris Naujoks. Metamodel Assisted Multiobjective Optimisation Strategies and their Application in Airfoil Design. *Proc. of ACDM VI*, 2004. (Cited on page 75)

[Emmerich *et al.*, 2002] Michael Emmerich, Alexios Giotis, Mutlu Özdemir, Thomas Bäck, and Kyriakos Giannakoglou. Metamodel-Assisted Evolution Strategies. In *Proceedings of the 7th International Conference on Parallel Problem Solving from Nature*, PPSN VII, pages 361–370, London, UK, UK, 2002. Springer-Verlag. (Cited on pages 68 and 70)

[Emmerich *et al.*, 2005] Michael Emmerich, Nicola Beume, and Boris Naujoks. An EMO Algorithm Using the Hypervolume Measure as Selection Criterion. In *2005 Int'l Conference, March 2005*, pages 62–76. Springer, 2005. (Cited on pages 39, 42, 43, and 184)

[Emmerich *et al.*, 2006a] M. Emmerich, K. Giannakoglou, and B. Naujoks. Single and multiobjective evolutionary optimization assisted by Gaussian random field metamodels. *IEEE Transactions on Evolutionary Computation*, 10:421—439, 2006. (Cited on pages 75 and 131)

[Emmerich *et al.*, 2006b] Michael T.M. Emmerich, Kyriakos C. Giannakoglou, and Boris Naujoks. Single- and Multiobjective Evolutionary Optimization Assisted by Gaussian Random Field Metamodels. *IEEE TEC*, 10(4):421–439, 2006. (Cited on page 53)

[Fan *et al.*, 2008] R.E. Fan, K.W. Chang, C.J. Hsieh, X.R. Wang, and C.J. Lin. LIBLINEAR: A library for large linear classification. *The Journal of Machine Learning Research*, 9:1871–1874, 2008. (Cited on page 130)

[Farina, 2002] Marco Farina. A Neural Network Based Generalized Response Surface Multiobjective Evolutionary Algorithm. In David B. Fogel, Mohamed A. El-Sharkawi, Xin Yao, Garry Greenwood, Hitoshi Iba, Paul Marrow, and Mark Shackleton, editors, *IEEE Congress on Evolutionary Computation*, pages 956–961. IEEE Press, 2002. (Cited on page 74)

[Fialho *et al.*, 2010] Álvaro Fialho, Raymond Ros, Marc Schoenauer, and Michèle Sebag. Comparison-based Adaptive Strategy Selection with Bandits in Differential Evolution. In *11th International Conference on Parallel Problem Solving From Nature - PPSN*, Krakow, Poland, September 2010. (Cited on pages 19 and 102)

[Finck *et al.*, 2010] S. Finck, N. Hansen, R. Ros, and A. Auger. Real-parameter black-box optimization benchmarking 2010: Experimental setup. Technical Report 2009/21, Research Center PPE, 2010. (Cited on pages 31, 32, and 33)

[Fisher, 1930] R.A. Fisher. *The genetical theory of natural selection.* Clarendon Press, Oxford, 1930. (Cited on page 12)

[Fisher, 1935] R Fisher. *The design of experiments.* Hafner Press, New York, 1935. (Cited on page 12)

[Fisher, 1936] R Fisher. Has Mendel's work been rediscovered? *Annals of Science*, 1(2):115–137, 1936. (Cited on page 12)

[Fletcher, 1987] R. Fletcher. *Practical methods of optimization, Volume 1.* Wiley, 1987. (Cited on page 56)

[Fogel *et al.*, 1966] L. J. Fogel, A. J. Owens, and M. J. Walsh. *Artificial Intelligence through Simulated Evolution.* John Wiley, New York, USA, 1966. (Cited on page 14)

[Fogel, 2006] D. B. Fogel. Nils Barricelli - artificial life, coevolution, self-adaptation. *Comp. Intell. Mag.*, 1(1):41–45, November 2006. (Cited on page 13)

[Fonseca *et al.*, 1993] C.M. Fonseca, P.J. Fleming, et al. Genetic algorithms for multiobjective optimization: Formulation, discussion and generalization. In *Proceedings of the*

fifth international conference on genetic algorithms, volume 1, page 416. Citeseer, 1993. (Cited on page 41)

[Fraser, 1957] A. S. Fraser. Simulation of genetic systems by automatic digital computers. II. Effects of linkage on rates of advance under selection. *Australian Journal of Biological Science*, 10:492–499, 1957. (Cited on page 13)

[Friedman, 1991] J.H. Friedman. Multivariate adaptive regression splines. *The annals of statistics*, pages 1–67, 1991. (Cited on page 51)

[Fursin *et al.*, 2005] G. Fursin, A. Cohen, M. O'Boyle, and O. Temam. A practical method for quickly evaluating program optimizations. *High Performance Embedded Architectures and Compilers*, pages 29–46, 2005. (Cited on page 3)

[García *et al.*, 2009] Salvador García, Daniel Molina, Manuel Lozano, and Francisco Herrera. A study on the use of non-parametric tests for analyzing the evolutionary algorithms' behaviour: a case study on the CEC'2005 Special Session on Real Parameter Optimization. *Journal of Heuristics*, 15:617–644, 2009. (Cited on page 31)

[Gelly *et al.*, 2007] S. Gelly, S. Ruette, and O. Teytaud. Comparison-based algorithms are robust and randomized algorithms anytime. *Evolutionary Computation*, 15(4):411–434, 2007. (Cited on page 30)

[Glasmachers and Igel, 2008] T. Glasmachers and C. Igel. Second-Order SMO Improves SVM Online and Active Learning. *Neural Computation*, 20(2):374–382, 2008. (Cited on page 240)

[Goldberg *et al.*, 1992] D.E. Goldberg, K. Deb, and J. rey Horn. Massive multimodality, deception, and genetic algorithms. *Urbana*, 51:61801, 1992. (Cited on page 23)

[Goldberg, 1989] David E. Goldberg. *Genetic Algorithms in Search, Optimization, and Machine Learning*. Addison-Wesley Professional, 1 edition, January 1989. (Cited on pages 16, 38, and 41)

[Google, 2012] Google. Google Scholar contributors. `http://scholar.google.com/`, 2012. Accessed August 24, 2012. (Cited on page 50)

[Gorissen *et al.*, 2009] Dirk Gorissen, Tom Dhaene, and Filip De Turck. Evolutionary Model Type Selection for Global Surrogate Modeling. *J. Mach. Learn. Res.*, 10:2039–2078, December 2009. (Cited on page 68)

[Graf and Borer, 2001] A. Graf and S. Borer. Normalization in support vector machines. *Pattern Recognition*, pages 277–282, 2001. (Cited on page 85)

[Gräning *et al.*, 2007] L. Gräning, Y. Jin, and B. Sendhoff. Individual-based management of meta-models for evolutionary optimization with application to three-dimensional blade optimization. *Evolutionary Computation in Dynamic and Uncertain Environments*, pages 225–250, 2007. (Cited on page 71)

[Hansen and Kern, 2004] Nikolaus Hansen and Stefan Kern. Evaluating the CMA Evolution Strategy on Multimodal Test Functions. In *PPSN'04*, pages 282–291, 2004. (Cited on page 185)

[Hansen and Ostermeier, 1996] Nikolaus Hansen and Andreas Ostermeier. Adapting Arbitrary Normal Mutation Distributions in Evolution Strategies: The Covariance Matrix Adaptation. In *International Conference on Evolutionary Computation*, pages 312–317, 1996. (Cited on pages 25, 26, 27, and 154)

[Hansen and Ostermeier, 2001] Nikolaus Hansen and Andreas Ostermeier. Completely Derandomized Self-Adaptation in Evolution Strategies. *Evol. Comput.*, 9(2):159–195, June 2001. (Cited on pages 23, 27, 98, and 155)

[Hansen and Ros, 2010a] Nikolaus Hansen and Raymond Ros. Benchmarking a weighted negative covariance matrix update on the BBOB-2010 noiseless testbed. In *GECCO '10: Proceedings of the 12th annual conference comp on Genetic and evolutionary computation*, pages 1673–1680, New York, NY, USA, 2010. ACM. (Cited on pages 27, 28, 29, 106, 113, and 188)

[Hansen and Ros, 2010b] Nikolaus Hansen and Raymond Ros. Benchmarking a weighted negative covariance matrix update on the BBOB-2010 noisy testbed. In *GECCO '10: Proceedings of the 12th annual conference comp on Genetic and evolutionary computation*, pages 1681–1688, New York, NY, USA, 2010. ACM. (Cited on page 120)

[Hansen *et al.*, 2003] N. Hansen, S.D. Müller, and P. Koumoutsakos. Reducing the time complexity of the derandomized evolution strategy with covariance matrix adaptation (CMA-ES). *Evolutionary Computation*, 11(1):1–18, 2003. (Cited on pages 4, 27, 29, 95, 153, and 155)

[Hansen *et al.*, 2008] N. Hansen, R. Ros, N. Mauny, M. Schoenauer, and A. Auger. PSO Facing Non-Separable and Ill-Conditioned Problems. Technical report, INRIA, 2008. (Cited on pages 20 and 22)

[Hansen *et al.*, 2009a] Nikolaus Hansen, Steffen Finck, Raymond Ros, and Anne Auger. Real-Parameter Black-Box Optimization Benchmarking 2009: Noiseless Functions Definitions. Research Report RR-6829, INRIA, 2009. (Cited on pages 32 and 113)

[Hansen *et al.*, 2009b] Nikolaus Hansen, Steffen Finck, Raymond Ros, and Anne Auger. Real-Parameter Black-Box Optimization Benchmarking 2009: Noisy Functions Definitions. Research Report RR-6869, INRIA, 2009. (Cited on pages 32 and 120)

[Hansen *et al.*, 2010a] N. Hansen, A. Auger, S. Finck, and R. Ros. Real-Parameter Black-Box Optimization Benchmarking 2010: Experimental Setup. Technical Report RR-7215, INRIA, 2010. (Cited on pages 6 and 29)

[Hansen *et al.*, 2010b] Nikolaus Hansen, Anne Auger, Raymond Ros, Steffen Finck, and Petr Pošík. Comparing results of 31 algorithms from the black-box optimization bench-

marking BBOB-2009. In *Proceedings of the 12th annual conference companion on Genetic and evolutionary computation*, GECCO 2010, pages 1689–1696, New York, NY, USA, 2010. ACM. (Cited on pages 4, 5, 24, 33, 34, and 184)

[Hansen *et al.*, 2011] N. Hansen, R. Ros, N. Mauny, M. Schoenauer, and A. Auger. Impacts of invariance in search: When CMA-ES and PSO face ill-conditioned and non-separable problems. *Applied Soft Computing*, 11(8):5755–5769, 2011. (Cited on page 31)

[Hansen *et al.*, 2012] N. Hansen, A. Auger, S. Finck, and R. Ros. Real-Parameter Black-Box Optimization Benchmarking 2012: Experimental Setup. Technical report, INRIA, 2012. (Cited on pages 113, 114, 120, 185, and 189)

[Hansen *et al.*, 2013] N. Hansen, D. V. Arnold, and A. Auger. Evolution Strategies. In Janusz Kacprzyk and Witold Pedrycz, editors, *Handbook of Computational Intelligence*. Springer, 2013. accepted. (Cited on pages 24 and 25)

[Hansen, 2006] N. Hansen. Compilation of results on the 2005 CEC benchmark function set. *Online, May*, 2006. (Cited on page 31)

[Hansen, 2008] N. Hansen. Adaptive encoding: How to render search coordinate system invariant. *Parallel Problem Solving from Nature–PPSN X*, pages 205–214, 2008. (Cited on pages 91, 151, 152, 153, 155, 163, and 164)

[Hansen, 2009] Nikolaus Hansen. Benchmarking a BI-population CMA-ES on the BBOB-2009 function testbed. In *GECCO Companion*, pages 2389–2396, 2009. (Cited on pages 29, 35, 97, 113, and 188)

[Hansen, 2011] Nikolaus Hansen. A CMA-ES for Mixed-Integer Nonlinear Optimization. Research Report RR-7751, INRIA, October 2011. (Cited on page 17)

[Hansen, 2012] Nikolaus Hansen. References to CMA-ES Applications. Website, August 2012. Available online at http://www.lri.fr/ hansen/cmaapplications.pdf. (Cited on pages 24 and 31)

[Hastie and Tibshirani, 1990] T.J. Hastie and R.J. Tibshirani. *Generalized additive models*. Chapman & Hall/CRC, 1990. (Cited on page 51)

[Hawkins, 2004] D. M. Hawkins. The Problem of Overfitting. *Journal of Chemical Information and Computer Sciences*, 44(1):1–12, 2004. (Cited on page 22)

[Hebbel and Nisticò, 2008] M. Hebbel and W. Nisticò. Learning to Walk with Model Assisted Evolution Strategies. *Frontiers in Evolutionary Robotics. I-Tech Education and Publishing, Vienna, Austria*, pages 209–220, 2008. (Cited on page 71)

[Helsgaun, 2009] Keld Helsgaun. General k-opt submoves for the Lin–Kernighan TSP heuristic. *Mathematical Programming Computation*, 2009. (Cited on page 17)

[Herbrich *et al.*, 1999] R. Herbrich, T. Graepel, and K. Obermayer. Support vector learning for ordinal regression. In *Artificial Neural Networks, 1999. ICANN 99. Ninth International Conference on (Conf. Publ. No. 470)*, volume 1, pages 97–102. IET, 1999. (Cited on pages 5, 62, and 80)

[Hoffmann and Holemann, 2006] F. Hoffmann and S. Holemann. Controlled Model Assisted Evolution Strategy with Adaptive Preselection. In *International Symposium on Evolving Fuzzy Systems*, pages 182–187. IEEE, 2006. (Cited on page 71)

[Holland, 1969] J.H. Holland. *Adaptive Plans Optimal for Payoff-only Environments*. Defense Technical Information Center, 1969. (Cited on page 15)

[Holland, 1975] J. H. Holland. *Adaptation in Natural and Artificial Systems*. University of Michigan Press, Ann Arbor, MI, USA, 1975. (Cited on page 15)

[Hooke and Jeeves, 1961] Robert Hooke and T. A. Jeeves. " Direct Search" Solution of Numerical and Statistical Problems. *J. ACM*, 8(2):212–229, April 1961. (Cited on pages 13 and 169)

[Horn *et al.*, 1994] J. Horn, N. Nafpliotis, and D. E. Goldberg. A niched Pareto genetic algorithm for multiobjective optimization. In *Evolutionary Computation, 1994. IEEE World Congress on Computational Intelligence., Proceedings of the First IEEE Conference on*, pages 82–87, 1994. (Cited on page 41)

[Horowitz, 2001] Joel L. Horowitz. The bootstrap. In *In Handbook of Econometrics*, pages 3159–3228. Elsevier Science, 2001. (Cited on page 66)

[Houle *et al.*, 2010] Michael E. Houle, Hans-Peter Kriegel, Peer Kröger, Erich Schubert, and Arthur Zimek. Can Shared-Neighbor Distances Defeat the Curse of Dimensionality? Scientific and Statistical Database Management. In Michael Gertz and Bertram Ludäscher, editors, *Scientific and Statistical Database Management*, volume 6187 of *LNCS*, chapter 34, pages 482–500. Springer Berlin / Heidelberg, Berlin, Heidelberg, 2010. (Cited on page 21)

[Huband *et al.*, 2005] Simon Huband, Luigi Barone, Lyndon While, and Phil Hingston. A scalable multi-objective test problem toolkit. In *Proceedings of the Third international conference on Evolutionary Multi-Criterion Optimization*, EMO'05, pages 280–295, Berlin, Heidelberg, 2005. Springer-Verlag. (Cited on page 46)

[Igel *et al.*, 2006] Christian Igel, Thorsten Suttorp, and Nikolaus Hansen. A computational efficient covariance matrix update and a (1+1)-CMA for evolution strategies. In *Proceedings of the 8th annual conference on Genetic and evolutionary computation*, GECCO 2006, pages 453–460, New York, NY, USA, 2006. ACM. (Cited on pages 34 and 43)

[Igel *et al.*, 2007a] C. Igel, T. Suttorp, and N. Hansen. Steady-state Selection and Efficient Covariance Matrix Update in the Multi-objective CMA-ES. In S. Obayashi et al.,

editor, *EMO'07*, volume 4403 of *LNCS*, pages 171–185. Springer-Verlag, 2007. (Cited on pages 43, 171, and 179)

[Igel *et al.*, 2007b] Christian Igel, Nikolaus Hansen, and Stefan Roth. Covariance Matrix Adaptation for Multi-objective Optimization. *Evolutionary Computation*, 15(1):1–28, March 2007. (Cited on pages 39, 41, 42, 43, 46, 142, 171, 178, and 179)

[Igel *et al.*, 2008] C. Igel, V. Heidrich-Meisner, and T. Glasmachers. Shark. *The Journal of Machine Learning Research*, 9:993–996, 2008. (Cited on page 86)

[Ingimundardottir and Runarsson, 2011] H. Ingimundardottir and T.P. Runarsson. Sampling Strategies in Ordinal Regression for Surrogate Assisted Evolutionary Optimization. In *11th International Conference on. Intelligent Systems Design and Applications (ISDA)*, page To appear, 2011. (Cited on pages 65 and 108)

[Ishibuchi *et al.*, 2008] Hisao Ishibuchi, Noritaka Tsukamoto, and Yusuke Nojima. Evolutionary many-objective optimization: A short review. In *IEEE Congress on Evolutionary Computation*, pages 2419–2426, 2008. (Cited on page 42)

[Jaakkola *et al.*, 1999] T. Jaakkola, M. Diekhans, and D. Haussler. Using the Fisher kernel method to detect remote protein homologies. In *Proceedings of the Seventh International Conference on Intelligent Systems for Molecular Biology*, pages 149–158, 1999. (Cited on page 92)

[Jastrebski and Arnold, 2006] Graheme A. Jastrebski and Dirk V. Arnold. Improving Evolution Strategies through Active Covariance Matrix Adaptation. In *IEEE Congress on Evolutionary Computation*, pages 2814–2821, 2006. (Cited on page 28)

[Jensen, 2003] M. T. Jensen. Reducing the run-time complexity of multiobjective EAs: The NSGA-II and other algorithms. *Trans. Evol. Comp*, 7(5):503–515, October 2003. (Cited on page 43)

[Jin *et al.*, 2001a] Yaochu Jin, Tatsuya Okabe, and Bernhard Sendhoff. Adapting Weighted Aggregation for Multiobjective Evolution Strategies. In *Proceedings of the First International Conference on Evolutionary Multi-Criterion Optimization*, EMO'01, pages 96–110, London, UK, UK, 2001. Springer-Verlag. (Cited on page 40)

[Jin *et al.*, 2001b] Yaochu Jin, Markus Olhofer, and Bernhard Sendhoff. Managing Approximate Models in Evolutionary Aerodynamic Design Optimization. In *IEEE Congress on Evolutionary Computation*, pages 592–599. IEEE Press, 2001. (Cited on page 69)

[Jin *et al.*, 2002] Yaochu Jin, Markus Olhofer, and Bernhard Sendhoff. A Framework for Evolutionary Optimization with Approximate Fitness Functions. *IEEE Transactions on Evolutionary Computation*, 6:481–494, 2002. (Cited on page 68)

[Jin, 2003] Yaochu Jin. Quality measures for approximate models in evolutionary computation. In *GECCO 2003: Proceedings of the Bird of a Feather Workshop, Genetic and*

Evolutionary Computation Conference, pages 170–173. AAAI, 2003. (Cited on pages 64, 70, and 75)

[Jin, 2005] Yaochu Jin. A Comprehensive Survey of Fitness Approximation in Evolutionary Computation. *Soft Computing*, 9(1):3–12, 2005. (Cited on pages 4, 5, 64, 98, 100, and 108)

[Jin, 2011] Yaochu Jin. Surrogate-assisted evolutionary computation: Recent advances and future challenges. *Swarm and Evolutionary Computation*, pages 61–70, 2011. (Cited on page 64)

[Joachims, 2005] T. Joachims. A support vector method for multivariate performance measures. In *Proceedings of the 22nd international conference on Machine learning*, pages 377–384. ACM, 2005. (Cited on pages 4, 5, 62, 80, and 135)

[Jones *et al.*, 1998] Donald R. Jones, Matthias Schonlau, and William J. Welch. Efficient Global Optimization of Expensive Black-Box Functions. *J. of Global Optimization*, 13(4):455–492, December 1998. (Cited on page 69)

[Kennedy and Eberhart, 1995] J. Kennedy and R. Eberhart. Particle swarm optimization. In *Neural Networks, 1995. Proceedings., IEEE International Conference on*, volume 4, pages 1942–1948 vol.4. IEEE, November 1995. (Cited on page 19)

[Kennedy and Mendes, 2002] James Kennedy and Rui Mendes. Population structure and particle swarm performance. In *IEEE Congress on Evolutionary Computation*, volume 2, pages 1671–1676. IEEE Press, 2002. (Cited on page 19)

[Kern *et al.*, 2006] S. Kern, N. Hansen, and P. Koumoutsakos. Local Meta-Models for Optimization Using Evolution Strategies. In Th. Runarsson et al., editor, *PPSN IX*, pages 939–948. LNCS 4193, Springer Verlag, 2006. (Cited on pages 65, 71, 72, 73, 74, 91, and 95)

[Kern *et al.*, 2007] Stefan Kern, Nikolaus Hansen, and Petros Koumoutsakos. Fast Quadratic Local Meta-Models for Evolutionary Optimization of Anguilliform Swimmers. In Neittaanmaki et al., editors, *EUROGEN 2007*, Helsinki, Finlande, 2007. (Cited on pages 51, 73, and 91)

[Kleijnen, 2009] J.P.C. Kleijnen. Kriging metamodeling in simulation: A review. *European Journal of Operational Research*, 192(3):707–716, 2009. (Cited on page 52)

[Knowles and Corne, 1999] Joshua Knowles and David Corne. Approximating the nondominated front using the Pareto Archived Evolution Strategy. *Evolutionary Computation*, 8:149–172, 1999. (Cited on page 41)

[Knowles and Nakayama, 2008] J. Knowles and H. Nakayama. Meta-modeling in multiobjective optimization. *Multiobjective Optimization*, pages 245–284, 2008. (Cited on page 4)

[Knowles *et al.*, 2001] J. Knowles, R. Watson, and D. Corne. Reducing local optima in single-objective problems by multi-objectivization. In *Evolutionary Multi-Criterion Optimization*, pages 269–283. Springer, 2001. (Cited on page 47)

[Knowles *et al.*, 2006] J. Knowles, L. Thiele, and E. Zitzler. A Tutorial on the Performance Assessment of Stochastic Multiobjective Optimizers. TIK Report 214, Computer Engineering and Networks Laboratory (TIK), ETH Zurich, February 2006. (Cited on pages 37, 46, and 143)

[Knowles, 2006] J. Knowles. ParEGO: a hybrid algorithm with on-line landscape approximation for expensive multiobjective optimization problems. *IEEE Transactions on Evolutionary Computation*, 10(1):50–66, February 2006. (Cited on page 75)

[Kohavi, 1995] Ron Kohavi. A study of cross-validation and bootstrap for accuracy estimation and model selection. In *Proceedings of the 14th international joint conference on Artificial intelligence - Volume 2*, IJCAI'95, pages 1137–1143, San Francisco, CA, USA, 1995. Morgan Kaufmann Publishers Inc. (Cited on pages 66 and 67)

[Koza, 1990] John R. Koza. Concept Formation and Decision Tree Induction Using the Genetic Programming Paradigm. In *PPSN*, pages 124–128, 1990. (Cited on pages 16 and 18)

[Koza, 1992] John R. Koza. *Genetic Programming: On the Programming of Computers by Means of Natural Selection (Complex Adaptive Systems)*. A Bradford Book, 1 edition, December 1992. (Cited on page 18)

[Kruisselbrink *et al.*, 2010] J.W. Kruisselbrink, M.T.M. Emmerich, A.H. Deutz, and T. Baeck. A robust optimization approach using Kriging metamodels for robustness approximation in the CMA-ES. In *IEEE Congress on Evolutionary Computation*, pages 1–8. IEEE, 2010. (Cited on pages 91 and 108)

[Kukkonen and Lampinen, 2005] Saku Kukkonen and Jouni Lampinen. GDE3: the third evolution step of generalized differential evolution. In *IEEE Congress on Evolutionary Computation*, pages 443–450. IEEE, 2005. (Cited on page 41)

[Kwok and Tsang, 2004] J.T.Y. Kwok and I.W.H. Tsang. The pre-image problem in kernel methods. *Neural Networks, IEEE Transactions on*, 15(6):1517–1525, 2004. (Cited on page 193)

[Larrañaga and Lozano, 2002] Pedro Larrañaga and Jose A. Lozano, editors. *Estimation of Distribution Algorithms: A New Tool for Evolutionary Computation*. Kluwer, Boston, MA, 2002. (Cited on page 17)

[LaTorre *et al.*, 2010] Antonio LaTorre, Santiago Muelas, and Na José Mar'ıa Pe. Benchmarking a MOS-based algorithm on the BBOB-2010 noiseless function testbed. In *GECCO '10: Proceedings of the 12th annual conference comp on Genetic and evolutionary computation*, pages 1649–1656, New York, NY, USA, 2010. ACM. (Cited on page 116)

[LeBlanc and Tibshirani, 1993] Michael LeBlanc and Robert Tibshirani. Combining Estimates in Regression and Classification. Technical report, Journal of the American Statistical Association, 1993. (Cited on page 67)

[Li and Zhang, 2009] Hui Li and Qingfu Zhang. Multiobjective Optimization Problems With Complicated Pareto Sets, MOEA/D and NSGA-II. *Evolutionary Computation, IEEE Transactions on*, 13(2):284–302, 2009. (Cited on pages 46, 178, and 181)

[Li *et al.*, 2006] Rui Li, Michael T. M. Emmerich, Ernst G. P. Bovenkamp, Jeroen Eggermont, Thomas Bäck, Jouke Dijkstra, and Johan H. C. Reiber. Mixed-Integer evolution strategies and their application to intravascular ultrasound image analysis. In *Proceedings of the 2006 international conference on Applications of Evolutionary Computing*, EuroGP'06, pages 415–426, Berlin, Heidelberg, 2006. Springer-Verlag. (Cited on page 17)

[Li *et al.*, 2011] R. Li, M.T.M. Emmerich, J. Eggermont, T. Bäck, M. Schütz, J. Dijkstra, and JHC Reiber. Mixed Integer Evolution Strategies for Parameter Optimization. *Evolutionary Computation*, pages 1–38, 2011. (Cited on page 17)

[Li, 2011] H. Li. Learning to rank for information retrieval and natural language processing. *Synthesis Lectures on Human Language Technologies*, 4:1–113, 2011. (Cited on page 79)

[Liang *et al.*, 2006] J. J. Liang, A. K. Qin, P. N. Suganthan, and S. Baskar. Comprehensive learning particle swarm optimizer for global optimization of multimodal functions. *IEEE Transactions on Evolutionary Computation*, 10(3):281–295, June 2006. (Cited on page 19)

[Liu *et al.*, 2009] Wudong Liu, Qingfu Zhang, Edward Tsang, and Botond Virginas. Fuzzy clustering based Gaussian process model for large training set and its application in expensive evolutionary optimization. In *IEEE Congress on Evolutionary Computation*, CEC'09, pages 2411–2415, Piscataway, NJ, USA, 2009. IEEE Press. (Cited on page 65)

[Loshchilov *et al.*, 2010a] I. Loshchilov, M. Schoenauer, and M. Sebag. A Mono Surrogate for Multiobjective Optimization. In J. Branke et al., editor, *Genetic and Evolutionary Computation Conference (GECCO)*, pages 471–478. ACM Press, July 2010. (Cited on page 132)

[Loshchilov *et al.*, 2010b] I. Loshchilov, M. Schoenauer, and M. Sebag. A Pareto-Compliant Surrogate Approach for Multiobjective Optimization. In J. Branke et al., editor, *Genetic and Evolutionary Computation Conference (GECCO)*, pages 1979–1982. ACM Press, July 2010. (Cited on page 132)

[Loshchilov *et al.*, 2010c] I. Loshchilov, M. Schoenauer, and M. Sebag. Comparison-Based Optimizers Need Comparison-Based Surrogates. In R. Schaefer et al., editor, *Parallel Problem Solving from Nature (PPSN XI)*, volume 6238 of *LNCS*, pages 364–373. Springer, September 2010. (Cited on pages 79, 90, and 91)

[Loshchilov *et al.*, 2010d] I. Loshchilov, M. Schoenauer, and M. Sebag. Dominance-Based Pareto-Surrogate for Multi-Objective Optimization. In R. Takahashi et al., editor, *Simulated Evolution and Learning (SEAL 2010)*, pages 230–239. LNCS 6457, Springer Verlag, December 2010. (Cited on page 132)

[Loshchilov *et al.*, 2011a] I. Loshchilov, M. Schoenauer, and M. Sebag. Adaptive Coordinate Descent. In N. Krasnogor et al., editor, *Genetic and Evolutionary Computation Conference (GECCO)*, pages 885–892. ACM Press, July 2011. (Cited on pages 151 and 152)

[Loshchilov *et al.*, 2011b] I. Loshchilov, M. Schoenauer, and M. Sebag. Not all parents are equal for MO-CMA-ES. In *Evolutionary Multi-Criterion Optimization 2011 (EMO 2011)*, pages 31–45. Springer Verlag, LNCS 6576, April 2011. (Cited on pages 151 and 170)

[Loshchilov *et al.*, 2012a] I. Loshchilov, M. Schoenauer, and M. Sebag. Alternative Restart Strategies for CMA-ES. In V. Cutello et al., editor, *Parallel Problem Solving from Nature (PPSN XII)*, LNCS, pages 296–305. Springer, September 2012. (Cited on page 152)

[Loshchilov *et al.*, 2012b] Ilya Loshchilov, Marc Schoenauer, and Michèle Sebag. Black-box Optimization Benchmarking of IPOP-saACM-ES and BIPOP-saACM-ES on the BBOB-2012 Noiseless Testbed. In Terence Soule and Jason H. Moore, editors, *Genetic and Evolutionary Computation Conference (GECCO Companion)*, pages 175–182. ACM Press, July 2012. (Cited on pages 79 and 98)

[Loshchilov *et al.*, 2012c] Ilya Loshchilov, Marc Schoenauer, and Michèle Sebag. Black-box Optimization Benchmarking of IPOP-saACM-ES on the BBOB-2012 Noisy Testbed. In Terence Soule and Jason H. Moore, editors, *Genetic and Evolutionary Computation Conference (GECCO Companion)*, pages 261–268. ACM Press, July 2012. (Cited on pages 79 and 98)

[Loshchilov *et al.*, 2012d] Ilya Loshchilov, Marc Schoenauer, and Michèle Sebag. Black-box Optimization Benchmarking of NIPOP-aCMA-ES and NBIPOP-aCMA-ES on the BBOB-2012 Noiseless Testbed. In Terence Soule and Jason H. Moore, editors, *Genetic and Evolutionary Computation Conference (GECCO Companion)*, pages 269–276. ACM Press, July 2012. (Cited on page 152)

[Loshchilov *et al.*, 2012e] Ilya Loshchilov, Marc Schoenauer, and Michèle Sebag. Self-Adaptive Surrogate-Assisted Covariance Matrix Adaptation Evolution Strategy. In Terence Soule and Jason H. Moore, editors, *Genetic and Evolutionary Computation Conference (GECCO)*, pages 321–328. ACM Press, July 2012. (Cited on pages 79 and 98)

[Loshchilov, 2009] Ilya G. Loshchilov. Darwin Solver — a system of evolutionary analog circuit design integrated with Microwave Office. In *Proceedings of the 19th International Crimean Conference on Microwave and Telecommunication Technology.*, CriMiCo 2009, pages 101 – 102. IEEE, 2009. (Cited on page 18)

[Madavan, 2002] N. K. Madavan. Multiobjective optimization using a Pareto differential evolution approach. In *IEEE Congress on Evolutionary Computation*, CEC 2002, pages 1145–1150, Washington, DC, USA, 2002. IEEE Computer Society. (Cited on page 41)

[Mahfoud, 1995] S.W. Mahfoud. Niching Methods for Genetic Algorithms. *Urbana*, 51:61801, 1995. (Cited on page 16)

[Marglin, 1967] Stephen A. Marglin. *Public investment criteria : benefit-cost analysis for planned economic growth* . Allen and Unwin, London, 1967. (Cited on page 39)

[Matheron, 1963] G. Matheron. Principles of geostatistics. *Economic geology*, 58(8):1246–1266, 1963. (Cited on page 52)

[Mühlenbein and Mahnig, 2002] H. Mühlenbein and Th. Mahnig. Evolutionary Computation and Wright's Equation. *Theoretical Computer Science*, 287:145–165, 2002. (Cited on page 17)

[Michalewicz, 2012] Z. Michalewicz. Quo Vadis, Evolutionary Computation? *Advances in Computational Intelligence*, pages 98–121, 2012. (Cited on page 4)

[Minsky and Seymour, 1969] M. Minsky and P. Seymour. *Perceptrons*. MIT press, 1969. (Cited on page 15)

[More and Wild, 2012] J. J. More and S. M. Wild. Do You Trust Derivatives or Differences? Preprint ANL/MCS-P2067-0312, Mathematics and Computer Science Division, Argonne National Laboratory, March 2012. (Cited on page 22)

[Mostaghim and Teich, 2003] S. Mostaghim and J. Teich. Strategies for finding good local guides in multi-objective particle swarm optimization (MOPSO). In *Proceedings of the IEEE swarm intelligence symposium*, pages 26–33, 2003. (Cited on page 41)

[Müller and Sbalzarini, 2011] Christian L. Müller and Ivo F. Sbalzarini. Global Characterization of the CEC 2005 Fitness Landscapes Using Fitness-Distance Analysis. In *EvoApplications (1)*, pages 294–303, 2011. (Cited on page 31)

[Mutseniyeks and Rastrigin, 1964] V. A. Mutseniyeks and L. A. Rastrigin. Extremal Control of Continuous Multiparameter Systems by the Method of Random Search. *Engineering Cybernetics*, pages 82–90, 1964. (Cited on page 14)

[Myers, 1990] R.H. Myers. *Classical and modern regression with applications*, volume 488. Duxbury Press Belmont, California, 1990. (Cited on page 51)

[Nain and Deb, 2003] P. K. S. Nain and Kalyanmoy Deb. Computationally effective search and optimization procedure using coarse to fine approximations using coarse to fine grained modeling. In Ruhul Sarker, Robert Reynolds, Hussein Abbass, Kay Chen Tan, Bob McKay, Daryl Essam, and Tom Gedeon, editors, *IEEE Congress on Evolutionary Computation*, pages 2081–2088, Canberra, 8-12 December 2003. IEEE Press. (Cited on page 74)

[Nelder and Mead, 1965] J. A. Nelder and R. Mead. A Simplex Method for Function Minimization. *The Computer Journal*, 7(4):308–313, January 1965. (Cited on page 22)

[Okabe *et al.*, 2004] T. Okabe, Y. Jin, M. Olhofer, and B. Sendhoff. On test functions for evolutionary multi-objective optimization. In *Parallel Problem Solving from Nature-PPSN VIII*, pages 792–802. Springer, 2004. (Cited on page 46)

[Oliveira *et al.*, 2011] Sabrina Oliveira, Mohamed Saifullah Hussin, Thomas Stutzle, Andrea Roli, and Marco Dorigo. A Detailed Analysis of the Population-Based Ant Colony Optimization Algorithm for the TSP and the QAP? Technical Report TR/IRIDIA/2011-006, IRIDIA, February 2011. (Cited on page 17)

[Oliwa and Rasheed, 2012] Tomasz Oliwa and Khaled Rasheed. A surrogate-assisted and informed linkage aware GA. In *GECCO (Companion)*, pages 1467–1468, 2012. (Cited on page 22)

[Orr, 1996] M. J. L. Orr. Introduction to radial basis function networks. Technical report, Centre for Cognitive Science, University of Edinburgh, Scotland, April 1996. (Cited on page 54)

[Orr, 2000] H. A. Orr. Adaptation and the cost of complexity. *Evolution; international journal of organic evolution*, 54(1):13–20, February 2000. (Cited on page 12)

[Pal *et al.*, 2012] Laszlo Pal, Tibor Csendes, Mihaly Csaba Markot, and Arnold Neumaier. Black-box optimization benchmarking of the GLOBAL method. *Evolutionary Computation*, to appear, 2012. (Cited on pages 6 and 34)

[Papadrakakis *et al.*, 1998] Manolis Papadrakakis, Nikos D. Lagaros, and Yiannis Tsompanakis. Structural optimization using evolution strategies and neural networks. *Comput. Methods Appl. Mech. Eng.*, 156(1-4):309–333, 1998. (Cited on page 69)

[Pilát and Neruda, 2011] M. Pilát and R. Neruda. ASM-MOMA: Multiobjective memetic algorithm with aggregate surrogate model. In *IEEE Congress on Evolutionary Computation*, pages 1202–1208. IEEE, 2011. (Cited on page 150)

[Pilát and Neruda, 2012] M. Pilát and R. Neruda. An evolutionary strategy for surrogate-based multiobjective optimization. In *IEEE Congress on Evolutionary Computation*, pages 1–7. IEEE, 2012. (Cited on page 150)

[Platt, 1998] J.C. Platt. Sequential minimal optimization: A fast algorithm for training support vector machines. *Advances in Kernel MethodsSupport Vector Learning*, 208(MSR-TR-98-14):1–21, 1998. (Cited on pages 59 and 80)

[Poland and Zell, 2001] Jan Poland and Andreas Zell. Main Vector Adaptation: A CMA Variant with Linear Time and Space Complexity. In L. Spector, editor, *Genetic and Evolutionary Computation Conference (GECCO 2001)*, pages 1050–1055. Morgan Kaufmann, 2001. (Cited on page 70)

[Poland, 2004] Jan Poland. Explicit Local Models: Towards "Optimal" Optimization Algorithms. In *ECML*, pages 569–571, 2004. (Cited on page 71)

[Ponweiser *et al.*, 2008] Wolfgang Ponweiser, Tobias Wagner, Dirk Biermann, and Markus Vincze. Multiobjective Optimization on a Limited Budget of Evaluations Using Model-Assisted S-Metric Selection. In *Proceedings of the 10th international conference on Parallel Problem Solving from Nature: PPSN X*, pages 784–794, Berlin, Heidelberg, 2008. Springer-Verlag. (Cited on pages 75 and 131)

[Pošík, 2004] Petr Pošík. Kernel Principal Components Analysis as an Efficient Crossover Operator in Real-Valued Evolutionary Algorithms. In *IEEE 4th International Conference on Intelligent Systems Design and Applications 2004*, pages 25–30, 2004. (Cited on page 169)

[Pošık, 2007] P. Pošık. *On the Use of Probabilistic Models and Coordinate Transforms in Real-Valued Evolutionary Algorithms.* PhD thesis, PhD thesis, Czech Technical University in Prague, Prague, Czech Republic, 2007. (Cited on page 193)

[Powell, 1987] M.J.D. Powell. Updating conjugate directions by the bfgs formula. *Mathematical Programming*, 38(1):29–46, 1987. (Cited on page 194)

[Powell, 2006] M. Powell. The NEWUOA software for unconstrained optimization without derivatives. In G. Pillo, M. Roma, and Panos Pardalos, editors, *Large-Scale Nonlinear Optimization*, volume 83 of *Nonconvex Optimization and Its Applications*, pages 255–297. Springer US, 2006. (Cited on pages 5, 6, and 34)

[Queipo *et al.*, 2005] Nestor V. Queipo, Raphael T. Haftka, Wei Shyy, Tushar Goel, Rajkumar Vaidyanathan, and P. Kevin Tucker. Surrogate-based analysis and optimization. *Progress in Aerospace Sciences*, 41(1):1 – 28, 2005. (Cited on page 66)

[Radcliffe and Surry, 1994] N. Radcliffe and P. Surry. Formal memetic algorithms. *Evolutionary Computing*, pages 1–16, 1994. (Cited on page 16)

[Rasheed and Hirsh, 2000] Khaled Rasheed and Haym Hirsh. Informed operators: Speeding up genetic-algorithm-based design optimization using reduced models. In *In Proceedings of the Genetic and Evolutionary Computation Conference (GECCO*, pages 628–635. Morgan Kaufmann, 2000. (Cited on pages 68 and 140)

[Rasmussen, 2004] C. Rasmussen. Gaussian processes in machine learning. *Advanced Lectures on Machine Learning*, pages 63–71, 2004. (Cited on page 52)

[Rastrigin, 1960] L. A. Rastrigin. Extremal control by the method of random scanning. *Automation and Remote Control*, pages 891–896, 1960. (Cited on pages 13 and 14)

[Rastrigin, 1963a] L. A. Rastrigin. *The convergence of the random search method in the extremal control of a many parameter system.* Automation and Remote Control, 1963. (Cited on pages 13 and 14)

[Rastrigin, 1963b] L. A. Rastrigin. *In the world of random events (in Russian)*. Latvian Academy of Science, USSR, Riga, 1963. (Cited on pages 13 and 14)

[Rechenberg, 1973] I. Rechenberg. *Evolutionsstrategie: optimierung technischer systeme nach prinzipien der biologischen evolution*. Frommann-Holzboog, 1973. (Cited on pages 14, 24, 25, 31, and 154)

[Richard Bellman, 1957] Rand Corporation Richard Bellman. *Dynamic Programming*. Princeton University Press, 1957. (Cited on page 21)

[Robič and Filipič, 2005] T. Robič and B. Filipič. DEMO: Differential evolution for multiobjective optimization. In *Evolutionary Multi-Criterion Optimization*, pages 520–533. Springer, 2005. (Cited on page 41)

[Ros and Hansen, 2008] Raymond Ros and Nikolaus Hansen. A Simple Modification in CMA-ES Achieving Linear Time and Space Complexity. In *Proceedings of the 10th international conference on Parallel Problem Solving from Nature: PPSN X*, pages 296–305, Berlin, Heidelberg, 2008. Springer-Verlag. (Cited on pages 35, 167, and 168)

[Ros, 2009] R. Ros. Benchmarking the BFGS algorithm on the BBOB-2009 function testbed. In *Proceedings of the 11th Annual Conference Companion on Genetic and Evolutionary Computation Conference: Late Breaking Papers*, pages 2409–2414. ACM, 2009. (Cited on page 194)

[Rosenblatt, 1958] F. Rosenblatt. The perceptron: A probabilistic model for information storage and organization in the brain. *Psychological review*, 65(6):386, 1958. (Cited on page 53)

[Rosenbrock, 1960] H.H. Rosenbrock. An automatic method for finding the greatest or least value of a function. *The Computer Journal*, 3(3):175–184, 1960. (Cited on page 153)

[Rosipal and Trejo, 2002] R. Rosipal and L.J. Trejo. Kernel partial least squares regression in reproducing kernel Hilbert space. *The Journal of Machine Learning Research*, 2:97–123, 2002. (Cited on page 51)

[Roslund *et al.*, 2009] J. Roslund, O.M. Shir, T. Bäck, and H. Rabitz. Accelerated optimization and automated discovery with covariance matrix adaptation for experimental quantum control. *Physical Review A*, 80(4):043415, 2009. (Cited on page 3)

[Rubinstein and Kroese, 2004] Reuven Y. Rubinstein and Dirk P. Kroese. *The Cross-Entropy Method: A Unified Approach to Combinatorial Optimization, Monte-Carlo Simulation and Machine Learning (Information Science and Statistics)*. Springer, 1 edition, July 2004. (Cited on page 17)

[Runarsson, 2004] Thomas Philip Runarsson. Constrained Evolutionary Optimization by Approximate Ranking and Surrogate Models. In *PPSN*, pages 401–410, 2004. (Cited on pages 70, 72, 94, and 98)

[Runarsson, 2006] Thomas P. Runarsson. Ordinal Regression in Evolutionary Computation. In Th. Runarsson et al., editor, *PPSN IX*, pages 1048–1057. LNCS 4193, Springer Verlag, 2006. (Cited on pages 5, 65, 71, 90, and 108)

[Salomon, 1995] Ralf Salomon. Reevaluating Genetic Algorithm Performance under Coordinate Rotation of Benchmark Functions - A survey of some theoretical and practical aspects of genetic algorithms. *BioSystems*, 39:263–278, 1995. (Cited on page 22)

[Sareni and Krahenbuhl, 1998] B. Sareni and L. Krahenbuhl. Fitness sharing and niching methods revisited. *Evolutionary Computation, IEEE Transactions on*, 2(3):97–106, September 1998. (Cited on page 16)

[Schaffer, 1985] J. David Schaffer. Multiple Objective Optimization with Vector Evaluated Genetic Algorithms. In *Proceedings of the 1st International Conference on Genetic Algorithms*, pages 93–100, Hillsdale, NJ, USA, 1985. L. Erlbaum Associates Inc. (Cited on pages 40 and 41)

[Schaul, 2011] Tom Schaul. *Studies in Continuous Black-box Optimization*. Dissertation, Technische Universität München, München, 2011. (Cited on page 30)

[Scholkopf *et al.*, 1996] B. Scholkopf, A. Smola, and K.-R. Muller. Nonlinear Component Analysis as a Kernel Eigenvalue Problem. Technical Report 44, Max Planck Institute for Biological Cybernetics, Tübingen, Germany, 1996. (Cited on pages 169 and 193)

[Scholkopf *et al.*, 1999] B. Scholkopf, S. Mika, C.J.C. Burges, P. Knirsch, K.R. Muller, G. Ratsch, and A.J. Smola. Input space versus feature space in kernel-based methods. *Neural Networks, IEEE Transactions on*, 10(5):1000–1017, 1999. (Cited on page 83)

[Schölkopf *et al.*, 2000] B. Schölkopf, A.J. Smola, R.C. Williamson, and P.L. Bartlett. New support vector algorithms. *Neural computation*, 12(5):1207–1245, 2000. (Cited on page 61)

[Schölkopf *et al.*, 2001] B. Schölkopf, J.C. Platt, J. Shawe-Taylor, A.J. Smola, and R.C. Williamson. Estimating the support of a high-dimensional distribution. *Neural computation*, 13(7):1443–1471, 2001. (Cited on pages 6, 61, 62, and 132)

[Schumer and Steiglitz, 1968] M. Schumer and K. Steiglitz. Adaptive step size random search. *Automatic Control, IEEE Transactions on*, 13:270–276, 1968. (Cited on pages 14, 25, and 31)

[Schwefel, 1965] H. P. Schwefel. *Kybernetische Evolution als Strategie der experimentellen Forschung in der Strömungstechnik*. Master's thesis. Technical University of Berlin, 1965. (Cited on pages 14 and 24)

[Schwefel, 1993] Hans-Paul Paul Schwefel. *Evolution and Optimum Seeking: The Sixth Generation*. John Wiley & Sons, Inc., New York, NY, USA, 1993. (Cited on pages 14, 15, 70, and 155)

[Sewell, 2011] M. Sewell. The Fisher Kernel: A Brief Review. *RN*, 11(06):06, 2011. (Cited on page 92)

[Shanno, 1970] D. F. Shanno. Conditioning of Quasi-Newton Methods for Function Minimization. *Mathematics of Computation*, 24(111):647–656, 1970. (Cited on pages 5, 6, 23, 34, and 169)

[Shevade *et al.*, 2000] S.K. Shevade, SS Keerthi, C. Bhattacharyya, and K.R.K. Murthy. Improvements to the SMO algorithm for SVM regression. *Neural Networks, IEEE Transactions on*, 11(5):1188–1193, 2000. (Cited on page 80)

[Shi and Ólafsson, 2000] Leyuan Shi and Sigurdur Ólafsson. Nested Partitions Method for Global Optimization. *Oper. Res.*, 48(3):390–407, May 2000. (Cited on page 23)

[Shi and Rasheed, 2008] Liang Shi and Khaled Rasheed. ASAGA: an adaptive surrogate-assisted genetic algorithm. In *Proceedings of the 10th annual conference on Genetic and evolutionary computation*, GECCO 2008, pages 1049–1056, 2008. (Cited on page 68)

[Shir and Bäck, 2006] O. Shir and T. Bäck. Niche radius adaptation in the CMA-ES niching algorithm. *Parallel Problem Solving from Nature-PPSN IX*, pages 142–151, 2006. (Cited on page 197)

[Singh and Deb, 2006] Gulshan Singh and Kalyanmoy Deb, Dr. Comparison of multimodal optimization algorithms based on evolutionary algorithms. In *Proceedings of the 8th annual conference on Genetic and evolutionary computation*, GECCO 2006, pages 1305–1312, New York, NY, USA, 2006. ACM. (Cited on page 21)

[Smit and Eiben, 2010] SK Smit and AE Eiben. Beating the 'world champion' Evolutionary Algorithm via REVAC Tuning. In *IEEE Congress on Evolutionary Computation*, pages 1–8, 2010. (Cited on page 31)

[Smola and Schölkopf, 2004] A.J. Smola and B. Schölkopf. A tutorial on support vector regression. *Statistics and computing*, 14(3):199–222, 2004. (Cited on pages 60, 132, and 240)

[Smola *et al.*, 1998] A. J. Smola, N. Murata, B. Schölkopf, and K.-R. Müller. Asymptotically optimal choice of ε-loss for support vector machines. In L. Niklasson, M. Boden, and T. Ziemke, editors, *Proceedings of the International Conference on Artificial Neural Networks*, Perspectives in Neural Computing, pages 105–110, Berlin, 1998. Springer. (Cited on page 112)

[Socha and Dorigo, 2008] Krzysztof Socha and Marco Dorigo. Ant colony optimization for continuous domains. *European Journal of Operational Research*, 185(3):1155–1173, March 2008. (Cited on page 18)

[Spearman, 1904] C. Spearman. The proof and measurement of association between two things. *The American journal of psychology*, 100(3-4):441–471, 1904. (Cited on page 64)

[Srinivas and Deb, 1994] N. Srinivas and Kalyanmoy Deb. Multiobjective Optimization Using Nondominated Sorting in Genetic Algorithms. *Evolutionary Computation*, 2:221–248, 1994. (Cited on pages 41 and 42)

[Stanley and Miikkulainen, 2002] K.O. Stanley and R. Miikkulainen. Evolving neural networks through augmenting topologies. *Evolutionary computation*, 10(2):99–127, 2002. (Cited on page 53)

[Stanley *et al.*, 2009] K.O. Stanley, D.B. D'Ambrosio, and J. Gauci. A hypercube-based encoding for evolving large-scale neural networks. *Artificial Life*, 15(2):185–212, 2009. (Cited on page 53)

[Stone, 1974] M. Stone. Cross-validatory choice and assessment of statistical predictions. *Roy. Stat. Soc.*, 36:111–147, 1974. (Cited on page 66)

[Storn and Price, 1995] R. Storn and K. Price. Differential Evolution- A Simple and Efficient Adaptive Scheme for Global Optimization over Continuous Spaces. Technical report, Berkeley, 1995. (Cited on page 18)

[Storn and Price, 1997] Rainer Storn and Kenneth Price. Differential Evolution – A Simple and Efficient Heuristic for Global Optimization over Continuous Spaces. *J. of Global Optimization*, 11(4):341–359, December 1997. (Cited on pages 19 and 114)

[Stracquadanio *et al.*, 2011] G. Stracquadanio, A. La Ferla, M. De Felice, and G. Nicosia. Design of Robust Space Trajectories. In *Research and Development in Intelligent Systems XXVIII*, pages 341–354. Springer Verlag, 2011. (Cited on page 191)

[Suganthan *et al.*, 2005] P. N. Suganthan, N. Hansen, J. J. Liang, K. Deb, Y. P. Chen, A. Auger, and S. Tiwari. Problem Definitions and Evaluation Criteria for the CEC 2005 Special Session on Real-Parameter Optimization. Technical report, Nanyang Technological University, Singapore, 2005. (Cited on page 31)

[Sun *et al.*, 2011] Y. Sun, F. Gomez, T. Schaul, and J. Schmidhuber. A Linear Time Natural Evolution Strategy for Non-Separable Functions. *arXiv preprint arXiv:1106.1998*, 2011. (Cited on page 168)

[Sutton and Barto, 1998] R.S. Sutton and A.G. Barto. *Reinforcement learning: An introduction*, volume 1. Cambridge Univ Press, 1998. (Cited on page 6)

[Suttorp *et al.*, 2009] T. Suttorp, N. Hansen, and C. Igel. Efficient covariance matrix update for variable metric evolution strategies. *Machine Learning*, 75(2):167–197, 2009. (Cited on pages 166 and 168)

[Tamiz *et al.*, 1998] Mehrdad Tamiz, Dylan Jones, and Carlos Romero. Goal programming for decision making: An overview of the current state-of-the-art. *European Journal of Operational Research*, 111(3):569–581, 1998. (Cited on page 39)

[Tax and Duin, 2004] D.M.J. Tax and R.P.W. Duin. Support vector data description. *Machine learning*, 54(1):45–66, 2004. (Cited on page 61)

[Tenne and Armfield, 2007] Y. Tenne and S. Armfield. A memetic algorithm using a trust-region derivative-free optimization with quadratic modelling for optimization of expensive and noisy black-box functions. *Evolutionary computation in dynamic and uncertain environments*, pages 389–415, 2007. (Cited on page 129)

[Tenne and Armfield, 2008] Yoel Tenne and Steven William Armfield. Metamodel accuracy assessment in evolutionary optimization. In *IEEE Congress on Evolutionary Computation*, pages 1505–1512, 2008. (Cited on page 67)

[Tesauro *et al.*, 2007] G. Tesauro, N.K. Jong, R. Das, and M.N. Bennani. On the use of hybrid reinforcement learning for autonomic resource allocation. *Cluster Computing*, 10(3):287–299, 2007. (Cited on page 3)

[Tezuka *et al.*, 2004] Masaru Tezuka, Masaharu Munetomo, and Kiyoshi Akama. Linkage Identification by Nonlinearity Check for Real-Coded Genetic Algorithms. In *GECCO 2004*, pages 222–233, 2004. (Cited on page 22)

[Tripathi *et al.*, 2007] P. K. Tripathi, S. Bandyopadhyay, and S. K. Pal. Multi-Objective Particle Swarm Optimization with time variant inertia and acceleration coefficients. *Information Sciences*, 177(22), 2007. (Cited on page 41)

[Tseng, 2001] P. Tseng. Convergence of Block Coordinate Descent Method for Nondifferentiable Minimization. *J. Optim. Theory Appl.*, 109:475–494, 2001. (Cited on page 156)

[Tusar, 2007] Tea Tusar. *Design of an Algorithm for Multiobjective Optimization with Differential Evolution*. M.Sc. Thesis. University of Ljubljana, 2007. (Cited on page 39)

[Ulmer *et al.*, 2003a] Holger Ulmer, Felix Streichert, and Andreas Zell. Evolution Strategies assisted by Gaussian Processes with Improved Pre-Selection Criterion. In *IEEE Congress on Evolutionary Computation*, pages 692–699, 2003. (Cited on pages 70 and 108)

[Ulmer *et al.*, 2003b] Holger Ulmer, Felix Streichert, and Andreas Zell. Model-assisted steady-state evolution strategies. In *Proceedings of the 2003 international conference on Genetic and evolutionary computation*, GECCO 2003, pages 610–621. Springer-Verlag, 2003. (Cited on page 70)

[Ulmer *et al.*, 2004] H. Ulmer, F. Streichert, and A. Zell. Evolution strategies with controlled model assistance. In *IEEE Congress on Evolutionary Computation*, pages 1569 – 1576, 2004. (Cited on pages 65, 68, 70, 71, and 108)

[Vapnik and Chervonenkis, 1971] V.N. Vapnik and A.Y. Chervonenkis. On the uniform convergence of relative frequencies of events to their probabilities. *Theory of Probability and its Applications*, 16(2):264–280, 1971. (Cited on pages 54 and 58)

[Vapnik, 1979] V. Vapnik. Estimation of dependences based on empirical data. *Nauka*, 1979. (Cited on page 135)

[Vapnik, 1995] V.N. Vapnik. *The nature of statistical learning theory*. Springer-Verlag New York, Inc., 1995. (Cited on pages 4, 6, 54, 59, and 60)

[Viana and Haftka, 2008] F. A. C. Viana and R. T. Haftka. Using Multiple Surrogates for Metamodeling. In *7th ASMO-UK/ISSMO International Conference on Engineering Design Optimization*, pages 1505–1512, 2008. (Cited on pages 50 and 67)

[Viana, 2011] F.A.C. Viana. *Multiple surrogates for prediction and optimization*. PhD thesis, UNIVERSITY OF FLORIDA, 2011. (Cited on page 67)

[Vinko and Izzo, 2008] T. Vinko and D. Izzo. Global Optimisation Heuristics and Test Problems for Preliminary Spacecraft Trajectory Design. Technical Report GOHTPP-STD, European Space Agency, 2008. (Cited on pages 185 and 190)

[Voglis *et al.*, 2009] C. Voglis, PE Hadjidoukas, IE Lagaris, and DG Papageorgiou. A numerical differentiation library exploiting parallel architectures. *Computer Physics Communications*, 180(8):1404–1415, 2009. (Cited on page 195)

[Voglis *et al.*, 2012] C. Voglis, G.S. Piperagkas, K.E. Parsopoulos, D.G. Papageorgiou, and I.E. Lagaris. MEMPSODE: comparing particle swarm optimization and differential evolution within a hybrid memetic global optimization framework. In *Proceedings of the fourteenth international conference on Genetic and evolutionary computation conference companion*, pages 253–260. ACM, 2012. (Cited on page 195)

[Voß *et al.*, 2009] Thomas Voß , Nikolaus Hansen, and Christian Igel. Recombination for Learning Strategy Parameters in the MO-CMA-ES. In *Proceedings of the 5th International Conference on Evolutionary Multi-Criterion Optimization*, EMO '09, pages 155–168, Berlin, Heidelberg, 2009. Springer-Verlag. (Cited on page 46)

[Voß *et al.*, 2010] Thomas Voß , Nikolaus Hansen, and Christian Igel. Improved step size adaptation for the MO-CMA-ES. In *Proceedings of the 12th annual conference on Genetic and evolutionary computation*, GECCO '10, pages 487–494, New York, NY, USA, 2010. ACM. (Cited on page 45)

[Voutchkov and Keane, 2006] I. Voutchkov and A.J. Keane. Multiobjective optimization using surrogates. In *Proceedings of the 7th International Conference on Adaptive Computing in Design and Manufacture*, pages 167–175. The M.C.Escher Company, April 2006. (Cited on page 74)

[Weyland, 2010] Dennis Weyland. A Rigorous Analysis of the Harmony Search Algorithm: How the Research Community can be Misled by a "Novel" Methodology. *Int. J. of Applied Metaheuristic Computing*, 1(2):50–60, 2010. (Cited on page 20)

[Wierstra *et al.*, 2008] Daan Wierstra, Tom Schaul, Jan Peters, and Jürgen Schmidhuber. Natural Evolution Strategies. In *IEEE Congress on Evolutionary Computation*, pages 3381–3387, 2008. (Cited on pages 4 and 29)

[Wolpert and Macready, 1997] David H. Wolpert and William G. Macready. No free lunch theorems for optimization. *IEEE Transactions on Evolutionary Computation*, 1(1):67–82, 1997. (Cited on pages 20 and 23)

[Wright, 1991] Alden H. Wright. Genetic Algorithms for Real Parameter Optimization. In *Foundations of Genetic Algorithms*, pages 205–218. Morgan Kaufmann, 1991. (Cited on page 16)

[Yagoubi and Schoenauer, 2012] Mouadh Yagoubi and Marc Schoenauer. Asynchronous master/slave moeas and heterogeneous evaluation costs. In *Proceedings of the fourteenth international conference on Genetic and evolutionary computation conference*, GECCO '12, pages 1007–1014, New York, NY, USA, 2012. ACM. (Cited on page 74)

[Yagoubi, 2012] M. Yagoubi. *Optimisation évolutionnaire multi-objectif parallèle: application à la combustion Diesel*. PhD thesis, Université Paris Sud-Paris XI, 2012. (Cited on pages 3 and 150)

[Yang *et al.*, 2002] B. S. Yang, Y. S. Yeun, and W. S. Ruy. Managing approximation models in multiobjective optimization. *Structural and Multidisciplinary Optimization*, 24:141—-156, 2002. (Cited on page 74)

[Yew-Soon *et al.*, 2006] Ong Yew-Soon, Zhou Zongzhao, and Lim Dudy. Curse and Blessing of Uncertainty in Evolutionary Algorithm Using Approximation. In Gary G. Yen, Simon M. Lucas, Gary Fogel, Graham Kendall, Ralf Salomon, Byoung-Tak Zhang, Carlos A. Coello Coello, and Thomas Philip Runarsson, editors, *Proceedings of the 2006 IEEE Congress on Evolutionary Computation*, pages 2928–2935, Vancouver, BC, Canada, 16-21 July 2006. IEEE Press. (Cited on page 64)

[Yu *et al.*, 2008] T. Yu, L. Davis, C. Baydar, and R. Roy. *Evolutionary Computation in Practice*, volume 88. Springer, 2008. (Cited on page 4)

[Yun *et al.*, 2004] Y. Yun, H. Nakayama, and M. Arakava. Generation of pareto frontiers using support vector machine. *MCDM'04*, 2004. (Cited on page 131)

[Zadeh, 1963] L. A. Zadeh. Optimality and Non-Scalar-Valued Performance Criteria. *IEEE Transactions on Automatic Control*, 8:59–60, 1963. (Cited on page 39)

[Zhang and Li, 2007] Qingfu Zhang and Hui Li. MOEA/D: A Multiobjective Evolutionary Algorithm Based on Decomposition. *IEEE Transactions on Evolutionary Computation*, 11(6):712–731, December 2007. (Cited on page 40)

[Zhang *et al.*, 2008] Q. Zhang, A. Zhou, and Y. Jin. RM-MEDA: A Regularity Model-Based Multiobjective Estimation of Distribution Algorithm. *Evolutionary Computation, IEEE Transactions on*, 12(1):41–63, 2008. (Cited on page 41)

[Zhang *et al.*, 2010] Qingfu Zhang, Wudong Liu, Edward Tsang, and Botond Virginas. Expensive multiobjective optimization by MOEA/D with Gaussian process model. *Trans. Evol. Comp*, 14(3):456–474, June 2010. (Cited on page 75)

[Zhang, 1993] P. Zhang. Model Selection Via Multifold Cross Validation. *The Annals of Statistics*, 21:299–313, 1993. (Cited on page 67)

[Zhou *et al.*, 2007] Z. Z. Zhou, Y. S. Ong, P. B. Nair, A. J. Keane, , and K. Y. Lum. Combining Global and Local Surrogate Models to Accelerate Evolutionary Optimization. *IEEE Trans. Systems, Man and Cybernetics - Part C*, 37(1):66–76, 2007. (Cited on page 67)

[Zitzler and Künzli, 2004] Eckart Zitzler and Simon Künzli. Indicator-based selection in multiobjective search. In *in Proc. 8th International Conference on Parallel Problem Solving from Nature (PPSN VIII*, pages 832–842. Springer, 2004. (Cited on pages 38, 39, and 42)

[Zitzler and Thiele, 1998] E. Zitzler and L. Thiele. Multiobjective optimization using evolutionary algorithms – a comparative case study. In A.E. Eiben et al., editor, *PPSN V*, volume 1498 of *LNCS*, pages 292–301. Springer Verlag, 1998. (Cited on pages 38 and 41)

[Zitzler *et al.*, 2000] Eckart Zitzler, Kalyanmoy Deb, and Lothar Thiele. Comparison of Multiobjective Evolutionary Algorithms: Empirical Results. *Evolutionary Computation*, 8:173–195, 2000. (Cited on pages 46 and 142)

[Zitzler *et al.*, 2002a] E. Zitzler, M. Laumanns, and L. Thiele. SPEA2: Improving the Strength Pareto Evolutionary Algorithm for Multiobjective Optimization. In K.C. Giannakoglou et al., editors, *Evolutionary Methods for Design, Optimisation and Control with Application to Industrial Problems (EUROGEN 2001)*, pages 95–100. International Center for Numerical Methods in Engineering (CIMNE), 2002. (Cited on pages 38, 39, and 41)

[Zitzler *et al.*, 2002b] Eckart Zitzler, Lothar Thiele, Marco Laumanns, Carlos M. Fonseca, and Viviane Grunert da Fonseca. Performance Assessment of Multiobjective Optimizers: An Analysis and Review. *IEEE Transactions on Evolutionary Computation*, 7:117–132, 2002. (Cited on pages 37 and 38)

Appendix A

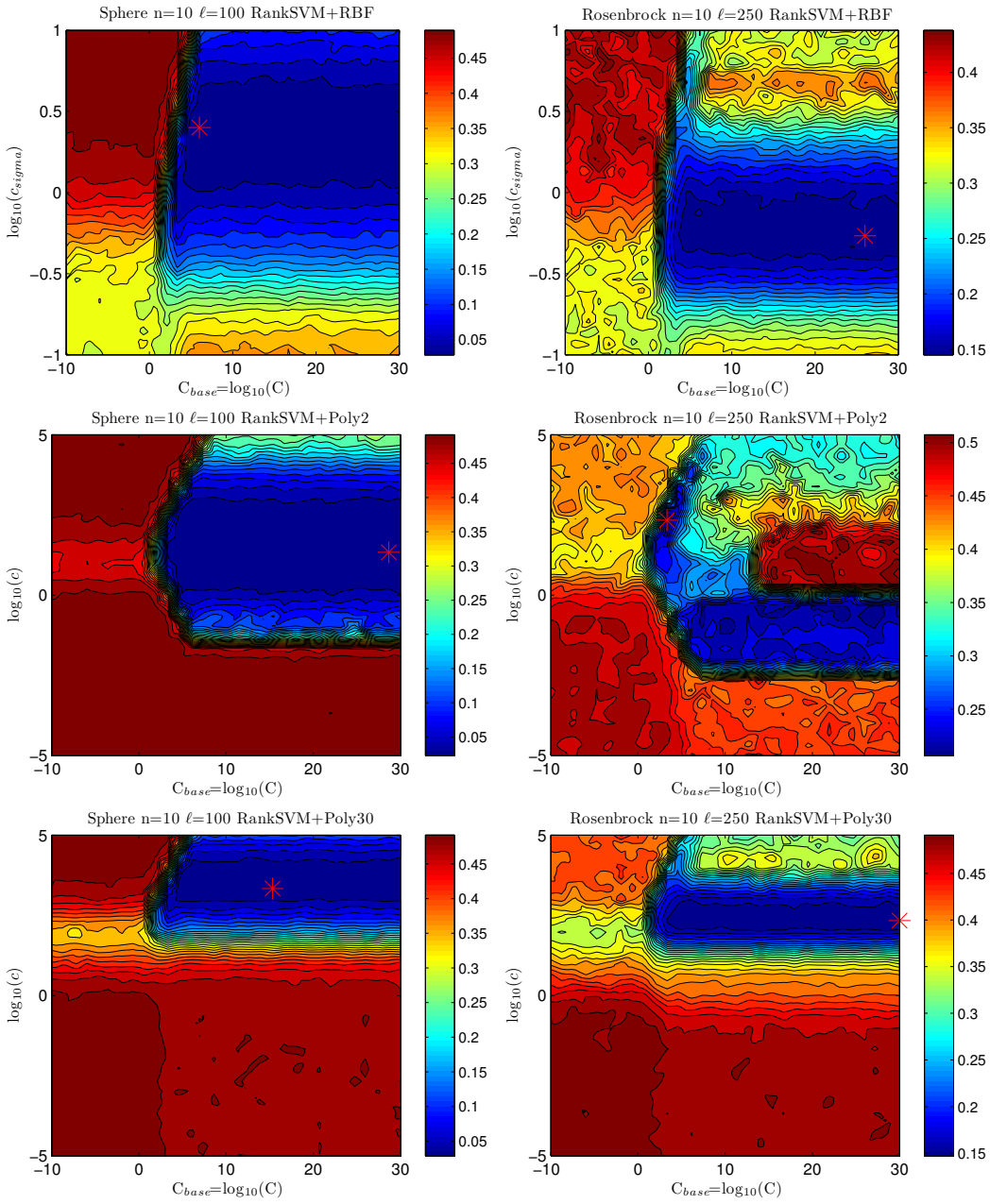

Figure 1: Average surrogate model error in the space of model hyper-parameters measured in 10 runs of Ranking SVM with RBF kernel **(First Row)**, Polynomial kernel with degree 2 **(Second Row)** and Polynomial kernel with degree 30 **(Third Row)** on Sphere **(Left Column)** and Rosenbrock **(Right Column)** functions in 10-D after 1000ℓ iterations of the SMO algorithm. The observed best pair of hyper-parameters is denoted as '*'.

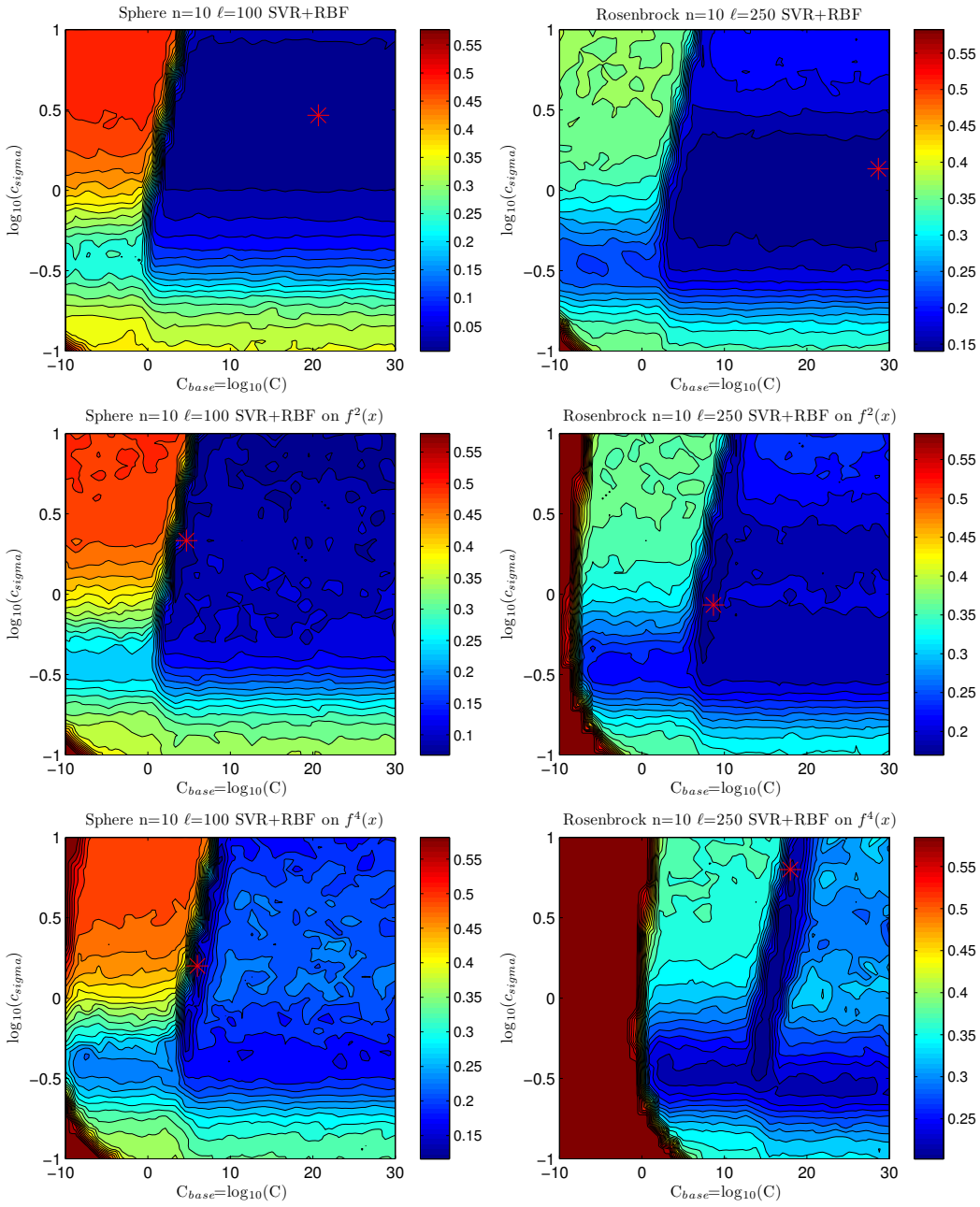

Figure 2: Average surrogate model error in the space of model hyper-parameters measured in 10 runs of SVR with RBF kernel on **(Left Column)** Sphere and **(Right Column)** Rosenbrock functions in 10-D **(First Row)** and its scaled variants f^2 and f^4 **(Second and Third Rows)** after 100ℓ iterations of the SMO algorithm. The observed best pair of hyper-parameters is denoted as '*'.

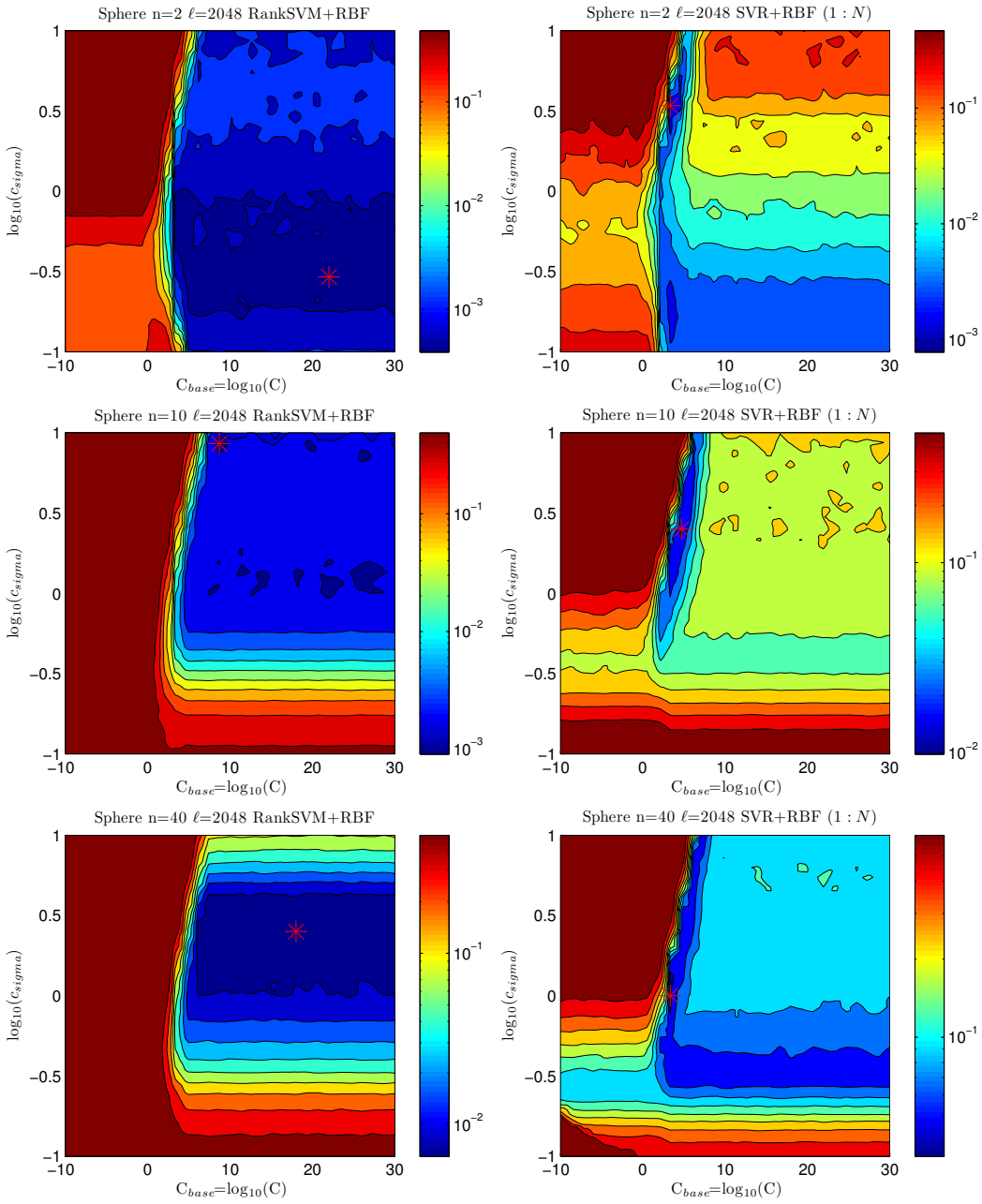

Figure 3: Average surrogate model error in the space of model hyper-parameters measured in 10 runs of Ranking SVM **(Left Column)** and (1:N) rank-based SVR **(Right Column)** with RBF kernel and $\ell = 2048$ training points on Sphere function in 2-D **(First Row)**, 10-D **(First Row)** and 40-D **(First Row)** after 1000ℓ (respectively, 100ℓ) iterations of the SMO algorithm for Ranking SVM (respectively, SVR). The observed best pair of hyper-parameters is denoted as '*'.

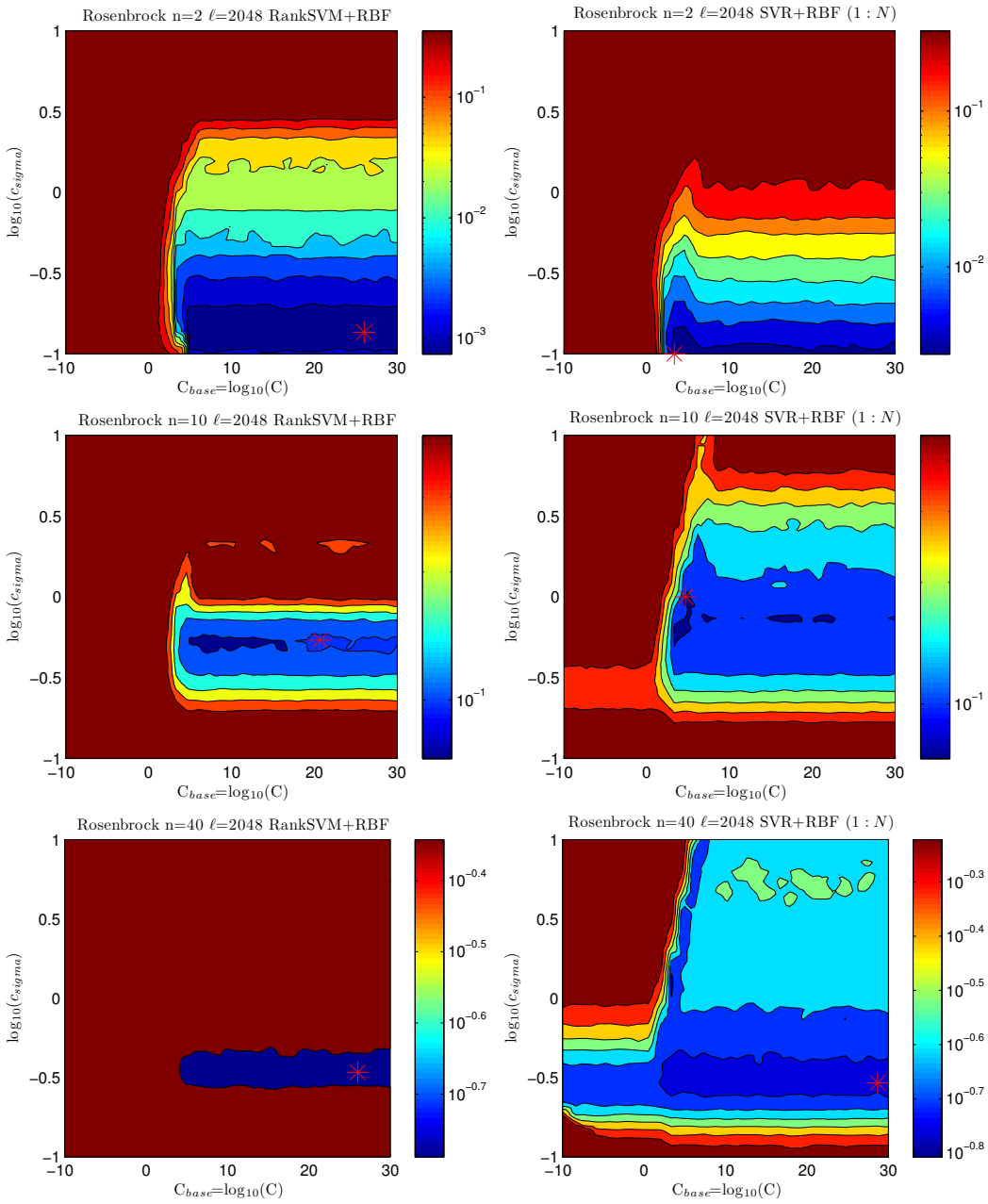

Figure 4: Average surrogate model error in the space of model hyper-parameters measured in 10 runs of Ranking SVM **(Left Column)** and (1:N) rank-based SVR **(Right Column)** with RBF kernel and $\ell = 2048$ training points on Rosenbrock function in 2-D **(First Row)**, 10-D **(First Row)** and 40-D **(First Row)** after 1000ℓ (respectively, 100ℓ) iterations of the SMO algorithm for Ranking SVM (respectively, SVR). The observed best pair of hyper-parameters is denoted as '*'.

Appendix B

B.1 Dual Form of ASM Learning Problem

Introducing the non-negative Lagrangian multipliers $\alpha_i^{(*)}$ and $\beta_i^{(*)}$ for each constraint (5.2-5.7) respectively (where $^{(*)}$ is either $^{(up)}$ or $^{(low)}$), the *dual* form is:

$$\begin{aligned} L(w,\rho,\xi^{(*)},\alpha^{(*)},\beta^{(*)}) &= \frac{1}{2}||w||^2 \\ &+C\sum_{i=1}^{\ell}(\xi_i^{up}+\xi_i^{low})+C\sum_{i=\ell+1}^{m}\xi_i^{up}+\rho \\ &-\sum_{i=1}^{\ell}\alpha_i^{up}(\rho+\epsilon+\xi_i^{up}-<w,\Phi(\boldsymbol{x}_i)>) \\ &-\sum_{i=1}^{\ell}\alpha_i^{low}(<w,\Phi(\boldsymbol{x}_i)>-\rho+\epsilon+\xi_i^{low}) \\ &-\sum_{i=\ell+1}^{m}\alpha_i^{up}(\rho-\epsilon+\xi_i^{up}-<w,\Phi(\boldsymbol{x}_i)>) \\ &-\sum_{i=1}^{\ell}\beta_i^{up}\xi_i^{up} \\ &-\sum_{i=1}^{\ell}\beta_i^{low}\xi_i^{low} \\ &-\sum_{i=\ell+1}^{m}\beta_i^{up}\xi_i^{up} \end{aligned}$$

Computing the KKT conditions leads to:

$$\frac{\partial L}{\partial w} = w+\sum_{i=1}^{\ell}(\alpha_i^{up}-\alpha_i^{low})\Phi(\boldsymbol{x}_i)+\sum_{i=\ell+1}^{m}\alpha_i^{up}\Phi(\boldsymbol{x}_i)=0 \tag{1}$$

$$\frac{\partial L}{\partial \rho} = 1-\sum_{i=1}^{\ell}(\alpha_i^{up}-\alpha_i^{low})-\sum_{i=\ell+1}^{m}\alpha_i^{up}=0 \tag{2}$$

$$\frac{\partial L}{\partial \xi_i^{up}} = C-\alpha_i^{up}-\beta_i^{up}=0 \tag{3}$$

$$\frac{\partial L}{\partial \xi_i^{low}} = C-\alpha_i^{low}-\beta_i^{low}=0 \tag{4}$$

$$\frac{\partial L}{\partial \xi_i^{up}} = C-\alpha_i^{up}-\beta_i^{up}=0 \tag{5}$$

Therefore, at the saddle point we have:

$$w=\sum_{i=1}^{\ell}\alpha_i^{low}\Phi(\boldsymbol{x}_i)-\sum_{i=1}^{m}\alpha_i^{up}\Phi(\boldsymbol{x}_j) \tag{6}$$

$$1=\sum_{i=1}^{m}\alpha_i^{up}-\sum_{i=1}^{\ell}\alpha_i^{low} \tag{7}$$

$$C=\alpha_i^{up}+\beta_i^{up}=\alpha_i^{low}+\beta_i^{low} \tag{8}$$

Reporting these equalities, the Lagrangian becomes:

$$\begin{aligned} L(w,\rho,\xi,\alpha,\beta) &= \\ &= -\tfrac{1}{2}||w||^2 - \epsilon\left(\textstyle\sum_{i=1}^{\ell}(\alpha_i^{up}+\alpha_i^{low}) - \sum_{i=\ell+1}^{m}\alpha_i^{up}\right) \\ &= -\tfrac{1}{2}||w||^2 - \epsilon\left(2\textstyle\sum_{i=1}^{\ell}\alpha_i^{up} - 1\right) \end{aligned}$$

Let us first define some additional notations. Denote

$$K_{ij} = K(\boldsymbol{x}_i, \boldsymbol{x}_j) =< \Phi(\boldsymbol{x}_i), \Phi(\boldsymbol{x}_j) >$$

and

$$\gamma_i = \begin{cases} (\alpha_i^{up} - \alpha_i^{low}) & \text{if } \ i = 1 \dots \ell \\ \alpha_i^{up} & \text{otherwise} \end{cases}$$

Then:

$$L(w,\rho,\xi,\alpha,\beta) = -\frac{1}{2}\sum_{i,j=1}^{m}\gamma_i\gamma_j K(\boldsymbol{x}_i,\boldsymbol{x}_j) - \epsilon\left(2\sum_{i=1}^{\ell}\alpha_i^{up} - 1\right)$$

Eliminating the $\beta^{(*)}$ thanks to relations (8), the dual problem to solve in $(\alpha^{(*)})$ is: Maximize

$$\widetilde{\mathcal{L}}(\alpha^{(*)}) = -\frac{1}{2}||w||^2 - \epsilon\left(2\sum_{i=1}^{\ell}\alpha_i^{up} - 1\right) \tag{9}$$

subject to

$$\sum_{i=1}^{m}\gamma_i = \sum_{i=1}^{m}\alpha_i^{up} - \sum_{i=1}^{\ell}\alpha_i^{low} = 1 \tag{10}$$

$$0 \le \alpha_i^{(*)} \le C \tag{11}$$

B.2 Solving the Dual Problem

Following [Smola and Schölkopf, 2004], the idea is to iterate exact resolutions of the maximization problem by varying only two of the α's multipliers. Thanks to the sum constraint (Eq. (7) or (10)), one of the α variables can be eliminated. As the resulting function, now depending on a single variable, is quadratic, its optimization can be solved analytically. It remains to choose the pair of α indices; this choice has a large impact on the overall computational cost for large regression problems, and several heuristics have been proposed [Glasmachers and Igel, 2008]. It turns out that the best results in our problem were obtained for a uniform selection of the α indices.

B.2.1 The One-dimensional Maximization Problem

Using the same formulation as [13], let φ_i denote the model value at point $\boldsymbol{x}_i$, that is

$$\varphi_i = \mathcal{F}(\boldsymbol{x}_i) =< w, \Phi(\boldsymbol{x}_i) >= \sum_{j=1}^{m} \gamma_j K_{ij}$$

Maximizing the Lagrangian as a function of variables i and j only, amounts to maximize (after removing terms that do not depend on those variables):

$$\begin{array}{l} \widehat{\mathcal{L}_{ij}}(\alpha_i^{(*)}, \alpha_j^{(*)}) = -\frac{1}{2}\Big[\gamma_i^2 K_{ii} + \gamma_j^2 K_{jj} + 2\gamma_i\gamma_j K_{ij}\Big] \\ \quad -\gamma_i\Big[\sum_{k\neq i,j} \gamma_k K_{ki}\Big] - \gamma_j\Big[\sum_{k\neq i,j} \gamma_k K_{kj}\Big] - \epsilon\Big(\widehat{\gamma}_i + \widehat{\gamma}_j\Big) \end{array} \tag{12}$$

where $\widehat{\gamma}_i = 2 * \alpha_i^{up}$ for Pareto points, and $\widehat{\gamma}_i = 0$ for dominated points.

From Eq. (10), it comes:

$$\gamma_i + \gamma_j = \gamma_i^{old} + \gamma_j^{old} \stackrel{def}{=} \Gamma \tag{13}$$

Moreover,for all i

$$\sum_{k\neq i,j} \gamma_k K_{ki} = \varphi_i - \gamma_i^{old} K_{ii} - \gamma_j^{old} K_{ij}$$

Using the above in (12) for i and j, and eliminating j thanks to the summation constraint ($\gamma_i = \Gamma - \gamma_j$) leads to a "single" variable maximization problem with unknown either α_i^*, if $\boldsymbol{x}_i$ is a dominated point, or α_i^{up} / α_i^{low}, knowing that at most one is non-zero:

$$\begin{array}{rl} \widehat{\mathcal{L}}(\alpha_i^{(*)}) = & -\frac{1}{2}\Big[\gamma_i^2 K_{ii} + (\Gamma-\gamma_i)^2 K_{jj} + \gamma_i(\Gamma-\gamma_i) K_{ij}\Big] \\ & -\gamma_i\Big[\varphi_i - \gamma_i^{old} K_{ii} - (\Gamma - \gamma_i^{old}) K_{ij}\Big] \\ & -(\Gamma-\gamma_i)\Big[\varphi_j - (\Gamma-\gamma_i^{old}) K_{jj} - \gamma_i^{old} K_{ij}\Big] \\ & -\epsilon\Big(\widehat{\gamma}_i + \widehat{\gamma}_j\Big) \\ = & -\frac{1}{2}\gamma_i^2\eta - \gamma_i(\varphi_i - \varphi_j - \gamma_i^{old}\eta) - \epsilon(\widehat{\gamma}_i + \widehat{\gamma}_j) \end{array} \tag{14}$$

where

$$\begin{array}{l} \eta \stackrel{def}{=} K_{ii} + K_{jj} - 2K_{ij} = \\ \quad =< \Phi(\boldsymbol{x}_i) - \Phi(\boldsymbol{x}_j), \Phi(\boldsymbol{x}_i) - \Phi(\boldsymbol{x}_j) > \ > 0 \text{ if } i \neq j \end{array} \tag{15}$$

and after having neglected with no loss of generality the terms that do not depend on any of the $\alpha_i^{(*)}$.

We now need to distinguish the different cases to instantiate the $\gamma_i^{(*)}$ and $\widehat{\gamma}_i$.

Dominated-Dominated

When both $\boldsymbol{x}_i$ and $\boldsymbol{x}_j$ are dominated, we have

$$\gamma_i = \alpha_i^{up} \text{ and } \widehat{\gamma}_i = 0$$

and same holds for j. Thanks to the reduced sum-constraint (13), the one-dimensional Lagrangian becomes

$$\widehat{\mathcal{L}}(\alpha_i^{up}) = -\frac{1}{2}(\alpha_i^{up})^2\eta - \alpha_i^{up}(\varphi_i - \varphi_j - \alpha_i^{up,old}\eta) \tag{16}$$

The maximum is thus reached for

$$\alpha_i^{up} = \alpha_i^{up,old} + \frac{\varphi_j - \varphi_i}{\eta} \tag{17}$$

Because $\alpha_k^{up} \in [0, C]$ for all k, the bounds for α_i^{up} are now $[\max(0, \Gamma - C), \min(C, \Gamma)]$. Whenever one of the bounds is violated, α_i^{up} is reset to the bound, and in all cases, α_j^{up} is computed according to the sum-constraint (13).

Pareto-Dominated

Suppose that $\boldsymbol{x}_i$ is non-dominated, and $\boldsymbol{x}_j$ is dominated. Then

$$\begin{aligned} \gamma_i = \alpha_i^{up} - \alpha_i^{low} \quad &\text{and} \quad \widehat{\gamma}_i = 2 * \alpha_i^{up} \\ \gamma_j = \alpha_j^{up} \quad &\text{and} \quad \widehat{\gamma}_j = 0 \end{aligned}$$

We have to distinguish 2 cases, depending on which of $\alpha_i^{up,old}$ and $\alpha_i^{low,old}$ is not 0.

$\underline{\alpha_i^{up,old} \neq 0}$
In this case, at least in some neighborhood of the current value $\alpha_i^{up,old}$,

$$\gamma_i = \alpha_i^{up} \text{ and } \widehat{\gamma}_i = 2 * \alpha_i^{up}$$

Thanks to the reduced sum-constraint (13), the one-dimensional Lagrangian becomes

$$\widehat{\mathcal{L}}(\alpha_i^{up}) = -\frac{1}{2}(\alpha_i^{up})^2\eta - \alpha_i^{up}(\varphi_i - \varphi_j - \alpha_i^{up,old}\eta + 2\varepsilon) \tag{18}$$

The maximum is thus reached for

$$\alpha_i^{up} = \alpha_i^{up,old} + \frac{\varphi_j - \varphi_i - 2\varepsilon}{\eta} \tag{19}$$

From the reduced sum-constraint (13) we deduce the same bounds as in previous section for α_i^{up}, i.e. $[\max(0, \Gamma - C), \min(C, \Gamma)]$. However, whereas the same action must be taken when the upper-bound is reached (set α_i^{up} to the upper bound, and compute α_j^{up} according to the sum-constraint (13), the situation is different if α_i^{up} violates its lower bound: if that bound is strictly positive (i.e. $\Gamma - C$ with $\Gamma > C$), again α_j^{up} should simply

be computed according to the sum-constraint (13). But if the lower bound is 0, it is likely that increasing α_i^{low} might increase the Lagrangian further.

In the latter case, one has to consider again the reduced Lagrangian (12), but with now

$$\gamma_i = -\alpha_i^{low} \text{ and } \widehat{\gamma}_i = 0 \text{ but with } \gamma_i^{old} = \alpha_i^{up,old}$$

which hence gives

$$\widehat{\mathcal{L}}(\alpha_i^{up}) = -\frac{1}{2}(\alpha_i^{low})^2\eta + \alpha_i^{low}(\varphi_i - \varphi_j - \alpha_i^{up,old}\eta) \tag{20}$$

whose maximum is reached for

$$\alpha_i^{low} = -\alpha_i^{up,old} + \frac{\varphi_i - \varphi_j}{\eta} \tag{21}$$

$\underline{\alpha_i^{low,old} \neq 0}$

In this case, at least in some neighborhood of the current value $\alpha_i^{low,old}$,

$$\gamma_i = -\alpha_i^{low} \text{ and } \widehat{\gamma}_i = 0$$

The reduced sum constraint (13) becomes

$$-\alpha_i^{low} + \alpha_j^{up} = \Gamma \tag{22}$$

and the one-dimensional Lagrangian now reads

$$\widehat{\mathcal{L}}(\alpha_i^{low}) = -\frac{1}{2}(\alpha_i^{low})^2\eta + \alpha_i^{low}(\varphi_i - \varphi_j + \alpha_i^{low,old}\eta) \tag{23}$$

Its maximum is this reached for

$$\alpha_i^{low} = \alpha_i^{low,old} + \frac{\varphi_i - \varphi_j}{\eta} \tag{24}$$

The bounds for α_i^{low} are now $[\max(0, -\Gamma), \min(C, C - \Gamma)]$. As in the previous case, if α_i^{low} hits it upper bound, or its strictly positive lower bound, α_j^{up} should simply be computed according to the constraint (22). But if it hits its 0 as its lower bound, here again maximization might be pursued, in a similar way than in previous section: the solution is given by

$$\alpha_i^{up} = -\alpha_i^{low,old} + \frac{\varphi_j - \varphi_i - 2\varepsilon}{\eta} \tag{25}$$

$\underline{\alpha_i^{up,old} = \alpha_i^{low,old} = 0}$

In this case, that could probably enter in both previous cases, both options should be explored: looking into the domain where $\alpha_i^{up} > 0$, it comes from equation (19) that the maximum value is reached for $\alpha_i^{up} = \frac{\varphi_j - \varphi_i - 2\varepsilon}{\eta}$ while in the domain $\alpha_i^{low} > 0$, equation (24) gives that the maximum is reached for $\alpha_i^{low} = \frac{\varphi_i - \varphi_j}{\eta}$. If both quantities are negative (i.e. $0 < \phi_j - \phi_i < 2\varepsilon$), the solution is $\alpha_i^{up} = \alpha_i^{low} = 0$. Otherwise, only one of these quantities is positive, and should be retained – with the same truncations than in sections B.2.1 or B.2.1.

Pareto-Pareto

Suppose now that both $\boldsymbol{x}_i$ and $\boldsymbol{x}_j$ belong to the Pareto front. Then

$$\gamma_i = \alpha_i^{up} - \alpha_i^{low} \text{ and } \widehat{\gamma_i} = 2 * \alpha_i^{up}$$
$$\gamma_j = \alpha_j^{up} - \alpha_j^{low} \text{ and } \widehat{\gamma_j} = 2 * \alpha_j^{up}$$

As in previous section, we have to distinguish different cases depending on which is non zero from α_i^{up} and α_i^{low}, and from α_j^{up} and α_j^{low}.

$\underline{\alpha_i^{up,old} > 0 \text{ and } \alpha_j^{up,old} > 0}$
Thanks to the reduced sum-constraint $\alpha_i^{up} + \alpha_j^{up} = \Gamma$, the one-dimensional Lagrangian now reads

$$\widehat{\mathcal{L}}(\alpha_i^{up}) = -\frac{1}{2}(\alpha_i^{up})^2\eta - \alpha_i^{up}(\varphi_i - \varphi_j - \alpha_i^{up,old}\eta) \tag{26}$$

Its maximum is this reached for

$$\alpha_i^{up} = \alpha_i^{up,old} + \frac{\varphi_j - \varphi_j}{\eta} \tag{27}$$

The bounds for α_i^{low} are, again, $[\max(0, \Gamma - C), \min(C, \Gamma)]$. If either α_i^{up} or α_j^{up} hits the 0 lower bound, maximization should be continued in the corresponding domain (either $\alpha_i^{up} = 0, \alpha_i^{low} > 0$ or $\alpha_j^{up} = 0, \alpha_j^{low} > 0$).

$\underline{\alpha_i^{low,old} > 0 \text{ and } \alpha_j^{up,old} > 0}$
The reduced sum-constraint now reads $-\alpha_i^{low} + \alpha_j^{up} = \Gamma$, and the one-dimensional Lagrangian becomes

$$\widehat{\mathcal{L}}(\alpha_i^{low}) = -\frac{1}{2}(\alpha_i^{low})^2\eta + \alpha_i^{low}(\varphi_i - \varphi_j + \alpha_i^{low,old}\eta - 2\varepsilon) \tag{28}$$

Its maximum is this reached for

$$\alpha_i^{low} = \alpha_i^{low,old} + \frac{\varphi_i - \varphi_i - 2\varepsilon}{\eta} \tag{29}$$

The bounds for α_i^{low} are here $[\max(0, -\Gamma), \min(C, C - \Gamma)]$. Again, if one of the α's hits the 0 bound, maximization should be continued in the other domain.

$\underline{\alpha_i^{up,old} > 0 \text{ and } \alpha_j^{low,old} > 0}$
Similarly, the reduced sum-constraint now reads $\alpha_i^{up} - \alpha_j^{low} = \Gamma$, and the one-dimensional Lagrangian becomes

$$\widehat{\mathcal{L}}(\alpha_i^{up}) = -\frac{1}{2}(\alpha_i^{up})^2\eta - \alpha_i^{up}(\varphi_i - \varphi_j - \alpha_i^{up,old}\eta + 2\varepsilon) \tag{30}$$

Its maximum is this reached for

$$\alpha_i^{up} = \alpha_i^{up,old} + \frac{\varphi_j - \varphi_i - 2\varepsilon}{\eta} \tag{31}$$

The bounds for α_i^{up} are here $[\max(0,\Gamma),\min(C,C+\Gamma)]$. Again, if one of the α's hits the 0 bound, maximization should be continued in the other domain.

$\underline{\alpha_i^{low,old} > 0 \text{ and } \alpha_j^{low,old} > 0}$

The reduced sum-constraint now reads $\alpha_i^{low} + \alpha_j^{up} = -\Gamma$, the term in ϵ hence vanishes, and the onedimensional Lagrangian becomes

$$\widehat{\mathcal{L}}(\alpha_i^{low}) = -\frac{1}{2}(\alpha_i^{low})^2\eta + \alpha_i^{low}(\varphi_i - \varphi_j + \alpha_i^{low,old}\eta) \tag{32}$$

Its maximum is this reached for

$$\alpha_i^{low} = \alpha_i^{low,old} + \frac{\varphi_i - \varphi_j}{\eta} \tag{33}$$

The bounds for α_i^{low} are here $[\max(0,-C-\Gamma),\min(C,-\Gamma)]$, and again, if one of the α's hits the 0 bound, maximization should be continued in the other domain.